THIN AIRFOIL THEORY APPLICATION: ANALYSIS EXAMPLE

Consider a thin airfoil with a simple parabolic-arc camber line, with a maximum camber height εc.

$$Z(x) = 4\varepsilon x\left(1 - \frac{x}{c}\right)$$

$$\frac{dZ}{dx} = 4\varepsilon\left(1 - 2\frac{x}{c}\right) = 4\varepsilon\cos\theta_o$$

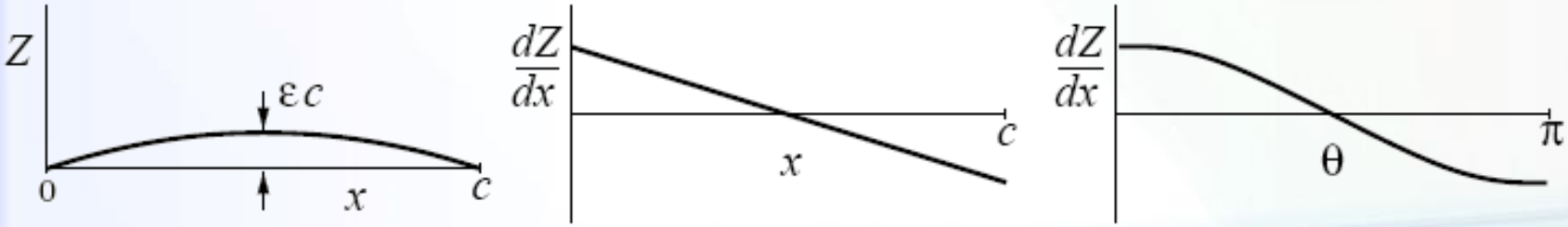

FOURIER COEFFICIENT CALCULATION

$$A_0 = \alpha - \frac{1}{\pi}\int_0^{\pi} \frac{dZ}{dx}\, d\theta = \alpha - \frac{1}{\pi}\int_0^{\pi} 4\varepsilon \cos\theta \, d\theta$$

$$A_n = \frac{2}{\pi}\int_0^{\pi} \frac{dZ}{dx} \cos n\theta \, d\theta = \frac{2}{\pi}\int_0^{\pi} 4\varepsilon \cos\theta \cos n\theta \, d\theta$$

The integral in the An expression can be evaluated by using the orthogonality property of the cosine functions.

$$\int_0^{\pi} \cos n\theta \cos m\theta \, d\theta = \begin{cases} \pi & (\text{if } n = m = 0) \\ \pi/2 & (\text{if } n = m \neq 0) \\ 0 & (\text{if } n \neq m) \end{cases}$$

$$\begin{aligned} A_0 &= \alpha \\ A_1 &= 4\varepsilon \\ A_2 &= 0 \\ A_3 &= 0 \\ &\vdots \end{aligned}$$

LIFT AND MOMENT COEFFICIENTS

$$c_\ell = \pi(2A_0 + A_1) = 2\pi(\alpha + 2\varepsilon) \Rightarrow \alpha_{L=0} = -2\varepsilon$$

$$c_{m,c/4} = \frac{\pi}{4}(A_2 - A_1) = -\pi\varepsilon$$

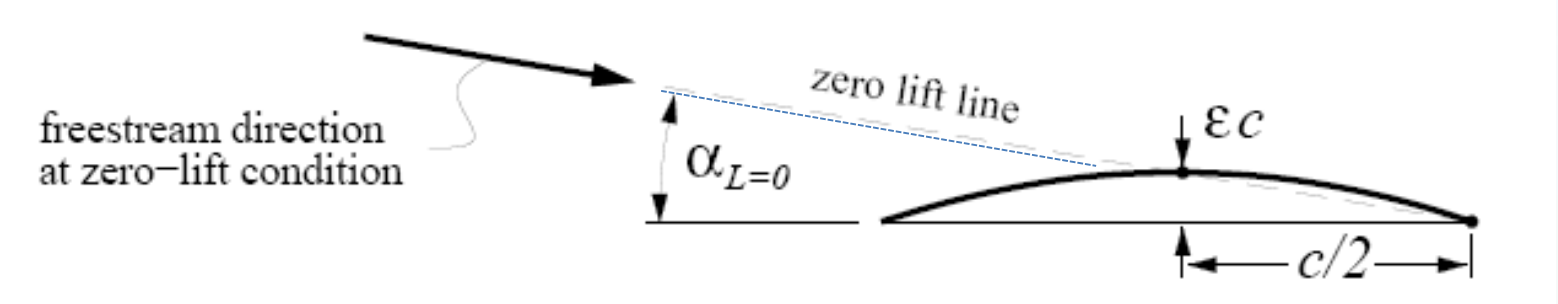

$$\alpha_{L=0} = \frac{1}{\pi}\int_0^\pi \frac{dZ}{dx}(1 - \cos\theta_o)\, d\theta_o = \frac{1}{\pi}\int_0^\pi 4\varepsilon \cos\theta_o (1 - \cos\theta_o)\, d\theta_o = -2\varepsilon$$

SURFACE LOADING (FURTHER DETAILS)

In many applications, obtaining just the cℓ and *cm* of the entire airfoil is sufficient. But in some cases, we may also want to know the force and moment on only a portion of the airfoil. For example, the force and moment on a flap are of considerable interest, since the flap hinge and flap control linkage must be designed to withstand these loads. We therefore need to know how the loading Δp(x) is distributed over the chord, and over the flap in particular.

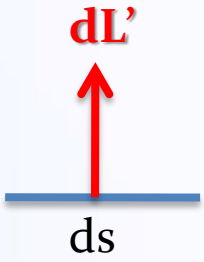

$dL' = \Delta p(x)\, ds = \rho V_\infty \gamma ds$

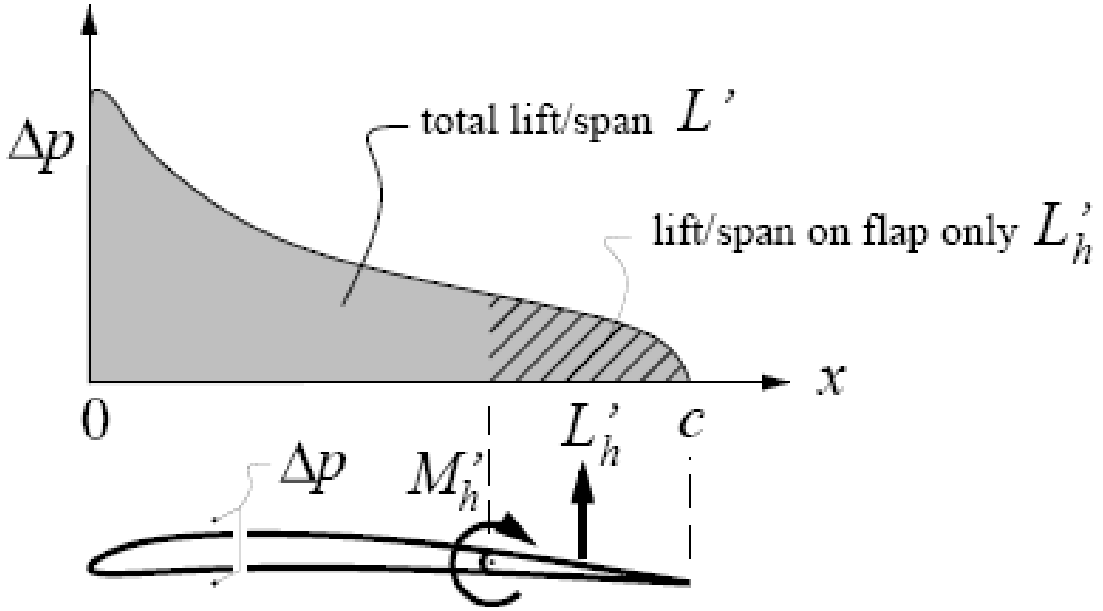

$$\Delta p(x) = \rho V_\infty \gamma(x) = \frac{1}{2}\rho V_\infty^2 \Delta C_p(x)$$

THIN AIRFOIL THEORY APPLICATION: ANALYSIS EXAMPLE

$$\gamma(\theta) = 2V_\infty \left(A_0 \frac{1+\cos\theta}{\sin\theta} + \sum_{n=1}^{N} A_n \sin n\theta \right)$$

$$\gamma(\theta) = 2V_\infty \left(\alpha \frac{1+\cos\theta}{\sin\theta} + 4\varepsilon \sin\theta \right)$$

$$\Delta C_p(\theta) = 2\frac{\gamma(\theta)}{V_\infty} = 4\alpha \frac{1+\cos\theta}{\sin\theta} + 16\varepsilon \sin\theta$$

$$\cos\theta = 1 - 2x/c \qquad \sin\theta = \sqrt{1-\cos^2\theta} = \sqrt{1-(1-2x/c)^2} = 2\sqrt{x/c-(x/c)^2}$$

$$\Delta C_p(x) = 4\alpha \sqrt{\frac{c}{x}-1} + 32\varepsilon \sqrt{\frac{x}{c}-\left(\frac{x}{c}\right)^2}$$

THIN AIRFOIL THEORY APPLICATION: ANALYSIS EXAMPLE

$$\Delta C_p(x) = 4\alpha\sqrt{\frac{c}{x}-1} + 32\varepsilon\sqrt{\frac{x}{c}-\left(\frac{x}{c}\right)^2}$$

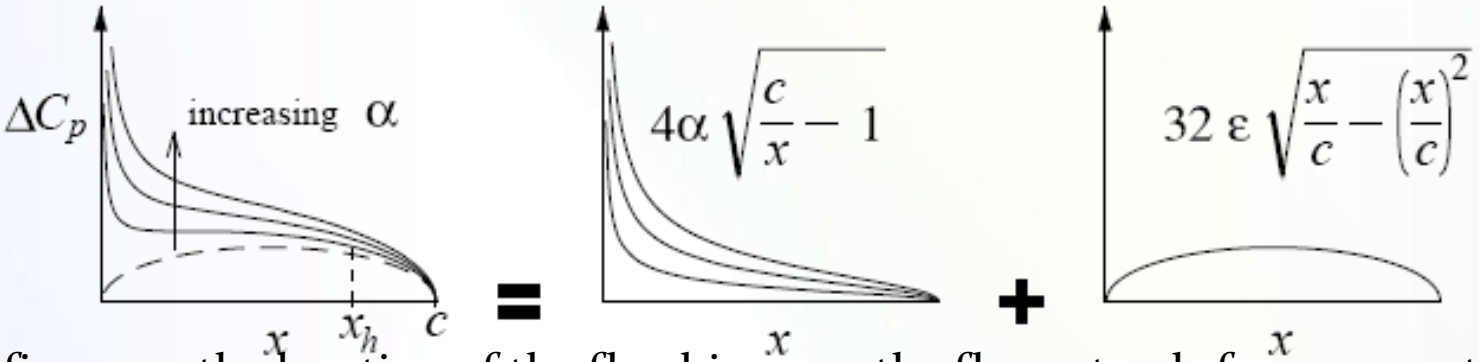

Define x_h as the location of the flap hinge, so the flap extends from $x = x_h$, to the trailing edge at $x = c$.

The corresponding θ locations $\theta = \arccos(1-2x_h/c) \equiv \theta_h$, and $\theta = \pi$ respectively. The load/span and moment/span coefficients on the flap hinge can now be computed by integrating the pressure loading.

$$c_{\ell_h} \equiv \frac{L'_h}{\frac{1}{2}\rho V_\infty^2 c} = \frac{1}{c}\int_{x_h}^{c} \Delta C_p(x)\,dx = \frac{1}{2}\int_{\theta_h}^{\pi} \Delta C_p(\theta)\,\sin\theta\,d\theta$$

$$c_{m_h} \equiv \frac{M'_h}{\frac{1}{2}\rho V_\infty^2 c^2} = \frac{1}{c^2}\int_{x_h}^{c} \Delta C_p(x)\,(x_h - x)\,dx = \frac{1}{4}\int_{\theta_h}^{\pi} \Delta C_p(\theta)\,(\cos\theta - \cos\theta_h)\,\sin\theta\,d\theta$$

INTRODUCTION TO CONFORMAL MAPPING IN AERODYNAMICS

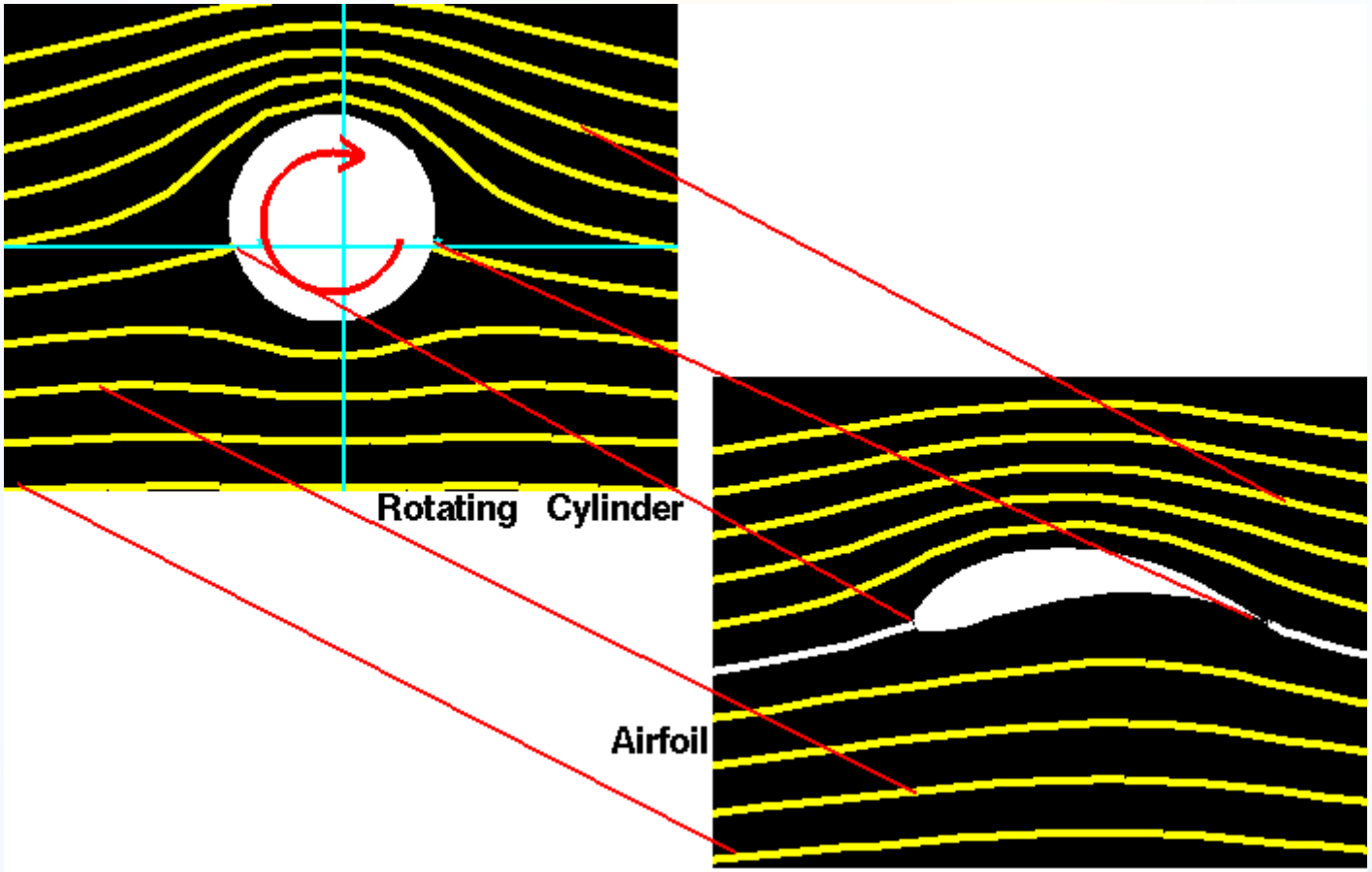

- We have shown that in a two-dimensional, incompressible, irrotational flow, both velocity potential (ϕ) and stream function (ψ), satisfy Laplace's equation.

$$\nabla^2\phi = 0 \qquad\qquad \nabla^2\psi = 0$$

- This fact gives rise to a particularly powerful method of analysing such flows, based on the properties of functions of a **Complex Variable**.

INTRODUCTION TO CONFORMAL MAPPING IN AERODYNAMICS

A complex number can be written in polar form using Euler's equation:

$$z = x + iy = re^{i\theta} = r(\cos\theta + i\ \sin\theta)$$

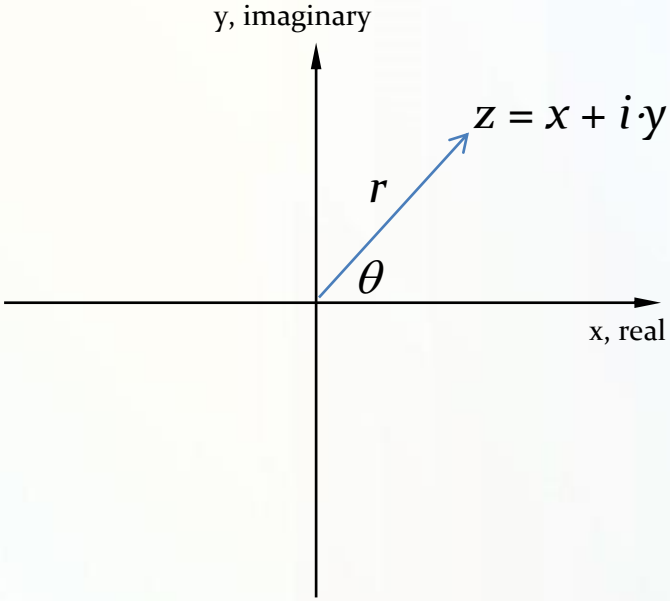

Where: $i^2 = -1$

$$r = |z| = \sqrt{x^2 + y^2} = \sqrt{z\bar{z}}$$

$$\theta = \arg z = \tan^{-1}\frac{y}{x}$$

Complex multiplication:

$$z_1 z_2 = (x_1 + iy_1)(x_2 + iy_2) = (x_1 x_2 - y_1 y_2) + i\,(x_1 y_2 + y_1 x_2)$$
$$= r_1 e^{i\theta_1} + r_2 e^{i\theta_2} = r_1 r_2 e^{i(\theta_1 + \theta_2)}$$

- Consider the function *f(z)* of the complex variable:

$$z=x+iy$$

- *f(x+iy)* has real and imaginary parts given by:

$$f\ (x\ +iy\ )=\alpha(x\ ,y\ )+i\ \beta(x\ ,y\ )$$

Where α (real part) and β (imaginary part) are called *conjugate functions*.

- Partial differentiation of f with respect to x and y yields:

$$\frac{\partial f}{\partial x} = \frac{\partial \alpha}{\partial x} + i\frac{\partial \beta}{\partial x} = \frac{df}{dz}\frac{\partial z}{\partial x} = \frac{df}{dz}$$

$$\frac{\partial f}{\partial y} = \frac{\partial \alpha}{\partial y} + i\frac{\partial \beta}{\partial y} = \frac{df}{dz}\frac{\partial z}{\partial y} = i\frac{df}{dz}$$

- Hence:

$$i\frac{df}{dz} = i\frac{\partial \alpha}{\partial x} - \frac{\partial \beta}{\partial x} = \frac{\partial \alpha}{\partial y} + i\frac{\partial \beta}{\partial y}$$

- Thus

$$\frac{\partial \alpha}{\partial x} = \frac{\partial \beta}{\partial y} \quad \text{and} \quad \frac{\partial \alpha}{\partial y} = -\frac{\partial \beta}{\partial x}$$

Cauchy-Riemann Equations

$$\frac{\partial \alpha}{\partial x} = \frac{\partial \beta}{\partial y} \quad \text{and} \quad \frac{\partial \alpha}{\partial y} = -\frac{\partial \beta}{\partial x}$$

- Partial differentiation of Cauchy-Riemann equations with respect to x and y gives:

$$\frac{\partial^2 \alpha}{\partial x \partial y} = \frac{\partial^2 \beta}{\partial y^2} = -\frac{\partial^2 \beta}{\partial x^2} \qquad \frac{\partial^2 \beta}{\partial x \partial y} = \frac{\partial^2 \alpha}{\partial x^2} = -\frac{\partial^2 \alpha}{\partial y^2}$$

$$\frac{\partial^2 \alpha}{\partial x^2} + \frac{\partial^2 \alpha}{\partial y^2} = 0 \qquad \frac{\partial^2 \beta}{\partial y^2} + \frac{\partial^2 \beta}{\partial x^2} = 0$$

α and β both satisfy Laplace's Equation

- We can substitude $\alpha=\phi$, $\beta=\psi$ and we can replace $f(z)$ by w:

$$w = \phi + i\psi$$

- w is known as the *complex potential* of the motion and is a function of the single complex variable z.

- Both components of the velocity can be obtained directly by differentiation of the complex potential w:

$$dw = \frac{\partial w}{\partial x}dx \; \frac{\partial w}{\partial y}dy = (u - iv)dx + (v + iu)dy = (u - iv)(dx + idy)$$

$$\Rightarrow \quad \frac{dw}{dz} = (u - iv)$$

COMPLEX ANALYSIS – ELEMENTARY PLANE FLOWS

- The basic flows used in potential flow theory such as *uniform flow*, *source*, *sink*, *doublet* and *vortex*, can all be represented using complex numbers.

- Uniform flow

$$w = Uze^{-i\alpha} = z\,(U\cos\alpha - iU\sin\alpha)$$

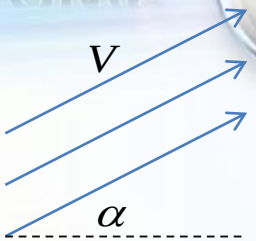

- Source flow

$$w = \frac{m}{2\pi}\ln z = \frac{m}{2\pi}\ln(re^{i\theta}) = \frac{m}{2\pi}\ln r - i\,\frac{m}{2\pi}\theta$$

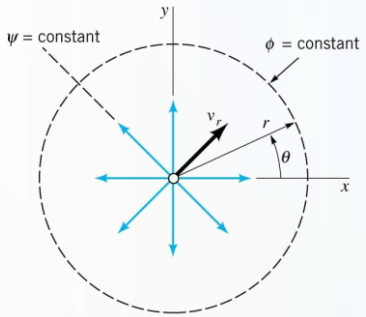

- Vortex

$$w = i\,\frac{\Gamma}{2\pi}\ln z = -\frac{\Gamma}{2\pi}\theta + i\,\frac{\Gamma}{2\pi}\ln r$$

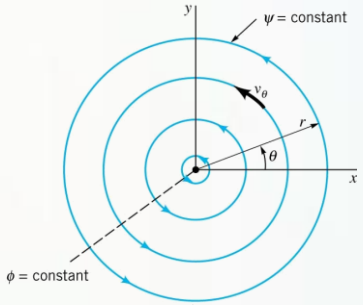

- Doublet

$$w = \frac{K}{z} = \frac{K}{x+iy} = \frac{K}{x^2+y^2}(x - iy)$$

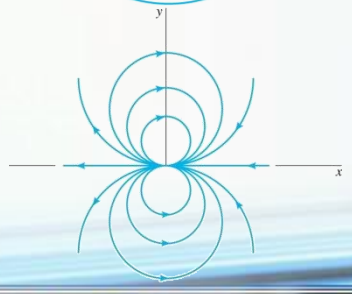

CONFORMAL MAPPING

- In the study of airfoils, we are interested in finding the flow pattern and pressure distribution.

  - **Direct** solution of the Laplace equation for the prescribed boundary shape of the airfoil is quite straightforward using a computer, but analytically difficult. In general, analytical solutions are possible only when the airfoil is assumed thin *(thin airfoil theory)*.

CONFORMAL MAPPING

- In the study of airfoils, we are interested in finding the flow pattern and pressure distribution.

- An **Indirect** way of solving the problem involves the method of conformal transformation. Many years ago, the Russian mathematician Joukowski developed a mapping function that converts a circular cylinder into a family of airfoil shapes.

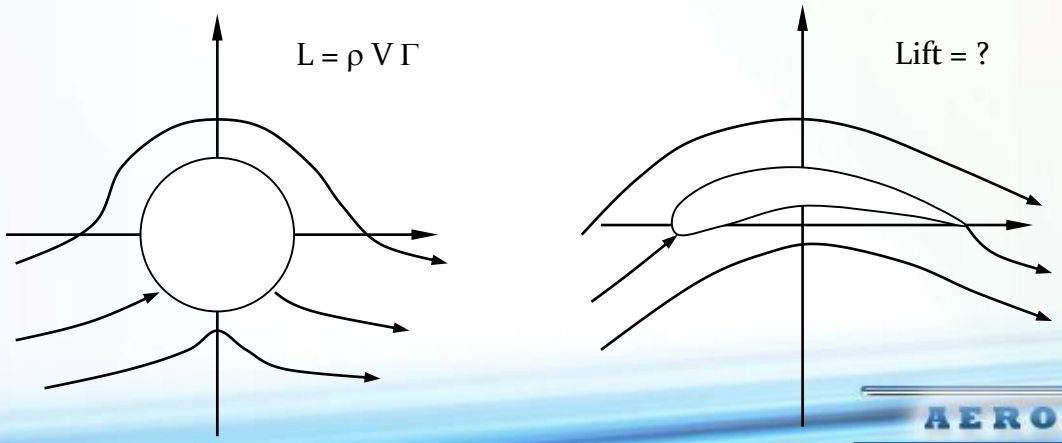

CONFORMAL MAPPING

- Conformal mapping is a mathematical technique used to convert (or map) one mathematical problem and solution into another. It involves the study of complex variables.

- A conformal mapping is performed through the transformation of a complex function from one coordinate system to another. A transformation function is applied to the original function to perform the mapping.

INTRODUCTION TO CONFORMAL MAPPING IN AERODYNAMICS

- We deal with a case in which a given transformation maps a *circle* into an *airfoil-like* shape and determine the properties of the airfoil generated thereby.

- This is the *Joukowski transformation* and is the most commonly used function for aerodynamic applications.

$$w = z + \frac{b^2}{z}$$

Here, b is a constant

INTRODUCTION TO CONFORMAL MAPPING IN AERODYNAMICS

$$w = z + \frac{b^2}{z}$$

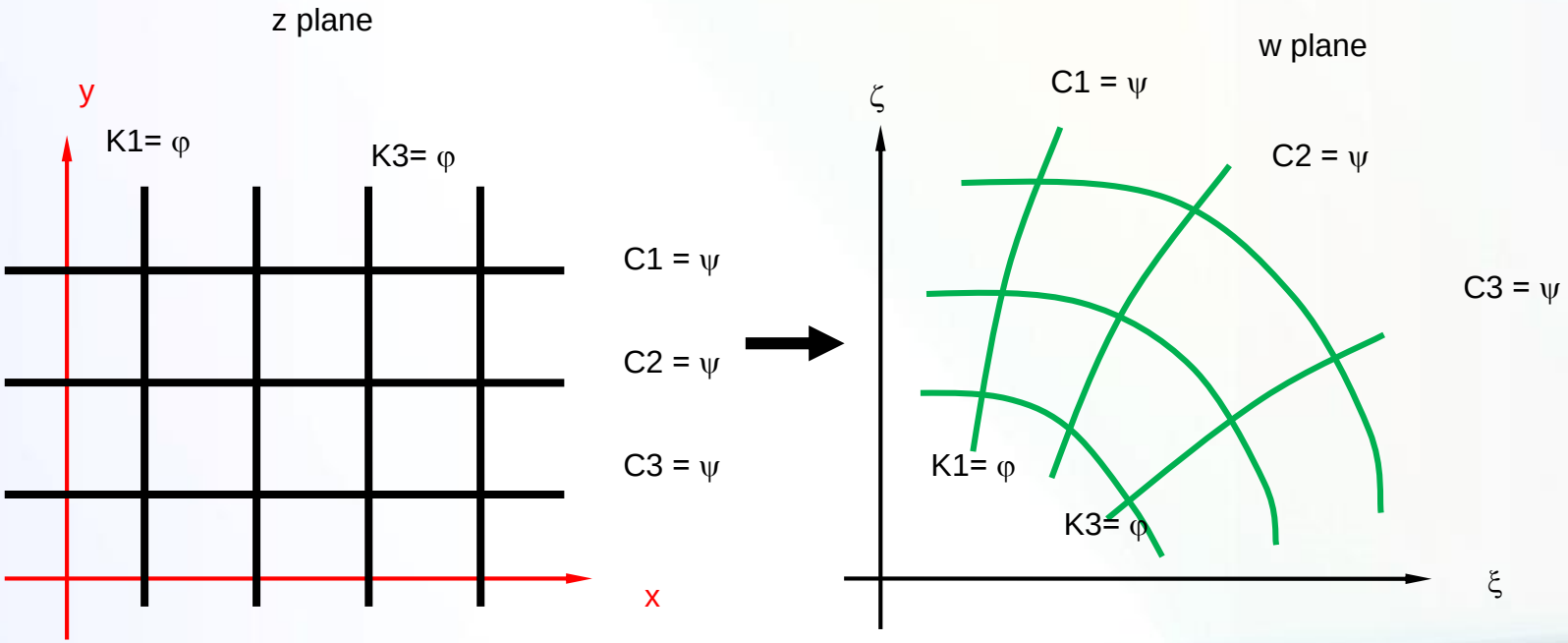

TRANSFORMATION OF A CIRCLE INTO A STRAIGHT LINE

Consider a circle, centered at the origin in the z-plane, whose radius b is same as the constant in the Joukowski transformation.

$$z = be^{i\theta}$$

$$w = z + \frac{b^2}{z} \quad \Rightarrow \quad w = be^{i\theta} + \frac{b^2}{be^{i\theta}} = be^{i\theta} + be^{-i\theta} = 2b\cos(\theta) + i0$$

The Joukowski transform maps the circle of radius b in z-plane, into a flat plate of length $4b$ in the w-plane.

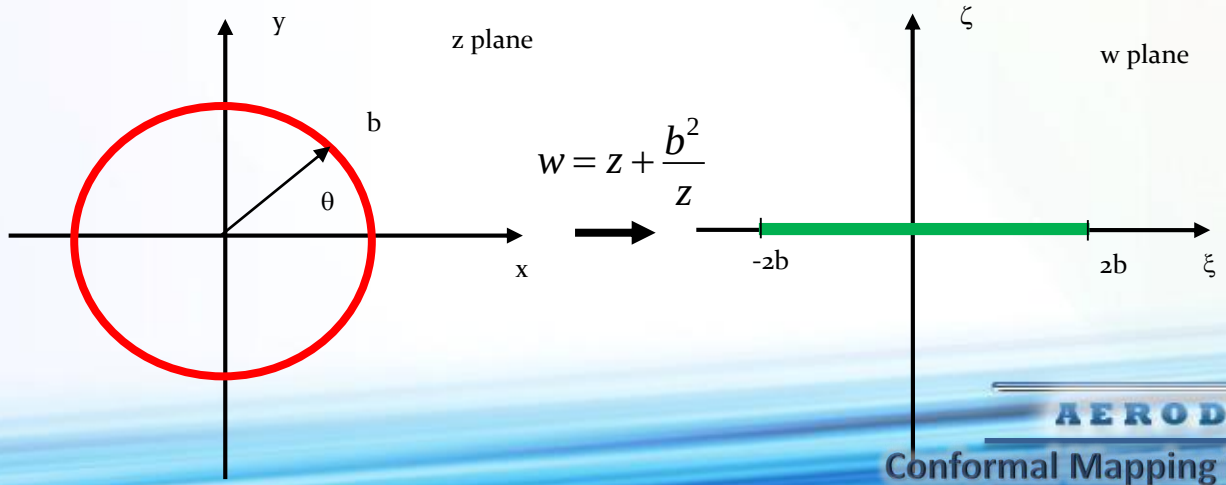

TRANSFORMATION OF A CIRCLE INTO AN ELLIPSE

If the circle originally had a radius slightly larger than the transform constant b:

$$z = ae^{i\theta}, \text{ with } a > b,$$

$$w = z + \frac{b^2}{z} = ae^{i\theta} + \frac{b^2}{ae^{i\theta}} = \left(a + \frac{b^2}{a}\right)\cos(\theta) + i\left(a - \frac{b^2}{a}\right)\sin(\theta) = \eta + i\zeta$$

$$\frac{\eta^2}{\left(a + \frac{b^2}{a}\right)^2} + \frac{\zeta^2}{\left(a - \frac{b^2}{a}\right)^2} = 1$$

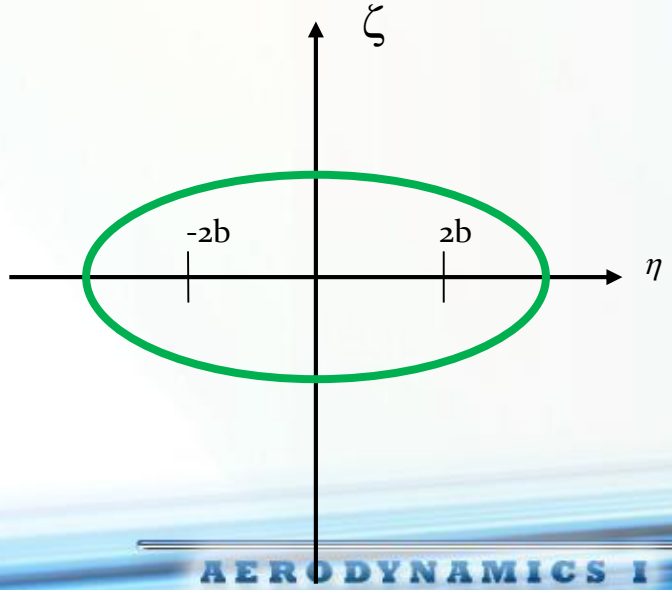

the circle would have formed an ellipse instead of the flat plate.

TRANSFORMATION OF A CIRCLE INTO A SYMMETRIC AIRFOIL

From and aerodynamics point of view, the most interesting application of the Joukowski transform is to an offset circle. If we consider a circle slightly offset from the origin along the negative real axis, one obtains a symmetric Joukowski airfoil.

The equation of the offset circle is: $z = ae^{i\theta} - eb$, where the constant e is a small number.

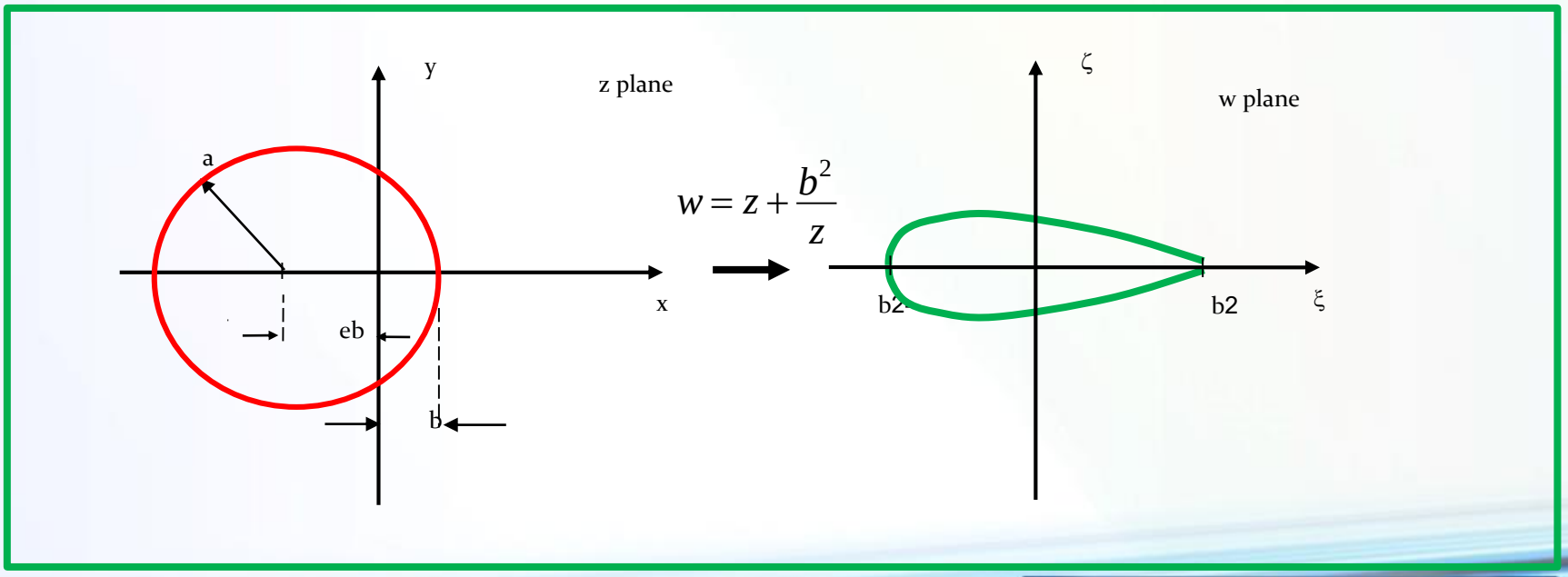

TRANSFORMATION OF A CIRCLE INTO A CAMBERED AIRFOIL

If the circle is displaced slightly along the complex axis as well, one obtains a cambered airfoil shape.

Here, the points *A* and *B* are the intercepts of the displaced circle on the real axis and their corresponding points in the transformed plane. The angle β is the angle formed by the line joining the point *A* (or *B)* and the origin with the real axis.

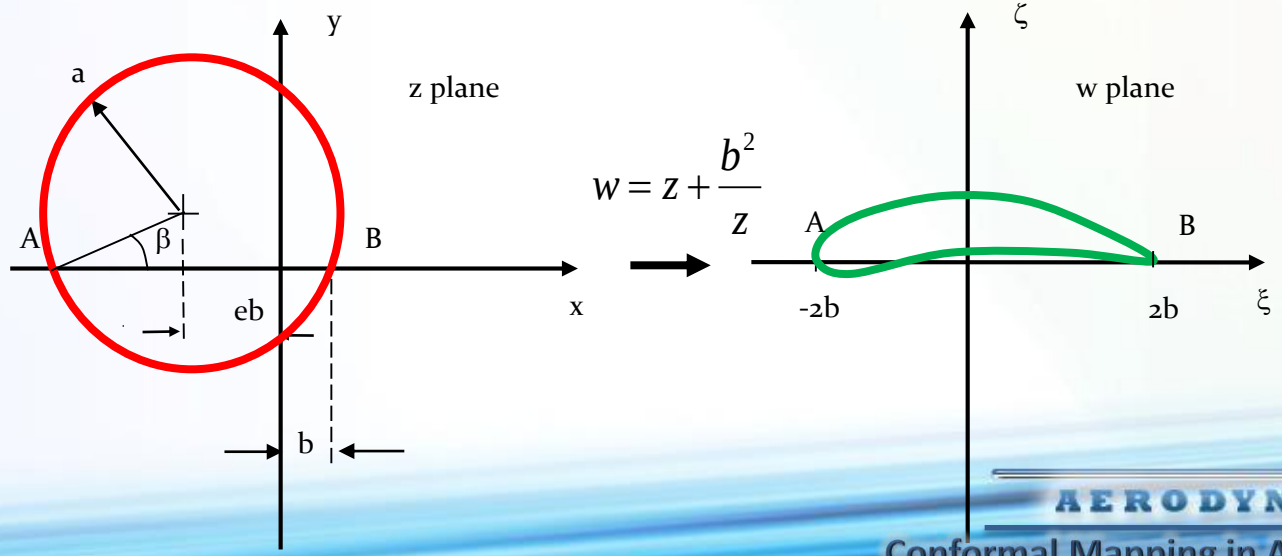

TRANSFORMATION OF A CIRCLE INTO A CAMBERED AIRFOIL

If lifting flow about the original circle had been imposed, the Joukowski transformation would have generated a lifting flow about the Joukowski airfoil;

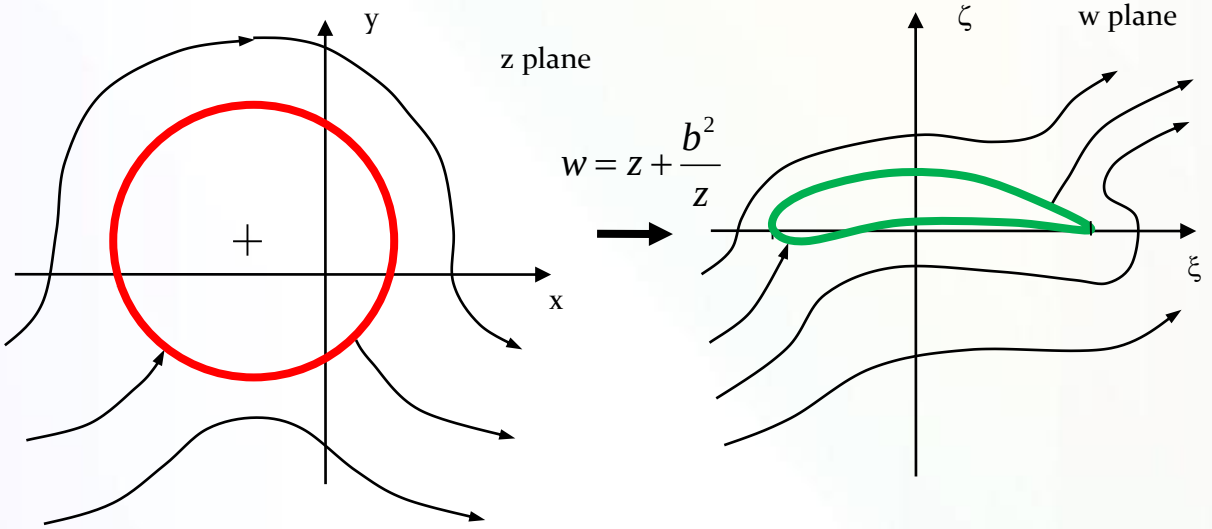

Although such a flow is mathematically possible, in reality it may not be realistic. The stagnation points on the cylinder map to stagnation points that are not always realistic.

TRANSFORMATION OF A CIRCLE INTO A CAMBERED AIRFOIL

The only means of making a realistic flow is to impose the **Kutta condition** where the stagnation point is forced to exist at the trailing edge thus making the streamlines flow smoothly from this point.

This is done by *adjusting the value of vorticity strength* Γ, such that the stagnation points on the cylinder reside at the cylinder's intercepts of the real axis. In this case, when the cylinder is transformed, one stagnation point will be forced to the trailing edge.

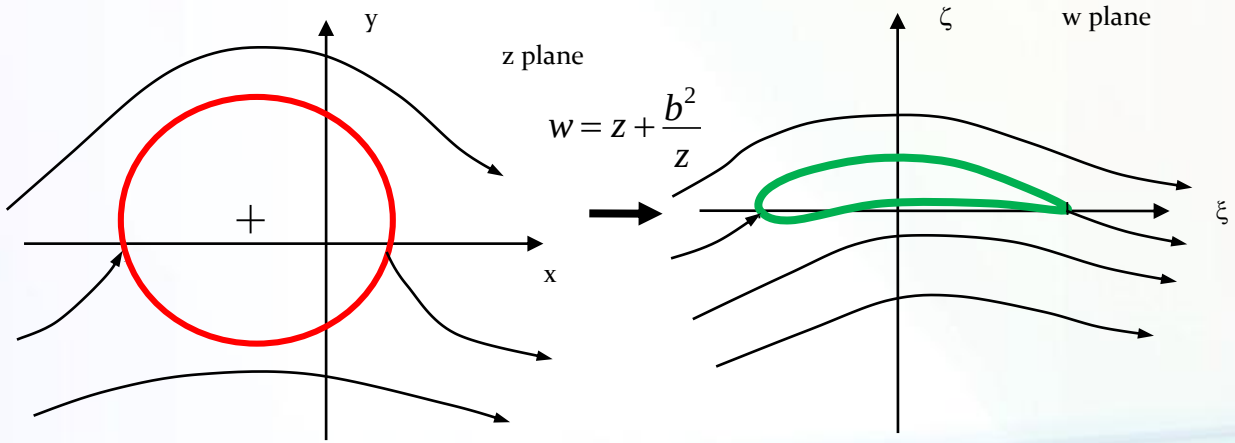

TRANSFORMATION OF A CIRCLE INTO A CAMBERED AIRFOIL

The lift force generated by the lifting flow over the cylinder is proportional to the circulation about the cylinder imposed by the added vortex flow according to the Kutta-Joukowski relation, $L' = \rho V_\infty \Gamma$.

The lifting force on the resulting Joukowski airfoil is not clear.

If the lifting flow about the cylinder is defined as function Q where $Q = Q(z)$ in the z plane and $Q = Q(w)$ in the w plane, the velocities in each plane are:

$$V_z = \frac{\partial Q}{\partial z} \qquad V_w = \frac{\partial Q}{\partial w}$$

TRANSFORMATION OF A CIRCLE INTO A CAMBERED AIRFOIL

$$\frac{\partial Q}{\partial z} = \frac{\partial Q}{\partial w}\frac{\partial w}{\partial z} \quad \Longrightarrow \quad V_z = V_w \frac{\partial w}{\partial z} \qquad \frac{\partial w}{\partial z} = \frac{z^2 - b^2}{z^2}$$

Clearly, the velocity field very close to the cylinder and its transformed counterpart are dissimilar as one would expect.
Farther away from these objects the velocity fields become identical as the magnitude of z becomes larger than the constant value of b.

Since the circulation can be calculated about any closed path, including paths very far from the object surface, the circulations must be the same in both planes.

$$\rho V_\infty \Gamma_{cylinder} = \rho V_\infty \Gamma_{Joukowski}$$

TRANSFORMATION OF A CIRCLE INTO A CAMBERED AIRFOIL – VORTEX STRENGTH

The appropriate vortex strength to impose the Kutta condition must be determined.

Consider the lifting flow about a cylinder. The velocity in the θ direction is

$$V_\theta = -\left(2V_\infty \sin(\theta) + \frac{\Gamma}{2\pi R}\right)$$

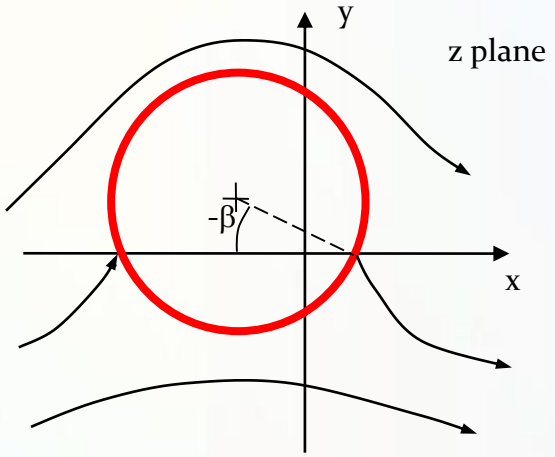

stagnation points:

$$0 = 2V_\infty \sin(\beta) - \frac{\Gamma}{2\pi R}$$

$$\Gamma = 4\pi V_\infty R \sin(\beta)$$

If the field is rotated by α to simulate an angle of attack,

$$\Gamma = 4\pi V_\infty R \sin(\beta + \alpha)$$

TRANSFORMATION OF A CIRCLE INTO A CAMBERED AIRFOIL

Since the chord length of the Joukowski airfoil is $4b$

$$C_L = \frac{L'}{\frac{1}{2}\rho V_\infty^2 c} = \frac{\rho V \Gamma}{\frac{1}{2}\rho V_\infty^2 4b} = \frac{\Gamma}{2V_\infty^2 b} = \frac{4\pi V_\infty^2 R \sin(\alpha+\beta)}{2V_\infty^2 b}$$

Making the assumption that $b \approx R$,

$$C_L = 2\pi \sin(\alpha+\beta) \approx 2\pi(\alpha+\beta)$$

EXAMPLE

A Joukowski airfoil is formed by displacing a circle of radius 1 by Δx = -0.08 (real axis) and Δy = 0.05 (imaginary axis).

Find:

a) Vortex strength Γ if $\alpha = 0^o$, *and* $V_\infty = 10\ m/s$

b) C_L at $\alpha = 0^o$ and $\alpha = 10^o$

$$\beta = \sin^{-1}\left(\frac{0.05}{1}\right) = 2.87^\circ$$

$$\tan(2.87^O) = \frac{0.05}{0.08 + b}$$

$$b = 0.9187$$

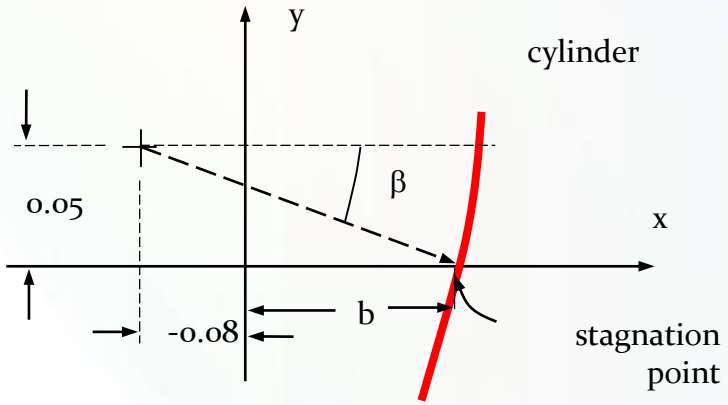

EXAMPLE

A Joukowski airfoil is formed by displacing a circle of radius 1 by Δx = -0.08 (real axis) and Δy = 0.05 (imaginary axis).

Find:

a) Vortex strength Γ if $\alpha = 0^o$, *and* $V_\infty = 10\ m/s$

b) C_L at $\alpha = 0^o$ and $\alpha = 10^o$

$$\Gamma = 4\pi V_\infty R\sin(\alpha+\beta) = 4\pi(10)(1)\sin(2.87) = 6.2831$$

$$\alpha = 0^o: \quad C_L = 2\pi\sin(2.87) = 0.31415$$

$$\alpha = 10^o: \quad C_L = 2\pi\sin(10 + 2.87) = 1.40$$

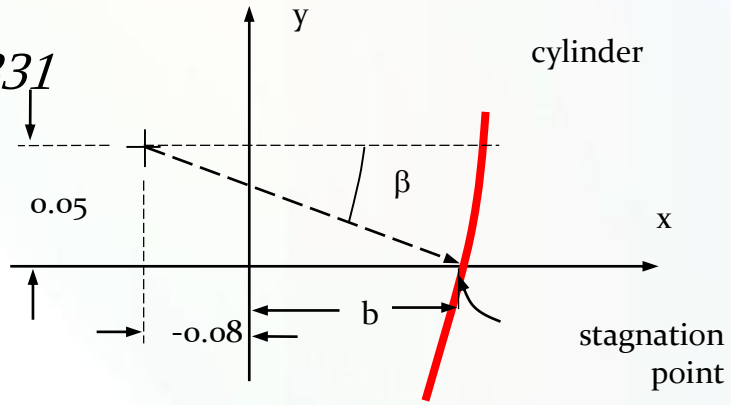

LIFTING FLOWS OVER ARBITRARY BODIES: THE VORTEX PANEL NUMERICAL METHOD

The thin airfoil theory applies only to thin airfoils at small angles of attack.

The advantage of thin airfoil theory is that closed-form expressions are obtained for the aerodynamic coefficients. Moreover, the results compare favorably with experimental data for airfoils of about 12 percent thickness or less.

We need a method that allows us to calculate the aerodynamic characteristics of bodies of arbitrary shape, thickness, and orientation.

REVIEW OF PANEL METHOD BASIC IDEAS

1. Approximate the surface of a given body by a series of panels.
2. Place distributions of singularities (such as sources, vortices or doublets) on each panel.
3. The problem is to find the values of the unknown strengths of the singularities for the given geometry. Find the unknown strengths by solving a linear set of algebraic equations.

With the aid of panel methods, the requirement to find the solution over the entire flowfield (a 3D problem) is replaced with the problem of finding the solution for the singularity distribution over a surface (a 2D problem).

REVIEW OF PANEL METHOD BASIC IDEAS

Possible differences in panel methods are in:

1. Using various types of singularities (sources, doublets and vortices or any combination of them)
2. Using various distributions of singularity strength over each panel (zero-, first-, second-order, etc.).
3. Using various panel geometries.

VORTEX PANEL METHOD

We treat the vortex panel method, which is a numerical technique that has come into widespread use since the early 1970s.

The vortex panel method is directly analogous to the source panel method. However, because a source has zero circulation, source panels are useful only for nonlifting cases. In contrast, vortices have circulation, and hence vortex panels can be used for lifting cases.

The philosophy of covering a body surface with a vortex sheet of such a strength to make the surface a streamline of the flow was discussed

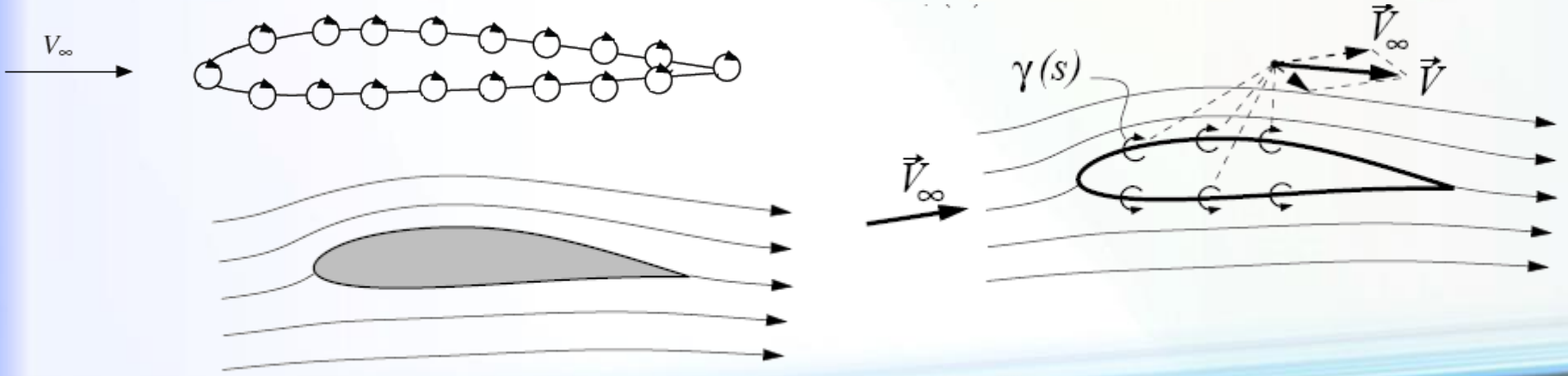

VORTEX PANEL METHOD

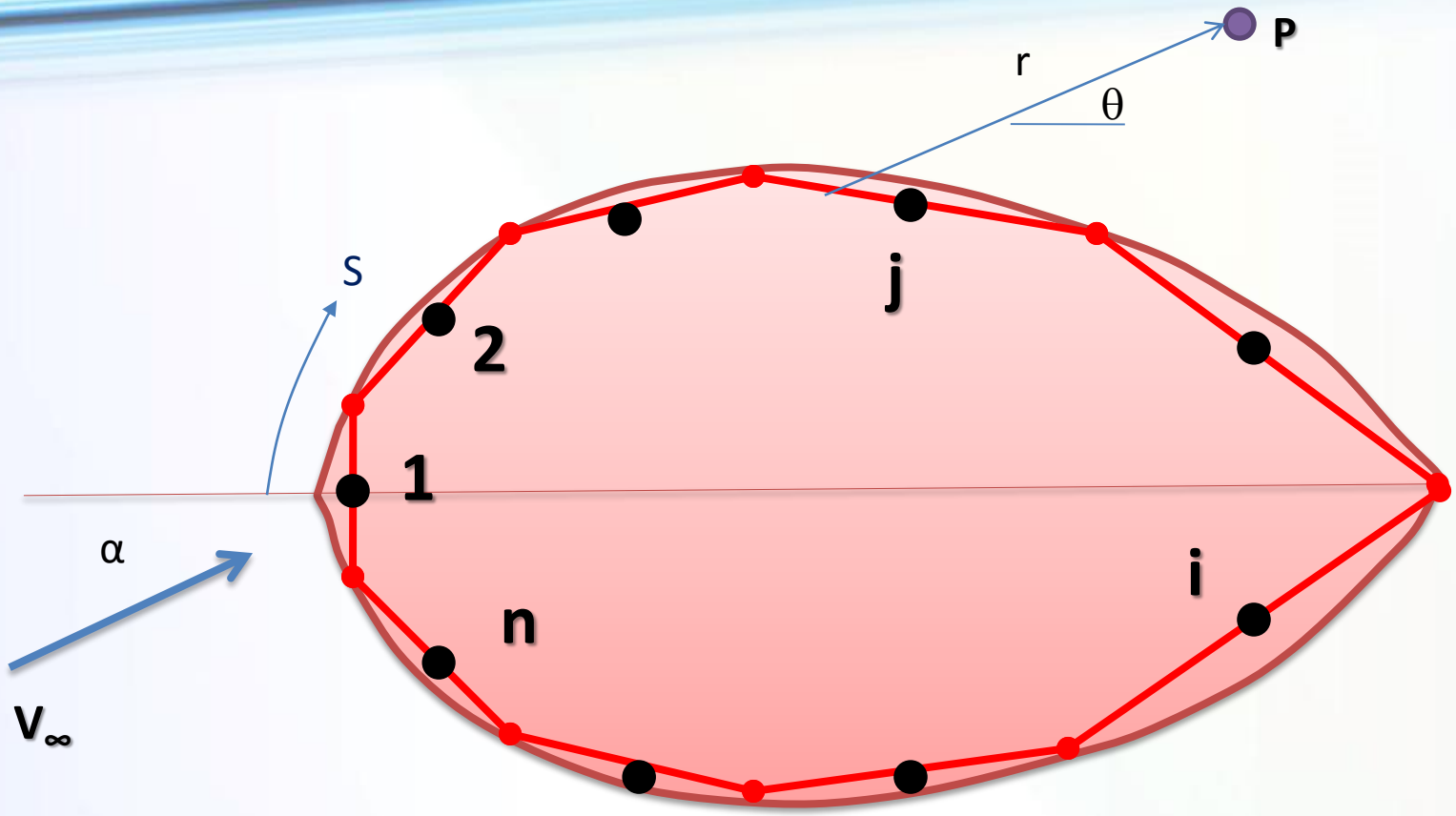

VORTEX PANEL METHOD

$$\phi(x,y) = -\int_0^{\ell} \frac{\gamma}{2\pi}\,\theta\,ds$$

$$\Delta\phi_j = -\frac{1}{2\pi}\int_j \theta_{pj}\gamma_j\,ds_j$$

$$\theta_{pj} = \tan^{-1}\frac{y-y_j}{x-x_j}$$

$$\phi(P) = \sum_{j=1}^{n}\phi_j = -\sum_{j=1}^{n}\frac{\gamma_j}{2\pi}\int_j \theta_{pj}\,ds_j$$

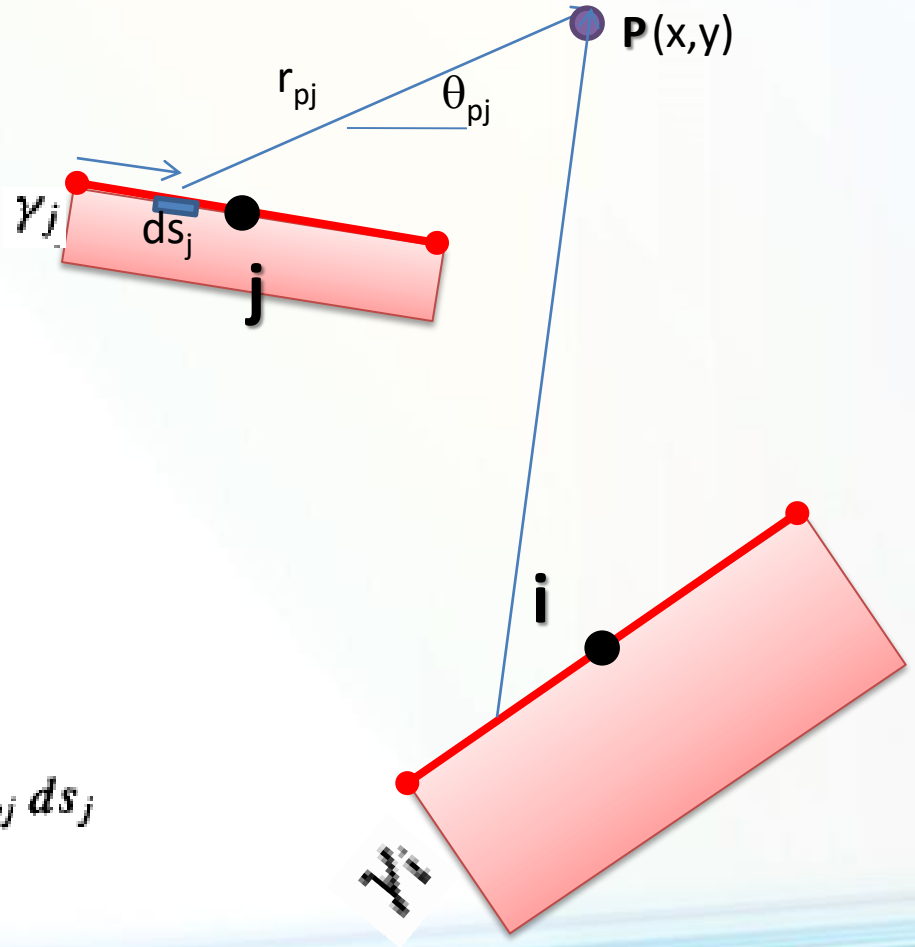

VORTEX PANEL METHOD

$$\theta_{ij} = \tan^{-1} \frac{y_i - y_j}{x_i - x_j}$$

$$\phi(x_i, y_i) = -\sum_{j=1}^{n} \frac{\gamma_j}{2\pi} \int_j \theta_{ij}\, ds_j$$

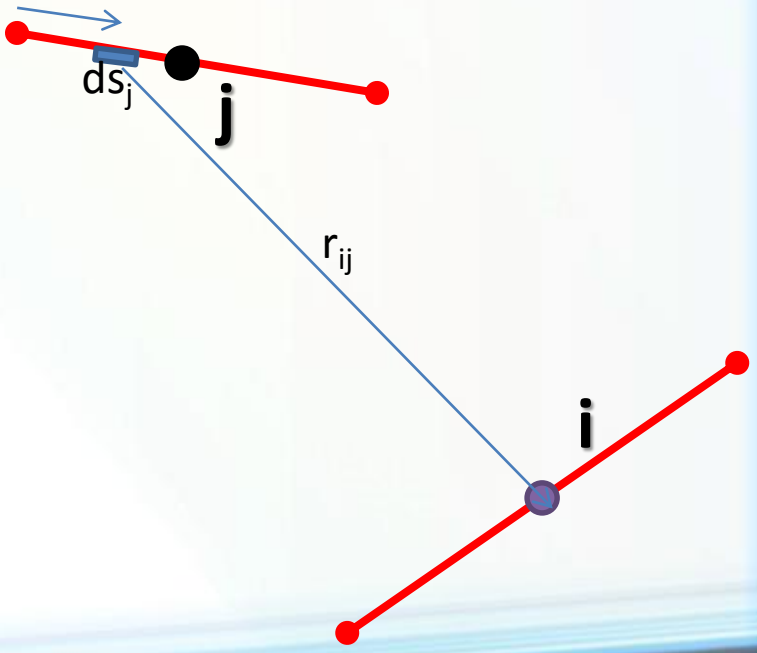

VORTEX PANEL METHOD

$$V_{\infty,n} + V_n = 0$$

$$V_n = \frac{\partial}{\partial n_i}[\phi(x_i, y_i)]$$

$$V_{\infty,n} = \mathbf{V}_\infty \cdot \mathbf{n}_i = V_\infty \cos(\beta_i - \alpha)$$

$$V_n = -\sum_{j=1}^{n} \frac{\gamma_j}{2\pi} \int_j \frac{\partial \theta_{ij}}{\partial n_i} ds_j$$

$$V_\infty \cos(\beta_i - \alpha) - \sum_{j=1}^{n} \frac{\gamma_j}{2\pi} \int_j \frac{\partial \theta_{ij}}{\partial n_i} ds_j = 0$$

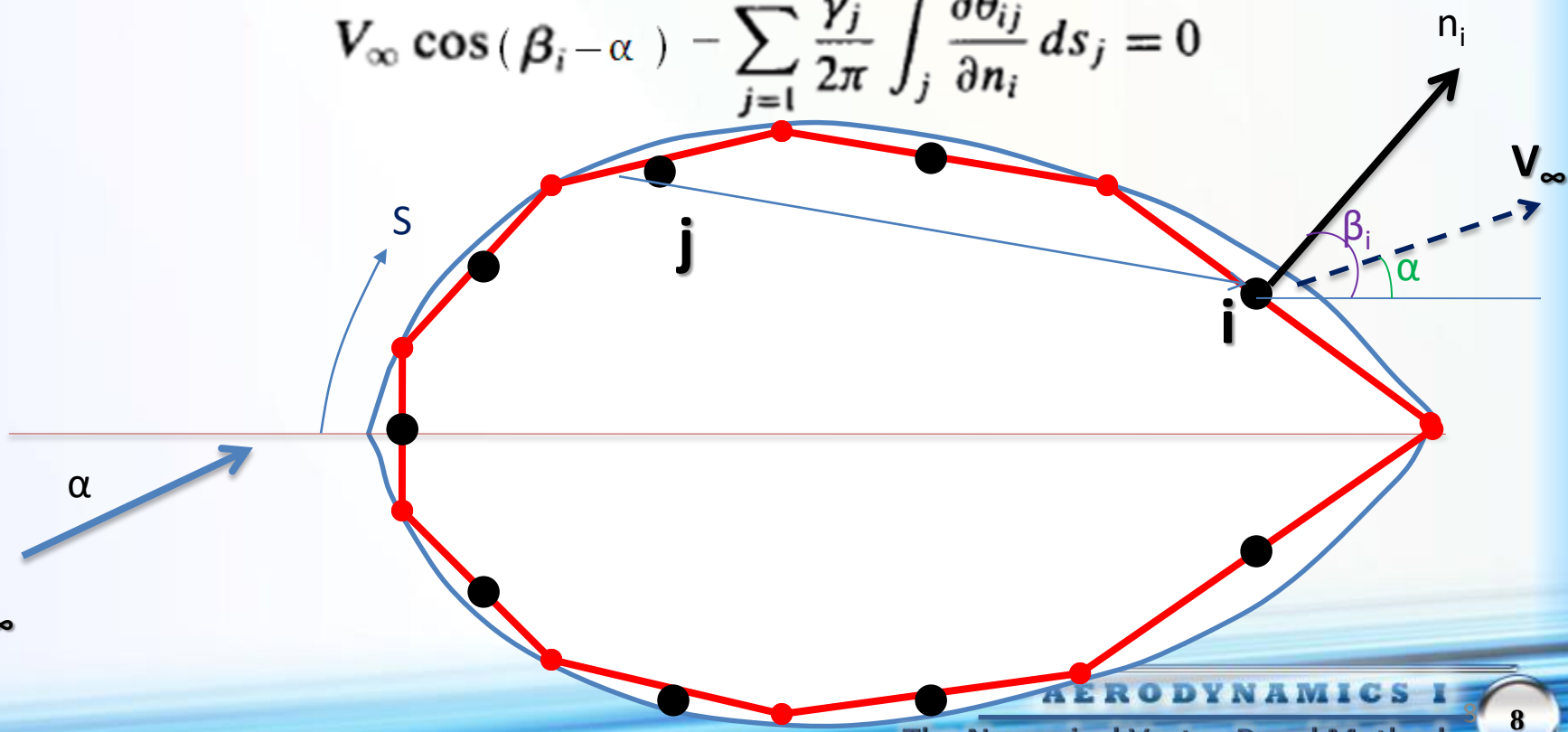

VORTEX PANEL METHOD

$$V_\infty \cos(\beta_i - \alpha) - \sum_{j=1}^{n} \frac{\gamma_j}{2\pi} \int_j \frac{\partial \theta_{ij}}{\partial n_i} ds_j = 0$$

$$V_\infty \cos(\beta_i - \alpha) - \sum_{j=1}^{n} \frac{\gamma_j}{2\pi} J_{i,j} = 0$$

The above equation is a linear algebraic equation with *n unknowns*, γ_1 , γ_2, ..., γ_n It represents the flow boundary condition evaluated at the control point of the *ith* panel.

If the equation is applied to the control points of *all the panels, we* obtain a system of *n linear equations with n unknowns.*

To this point, we have been deliberately paralleling the discussion of the source panel method; however, the similarity stops here.

VORTEX PANEL METHOD

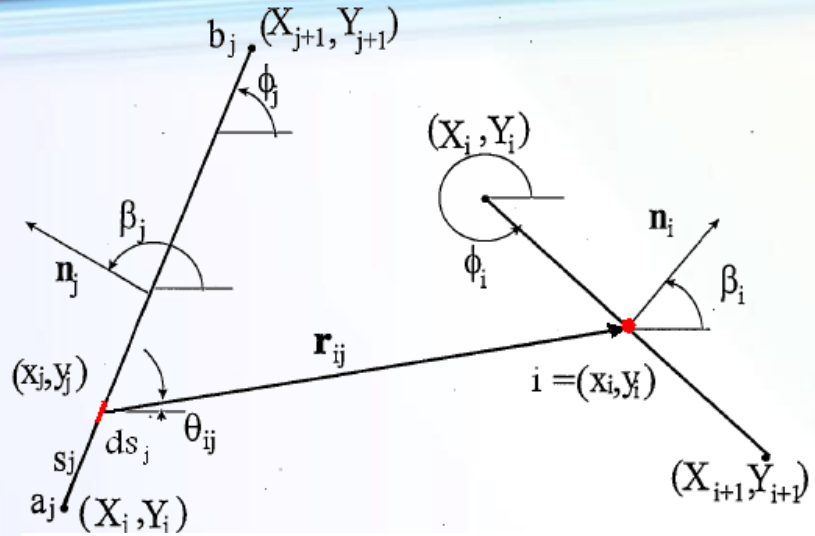

$$\beta_i = \phi_i + \frac{\pi}{2} - 2\pi \Rightarrow \begin{aligned} \cos\beta_i &= \sin\phi_i \\ \sin\beta_i &= \cos\phi_i \end{aligned}$$

$$x_i = \frac{X_i + X_{i+1}}{2}$$

$$\frac{\partial x_i}{\partial n_i} = \cos\beta_i \qquad y_i = \frac{Y_i + Y_{i+1}}{2}$$

$$\frac{\partial y_i}{\partial n_i} = \sin\beta_i \qquad \begin{aligned} x_j &= X_j + s_j\cos\phi_j \\ y_j &= Y_j + s_j\sin\phi_j \end{aligned}$$

$$V_\infty \cos(\beta_i - \alpha) - \sum_{j=1}^{n} \frac{\gamma_j}{2\pi} \int_j \frac{\partial \theta_{ij}}{\partial n_i} ds_j = 0$$

$$\beta_i = \phi_i + \frac{\pi}{2} - 2\pi$$

$$V_\infty \sin(\alpha - \phi_i) - \sum_{j=1}^{n} \frac{\gamma_j}{2\pi} \int_j \frac{\partial \theta_{ij}}{\partial n_i} ds_j = 0$$

$$r_{ij} = \sqrt{(x_i - x_j)^2 + (y_i - y_j)^2}$$

$$\theta_{ij} = \arctan\frac{y_i - y_j}{x_i - x_j}$$

$$S_j = \sqrt{(X_{j+1} - X_j)^2 + (Y_{j+1} - Y_j)^2}$$

VORTEX PANEL METHOD

$$V_\infty \sin(\alpha - \phi_i) = \frac{1}{2\pi} \sum_{j=1}^{M} \gamma_j \int_0^{S_j} \frac{1}{1 + \left(\frac{y_i - y_j}{x_i - x_j}\right)^2} \frac{\frac{\partial y_i}{\partial n_i}(x_i - x_j) - \frac{\partial x_i}{\partial n_i}(y_i - y_j)}{(x_i - x_j)^2} \mathrm{d}s_j$$

Replace the derivatives with their values:

$$\sin(\alpha - \phi_i) = \frac{1}{2\pi V_\infty} \sum_{j=1}^{M} \int_0^{S_j} \gamma_j \frac{\cos\phi_i(x_i - x_j) + \sin\phi_i(y_i - y_j)}{(x_i - x_j)^2 + (y_i - y_j)^2} \mathrm{d}s_j$$

$$\sin(\alpha - \phi_i) = \frac{1}{2\pi V_\infty} \sum_{j=1}^{M} \left[\gamma_j \int_0^{S_j} \frac{\cos\phi_i(x_i - X_j - s_j\cos\phi_j) + \sin\phi_i(y_i - Y_j - s_j\sin\phi_j)}{(x_i - X_j - s_j\cos\phi_j)^2 + (y_i - Y_j - s_j\sin\phi_j)^2} \mathrm{d}s_j \right.$$

KUTTA CONDITION

For the source panel method, the *n equations for the n unknown source strengths* are routinely solved, giving the flow over a nonlifting body. In contrast, for the lifting case with vortex panels, in addition to the *n* equations applied at all the panels, we must also satisfy the Kutta condition.

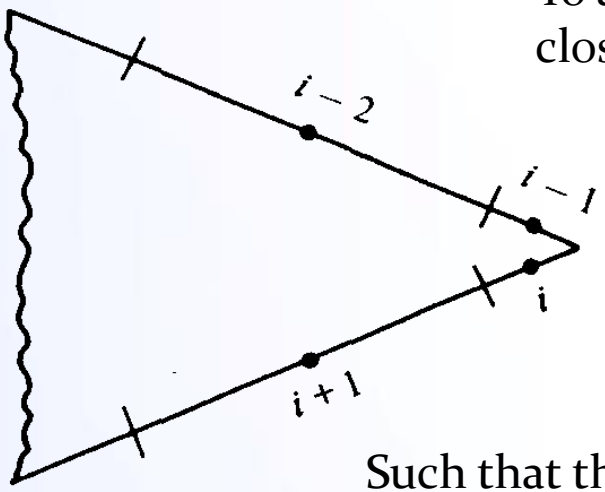

To approximate this numerically, if points *i and i - 1 are* close enough to the trailing edge, we can write:

$$\gamma_i = -\gamma_{i-1}$$

Such that the strengths of the two vortex panels i and i - 1 exactly cancel at the point where they touch at the trailing edge. Thus, in order to impose the Kutta condition on the solution of the flow

An *overdetermined system of n unknowns with* n + 1 equations.

We choose to ignore one of the control points, and we have n-1 equation the other n - 1 control points. This, in combination with Kutta condition, now gives a system of n linear algebraic equations with n unknowns, which can be solved by standard techniques.

The total circulation and the resulting lift are obtained as follows:
Let s_j be the length of the *jth* panel. Then the circulation due to the *jth* panel is $\gamma_j s_j$. In turn, the total circulation due to all the panels is

$$\Gamma = \sum_{j=1}^{n} \gamma_j s_j$$

$$L' = \rho_\infty V_\infty \sum_{j=1}^{n} \gamma_j s_j$$

VORTEX PANEL METHOD

Although the method may appear to be straightforward, its numerical implementation can sometimes be frustrating.

For example,

1- The results for a given body are sensitive to the number of panels used, their various sizes, and the way they are distributed over the body surface (i.e., it is usually advantageous to place a large number of small panels near the leading and trailing edges of an airfoil and a smaller number of larger panels in the middle).

2-The need to ignore one of the control points in order to have a determined system in *n equations for n unknowns also introduces some arbitrariness in the numerical* solution. Which control point do you ignore? Different choices sometimes yield different numerical answers for the distribution of *γ over the surface.*

3- Moreover, the resulting numerical distributions for γ *are not always smooth, but rather, they* have oscillations from one panel to the next as a result of numerical inaccuracies.

To overcome the problems:

The mentioned problems are usually overcome in different ways.
For example,

1- What is more common today is to use a *combination* of both source and vortex panels (source panels to basically simulate the airfoil thickness and vortex panels to introduce circulation) in a panel solution.

2-Higher–order panel method, we have used first order panel method in which the distribution of γ is constant along each panel. Other distributions for γ may be used. For example linear distribution of γ

HIGHER ORDER PANEL METHOD

Constant strength panels

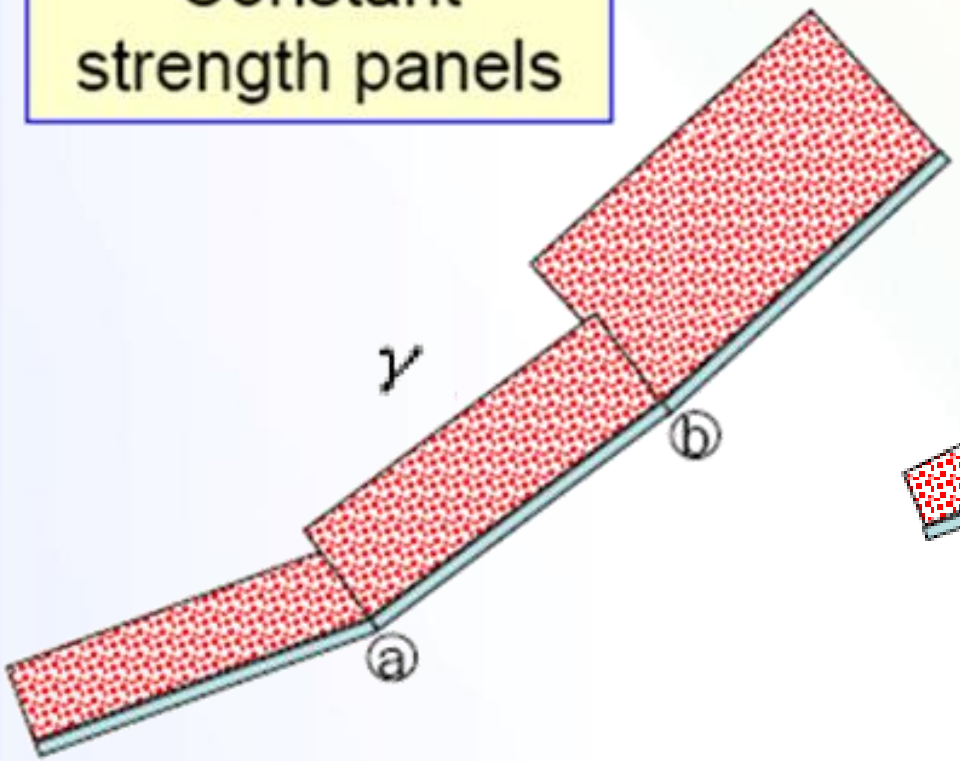

Linear strength panels

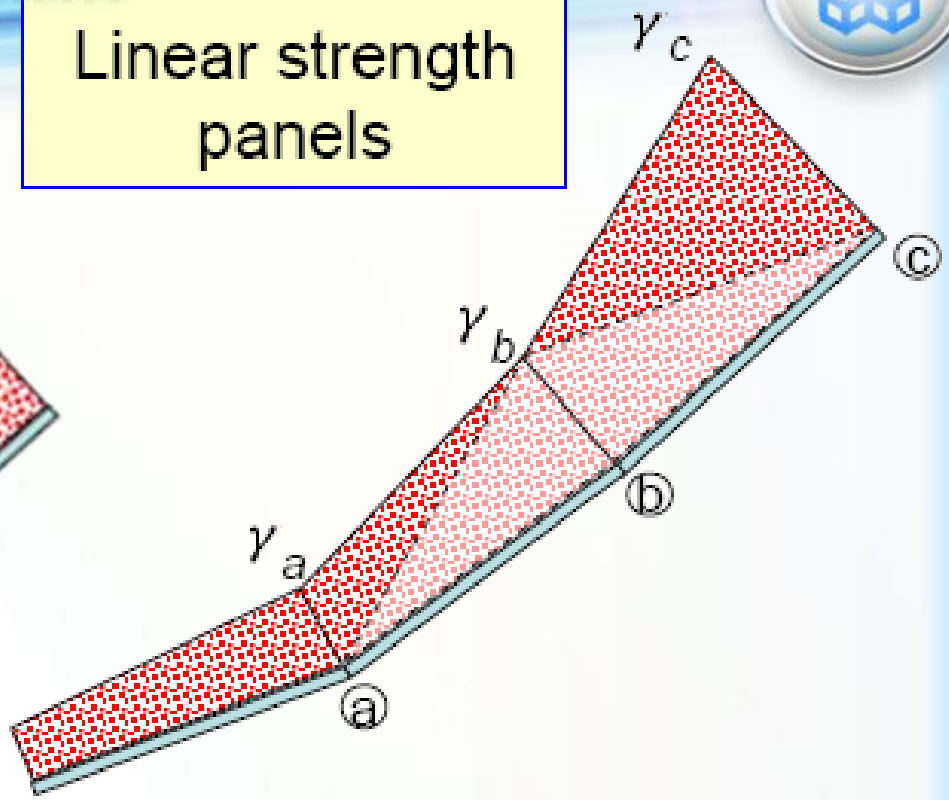

Influence of γ_b *depends on panel ab and panel bc*

LINEAR STRENGTH PANELS

$$\gamma(s_j) = \gamma_j + (\gamma_{j+1} - \gamma_j)\frac{s_j}{S_j}$$

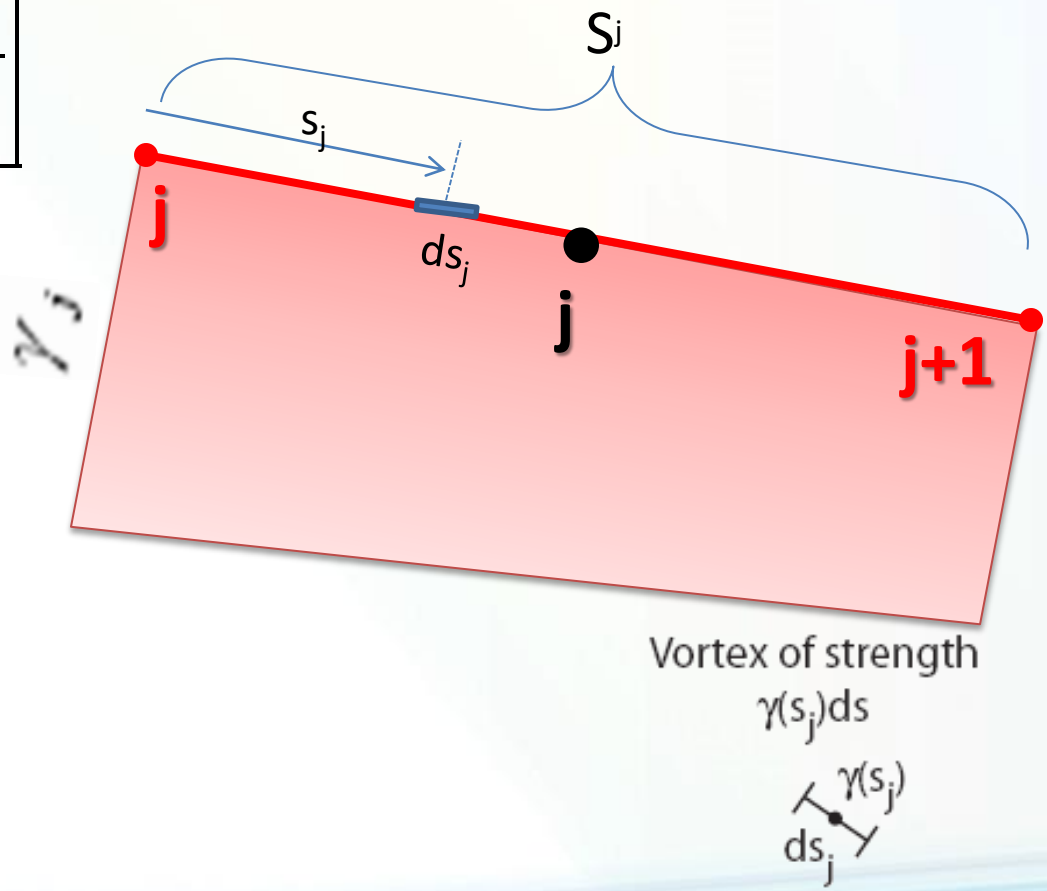

LINEAR STRENGTH PANELS

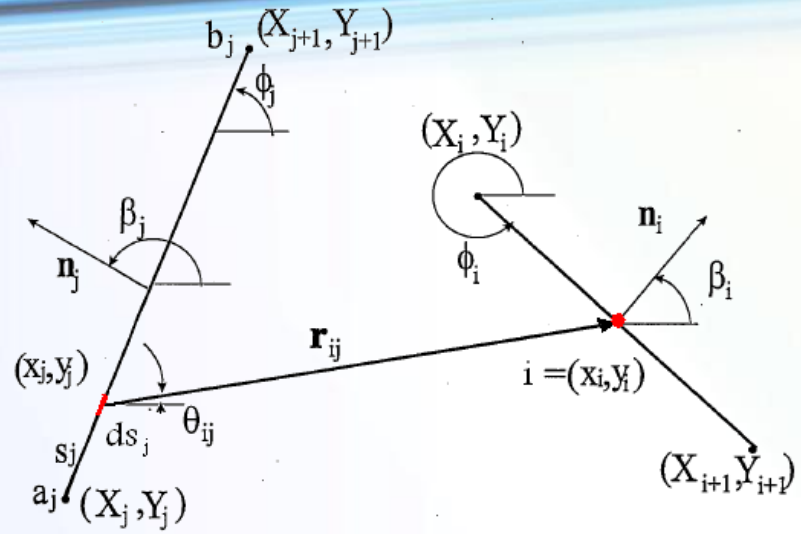

$$\beta_i = \phi_i + \frac{\pi}{2} - 2\pi \Rightarrow \begin{aligned} \cos\beta_i &= \sin\phi_i \\ \sin\beta_i &= \cos\phi_i \end{aligned}$$

$$x_i = \frac{X_i + X_{i+1}}{2}$$

$$\frac{\partial x_i}{\partial n_i} = \cos\beta_i \qquad y_i = \frac{Y_i + Y_{i+1}}{2}$$

$$\frac{\partial y_i}{\partial n_i} = \sin\beta_i \qquad \begin{aligned} x_j &= X_j + s_j\cos\phi_j \\ y_j &= Y_j + s_j\sin\phi_j \end{aligned}$$

$$V_\infty \cos(\beta_i - \alpha) - \sum_{j=1}^{n} \frac{1}{2\pi} \int_j \gamma(s_j) \frac{\partial \theta_{ij}}{\partial n_i} ds_j = 0$$

$$V_\infty \cos(\beta_i - \alpha) - \sum_{j=1}^{n} \frac{1}{2\pi} \int_j \left[\gamma_j + (\gamma_{j+1} - \gamma_j)\frac{s_j}{S_j} \right] \frac{\partial \theta_{ij}}{\partial n_i} ds_j = 0$$

$$V_\infty \sin(\alpha - \phi_i) - \sum_{j=1}^{n} \frac{1}{2\pi} \int_j \left[\gamma_j + (\gamma_{j+1} - \gamma_j)\frac{s_j}{S_j} \right] \frac{\partial \theta_{ij}}{\partial n_i} ds_j = 0$$

$$r_{ij} = \sqrt{(x_i - x_j)^2 + (y_i - y_j)^2}$$

$$\theta_{ij} = \arctan\frac{y_i - y_j}{x_i - x_j}$$

$$S_j = \sqrt{(X_{j+1} - X_j)^2 + (Y_{j+1} - Y_j)^2}$$

LINEAR STRENGTH PANELS

$$V_\infty \sin(\alpha - \phi_i) = \frac{1}{2\pi} \sum_{j=1}^{M} \int_0^{S_j} \left[\gamma_j + (\gamma_{j+1} - \gamma_j)\frac{s_j}{S_j}\right] \frac{1}{1 + \left(\dfrac{y_i - y_j}{x_i - x_j}\right)^2} \frac{\dfrac{\partial y_i}{\partial n_i}(x_i - x_j) - \dfrac{\partial x_i}{\partial n_i}(y_i - y_j)}{(x_i - x_j)^2} \mathrm{d}s_j$$

Replace the derivatives with their values:

$$\sin(\alpha - \phi_i) = \frac{1}{2\pi V_\infty} \sum_{j=1}^{M} \int_0^{S_j} \left[\gamma_j + (\gamma_{j+1} - \gamma_j)\frac{s_j}{S_j}\right] \frac{\cos\phi_i(x_i - x_j) + \sin\phi_i(y_i - y_j)}{(x_i - x_j)^2 + (y_i - y_j)^2} \mathrm{d}s_j$$

Factor out γ_j and γ_{j+1}:

$$\sin(\alpha - \phi_i) =$$

$$= \frac{1}{2\pi V_\infty} \sum_{j=1}^{M} \left[\gamma_j \int_0^{S_j} \left(1 - \frac{s_j}{S_j}\right) \frac{\cos\phi_i(x_i - X_j - s_j\cos\phi_j) + \sin\phi_i(y_i - Y_j - s_j\sin\phi_j)}{(x_i - X_j - s_j\cos\phi_j)^2 + (y_i - Y_j - s_j\sin\phi_j)^2} \mathrm{d}s_j + \right.$$

$$\left. \gamma_{j+1} \int_0^{S_j} \frac{s_j}{S_j} \frac{\cos\phi_i(x_i - X_j - s_j\cos\phi_j) + \sin\phi_i(y_i - Y_j - s_j\sin\phi_j)}{(x_i - X_j - s_j\cos\phi_j)^2 + (y_i - Y_j - s_j\sin\phi_j)^2} \mathrm{d}s_j \right]$$

LINEAR STRENGTH PANELS

Define

$$H_{ij} \equiv \int_0^{S_j} \left(1 - \frac{s_j}{S_j}\right) \frac{\cos\phi_i(x_i - X_j - s_j\cos\phi_j) + \sin\phi_i(y_i - Y_j - s_j\sin\phi_j)}{(x_i - X_j - s_j\cos\phi_j)^2 + (y_i - Y_j - s_j\sin\phi_j)^2}\mathrm{d}s_j$$

and

$$K_{ij} \equiv \int_0^{S_j} \frac{s_j}{S_j} \frac{\cos\phi_i(x_i - X_j - s_j\cos\phi_j) + \sin\phi_i(y_i - Y_j - s_j\sin\phi_j)}{(x_i - X_j - s_j\cos\phi_j)^2 + (y_i - Y_j - s_j\sin\phi_j)^2}\mathrm{d}s_j$$

$$\frac{1}{2\pi V_\infty}\sum_{j=1}^{M} H_{ij}\gamma_j + K_{ij}\gamma_{j+1} = \sin(\alpha - \phi_i)$$

LINEAR STRENGTH PANELS

$$A = -(x_i - X_j)\cos\phi_j - (y_i - Y_j)\sin\phi_j$$

$$B = (x_i - X_j)^2 + (y_i - Y_j)^2$$

$$C = \sin(\phi_i - \phi_j)$$

$$D = \cos(\phi_i - \phi_j)$$

$$E = (x_i - X_j)\sin\phi_j - (y_i - Y_j)\cos\phi_j$$

$$F = \ln\left(1 + \frac{S_j^2 + 2AS_j}{B}\right)$$

$$G = \arctan\left(\frac{ES_j}{B + AS_j}\right)$$

$$P = (x_i - X_j)\sin(\phi_i - 2\phi_j) + (y_i - Y_j)\cos(\phi_i - 2\phi_j)$$

$$Q = (x_i - X_j)\cos(\phi_i - 2\phi_j) - (y_i - Y_j)\sin(\phi_i - 2\phi_j)$$

LINEAR STRENGTH PANELS

$$K_{ij} = D + \frac{1}{2}\frac{QF}{S_j} - (AC + DE)\frac{G}{S_j}$$

$$K_{ii} = 1$$

$$H_{ij} = \frac{1}{2}DF + CG - K_{ij}$$

$$H_{ii} = -1$$

$$\frac{1}{2\pi V_\infty}\sum_{j=1}^{M} H_{ij}\gamma_j + K_{ij}\gamma_{j+1} = \sin(\alpha - \phi_i)$$

$$i = 1, 2, \ldots, M \text{ control points.}$$

Kutta condition $\gamma(TE) = 0$ requires $\gamma_1 = -\gamma_{M+1}$.

LINEAR STRENGTH PANELS

Then the γ_j values must satisfy the linear system

$$\sum_{j=1}^{M+1} L_{ij}\gamma_j = N_i \quad i = 1, 2, \ldots M+1$$

$$[L]\{\gamma\} = \{N\}$$

where, for $i = 1, 2 \ldots, M$,

$$L_{i1} = H_{i1}$$

$$L_{ij} = H_{ij} + K_{ij-1} \quad j = 2, 3, \ldots M$$

$$L_{iM+1} = K_{iM}$$

$$N_i = 2\pi V_\infty \sin(\alpha - \phi_i)$$

and, for $i = M + 1$,

$$L_{i1} = L_{iM+1} = 1$$

$$L_{ij} = 0 \quad j = 2, 3, \ldots, M$$

$$N_i = 0$$

LINEAR STRENGTH PANELS

$$\underbrace{\begin{bmatrix} L_{11} & L_{12} & & & L_{19} \\ L_{21} & L_{22} & & & \\ L_{31} & L_{32} & L_{33} & & \\ L_{41} & & & & \\ L_{51} & & & & \\ L_{61} & & & & \\ L_{71} & & & & \\ L_{81} & & & & \\ 1 & 0 & 0 & 0 & 1 \end{bmatrix}}_{L} \underbrace{\begin{bmatrix} \gamma_1 \\ \gamma_2 \\ \gamma_3 \\ . \\ . \\ . \\ . \\ \gamma_8 \\ \gamma_9 \end{bmatrix}}_{\gamma} = -\underbrace{\begin{bmatrix} 2\pi V_\infty \sin(\alpha - \phi_1) \\ 2\pi V_\infty \sin(\alpha - \phi_2) \\ . \\ . \\ . \\ \\ \\ 2\pi V_\infty \sin(\alpha - \phi_8) \\ 0 \end{bmatrix}}_{N}$$

LINEAR STRENGTH PANELS

$$L' = \frac{1}{2}\rho V_\infty \sum_{i=1}^{m} (\gamma_i + \gamma_{i+1}) S_i$$

$$\Rightarrow \boxed{C_l = \frac{L'}{\frac{1}{2}\rho V_\infty^2 c} = \sum_{i=1}^{m} \left(\frac{\gamma_i}{V_\infty} + \frac{\gamma_{i+1}}{V_\infty} \right) \frac{S_i}{c}}$$

Once the $M+1$ values of γ_j are known, one calculates the tangential component of the velocity at the control points using $V_{ti} = \dfrac{\partial \phi}{\partial s_i}$

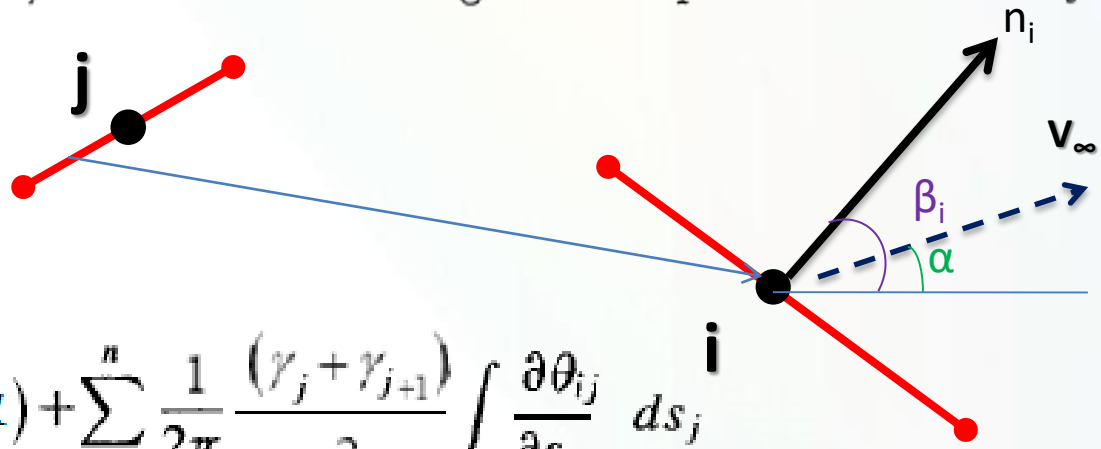

$$V_i = V_{\infty,s} + V_s = V_\infty \sin(\beta_i - \alpha) + \sum_{j=1}^{n} \frac{1}{2\pi} \frac{(\gamma_j + \gamma_{j+1})}{2} \int_j \frac{\partial \theta_{ij}}{\partial s_i} \, ds_j$$

LINEAR STRENGTH PANELS

$$T_{ij} = C + \frac{1}{2}\frac{PF}{S_j} + (AD - CE)\frac{G}{S_j}$$

$$R_{ij} = \frac{1}{2}CF - DG - T_{ij}$$

$$R_{ii} = T_{ii} = \frac{\pi}{2}$$

$$V_{ti} = V_\infty \left[\cos(\alpha - \phi_i) + \sum_{j=1}^{M+1} W_{ij}\frac{\gamma_j}{2\pi}\right] \quad i = 1, 2, \ldots, M$$

where

$$W_{i1} = R_{i1}$$

$$W_{ij} = R_{ij} + T_{ij-1} \quad j = 2, 3, \ldots, M$$

$$W_{iM+1} = T_{iM}$$

$$c_{pi} = 1 - \left(\frac{V_{ti}}{V_\infty}\right)^2$$

VORTEX PANEL METHOD - SUMMARY

1. Write down the velocities in terms of contributions from all the singularities.
2. Find the algebraic equations defining the influence coefficients.
3. Write down flow tangency conditions in terms of the velocities (N equations, N+1 unknowns)
4. Write down the Kutta condition equation to get the N+1 equation.
5. Solve the resulting linear algebraic system of equations
6. Write down the equations for tangential velocity at each control point.
7. Determine the pressure distribution from Bernoulli's equation using the tangential velocity on each panel.

VORTEX PANEL METHOD

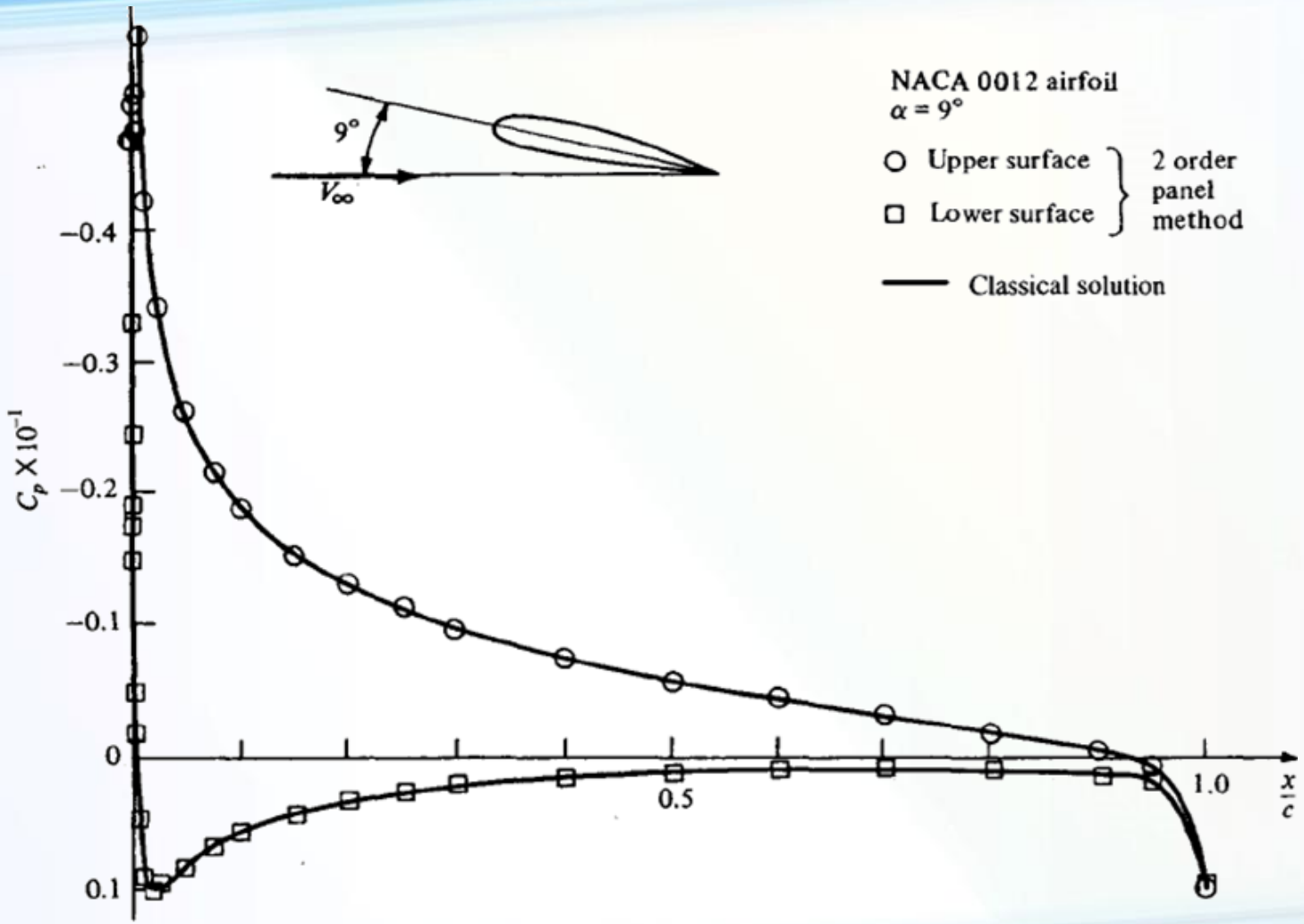

INVISCID – VISCOUS FLUID FLOW

- Most of our previous discussions have dealt with inviscid flows. A large number of practical aerodynamic applications are appropriately treated by assuming inviscid flow, as we have already seen.

- Inviscid flows do not truly exist in nature; however, there are many practical aerodynamic flows (more than you would think) where the influence of transport phenomena is small, and we can model the flow as being inviscid.

- Theoretically, inviscid flow is approached in the limit as the Reynolds number goes to infinity.

INVISCID – VISCOUS FLUID FLOW

- Some aspects of aerodynamics are inherently viscous in nature, such as skin-friction drag, aerodynamic heating and flow separation.

- To deal with these important aspects, we have to undertake the study of *Viscous Flow*.

WHTAT IS A BOUNDARY LAYER?

- For practical problems, many flows with high but finite *Re* can be assumed to be inviscid. For such flows, the influence of friction, is limited to a very thin region adjacent to the body surface called the boundary layer.

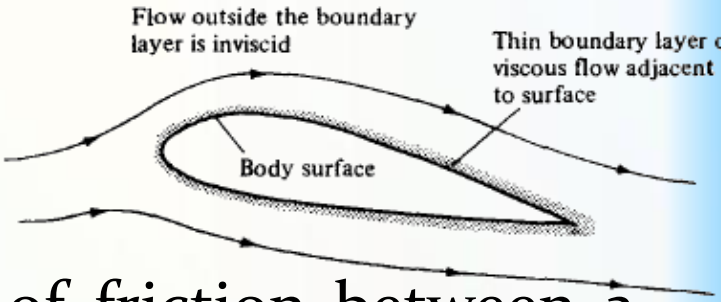

- The boundary layer is the thin region of flow adjacent to a surface, where the flow is retarded by the influence of friction between a solid surface and the fluid.

- Although the influence of friction is present every point throughout flow, it is usually of no consequence except in a thin region adjacent to the surface of a body immersed in the flow.

WHTAT IS A BOUNDARY LAYER?

- Consider the viscous flow over a flat plate. The viscous effects are contained within a thin layer adjacent to the surface.

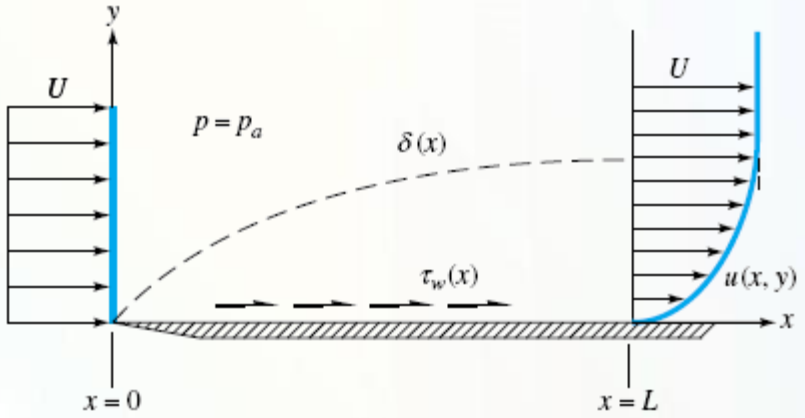

- The influence of friction is to create *V=o* right at the plate surface. This is called the *no-slip condition* which dominates viscous flow.

- Above the surface, the flow velocity increases in *y* direction until, for all practical purposes, it equals the freestream velocity.

WHTAT IS A BOUNDARY LAYER?

- Consider the viscous flow over a flat plate. The viscous effects are contained within a thin layer adjacent to the surface.

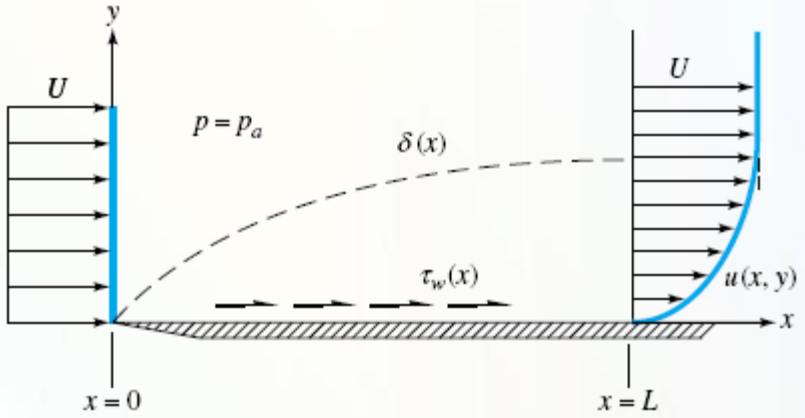

- δ (*boundary layer thickness*) is defined as that distance above the wall where $u=0.99U$; Here, U is the velocity at the outer edge of the boundary layer.

- At any x station, the variation of u between $y=0$ and $y=\delta$, that is, $u=u(y)$ is defined as the *velocity profile*.

WHTAT IS A BOUNDARY LAYER?

- Consider the viscous flow over a flat plate. The viscous effects are contained within a thin layer adjacent to the surface.

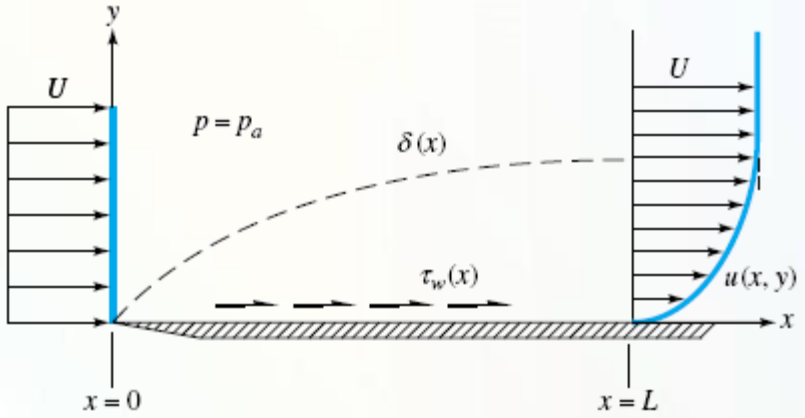

- The consequence of the velocity gradient at the wall is the generation of shear stress at the wall:

$$\tau_w = \mu \left(\frac{\partial u}{\partial y} \right)_w$$

EFFECT OF PRESSURE GRADIENT ON VELOCITY PROFILE

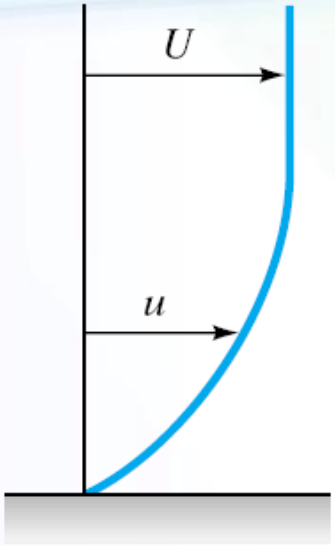

Favorable gradient:

$$\frac{dU}{dx} > 0$$

$$\frac{dp}{dx} < 0$$

No separation, PI inside wall

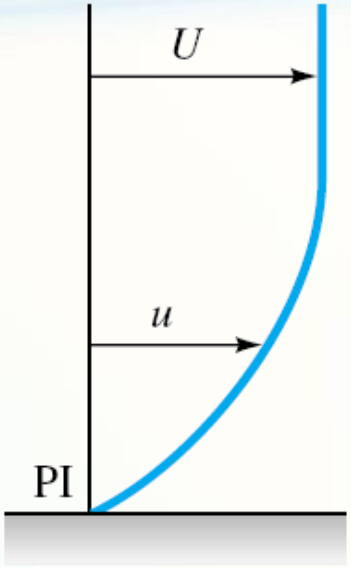

Zero gradient:

$$\frac{dU}{dx} = 0$$

$$\frac{dp}{dx} = 0$$

No separation, PI at wall

EFFECT OF PRESSURE GRADIENT ON VELOCITY PROFILE (SEPARATION)

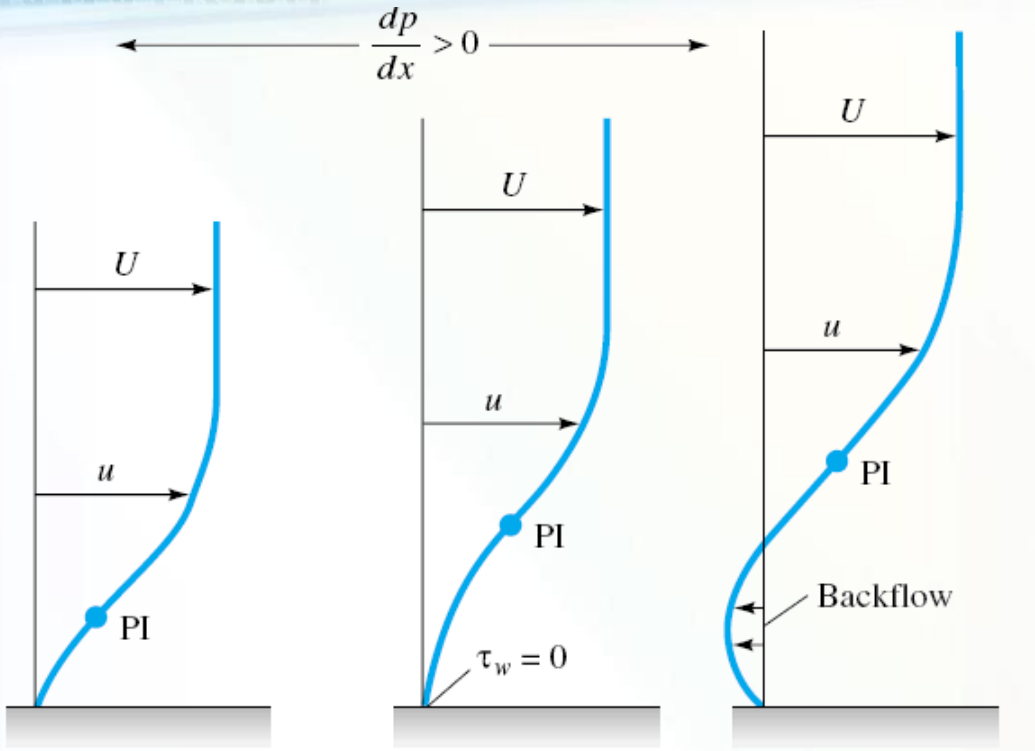

Weak adverse gradient:

$\frac{dU}{dx} < 0$

$\frac{dp}{dx} > 0$

Critical adverse gradient:

Zero slope at the wall:

Separation

Excessive adverse gradient:

Backflow at the wall:

Separated flow region

EFFECT OF PRESSURE GRADIENT ON VELOCITY PROFILE (SEPARATION)

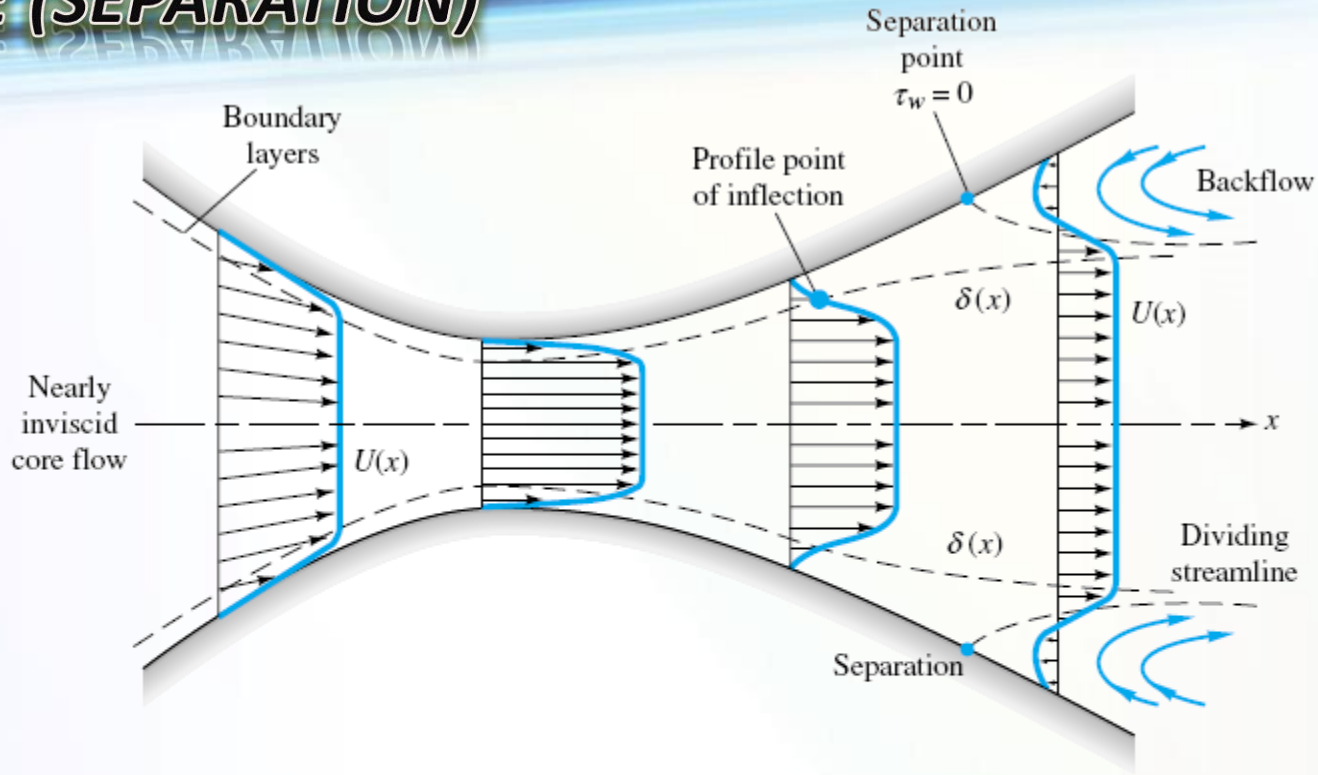

Nozzle:	*Throat*:	*Diffuser*:
Decreasing pressure and area	Constant pressure and area	Increasing pressure and area
Increasing velocity	Velocity constant	Decreasing velocity
Favorable gradient	Zero gradient	Adverse gradient (boundary layer thickens)

EFFECT OF PRESSURE GRADIENT ON VELOCITY PROFILE (SEPARATION)

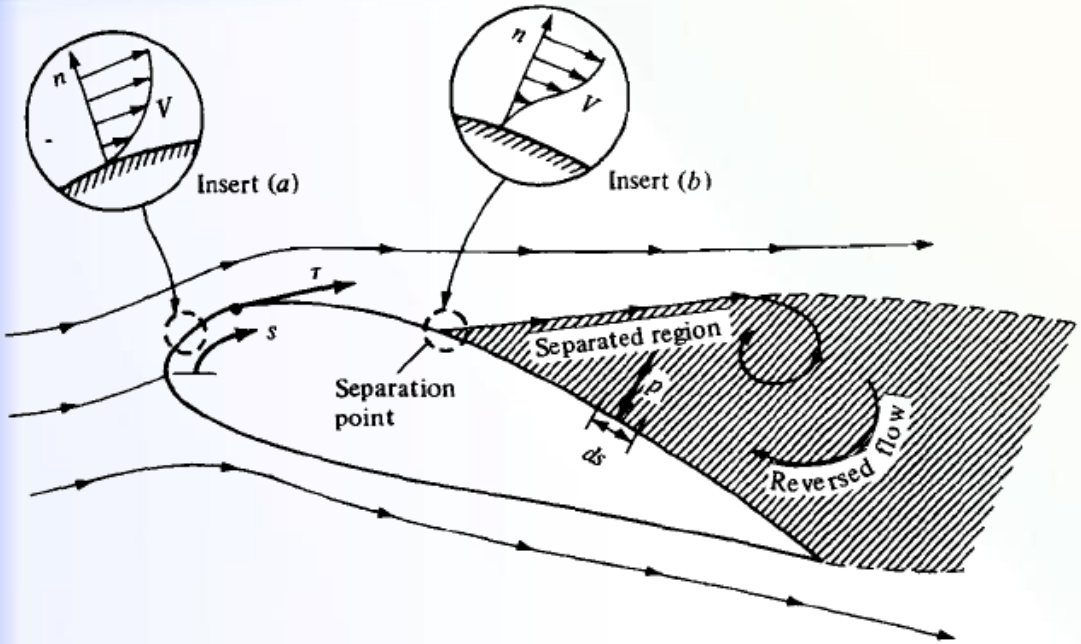

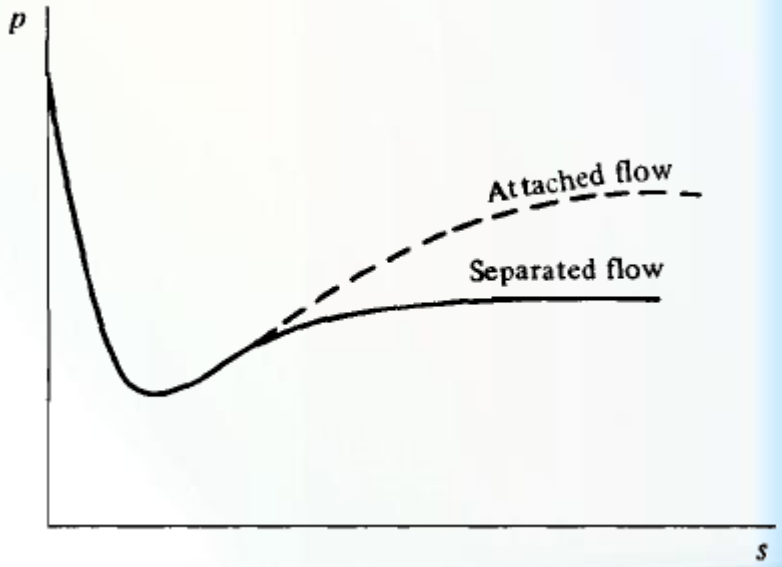

EFFECT OF PRESSURE GRADIENT ON VELOCITY PROFILE (SEPARATION)

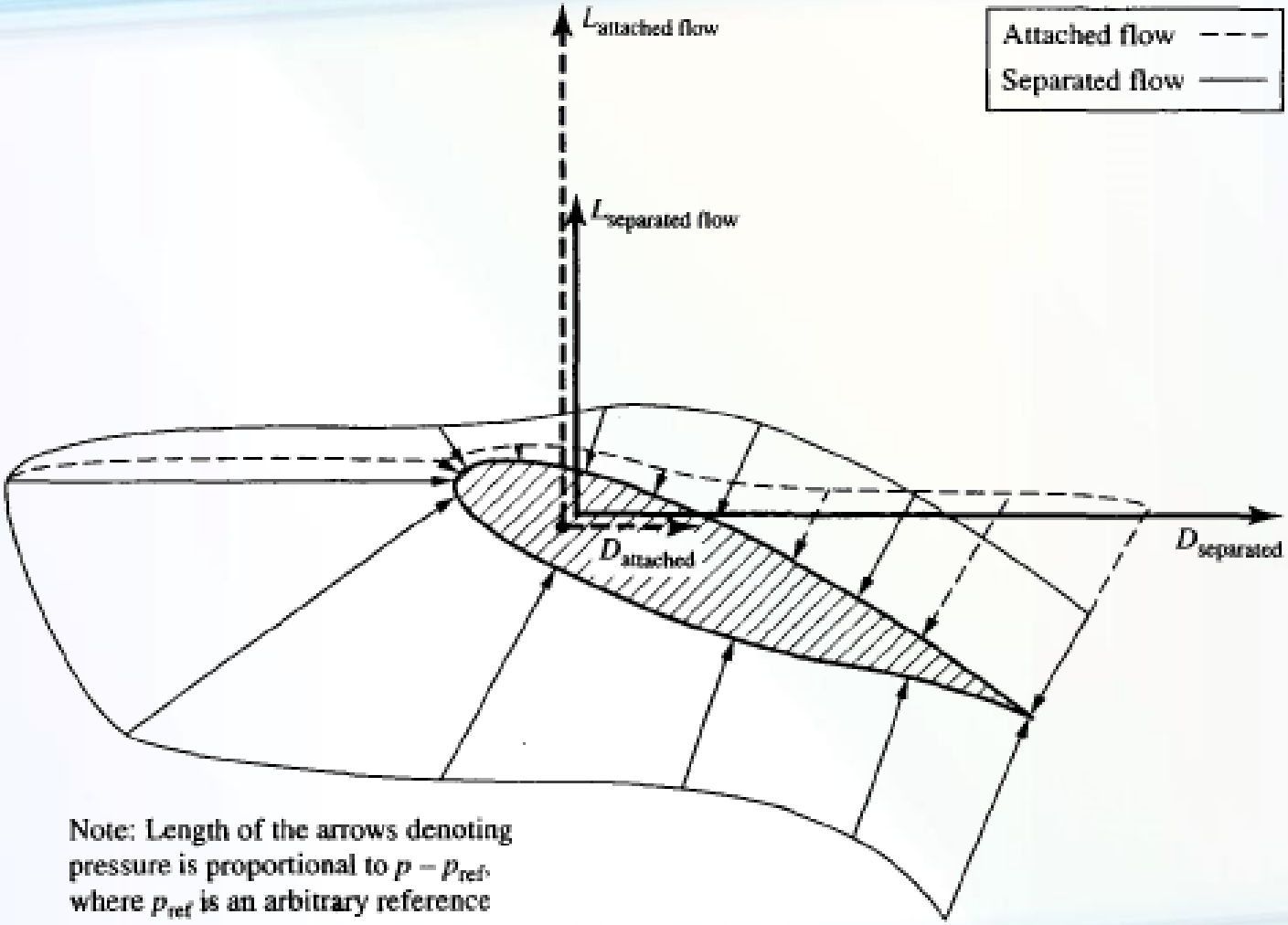

Note: Length of the arrows denoting pressure is proportional to $p - p_{ref}$, where p_{ref} is an arbitrary reference pressure slightly less than the minimum pressure on the airfoil

EFFECT OF PRESSURE GRADIENT ON VELOCITY PROFILE (SEPARATION)

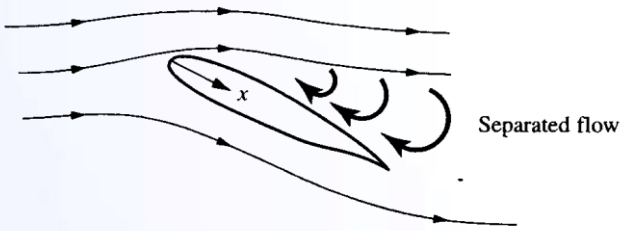

NASA LS(1) - 0417 airfoil
Angle of attack = 18.4°

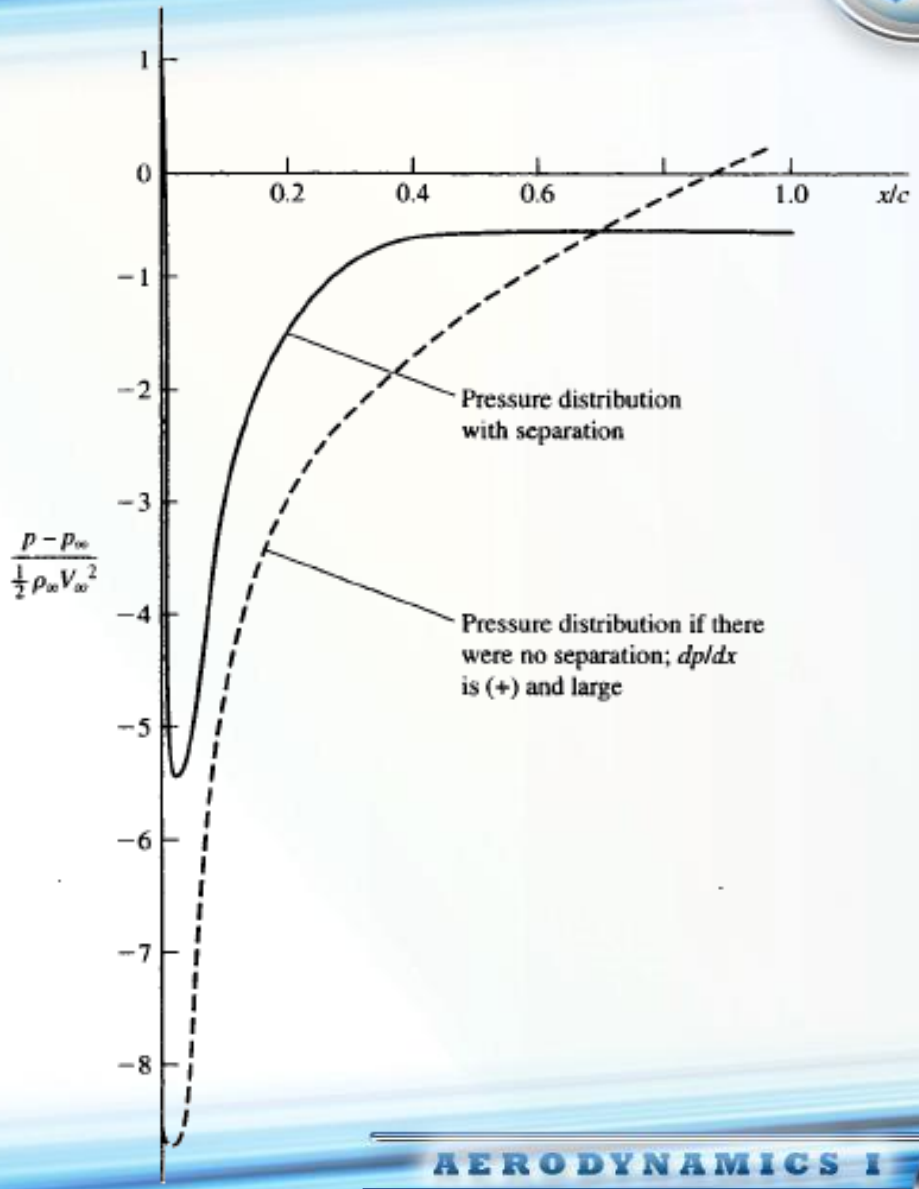

EFFECTS OF VISCOUSITY ON DRAG

- With the assumption of an inviscid flow, the integrated pressure distribution over body would give zero drag! (d' Alembert's paradox)

- The effects of viscosity are to produce two types of drag:
  1. *Skin-friction drag* (D_f): The component in the drag direction of the integral of the shear stress over body.
  2. *Pressure drag* (D_p) due to separation, that is, the component in the drag direction of the integral of the pressure distribution over body. Pressure drag is sometimes called *form drag*.
  3. The sum $D_f + D_p$ is called the *profile drag* of a two-dimensional body. This is frequently called *parasite drag*.

EFFECTS OF VISCOUSITY ON DRAG

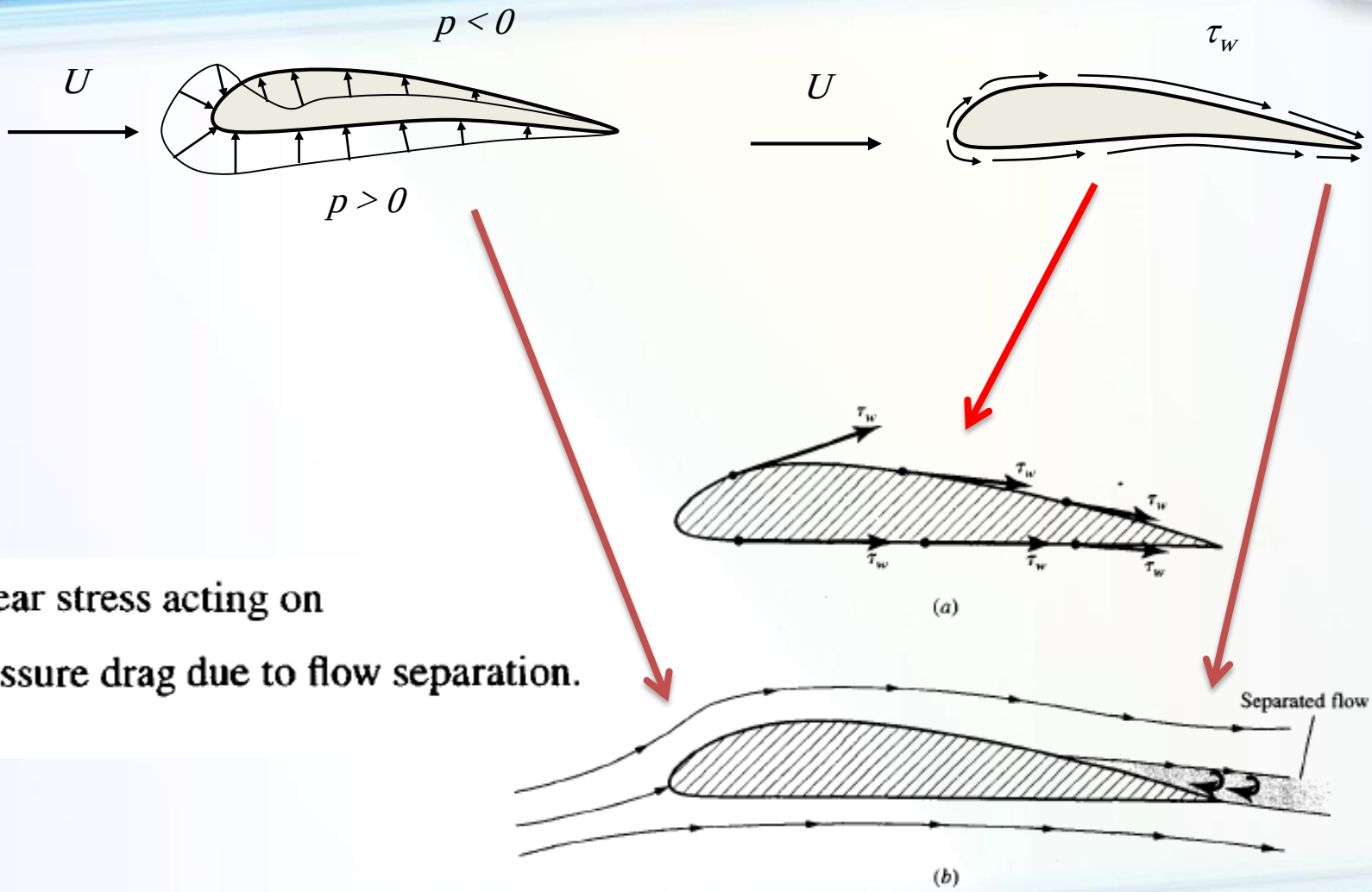

(*a*) shear stress acting on

(*b*) pressure drag due to flow separation.

LAMINAR AND TURBULENT FLOWS

- Consider the viscous flow over a surface.

  • Laminar flow: The path lines of various fluid elements are smooth and regular.
  • Turbulent flow: The motion of a fluid element is very irregular and tortuous.

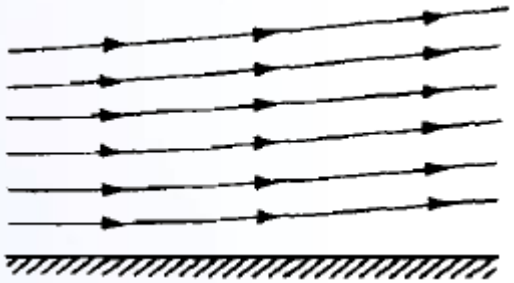

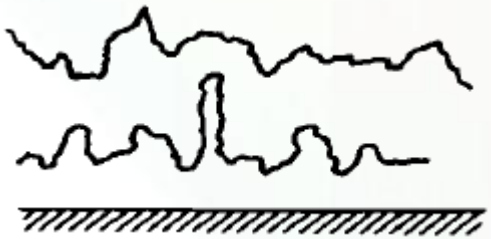

TRANSITION FROM LAMINAR TO TURBULENT BOUNDARY LAYERS

- For the laminar boundary layer over a flat plate, after a certain distance from the leading edge, instabilities will appear in the laminar flow.

- The instabilities rapidly grow, causing transition to turbulent flow.

- For purposes of analysis, we frequently model the Transition region as a single point, called the transition point.

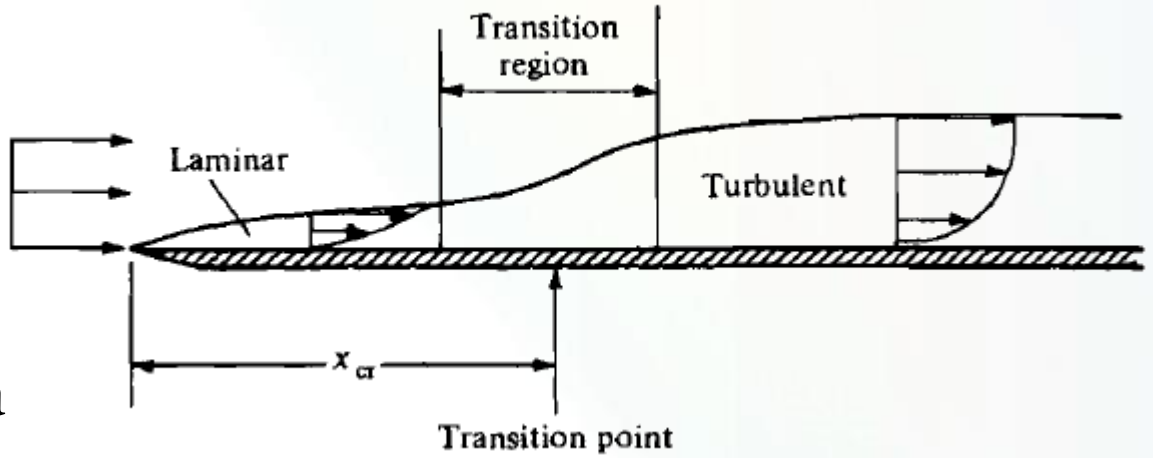

$$\mathrm{Re}_{cr} \equiv \frac{\rho_\infty V_\infty x_{cr}}{\mu_\infty}$$

TRANSITION FROM LAMINAR TO TURBULENT BOUNDARY LAYERS

- Some characteristics which encourage transition from laminar to turbulent flow, are:

1. Increased surface roughness
2. Increased turbulence in the freestream
3. Adverse pressure gradient
4. Heating of the fluid by the surface

FLOW PAST A CIRCULAR CYLINDER

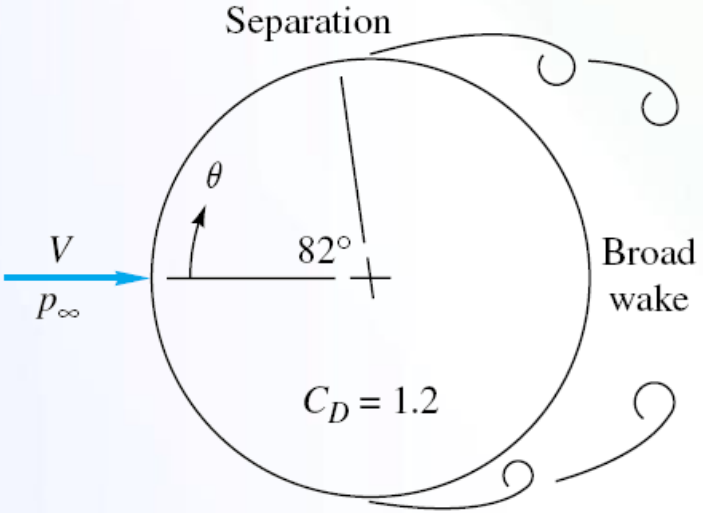

Laminar Separation

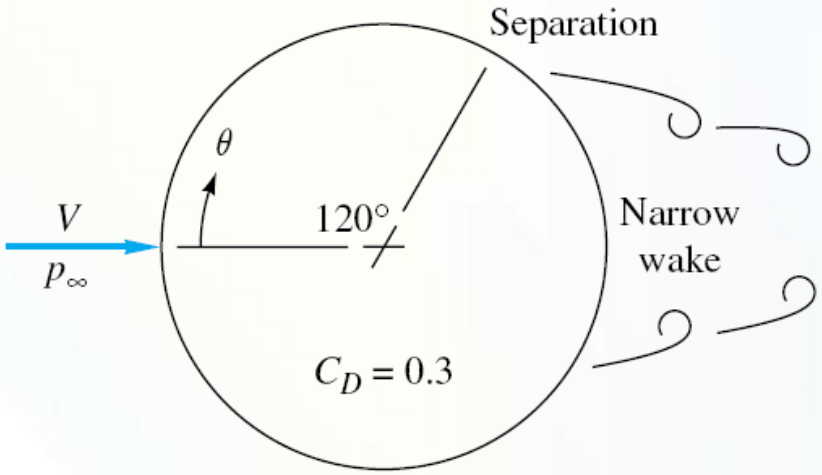

Turbulent Separation

FLOW PAST A CIRCULAR CYLINDER

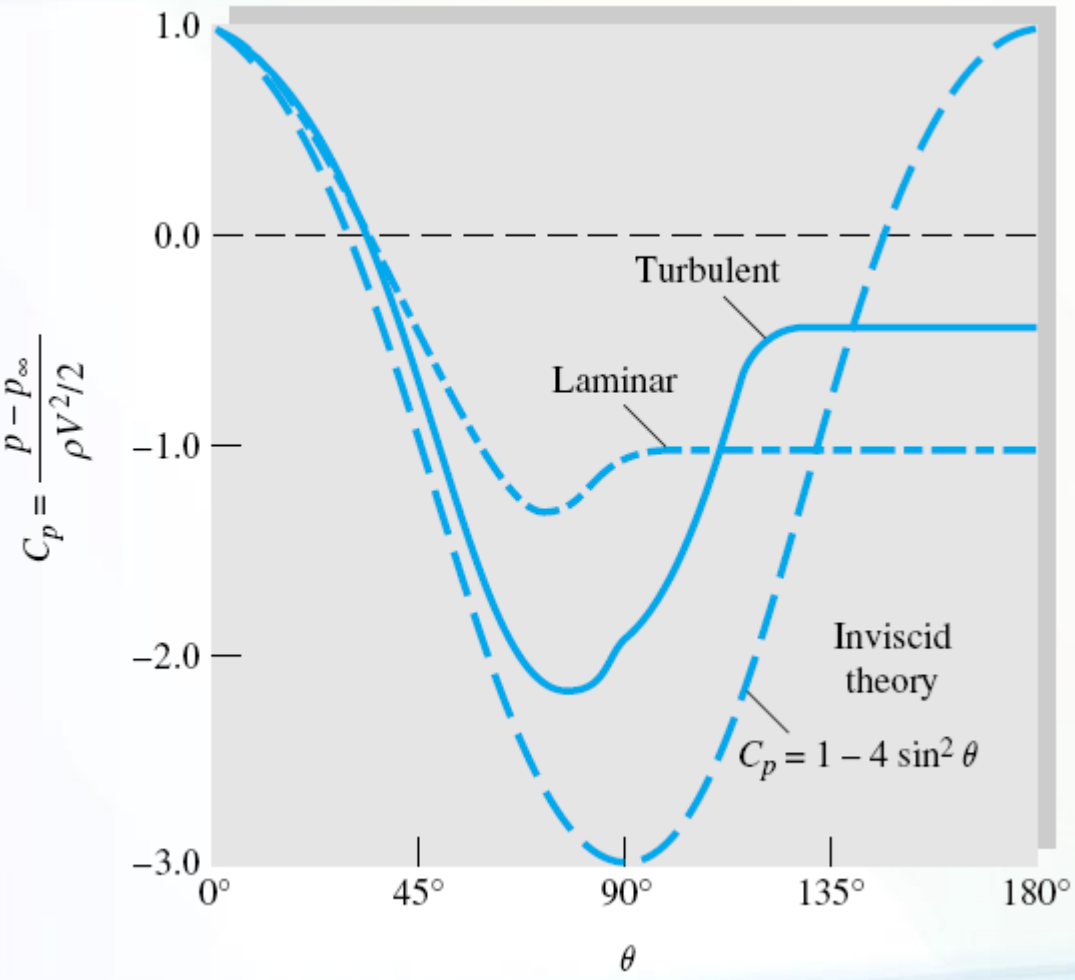

VELOCITY PROFILES FOR LAMINAR AND TURBULENT FLOWS

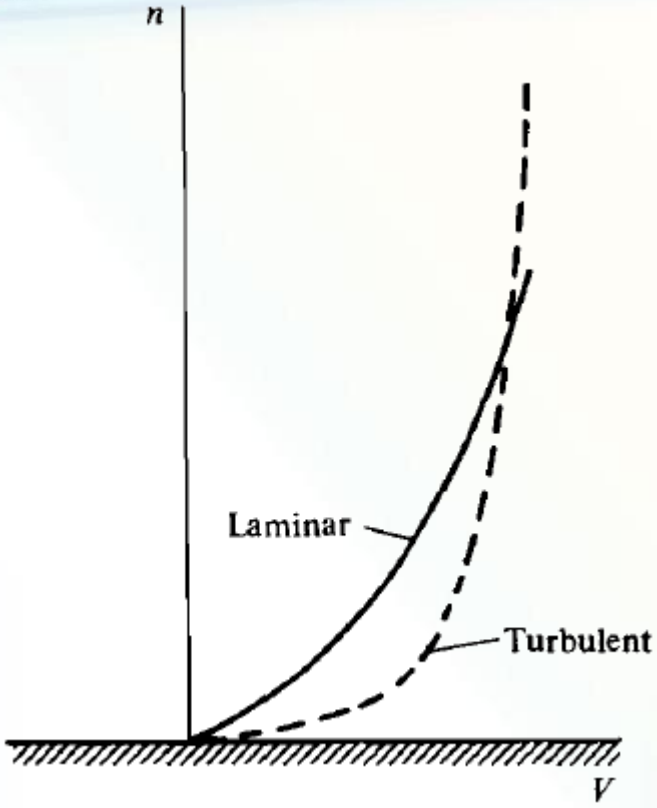

$$\left[\left(\frac{\partial V}{\partial n}\right)_{n=0}\right]_{\text{turbulent}} > \left[\left(\frac{\partial V}{\partial n}\right)_{n=0}\right]_{\text{laminar}}$$

DRAG COEFFICIENT OF LAMINAR AND TURBULENT BOUNDARY LAYERS

- Drag coefficient of laminar and turbulent boundary layers on smooth and rough flat plates:

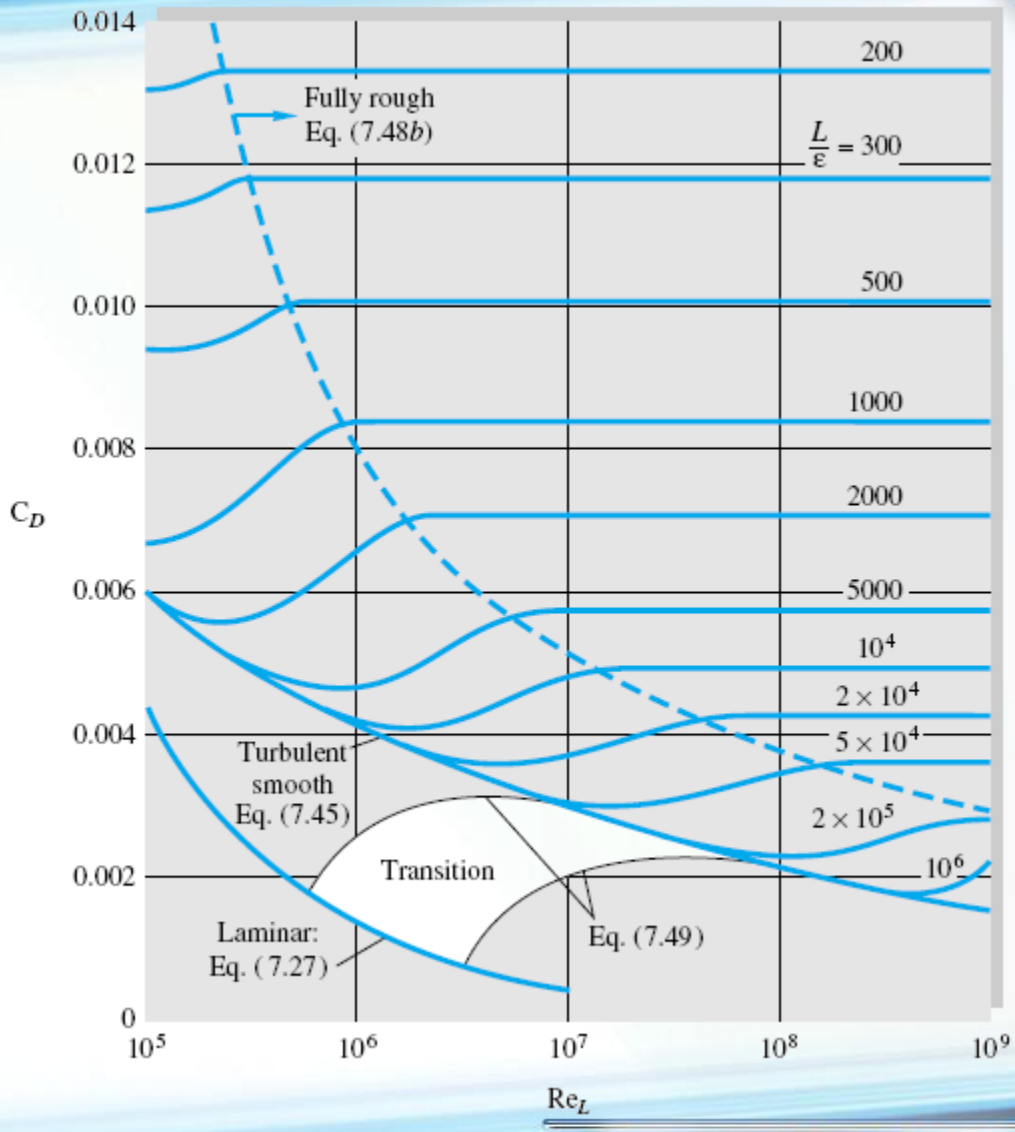

- Drag of a streamlined two-dimensional cylinder at $Re_c = 10^6$

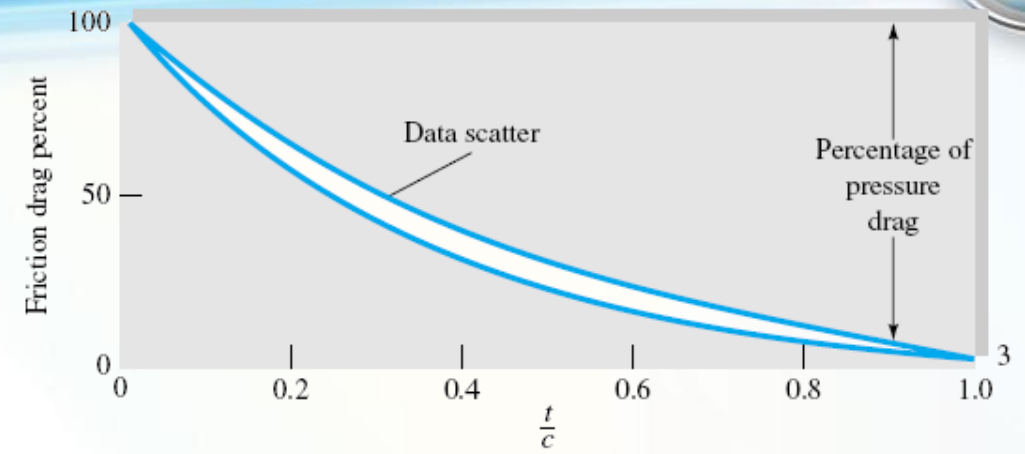

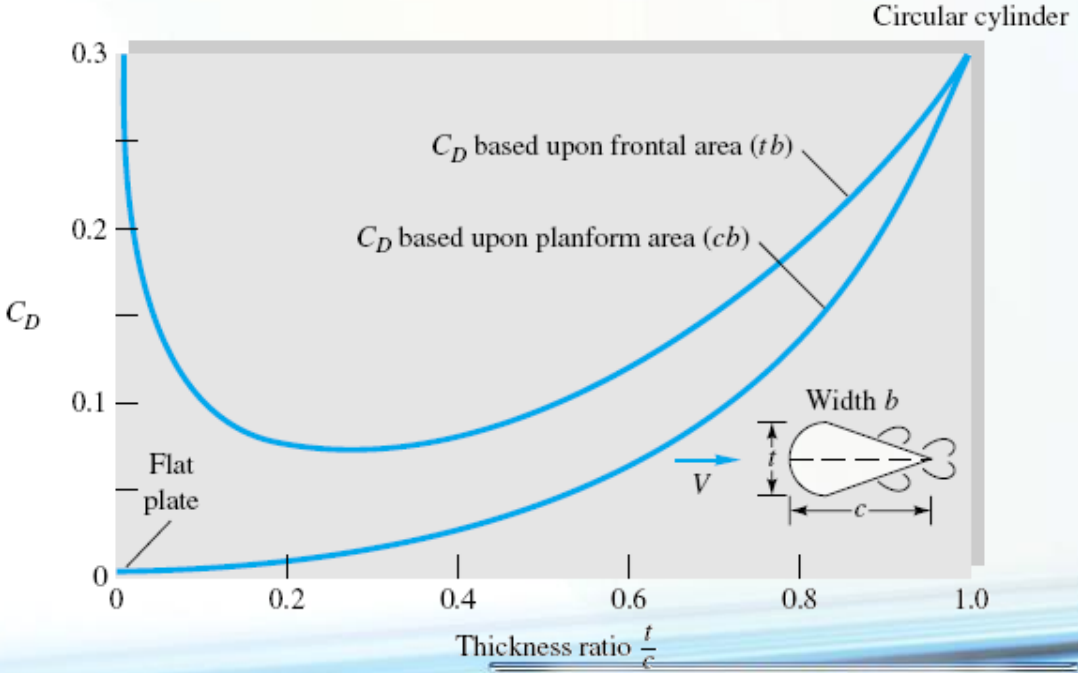

- The importance of streamlining in reducing drag of a body (C_D based on frontal area)

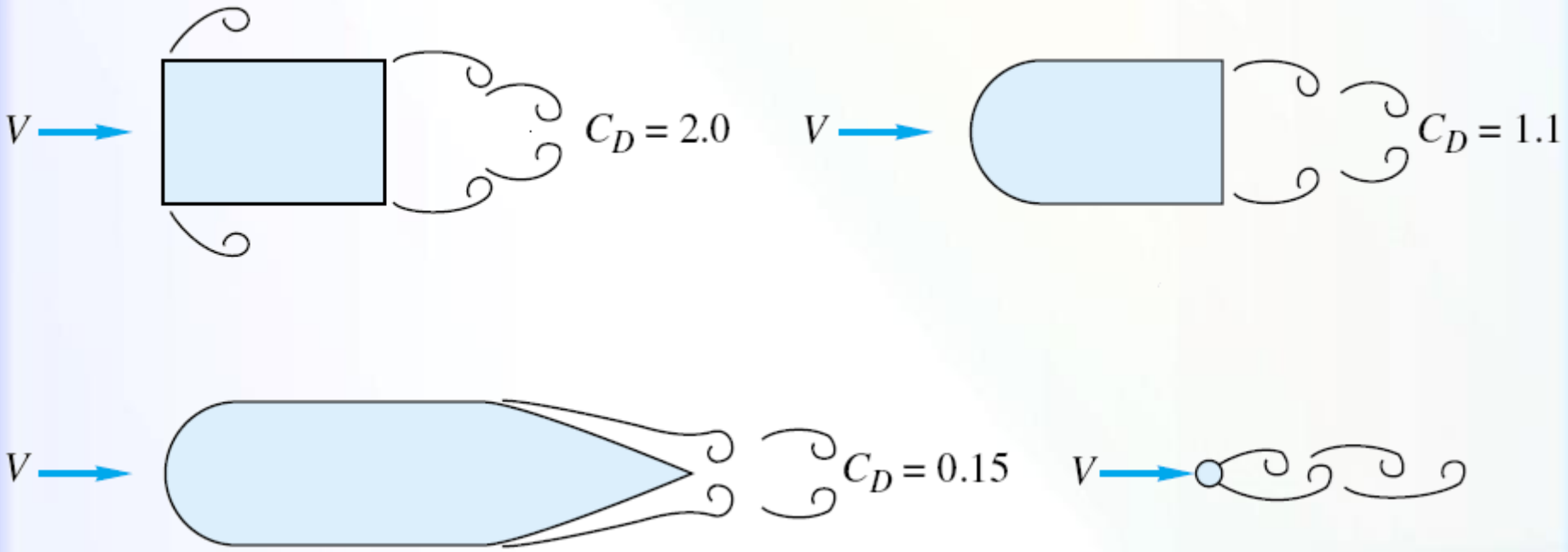

- Drag of two-dimensional bodies $Re>10^4$

Square cylinder:

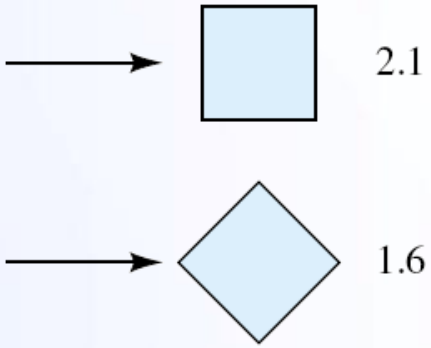

Half tube:

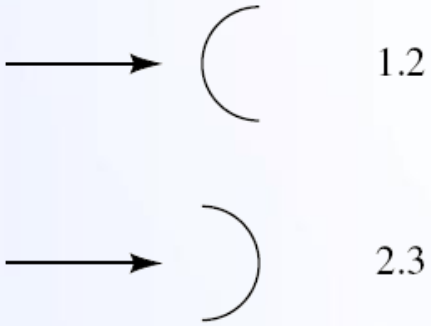

Half-cylinder:

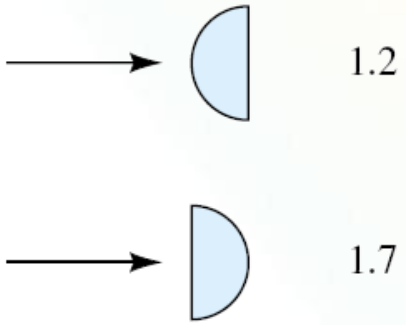

Equilateral triangle:

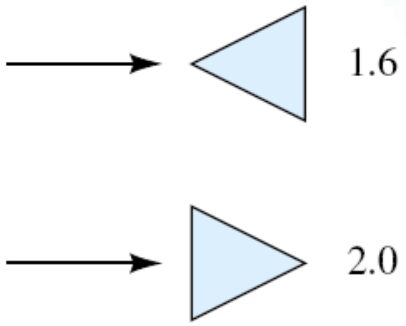

Plate:

Thin plate normal to a wall:

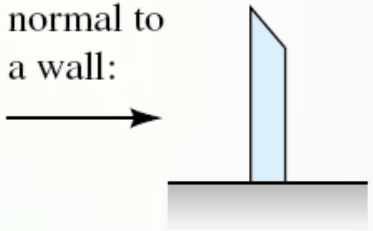

Hexagon:

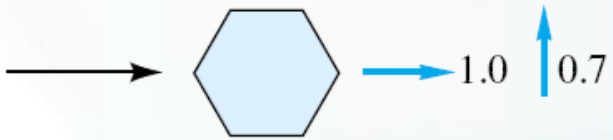

- Drag of two-dimensional bodies $Re > 10^4$

Rounded nose section:

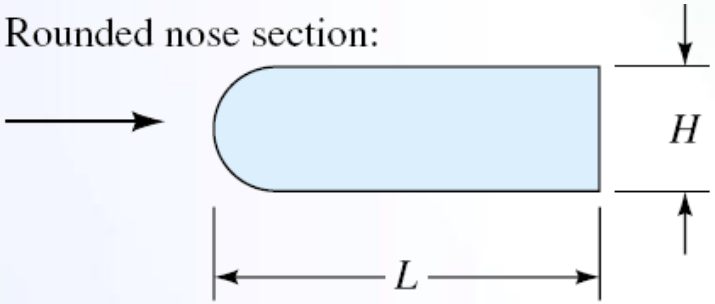

L/H:	0.5	1.0	2.0	4.0	6.0
C_D:	1.16	0.90	0.70	0.68	0.64

Flat nose section

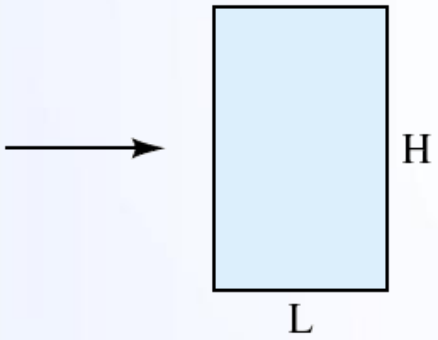

L/H:	0.1	0.4	0.7	1.2	2.0	2.5	3.0	6.0
C_D:	1.9	2.3	2.7	2.1	1.8	1.4	1.3	0.9

- Drag of two-dimensional bodies $Re > 10^4$

Elliptical cylinder:		Laminar	Turbulent
1:1 →	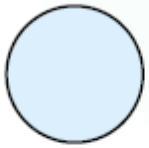	1.2	0.3
2:1 →		0.6	0.2
4:1 →		0.35	0.15
8:1 →		0.25	0.1

- Drag of three-dimensional bodies $Re > 10^4$

Cube:

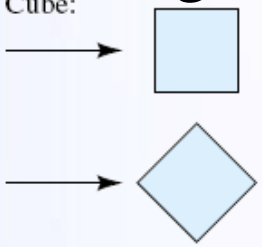

1.07

0.81

Cup:

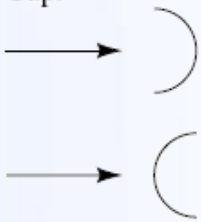

1.4

0.4

Disk:

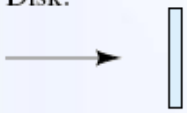

1.17

Parachute (Low porosity):

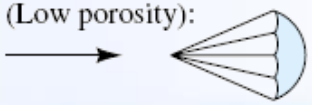

1.2

Cone:

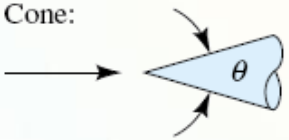

θ:	10°	20°	30°	40°	60°	75°	90°
C_D:	0.30	0.40	0.55	0.65	0.80	1.05	1.15

Short cylinder, laminar flow:

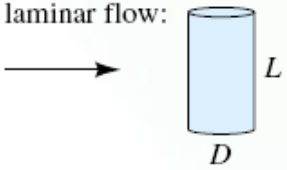

L/D:	1	2	3	5	10	20	40	∞
C_D:	0.64	0.68	0.72	0.74	0.82	0.91	0.98	1.20

Porous parabolic dish [23]:

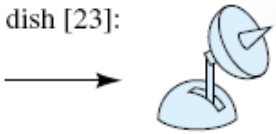

Porosity:	0	0.1	0.2	0.3	0.4	0.5
← C_D:	1.42	1.33	1.20	1.05	0.95	0.82
→ C_D:	0.95	0.92	0.90	0.86	0.83	0.80

Average person:

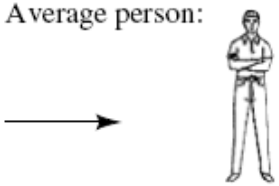

→ $C_D A \approx 9$ ft^2 ↑ $C_D A \approx 1.2$ ft^2

Pine and spruce trees [24]:

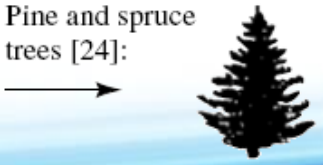

U, m/s:	10	20	30	40
C_D:	1.2 ± 0.2	1.0 ± 0.2	0.7 ± 0.2	0.5 ± 0.2

- Drag of three-dimensional bodies $Re>10^4$

Rectangular plate:

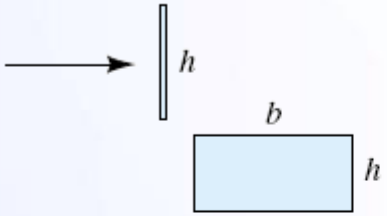

b/h	C_D
1	1.18
5	1.2
10	1.3
20	1.5
∞	2.0

Flat-faced cylinder:

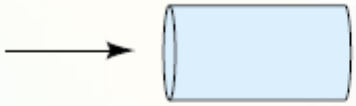

L/d	C_D
0.5	1.15
1	0.90
2	0.85
4	0.87
8	0.99

Ellipsoid:

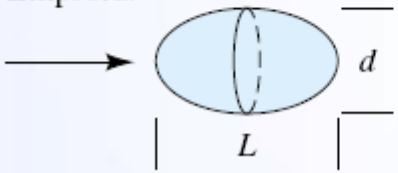

L/d	C_D Laminar	C_D Turbulent
0.75	0.5	0.2
1	0.47	0.2
2	0.27	0.13
4	0.25	0.1
8	0.2	0.08

- Aerodynamic force on road vehicles

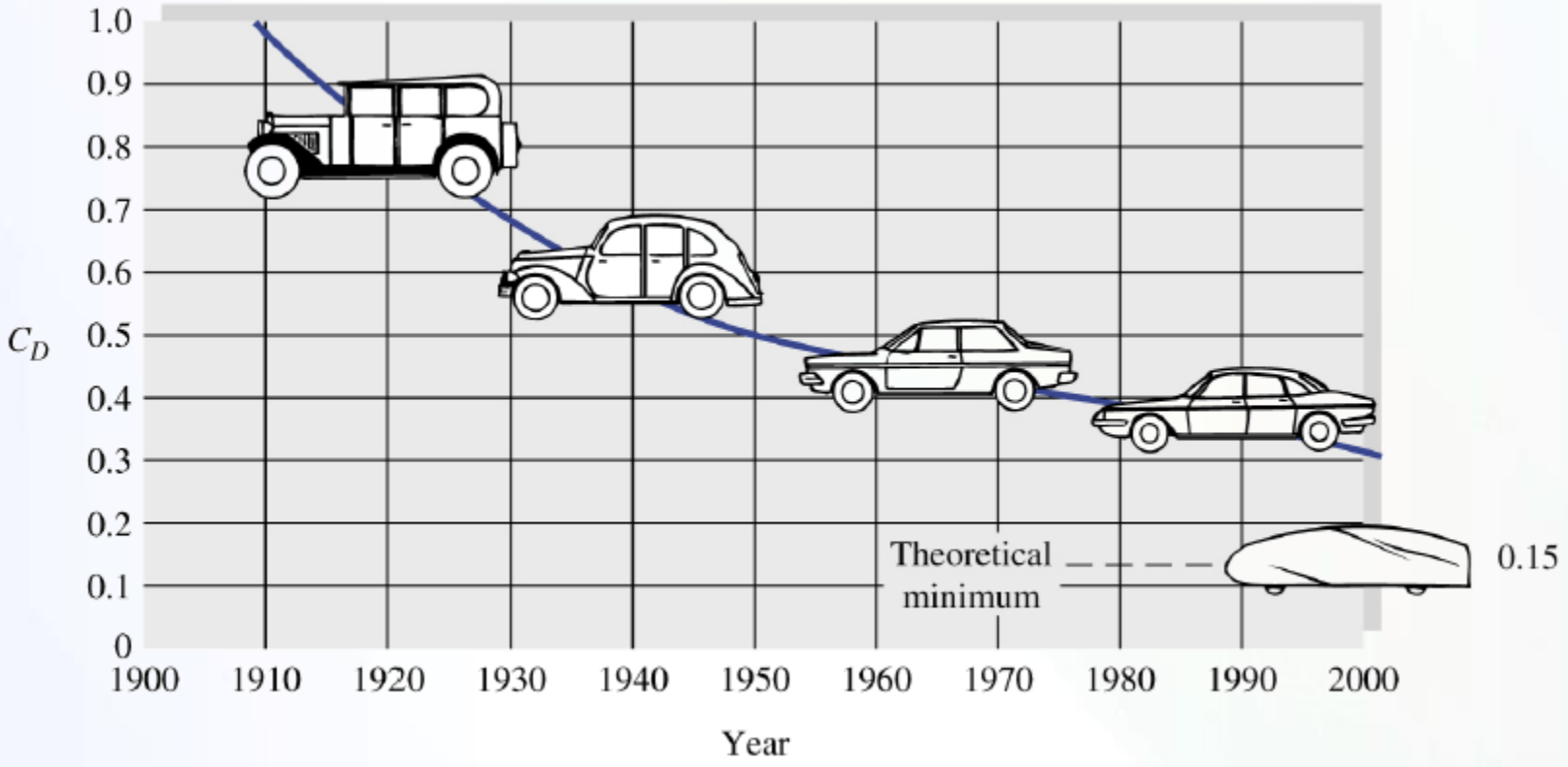

- Aerodynamics of automobiles

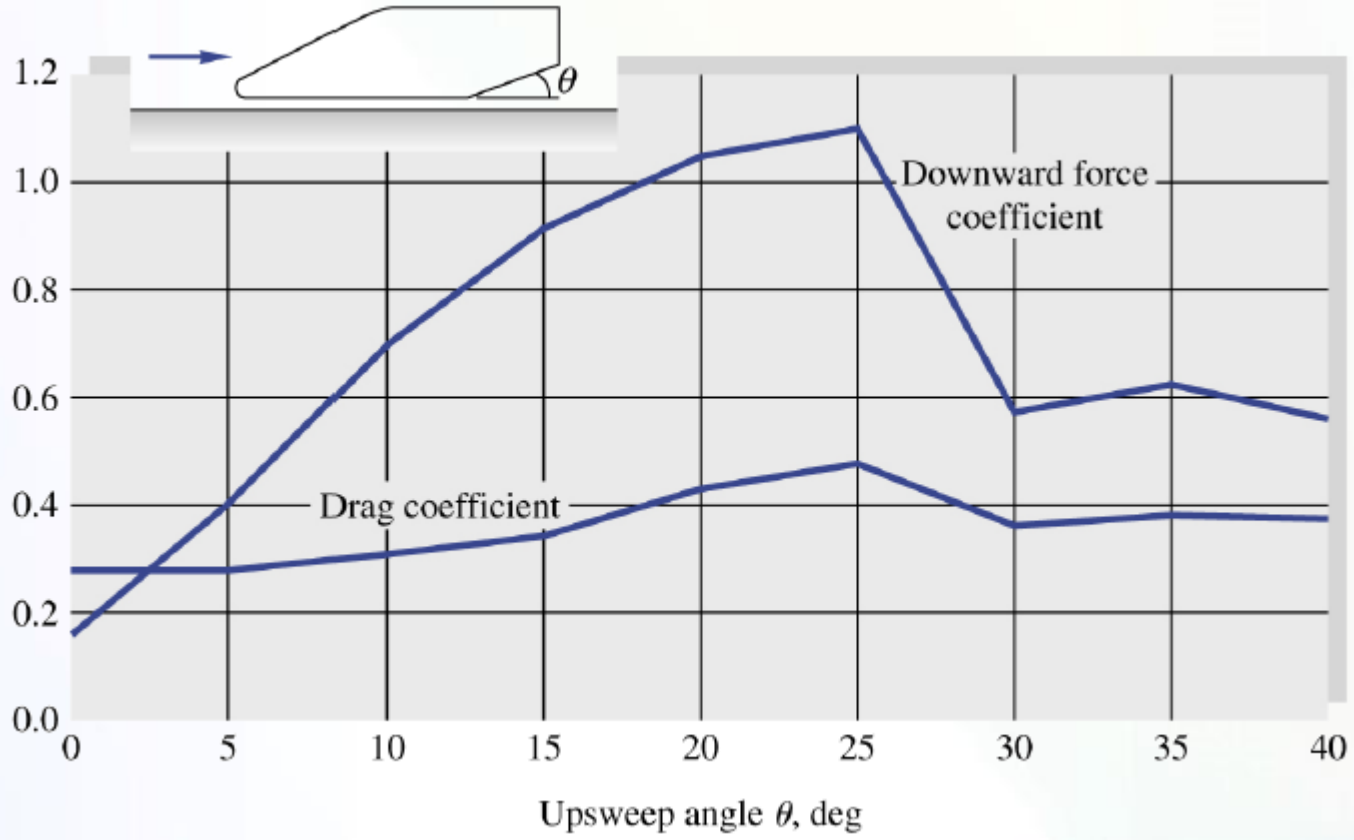

- Drag reduction of a tractor-trailer truck

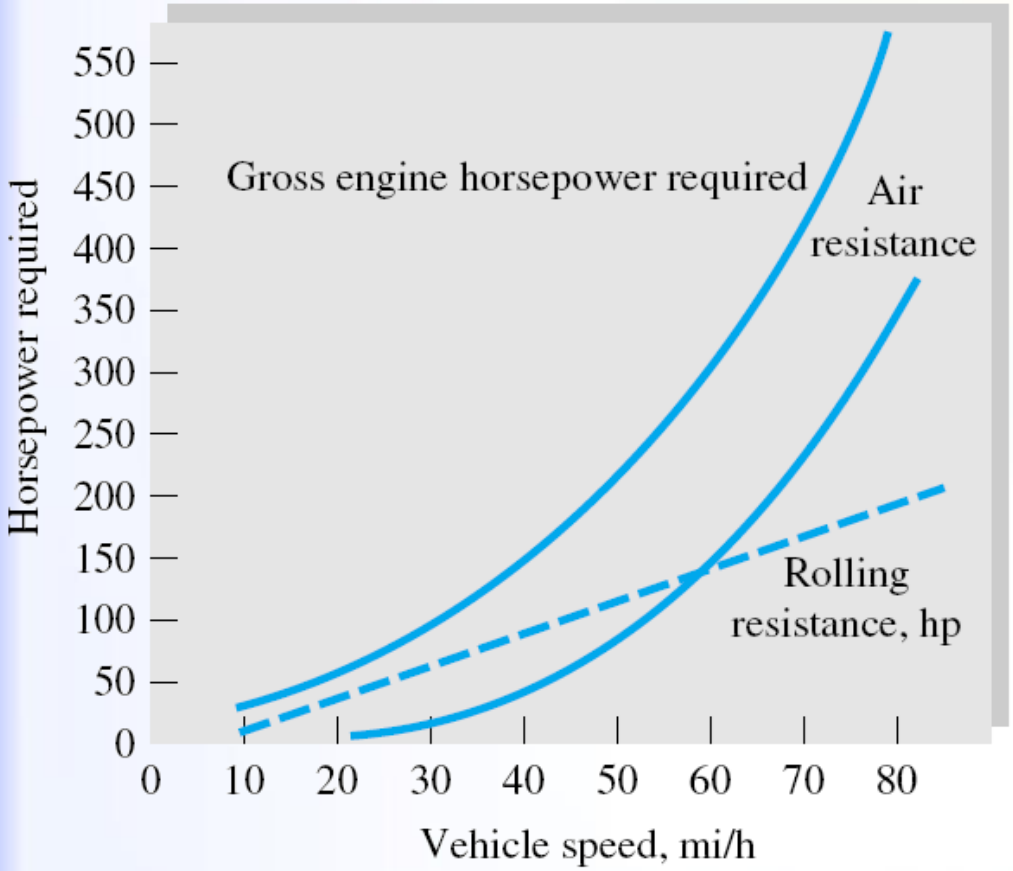

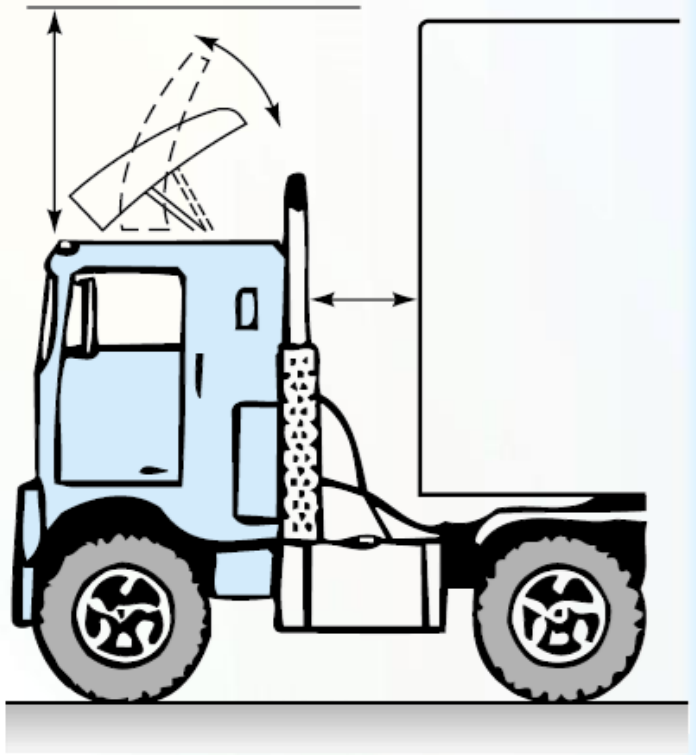

BIOLOGICAL DRAG REDUCTION

- A great deal of engineering effort goes into designing immersed bodies to reduce their drag. Most such effort concentrates on rigid-body shapes.

- A different process occurs in nature, as organisms adapt to survive high winds or currents. Flexible structure of a tree allows it to reconfigure in high winds and thus reduce drag and damage.

- as wind velocity increases, the shape of the tree changes to offer less Resistance.

U, m/s:	10	20	30	40
C_D:	1.2 ± 0.2	1.0 ± 0.2	0.7 ± 0.2	0.5 ± 0.2

BIOLOGICAL DRAG REDUCTION

- The individual branches and leaves of a tree also curl and cluster to reduce drag.

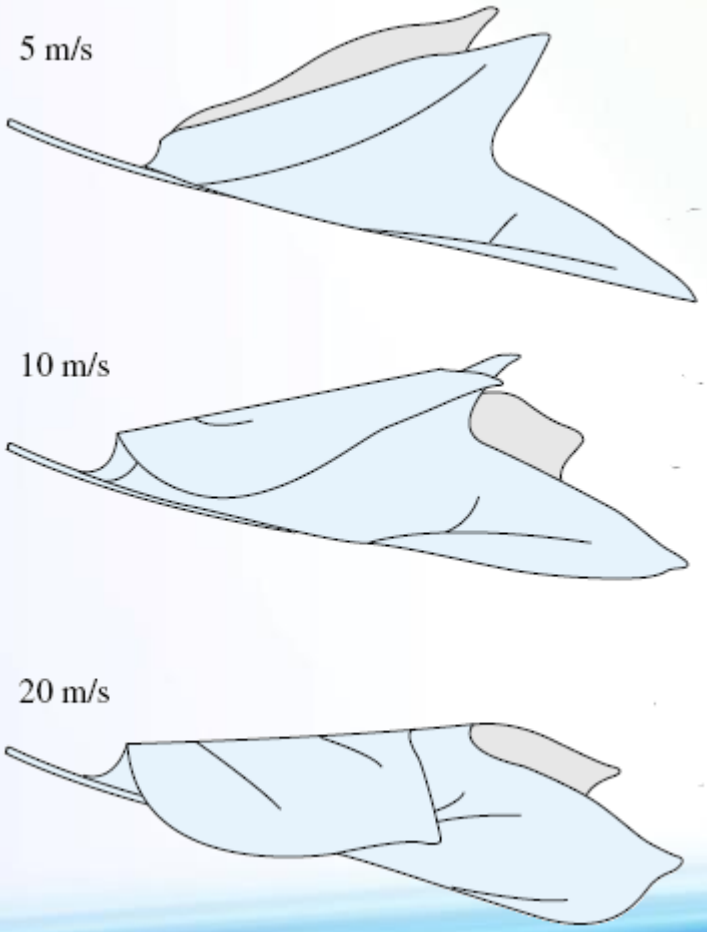

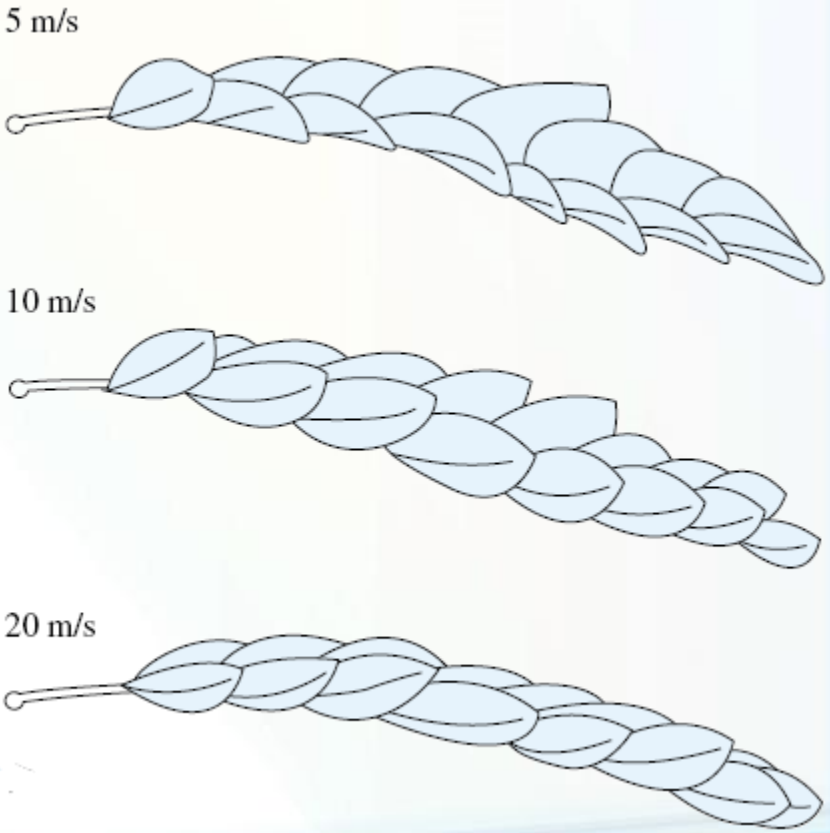

ESTIMATING SKIN-FRICTION DRAG OF A AIRFOIL

- We assume that skin-friction drag on an airfoil is essentially the same as the skin-friction drag on a flat plate at zero angle of attack.

- This approximation becomes more accurate the thinner the airfoil and the smaller the angle of attack.

ESTIMATING SKIN-FRICTION DRAG OF A AIRFOIL LAMINAR FLOW

- We first deal with the case of completely laminar flow over the airfoil (and hence the flat plate)

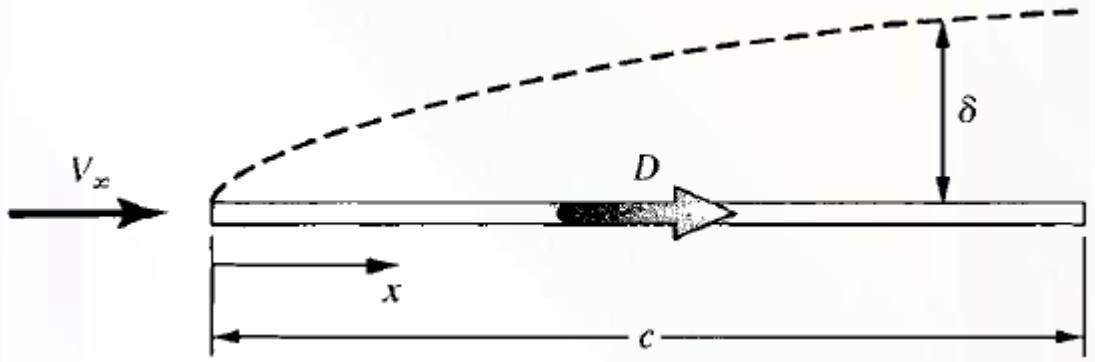

- There is an exact analytical solution for the laminar boundary-layer flow over a flat plate.

ESTIMATING SKIN-FRICTION DRAG OF A AIRFOIL LAMINAR FLOW

- The boundary-layer thickness for incompressible laminar flow over a flat plate at zero angle of attack is given by

$$\delta = \frac{5.0x}{\sqrt{\mathrm{Re}_x}}$$

Where

$$\mathrm{Re}_x = \frac{\rho_e V_\infty x}{\mu_\infty}$$

- The local shear stress, integrated over both the top and bottom surfaces of the flat plate, yields the net friction drag, D_f, on the plate

$$D_f = 2D_{f,\text{top}} = 2D_{f,\text{bottom}}$$

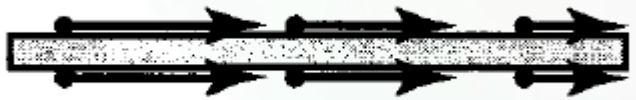

ESTIMATING SKIN-FRICTION DRAG OF A AIRFOIL LAMINAR FLOW

- Define the skin-friction drag coefficient for the flow over one surface as

$$C_f \equiv \frac{D_{f,\text{top}}}{q_\infty S} = \frac{D_{f,\text{bottom}}}{q_\infty S}$$

- The laminar skin-friction drag coefficient is a function of the Reynolds number

$$C_f = \frac{1.328}{\sqrt{\text{Re}_c}}$$

Where Re_c is the Reynolds number based on the chord length c.

$$\text{Re}_c = \frac{\rho_\infty V_\infty c}{\mu_\infty}$$

ESTIMATING SKIN-FRICTION DRAG OF A AIRFOIL LAMINAR FLOW (EXAMPLE)

Consider the NACA 2412 airfoil, data for which is given in Figure. The data are given for two values of the Reynolds number based on chord length. For the case where $Re_c = 3.1 \times 10^6$, estimate:

(a) the laminar boundary layer thickness at the trailing edge for a chord length of 1.5 m

(b) the net laminar skin-friction drag coefficient for the airfoil.

$$\delta = \frac{5.0c}{\sqrt{Re_c}} = \frac{(5.0)(1.5)}{\sqrt{3.1 \times 10^6}} = \boxed{0.00426 \text{ m}}$$

$$C_f = \frac{1.328}{\sqrt{Re_c}} = \frac{1.328}{\sqrt{3.1 \times 10^6}} = 7.54 \times 10^{-4}$$

$$\text{Net } C_f = 2(7.54 \times 10^{-4}) = \boxed{0.0015}$$

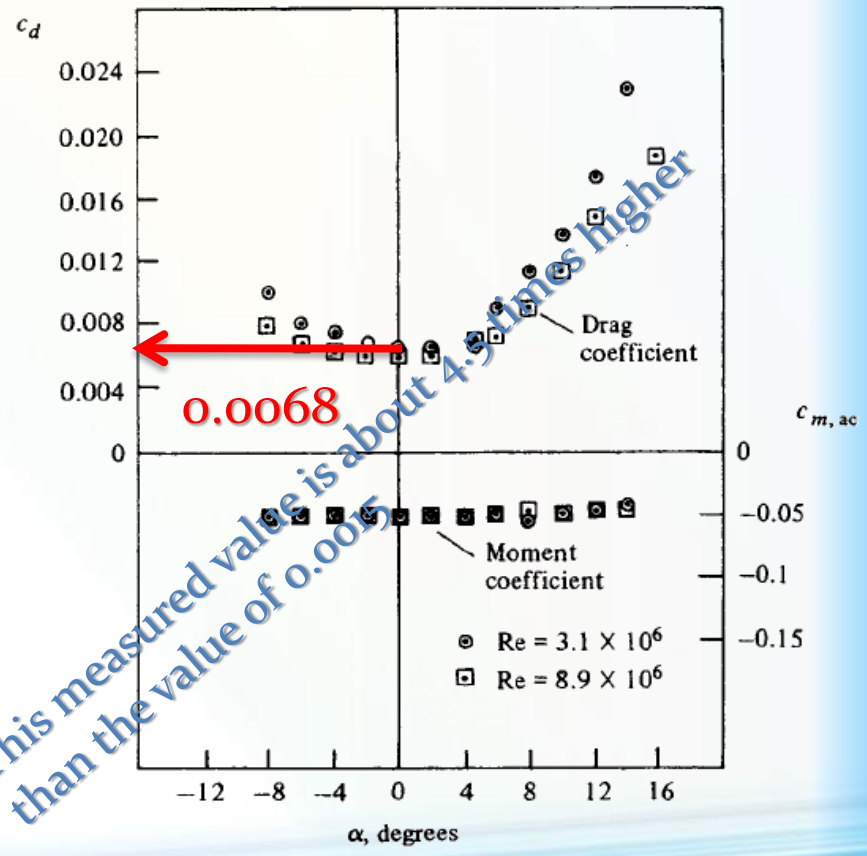

ESTIMATING SKIN-FRICTION DRAG OF A AIRFOIL TURBULENT FLOW

- There are no exact analytical solutions for turbulent flow.

- The analysis of any turbulent flow requires some amount of empirical data.

- All analyses of turbulent flow are approximate

ESTIMATING SKIN-FRICTION DRAG OF A AIRFOIL TURBULENT FLOW

- For incompressible flow over a flat plate, the boundary-layer thickness is given approximately by

$$\delta = \frac{0.37x}{\mathrm{Re}_x^{1/5}}$$

- With regard to skin friction drag, for incompressible turbulent flow over a flat plate, we have

$$C_f = \frac{0.074}{\mathrm{Re}_c^{1/5}}$$

- Note that, in contrast to the inverse square root variation with Reynolds number for laminar flow, the turbulent flow results show an inverse fifth root variation with Reynolds number

ESTIMATING SKIN-FRICTION DRAG OF A AIRFOIL TURBULENT FLOW (EXAMPLE)

Consider the NACA 2412 airfoil, data for which is given in Figure. The data are given for two values of the Reynolds number based on chord length. For the case where $Re_c = 3.1 \times 10^6$, estimate:

(a) the Turbulent boundary layer thickness at the trailing edge for a chord length of 1.5 m

(b) the net Turbulent skin-friction drag coefficient for the airfoil.

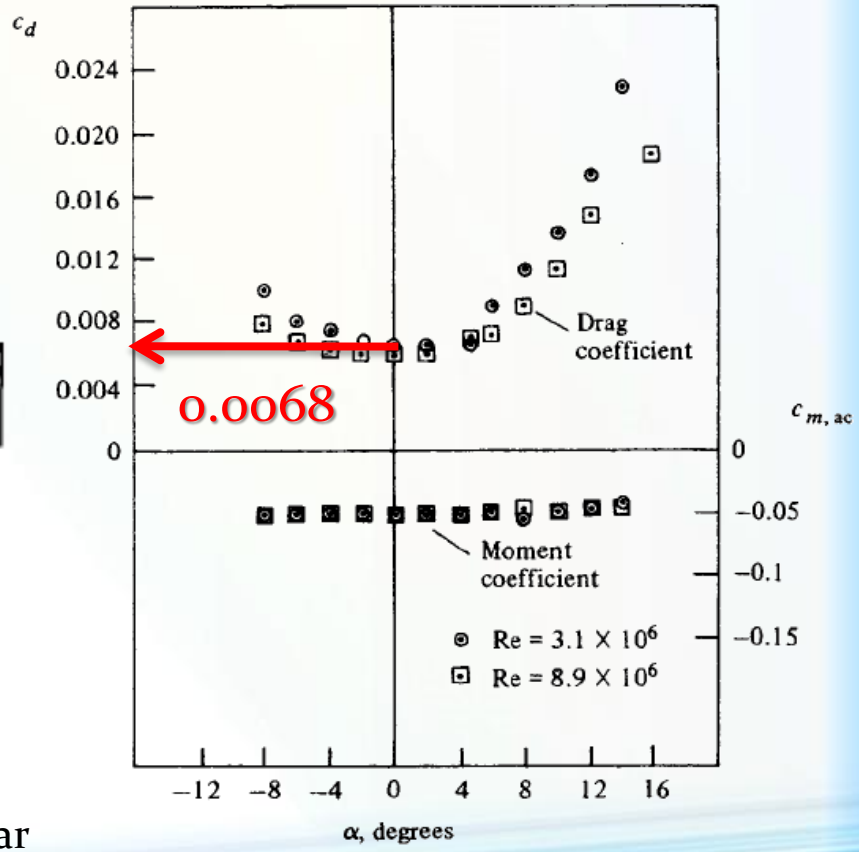

$$\delta = \frac{0.37x}{Re_x^{1/5}} = \frac{0.37(1.5)}{(3.1 \times 10^6)^{1/5}} = \boxed{0.0279 \text{ m}}$$

$$C_f = \frac{0.074}{Re_c^{1/5}} = \frac{0.074}{(3.1 \times 10^6)^{1/5}} = 0.00372$$

$$\text{Net } C_f = 2(0.00372) = \boxed{0.00744}$$

This result is a factor of five larger than for the laminar boundary layer

ESTIMATING SKIN-FRICTION DRAG OF A AIRFOIL TURBULENT FLOW

- The result for the skin friction drag coefficient in the previous example is larger than the measured drag coefficient of the airfoil of 0.0068, which is the sum of both skin friction drag and pressure drag due to flow separation. So our result in this example clearly overestimates the skin friction drag coefficient for the airfoil.

ESTIMATING SKIN-FRICTION DRAG OF A AIRFOIL LAMINAR/TURBULENT FLOW

- In actuality, the boundary layer over a body always starts out as a laminar boundary for some distance from the leading edge, and then transits to a turbulent boundary layer at some point downstream of the leading edge.

- The skin-friction drag is a combination of laminar skin friction over the forward part of the airfoil, and turbulent skin friction over the remaining part.

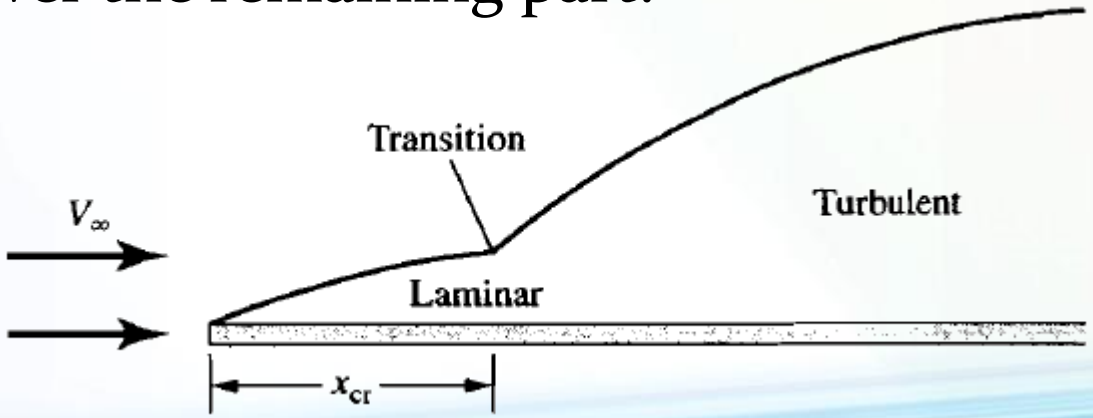

ESTIMATING SKIN-FRICTION DRAG OF A AIRFOIL LAMINAR/TURBULENT FLOW

- The value of x where transition is said to take place is the critical value x_{cr} . In turn, x_{cr} allows the definition of a critical Reynolds number for transition as

$$\mathrm{Re}_{x_{cr}} = \frac{\rho_\infty V_\infty x_{cr}}{\mu_\infty}$$

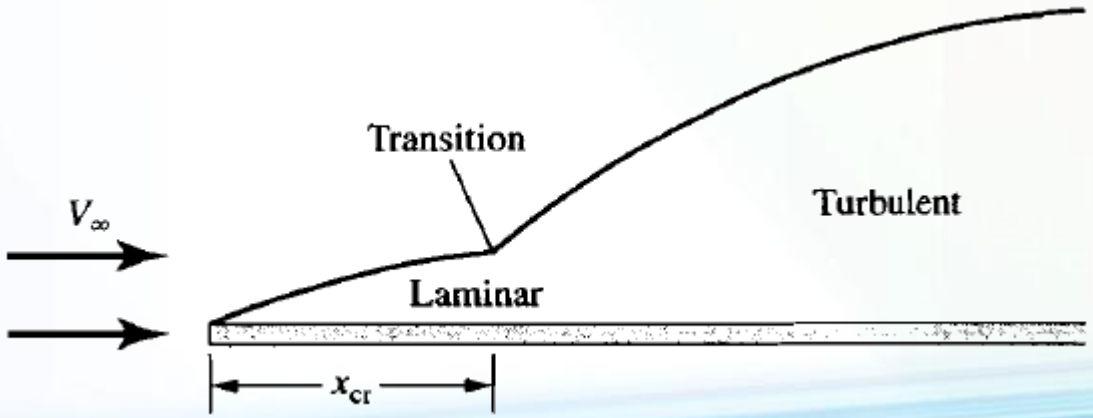

ESTIMATING SKIN-FRICTION DRAG OF A AIRFOIL LAMINAR/TURBULENT FLOW (EXAMPLE)

- For the NACA 2412 airfoil and the conditions in previous example, calculate the net skin friction drag coefficient assuming that the critical Reynolds number is 500,000.

$$\mathrm{Re}_{x_{cr}} = \frac{\rho_\infty V_\infty x_1}{\mu_\infty} = 5 \times 10^5$$

$$\mathrm{Re}_c = \frac{\rho_\infty V_\infty c}{\mu_\infty} = 3.1 \times 10^6$$

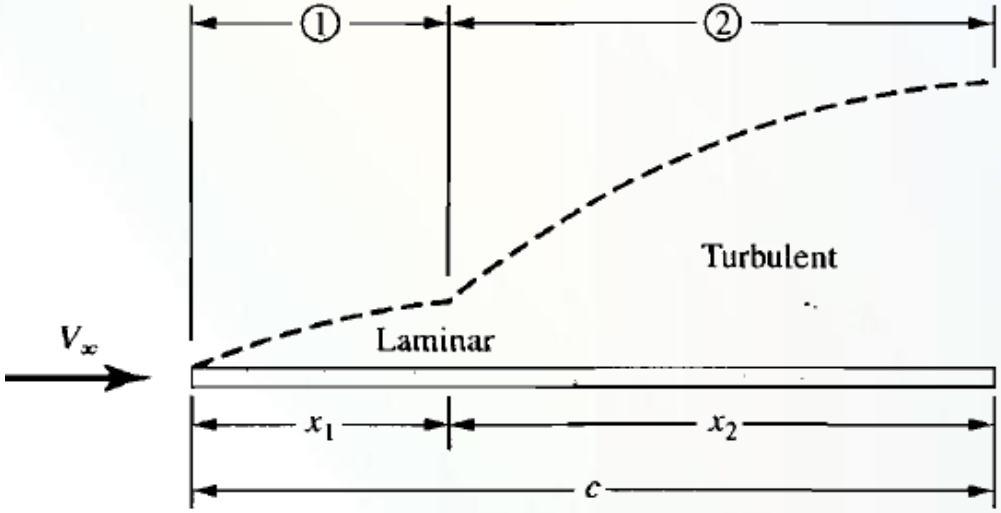

$$\frac{\mathrm{Re}_{x_{cr}}}{\mathrm{Re}_c} = \frac{5 \times 10^5}{3.1 \times 10^6} = 0.1613 = \frac{(\rho_\infty V_\infty x_1/\mu_\infty)}{(\rho_\infty V_\infty c/\mu_\infty)} = \frac{x_1}{c} \quad \Rightarrow \quad \frac{x_1}{c} = 0.1613$$

ESTIMATING SKIN-FRICTION DRAG OF A AIRFOIL LAMINAR/TURBULENT FLOW (EXAMPLE)

- Assuming all turbulent flow over the entire length of the plate, the drag (on one side of the plate) is $(D_{f,c})_{turbulent}$ where

$$(D_{f,c})_{\text{turbulent}} = q_\infty S (C_{f,c})_{\text{turbulent}}$$

$$S = c(1) \quad \Rightarrow \quad (D_{f,c})_{\text{turbulent}} = q_\infty c (C_{f,c})_{\text{turbulent}}$$

- The turbulent drag on just region 1 is

$$(D_{f,1})_{\text{turbulent}} = q_\infty x_1 (C_{f,1})_{\text{turbulent}}$$

- And the turbulent drag just on region 2 is:

$$(D_{f,2})_{\text{turbulent}} = (D_{f,c})_{\text{turbulent}} - (D_{f,1})_{\text{turbulent}}$$

$$(D_{f,2})_{\text{turbulent}} = q_\infty c (C_{f,c})_{\text{turbulent}} - q_\infty x_1 (C_{f,1})_{\text{turbulent}}$$

ESTIMATING SKIN-FRICTION DRAG OF A AIRFOIL LAMINAR/TURBULENT FLOW (EXAMPLE)

- The laminar drag on region 1 is:

$$(D_{f,1})_{\text{laminar}} = q_\infty S (C_{f,1})_{\text{laminar}} = q_\infty x_1 (C_{f,1})_{\text{laminar}}$$

- The total skin-friction drag on the plate, D_f, is then

$$D_f = (D_{f,1})_{\text{laminar}} + (D_{f,2})_{\text{turbulent}}$$

$$D_f = q_\infty x_1 (C_{f,1})_{\text{laminar}} + q_\infty c (C_{f,c})_{\text{turbulent}} - q_\infty x_1 (C_{f,1})_{\text{turbulent}}$$

- The total skin-friction drag coefficient is

$$C_f = \frac{D_f}{q_\infty S} = \frac{D_f}{q_\infty c}$$

$$C_f = \frac{x_1}{c}(C_{f,1})_{\text{laminar}} + (C_{f,c})_{\text{turbulent}} - \frac{x_1}{c}(C_{f,1})_{\text{turbulent}}$$

ESTIMATING SKIN-FRICTION DRAG OF A AIRFOIL LAMINAR/TURBULENT FLOW (EXAMPLE)

$$C_f = \frac{x_1}{c}(C_{f,1})_{\text{laminar}} + (C_{f,c})_{\text{turbulent}} - \frac{x_1}{c}(C_{f,1})_{\text{turbulent}}$$

$x_1/c = 0.1613$ ⇒ $C_f = 0.1613(C_{f,1})_{\text{laminar}} + (C_{f,c})_{\text{turbulent}} - 0.1613(C_{f,1})_{\text{turbulent}}$

$$(C_{f,1})_{\text{laminar}} = \frac{1.328}{\sqrt{\text{Re}_{x_1}}} = \frac{1.328}{\sqrt{5 \times 10^5}} = 0.00188$$

$$(C_{f,c})_{\text{turbulent}} = 0.00372 \quad \text{(for one side)}$$

$$(C_{f,1})_{\text{turbulent}} = \frac{0.074}{\text{Re}_{x_1}^{1/5}} = \frac{0.074}{(5 \times 10^5)^{0.2}} = 0.00536$$

$$C_f = 0.1613(0.00188) + 0.00372 - 0.1613(0.00536) = 0.003158$$

$$\text{Net } C_f = 2(0.003158) = \boxed{0.0063}$$

ESTIMATING SKIN-FRICTION DRAG OF A AIRFOIL LAMINAR/TURBULENT FLOW

- the measured airfoil drag coefficient is 0.0068, which includes both skin friction drag and pressure drag due to flow separation. The result from Example, therefore, is qualitatively reasonable,. giving a skin friction drag coefficient slightly less than the measure total drag coefficient.

- We do not know what the critical Reynolds number is for the experiments.

ESTIMATING SKIN-FRICTION DRAG OF A AIRFOIL LAMINAR/TURBULENT FLOW (EXAMPLE)

- Repeat the example but assuming the critical Reynolds number is 1 x 10^6.

$$\frac{x_1}{c} = \frac{1 \times 10^6}{3.1 \times 10^6} = 0.3226$$

$$C_f = 0.3226(C_{f,1})_{\text{laminar}} + (C_{f,c})_{\text{turbulent}} - 0.3226(C_{f,1})_{\text{turbulent}}$$

$$(C_{f,1})_{\text{laminar}} = \frac{1.328}{\sqrt{\text{Re}_{x_1}}} = \frac{1.328}{\sqrt{1 \times 10^6}} = 0.00042$$

$$(C_{f,c})_{\text{turbulent}} = 0.00372$$

$$(C_{f,1})_{\text{turbulent}} = \frac{0.074}{(\text{Re}_{x_1})^{1/5}} = \frac{0.074}{(1 \times 10^6)^{1/5}} = 0.002946$$

$$C_f = 0.3226(0.00042) + 0.00372 - 0.3226(0.002946) = 0.00291$$

$$\text{Net } C_f = 2(0.00291) = \boxed{0.00582}$$

ESTIMATING SKIN-FRICTION DRAG OF A AIRFOIL LAMINAR/TURBULENT FLOW (EXAMPLE)

- Comparing the results from the recent two Examples, we see that an increase in Re_{cr} from 500,000 to 1,000,000 resulted in a skin friction drag coefficient that is eight percent smaller. This difference underscores the importance of knowing where transition takes place on a surface for the calculation of skin friction drag.

- The result from the last example CF = 0.00582 would imply that the pressure drag due to flow separation is about 15 percent of the total drag.

- The drag on a streamlined two-dimensional shape is mostly skin friction drag, and by comparison the pressure drag is small.

INCOMPRESSIBLE FLOW OVER FINITE WINGS

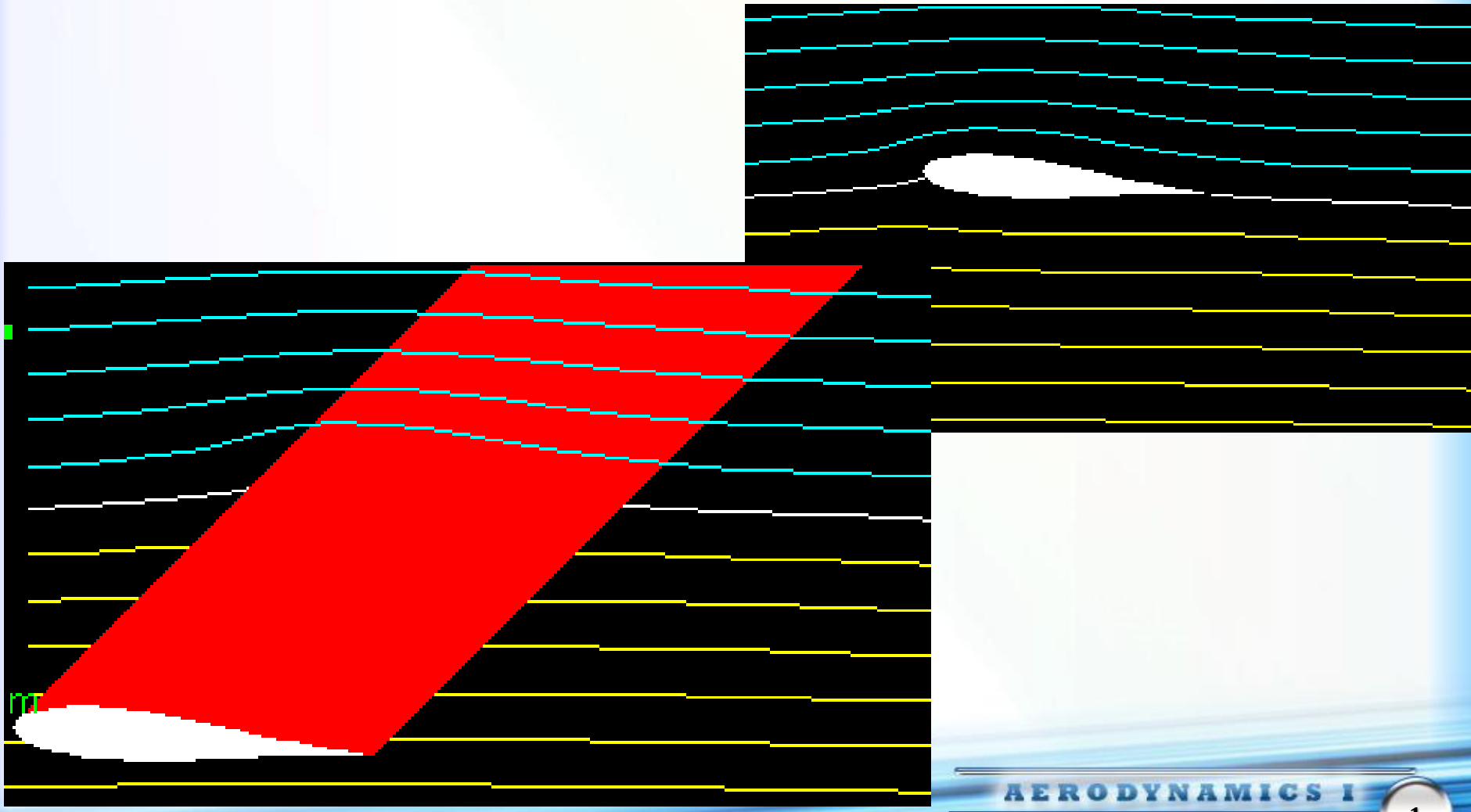

AIRFOILS AND WINGS

- The properties of *airfoils* are the same as the properties of a *wing of infinite span*.

- All real airplanes have wings of *finite span*, and our purpose is to apply our knowledge of airfoil properties to the analysis of finite wings.

AIRFOILS AND WINGS

- ***Question:*** *Why are the aerodynamic characteristics of a finite wing any different from the properties of its airfoil sections?*

- The flow over an airfoil is two-dimensional.

- A finite wing is a three-dimensional body, and consequently the flow over the finite wing is three-dimensional; that is, there is a component of flow in the spanwise direction.

THREE-DIMENSIONAL FLOW OVER A FINITE WING

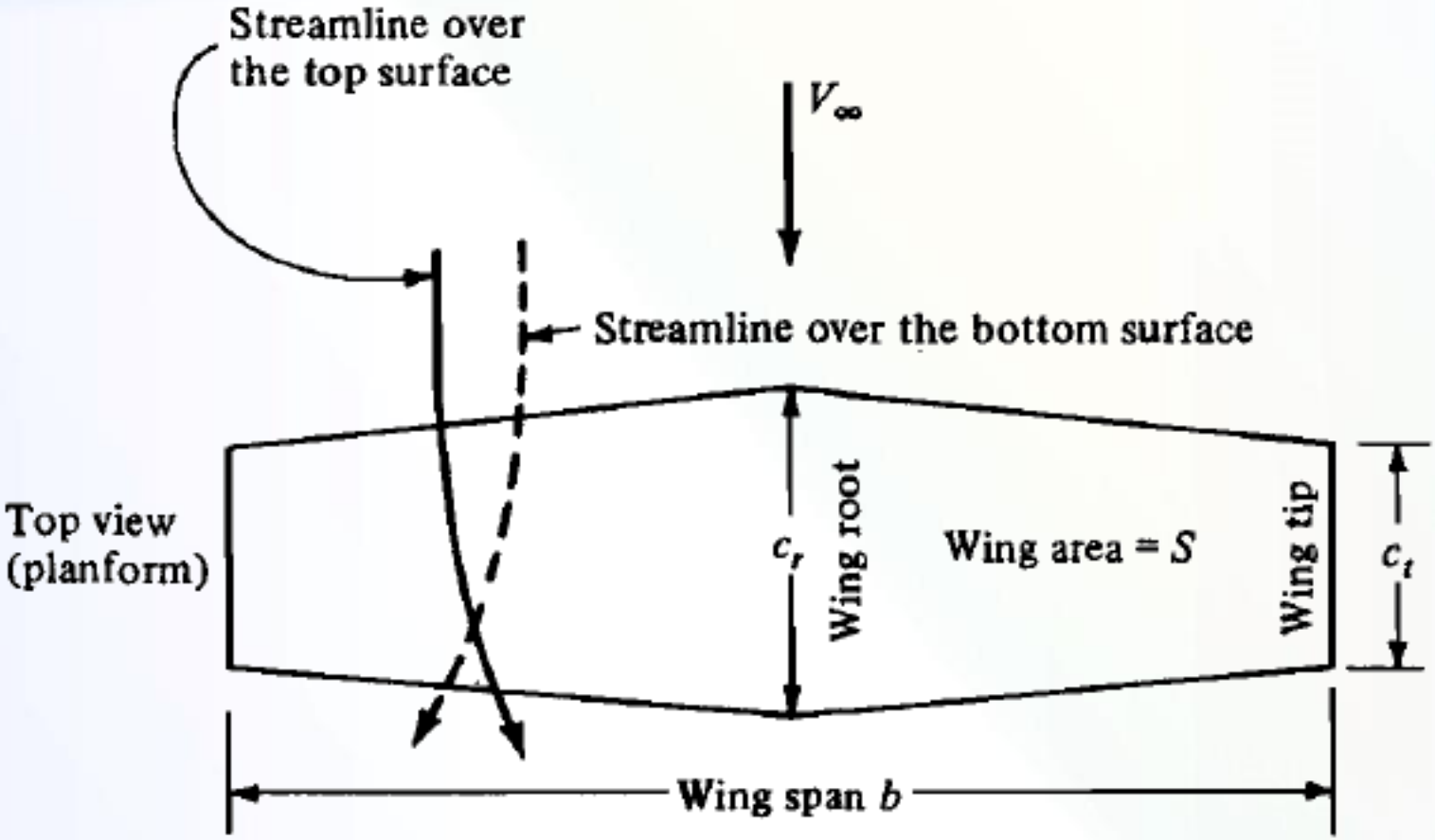

LIFT GENERATION BY WINGS

- The physical mechanism for generating lift on the wing is the existence of a high pressure on the bottom surface and a low pressure on the top surface.

- The net imbalance of the pressure distribution creates the lift.

WING-TIP VORTEX

- As a by-product of this pressure imbalance, the flow near the wing tips tends to curl around the tips, being forced from the high-pressure region just underneath the tips to the low-pressure region on top.

WING-TIP VORTEX

- As a result, on the top surface of the wing, there is generally a spanwise component of flow from the tip toward the wing root, causing the streamlines over the top surface to bend toward the root.

- On the bottom surface of the wing, there is generally a spanwise component of flow from the root toward the tip, causing the streamlines over the bottom surface to bend toward the tip.

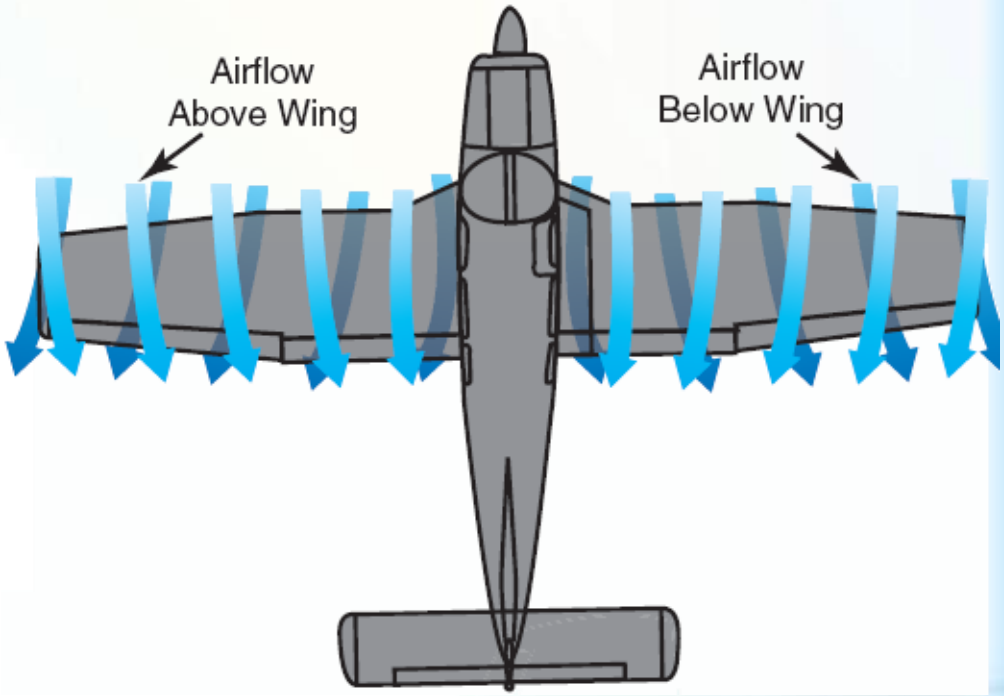

WING-TIP VORTEX

- The tendency for the flow to "leak" around the wing tips establishes a circulatory motion that trails downstream of the wing; that is, a trailing *vortex* is created at each wing tip.

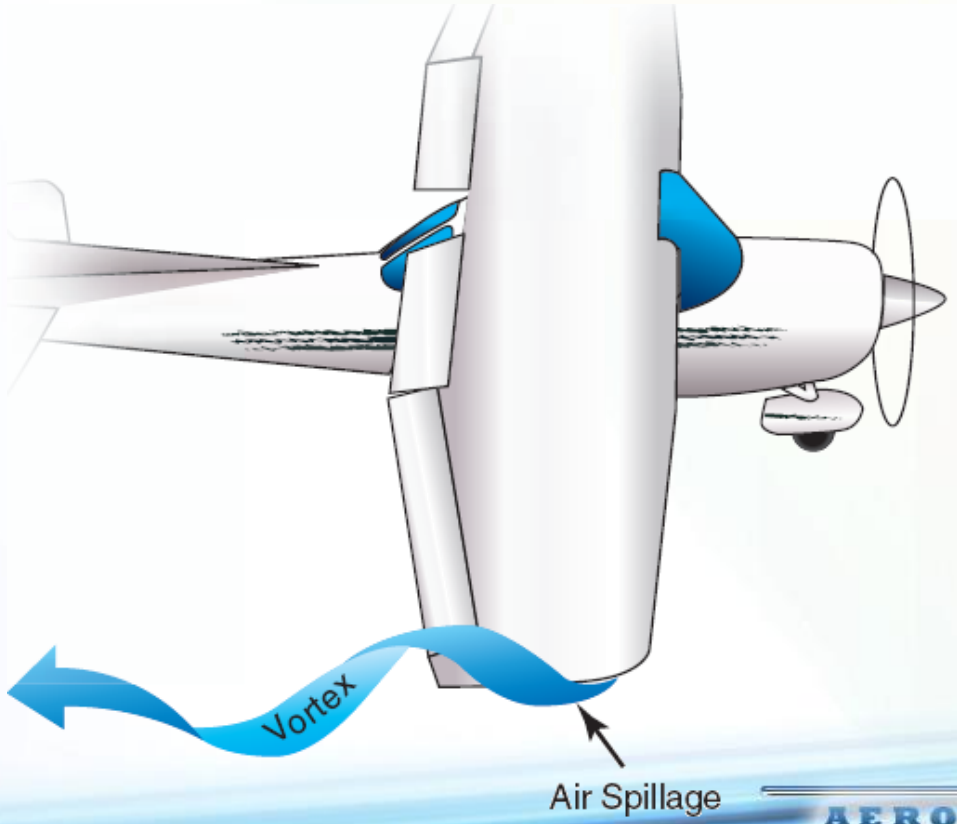

WING-TIP VORTEX

- The tip vortices are essentially weak "tornadoes“ that trail downstream of the finite wing.

- For large airplanes such as a Boeing 747, these tip vortices can be powerful enough to cause light airplanes following too closely to go out of control.

- This is one reason for large spacings between aircraft landing or taking off consecutively at airports.

DOWNWASH

- The two vortices tend to drag the surrounding air around with them, and this secondary movement induces a small velocity component in the downward direction at the wing.

- This downward component is called *downwash*, denoted by the symbol *w*.

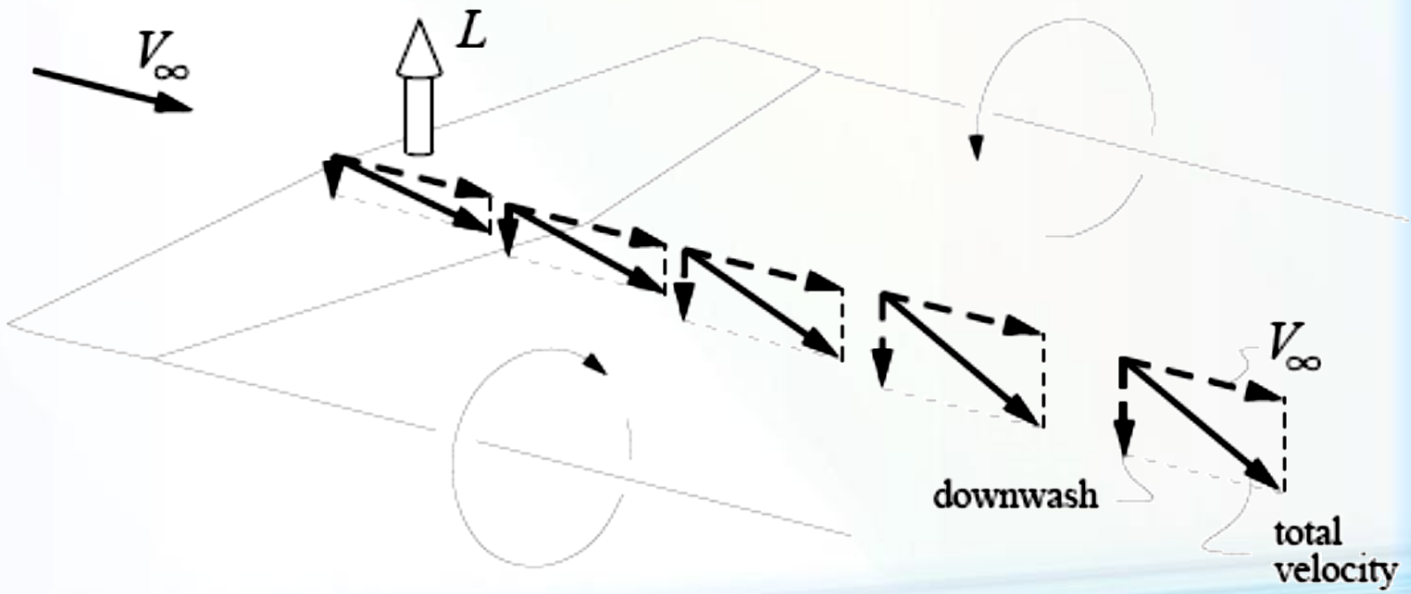

DOWNWASH

- The downwash combines with the freestream velocity V_∞ to produce a local relative wind which is canted downward in the vicinity of each airfoil section of the wing.

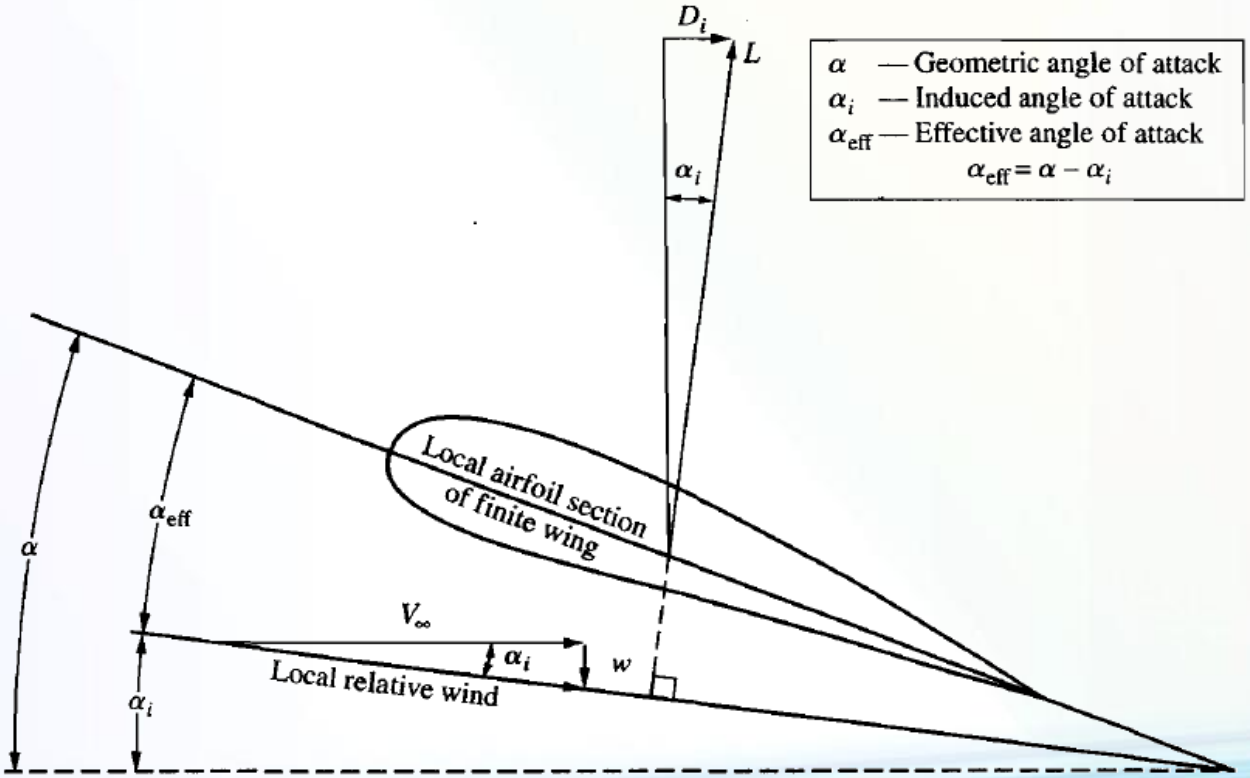

INDUCED DRAG

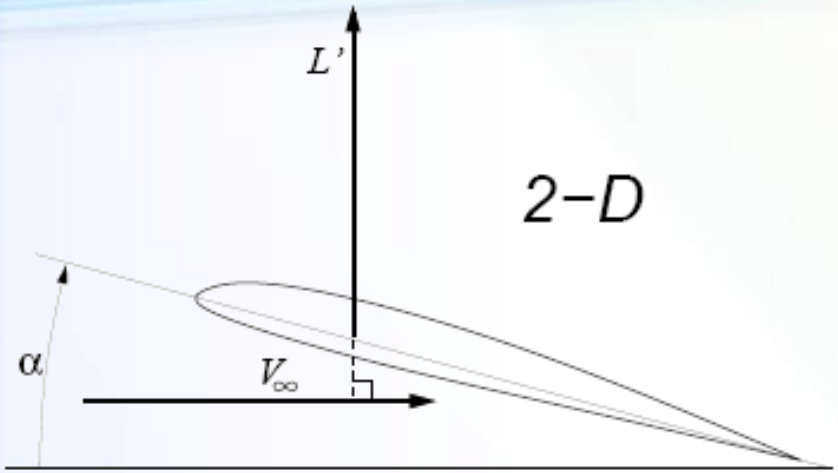

$$F' = \rho V_\infty \Gamma$$

$$L' = F' \cos\alpha_i \simeq F' = \rho V_\infty \Gamma$$

$$D_i' = F' \sin\alpha_i \simeq F'\alpha_i = -\rho w \Gamma$$

$$\alpha_i = \arctan\frac{-w}{V_\infty} \simeq \frac{-w}{V_\infty}$$

$|w| \ll V_\infty$

$$\alpha_{\text{eff}} = \alpha - \alpha_i$$

$$V_{\text{eff}} = \sqrt{V_\infty^2 + w^2} \simeq V_\infty$$

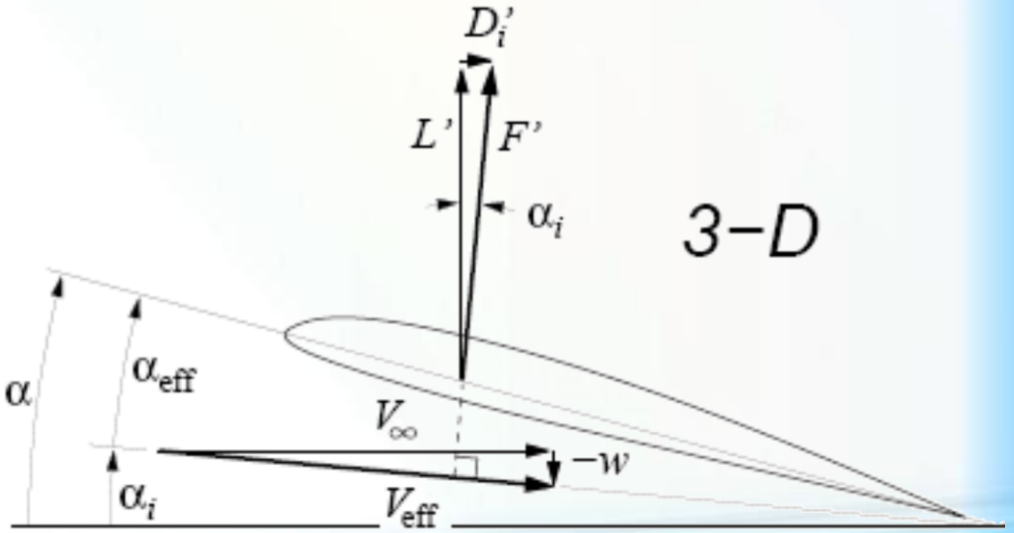

- Defining the profile drag coefficient as

$$c_d = \frac{D_f + D_p}{q_\infty S}$$

and the induced drag coefficient as

$$C_{D,i} = \frac{D_i}{q_\infty S}$$

the total drag coefficient for the finite wing C_D is given by

$$C_D = c_d + C_{D,i}$$

THE VORTEX FILAMENT

$$V_\theta = \frac{\Gamma}{2\pi r}$$

$$V_r = 0$$

$$V_z = 0$$

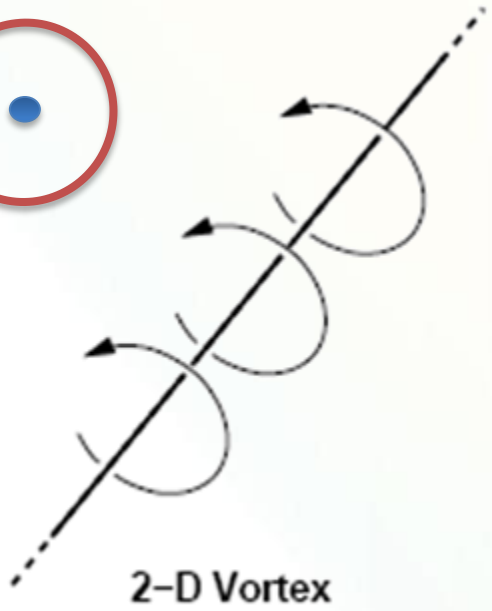

HELMHOLTZ'S THEOREMS

A general 3-D vortex can take any arbitrary shape. It is subject to the *Helmholtz's Vortex Theorems*:

1) The strength Γ of a vortex filament is constant all along its length.
2) The vortex filament cannot end inside the fluid. It must either
   a) extend to $\pm\infty$, or
   b) end at a solid boundary, or
   c) form a closed loop.

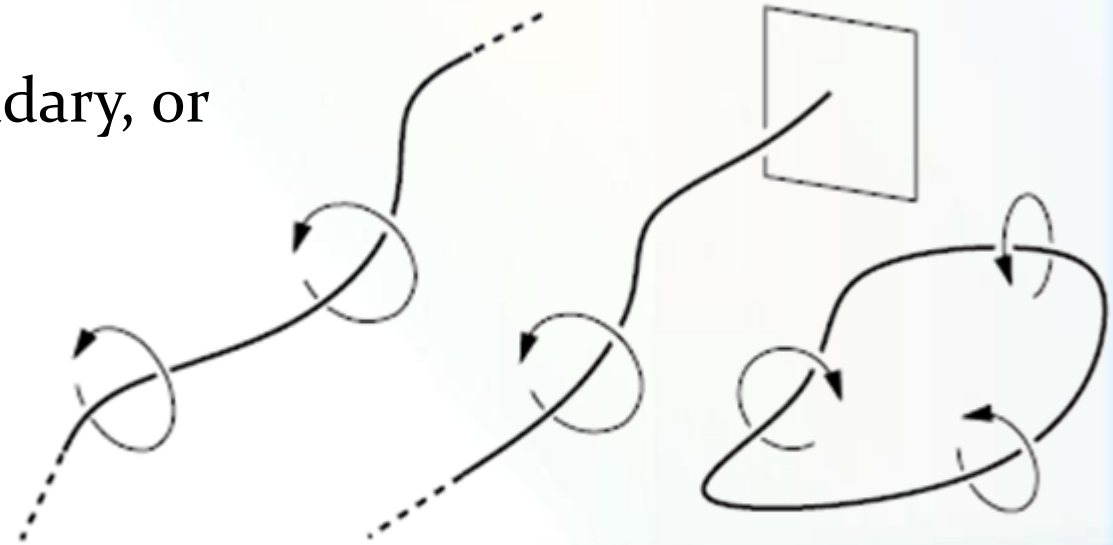

3–D Vortices

THE BIOT-SAVART LAW

The velocity field of a vortex of general shape is given by the *Biot-Savart Law*.

$$\vec{V}(x,y,z) = \frac{\Gamma}{4\pi}\int_{-\infty}^{+\infty}\frac{d\vec{\ell}\times\vec{r}}{|\vec{r}|^3} \qquad \text{(general 3-D vortex)}$$

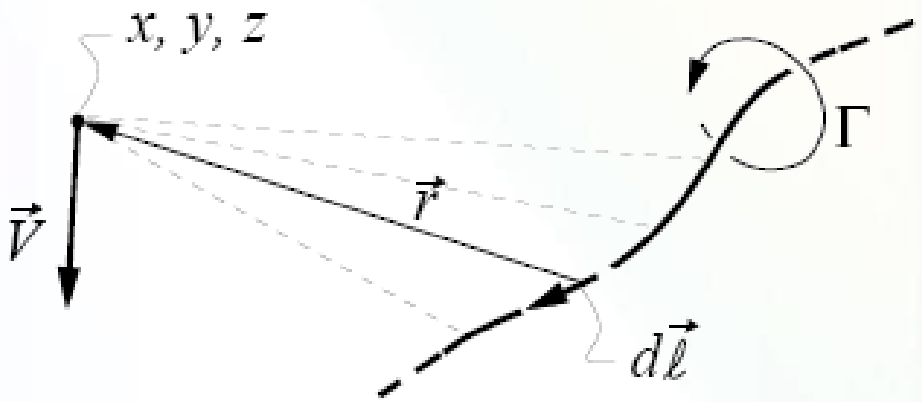

The magnetic field strength ***dB*** induced at point *P by a segment of the wire dl* with the current moving in the direction of ***dl*** is

$$\mathbf{dB} = \frac{\mu I}{4\pi}\frac{\mathbf{dl}\times\mathbf{r}}{|\mathbf{r}|^3}$$

where μ is the permeability

STRAIGHT-VORTEX FILAMENT

$$r \equiv |\vec{r}| = \frac{h}{\sin\theta}$$

$$\ell = -\frac{h}{\tan\theta}$$

$$d\ell = \frac{h}{\sin^2\theta}\, d\theta$$

$$d\vec{\ell} \times \vec{r} = (d\ell\, r\, \sin\theta)\, \hat{\theta}$$

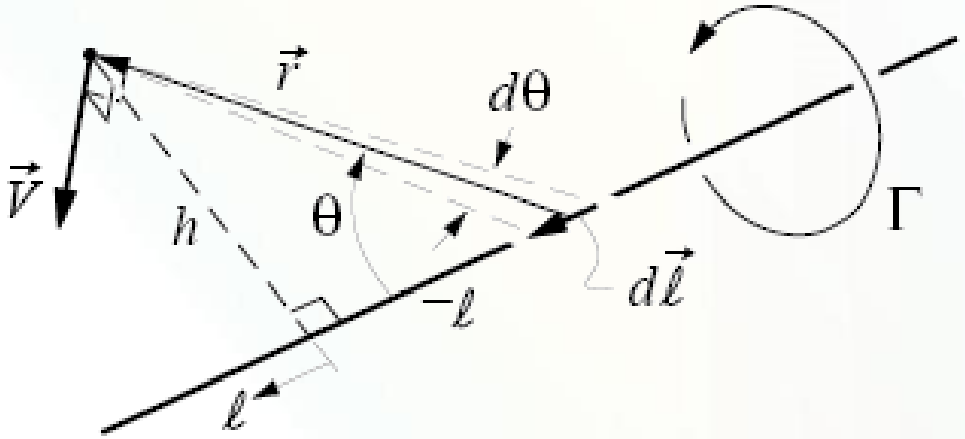

$$\vec{V}(x,y,z) = \frac{\Gamma}{4\pi}\int_{-\infty}^{+\infty}\frac{d\vec{\ell}\times\vec{r}}{|\vec{r}|^3}$$

$$\vec{V} = \frac{\Gamma}{4\pi h}\,\hat{\theta}\int_0^{\pi}\sin\theta\, d\theta = \frac{\Gamma}{2\pi h}\,\hat{\theta}$$

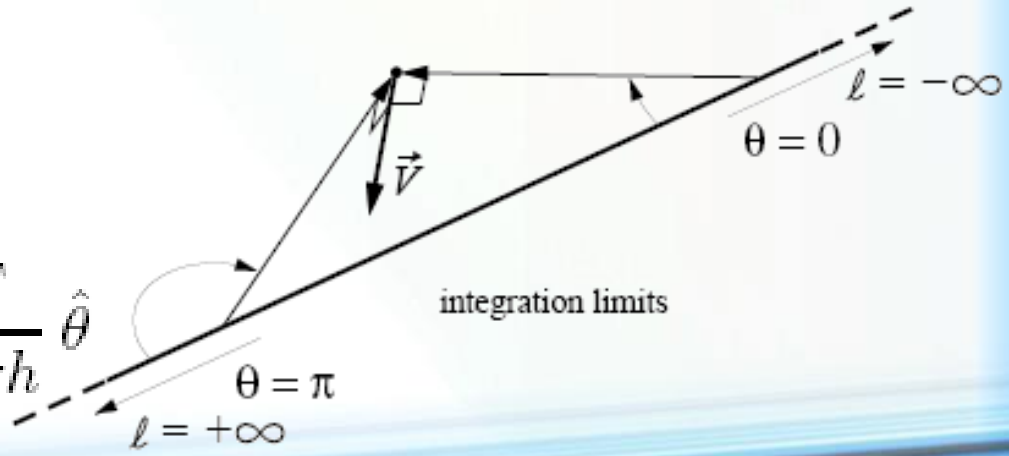

STRAIGHT-VORTEX FILAMENT

Consider the semi-infinite vortex filament shown in Figure. The filament extends from point A to ∞.

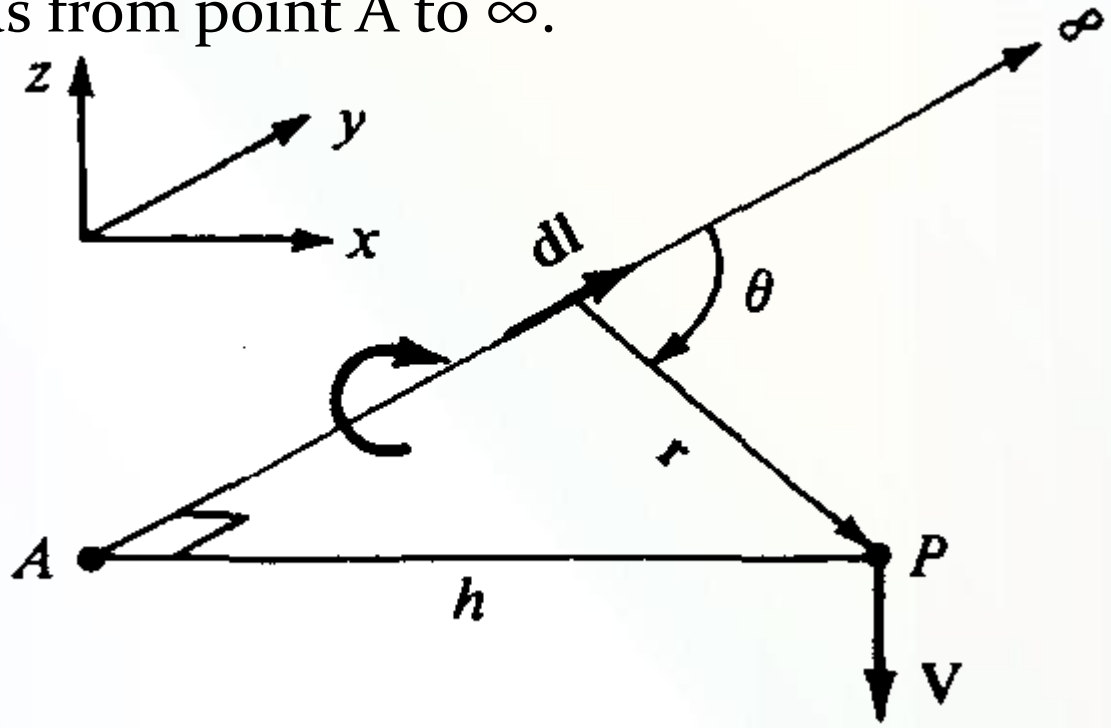

$$\vec{V} = \frac{\Gamma}{4\pi h}\hat{\theta}\int_0^{\frac{\pi}{2}} \sin\theta\, d\theta = \frac{\Gamma}{4\pi h}\hat{\theta}$$

Wing vortex model

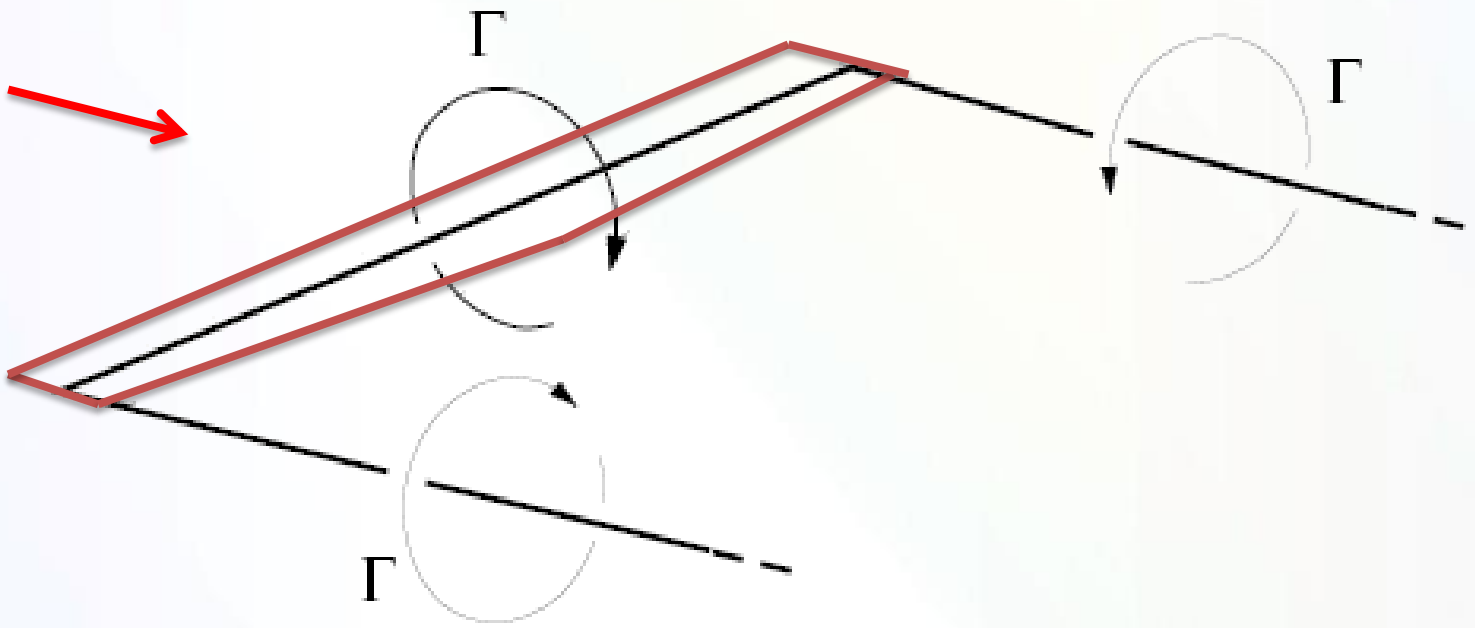

Horseshoe vortex

LIFTING-LINE THEORY

- A vortex filament of strength Γ that is somehow bound to a fixed location in a flow (*bound vortex*) will experience a force $L'=\rho_\infty V_\infty \Gamma$ from the Kutta-Joukowski theorem.

- The bound vortex is in contrast to a *free vortex*, which moves with the same fluid elements throughout a flow.

LIFTING-LINE THEORY

- Let us replace a finite wing of span b with a bound vortex, extending from y = -b/2 to y = b/2. Assume the vortex filament continues as two free vortices trailing downstream from the wing tips to infinity.

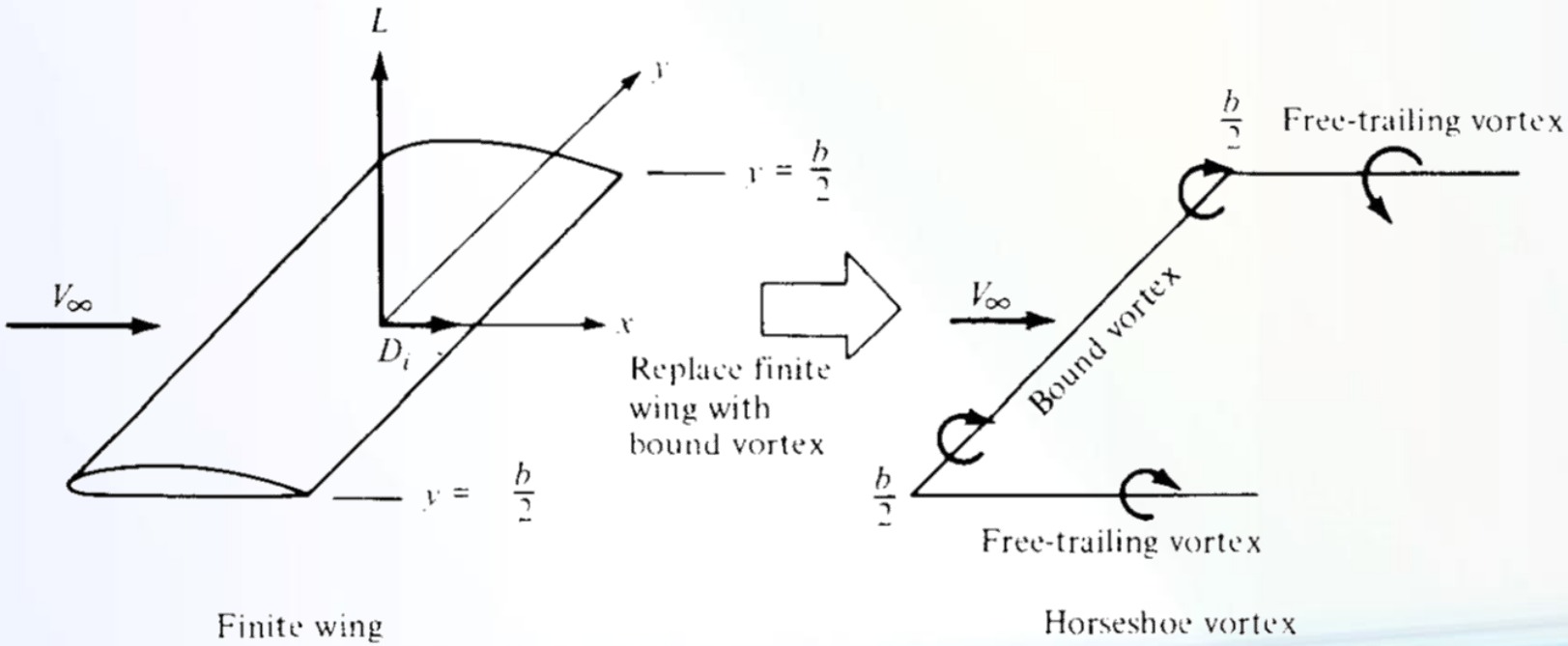

LIFTING-LINE THEORY

$$L' = \rho V_\infty \Gamma$$

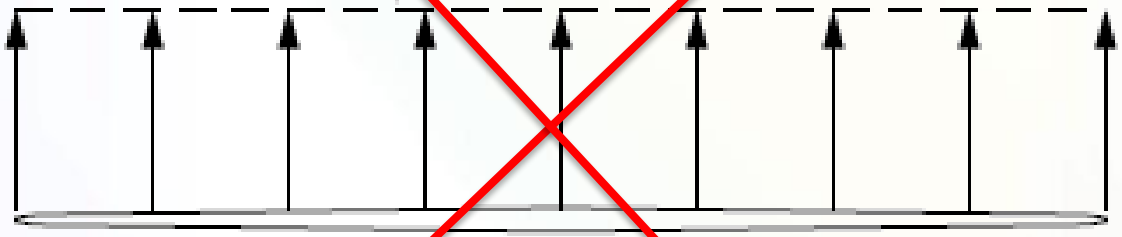

$$L'(y) = \rho V_\infty \Gamma(y)$$

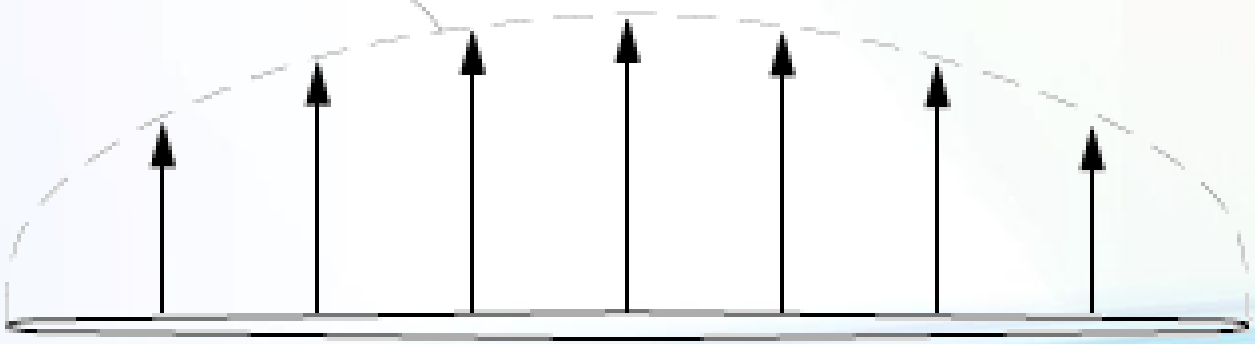

LIFTING-LINE THEORY

- Consider the downwash w induced along the bound vortex from -b/2 to b/2 by the horseshoe vortex.

  The bound vortex induces no velocity along itself

  The two trailing vortices both contribute to the induced velocity.

$$w(y) = -\frac{\Gamma}{4\pi(b/2 + y)} - \frac{\Gamma}{4\pi(b/2 - y)}$$

$$w(y) = -\frac{\Gamma}{4\pi}\frac{b}{(b/2)^2 - y^2}$$

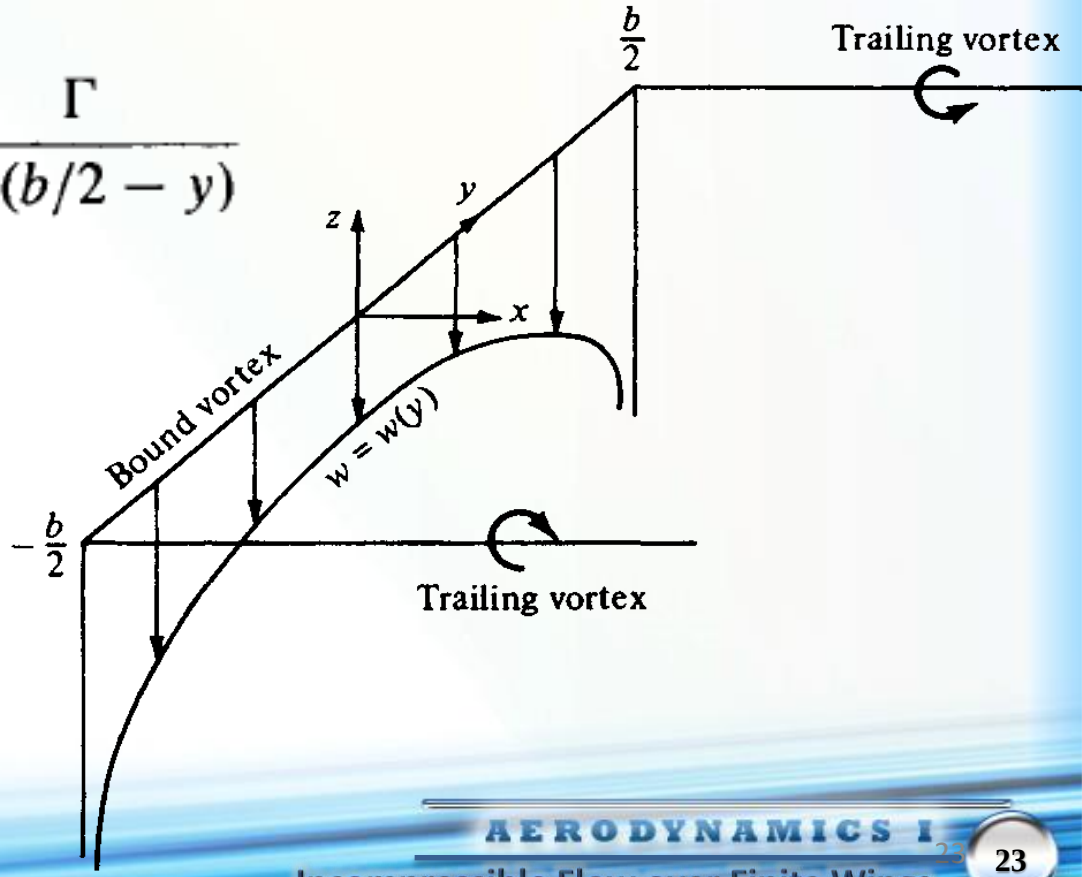

LIFTING-LINE THEORY

The downwash distribution due to the single horseshoe vortex does not realistically simulate that of a finite wing. A better flow field model employs multiple distributed horseshoe vortices.

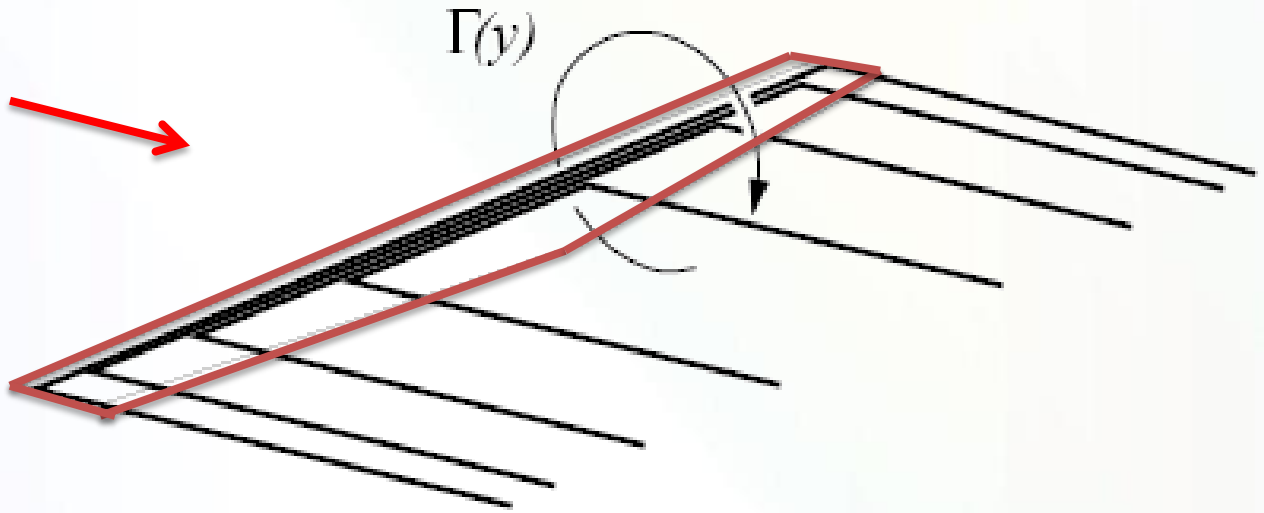

LIFTING-LINE THEORY

The figure shows 3 horseshoe vortices on the wing, each with different length of bound vortex, but with all bound vortices coincident along a single line. This line is called the *Lifting Line*.

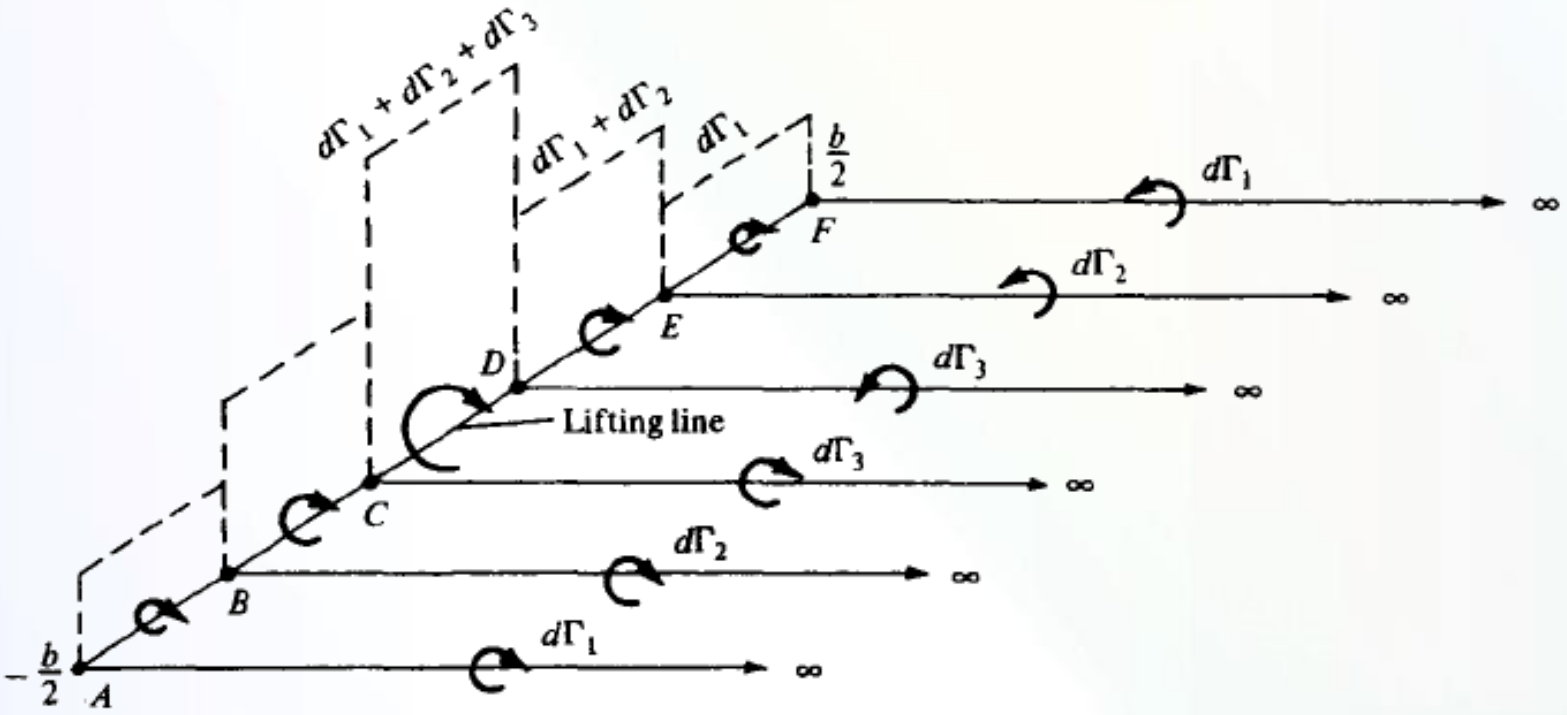

LIFTING-LINE THEORY

The figure shows infinite number of horseshoe vortices superimposed along lifting line, each with a vanishingly small strength $d\Gamma$.
It has a continuous distribution of $\Gamma = \Gamma(y)$ along the lifting line.

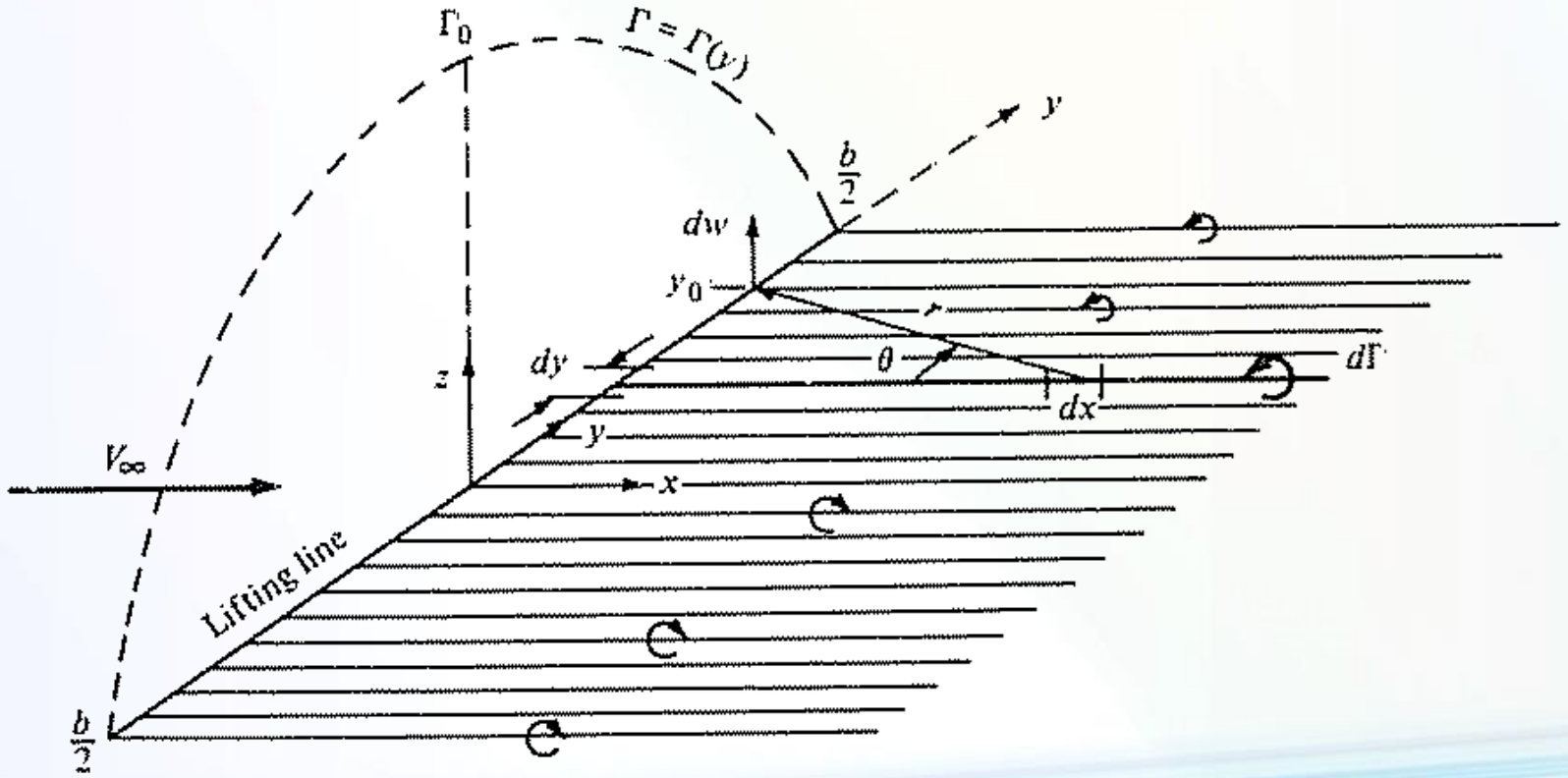

LIFTING-LINE THEORY

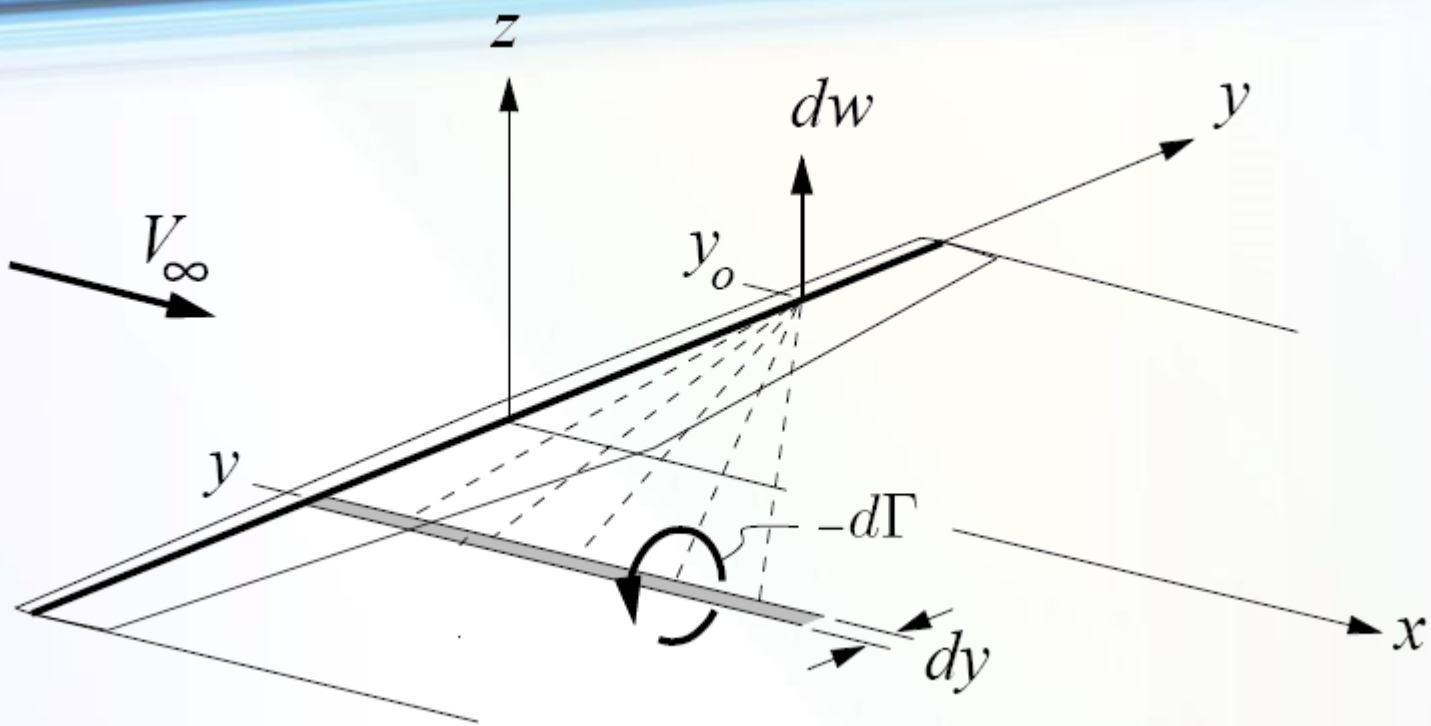

$$dw = -\frac{(d\Gamma/dy)\,dy}{4\pi(y_o - y)} \quad \Rightarrow \quad w(y_o) = -\frac{1}{4\pi}\int_{-b/2}^{b/2} \frac{d\Gamma}{dy}\frac{dy}{y_o - y}$$

LIFTING-LINE THEORY

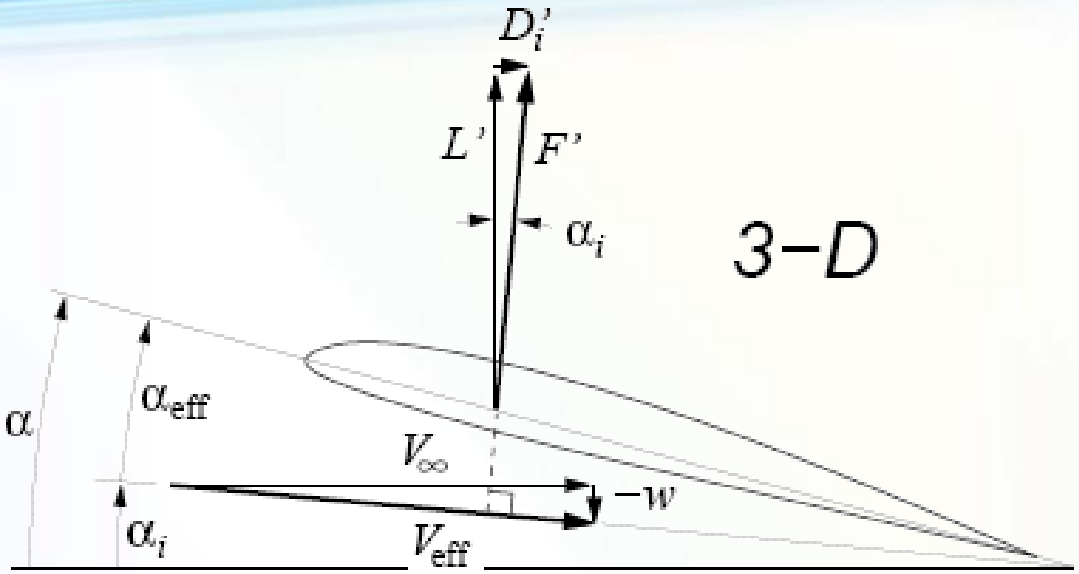

$$\alpha_i(y_0) = \tan^{-1}\left(\frac{-w(y_0)}{V_\infty}\right) \quad \Rightarrow \quad \alpha_i(y_0) = -\frac{w(y_0)}{V_\infty}$$

$$\alpha_i(y_o) = \frac{-w(y_o)}{V_\infty} = \frac{1}{4\pi V_\infty}\int_{-b/2}^{b/2}\frac{d\Gamma}{dy}\frac{dy}{y_o - y}$$

LIFTING-LINE THEORY

$$c_l = a_0[\alpha_{\text{eff}}(y_0) - \alpha_{L=0}] = 2\pi[\alpha_{\text{eff}}(y_0) - \alpha_{L=0}]$$

$$L' = \tfrac{1}{2}\rho_\infty V_\infty^2 c(y_0) c_l = \rho_\infty V_\infty \Gamma(y_0) \quad \Rightarrow \quad c_l = \frac{2\Gamma(y_0)}{V_\infty c(y_0)}$$

$$\alpha_{\text{eff}} = \frac{\Gamma(y_0)}{\pi V_\infty c(y_0)} + \alpha_{L=0}$$

$$\alpha_{\text{eff}} = \alpha - \alpha_i$$

$$\alpha(y_0) = \frac{\Gamma(y_0)}{\pi V_\infty c(y_0)} + \alpha_{L=0}(y_0) + \frac{1}{4\pi V_\infty} \int_{-b/2}^{b/2} \frac{(d\Gamma/dy)\, dy}{y_0 - y}$$

fundamental equation of Prandtl's lifting-line theory

The solution $\Gamma = \Gamma(y_o)$, gives us the three main aerodynamic characteristics of a finite wing, as follows:

1. The lift distribution is obtained from the Kutta-Joukowski theorem:

$$L'(y_0) = \rho_\infty V_\infty \Gamma(y_0)$$

2. The total lift is obtained by integrating $L'(y_o)$ over the span

$$L = \int_{-b/2}^{b/2} L'(y)\,dy \quad \Rightarrow \quad L = \rho_\infty V_\infty \int_{-b/2}^{b/2} \Gamma(y)\,dy$$

$$C_L = \frac{L}{q_\infty S} = \frac{2}{V_\infty S} \int_{-b/2}^{b/2} \Gamma(y)\,dy$$

The solution $\Gamma = \Gamma(y_o)$, gives us the three main aerodynamic characteristics of a finite wing, as follows:

3. The induced drag per unit span is

$$D_i' = L_i' \sin \alpha_i$$

Since α_i is small, this relation becomes

$$D_i' = L_i' \alpha_i$$

The total induced drag is obtained by integrating D'_i over the span:

$$D_i = \int_{-b/2}^{b/2} L'(y)\alpha_i(y)\,dy \quad \Rightarrow \quad D_i = \rho_\infty V_\infty \int_{-b/2}^{b/2} \Gamma(y)\alpha_i(y)\,dy$$

$$C_{D,i} = \frac{D_i}{q_\infty S} = \frac{2}{V_\infty S} \int_{-b/2}^{b/2} \Gamma(y)\alpha_i(y)\,dy$$

ELLIPTICAL LIFT DISTRIBUTION

Consider an elliptical spanwise circulation distribution given by:

$$\Gamma(y) = \Gamma_0 \sqrt{1 - \left(\frac{2y}{b}\right)^2}$$

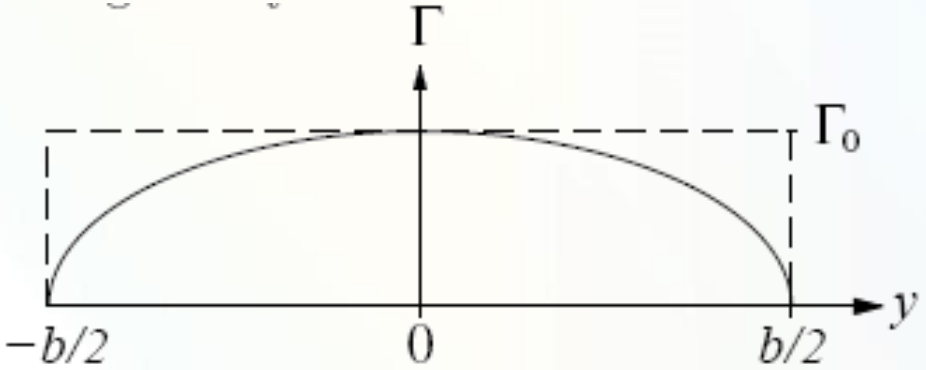

$$L'(y) = \rho V_\infty \Gamma(y)$$

$$L = \int_{-b/2}^{b/2} L'(y)\, dy = \int_{-b/2}^{b/2} \rho V_\infty \Gamma_0 \sqrt{1 - \left(\frac{2y}{b}\right)^2}\, dy = \frac{\pi}{4} \rho V_\infty \Gamma_0 b$$

ELLIPTICAL LIFT DISTRIBUTION DOWNWASH CALCULATION

$$\frac{d\Gamma}{dy} = -\frac{4\Gamma_0}{b^2} \frac{y}{(1 - 4y^2/b^2)^{1/2}}$$

$$w(y_0) = \frac{\Gamma_0}{\pi b^2} \int_{-b/2}^{b/2} \frac{y}{(1 - 4y^2/b^2)^{1/2}(y_0 - y)} dy$$

ELLIPTICAL LIFT DISTRIBUTION

As in thin airfoil theory, the mathematical problem is considerably simplified by making the trigonometric substitution

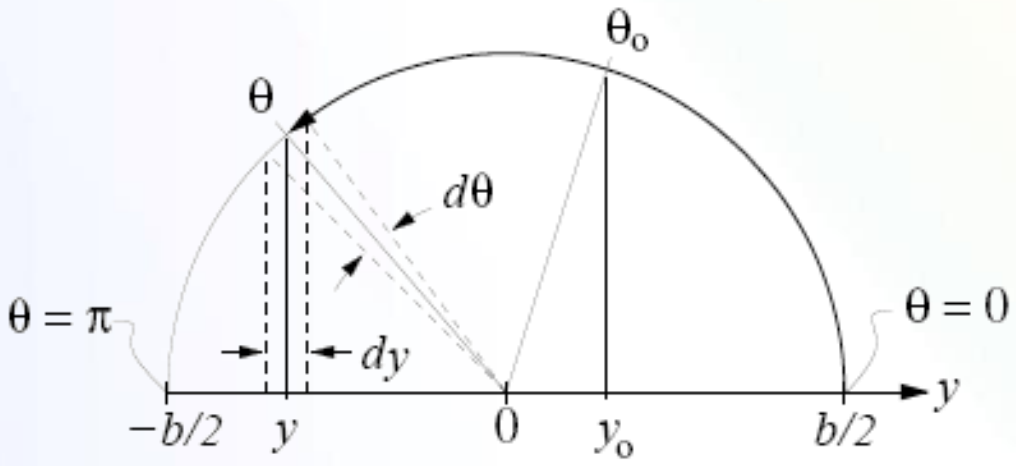

$$y_o = \frac{b}{2}\cos\theta_o$$

$$y = \frac{b}{2}\cos\theta$$

$$dy = -\frac{b}{2}\sin\theta\, d\theta$$

ELLIPTICAL LIFT DISTRIBUTION

$$w(\theta_o) = -\frac{\Gamma_0}{2\pi b}\int_{\pi}^{0}\frac{\cos\theta}{\cos\theta_o - \cos\theta}\,d\theta = \frac{\Gamma_0}{2\pi b}\int_{0}^{\pi}\frac{\cos\theta}{\cos\theta_o - \cos\theta}\,d\theta$$

$$\int_0^{\pi}\frac{\cos n\theta}{\cos\theta - \cos\theta_o}\,d\theta = \frac{\pi\,\sin n\theta_o}{\sin\theta_o} \quad \Rightarrow \quad w(\theta_o) = \frac{\Gamma_0}{2\pi b}\left(-\frac{\pi\,\sin\theta_o}{\sin\theta_o}\right) = -\frac{\Gamma_0}{2b}$$

$$L = \rho_\infty V_\infty \Gamma_0 \int_{-b/2}^{b/2}\left(1 - \frac{4y^2}{b^2}\right)^{1/2} dy \quad \Rightarrow \quad L = \rho_\infty V_\infty \Gamma_0 \frac{b}{2}\int_0^{\pi}\sin^2\theta\,d\theta = \rho_\infty V_\infty \Gamma_0 \frac{b}{4}\pi$$

We have the somewhat surprising result that the downwash is uniform over the span of a wing with an elliptical circulation distribution. There is a sharp upwash just outboard of the tips which rapidly dies off with distance, but this doesn't impact the flow angles seen by the wing itself.

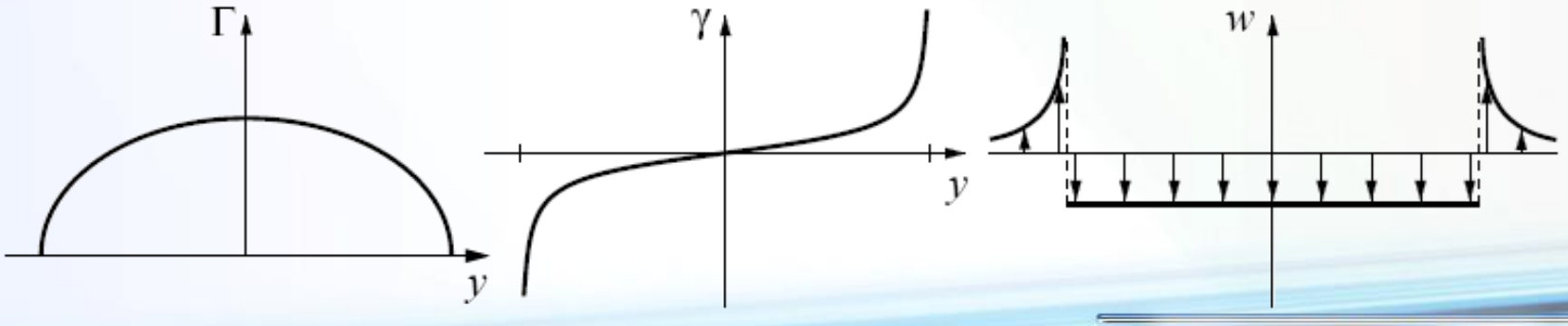

ELLIPTICAL LIFT DISTRIBUTION
INDUCED DRAG

$$L = \rho_\infty V_\infty \Gamma_0 \frac{b}{2} \int_0^\pi \sin^2\theta \, d\theta = \rho_\infty V_\infty \Gamma_0 \frac{b}{4}\pi$$

Solving above Equation for Γ_o, we have

$$\Gamma_0 = \frac{4L}{\rho_\infty V_\infty b\pi}$$

Which allows eliminating Γ_o from the w result to give a somewhat more convenient expression

$$w = -\frac{2L}{\rho V_\infty b^2 \pi}$$

Induced angle of attack

$$\alpha_i = -\frac{w}{V_\infty} = \frac{\Gamma_0}{2bV_\infty} = \frac{L}{\frac{1}{2}\rho V_\infty^2 b^2 \pi}$$

ELLIPTICAL LIFT DISTRIBUTION
INDUCED DRAG

$$C_L \equiv \frac{L}{\frac{1}{2}\rho V_\infty^2 S}$$

$$\text{AR} \equiv \frac{b^2}{S}$$

$$\alpha_i = -\frac{w}{V_\infty} = \frac{\Gamma_0}{2bV_\infty} = \frac{L}{\frac{1}{2}\rho V_\infty^2 b^2 \pi}$$

$$\Rightarrow \quad \alpha_i = \frac{S\,C_L}{b^2\,\pi} = \frac{C_L}{\pi\,AR}$$

Induced drag

$$D_i = \int_{-b/2}^{b/2} L'(y)\,\alpha_i\,dy = \alpha_i \int_{-b/2}^{b/2} L'(y)\,dy = \alpha_i\,L$$

$$D_i = \frac{(L/b)^2}{\frac{1}{2}\rho V_\infty^2\,\pi} \quad \Rightarrow \quad C_{Di} = \frac{C_L^2}{\pi\,AR}$$

TOTAL WING DRAG

$$D = D_p + D_i$$

$$C_D = C_{Dp} + C_{Di}$$

$$C_{Dp} = \frac{1}{S}\int_{-b/2}^{b/2} c_d(y)\, c(y)\, dy$$

Here c_d is the 2-D airfoil viscous airfoil drag, and is usually known in the form of a $c_d(c_\ell; Re)$ drag polar from wind tunnel data or from calculations. In general, $c_d(y)$ will vary across the span, although a very common approximation is to simply assume that it's constant, and determined using the overall wing C_L, and the Reynolds number based on the average chord.

$$c_d \simeq c_d\left(C_L; Re_{\text{avg}}\right) \quad , \quad Re_{\text{avg}} = \frac{V_\infty c_{\text{avg}}}{\nu}$$

TOTAL WING DRAG

In this case $C_{Dp} = c_d$, and together with the induced drag result the total drag coefficient can then be computed as follows.

$$C_D(C_L; Re_{\text{avg}}) = c_d(C_L; Re_{\text{avg}}) + \frac{C_L^2}{\pi AR}$$

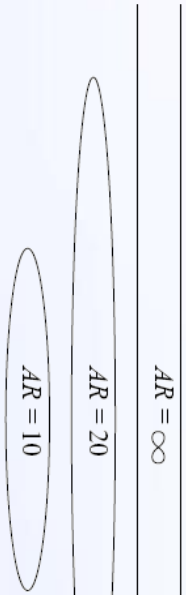

Atypical CD(CL) polar plot for one Reynolds number

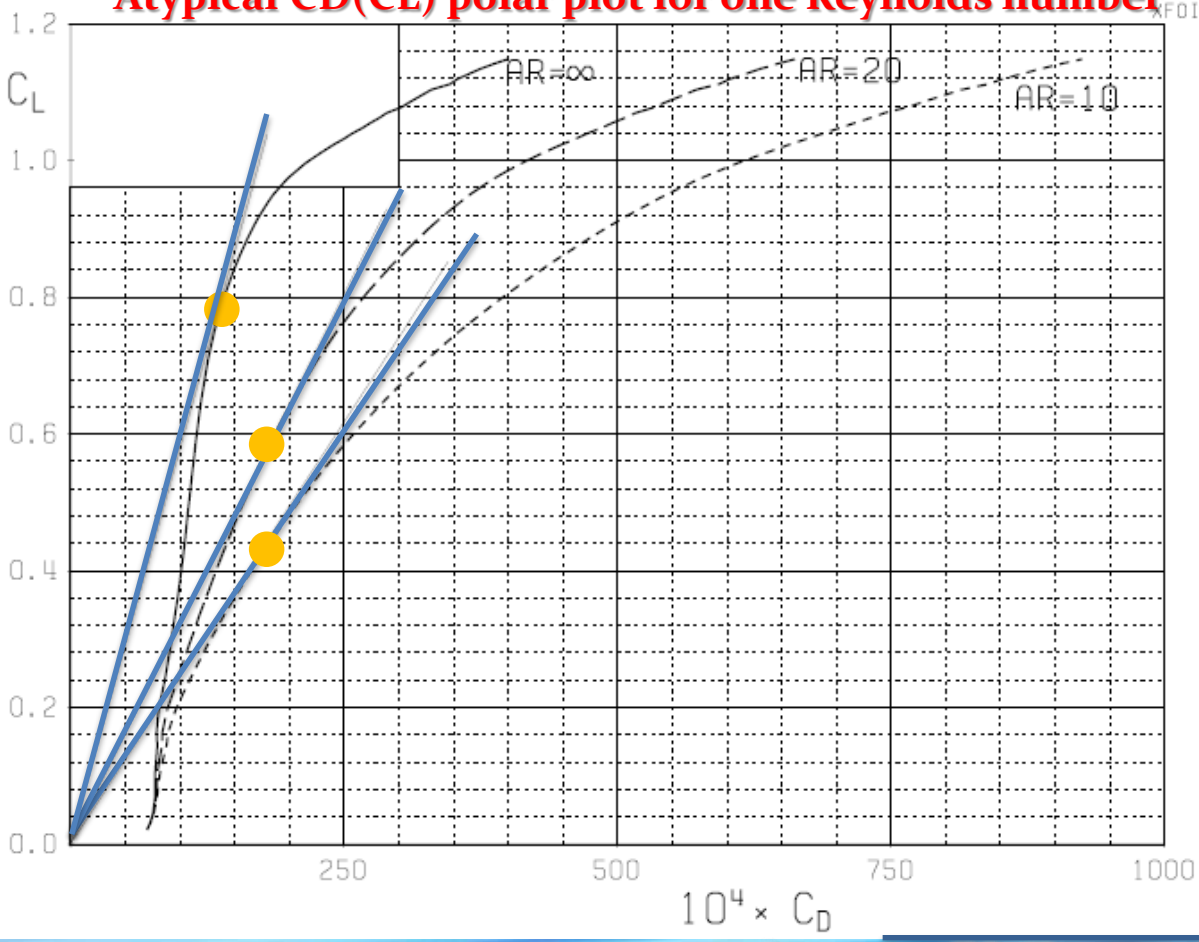

EFFECT OF ASPECT RATIO

The aspect ratio of the 1903 Wright Flyer was 6 and that today the aspect ratios of conventional subsonic aircraft range typically from 6 to 8. (Exceptions are the Lockheed U-2 high-altitude reconnaissance aircraft with AR = 14.3 and sailplanes with aspect ratios as high as 51.

A high aspect ratio wing is efficient because it reduces the formation of the vortex and associated drag.

In contrast, a low aspect ratio wing allows the high pressure on the bottom of the wing to escape more easily, resulting in a larger vortex and greater drag.

EFFECT OF ASPECT RATIO
LOCKHEED U-2

EFFECT OF ASPECT RATIO

ELLIPTICAL LIFT DISTRIBUTION

We have seen that α_i, is constant along the span. Hence, $\alpha_{eff} = \alpha - \alpha_i$ *is also constant* along the span.

$$c_l = \frac{a_0}{2\pi}(\alpha_{eff} - \alpha_{L=0}) \Rightarrow$$ $\mathbf{c_l}$ must be constant along the span.

$$L'(y) = q_\infty c c_l \Rightarrow c(y) = \frac{L'(y)}{q_\infty c_l}$$

The chord must vary *elliptically* along the span

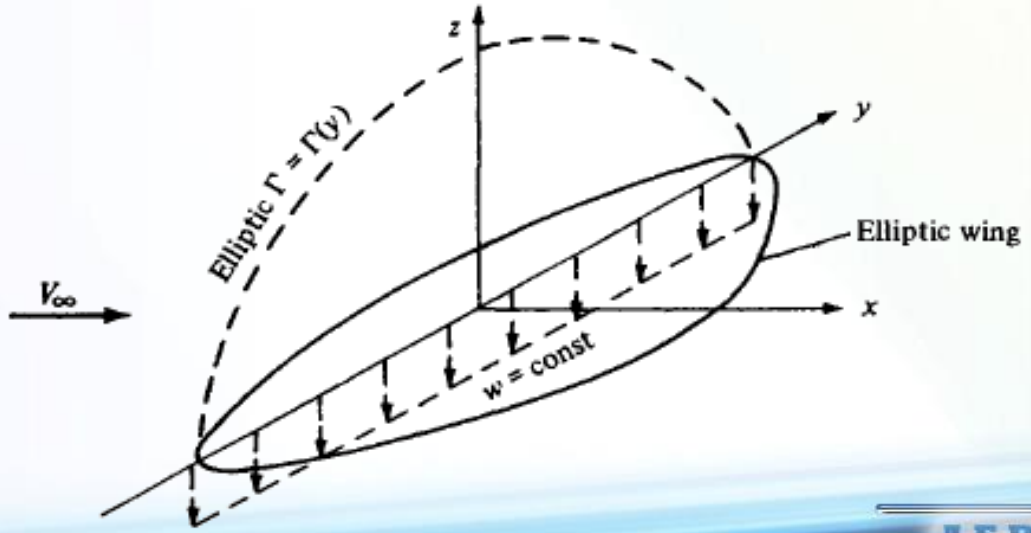

General circulation distribution and downwash

$$\Gamma(y) = \Gamma_0 \sqrt{1 - \left(\frac{2y}{b}\right)^2}$$

$$y = -\frac{b}{2}\cos\theta$$

$$\Gamma(\theta) = \Gamma_0 \sin\theta$$

This hints that a Fourier sine series would be an appropriate expression for the general circulation distribution along an arbitrary finite wing.

$$\Gamma(\theta) = 2bV_\infty \sum_{n=1}^{N} A_n \sin n\theta$$

GENERAL WINGS

$$\frac{\Gamma}{2bV_\infty}$$

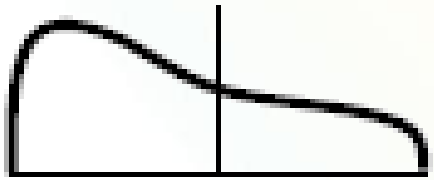

y

$A_1 \times \sin\theta$ $A_2 \times \sin 2\theta$ $A_3 \times \sin 3\theta$

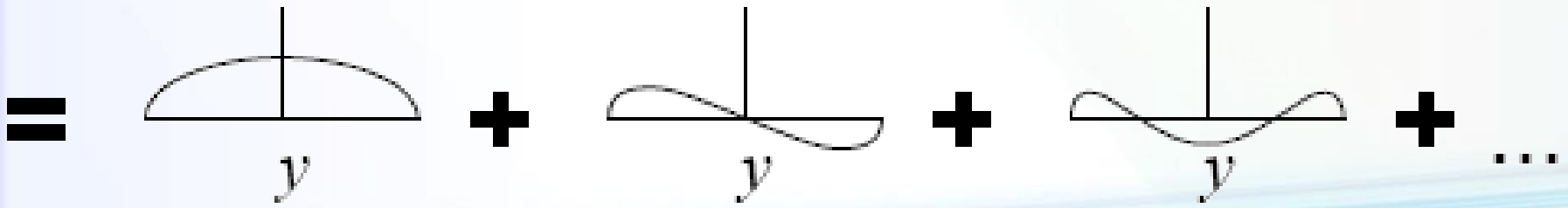

GENERAL WINGS

$$\frac{d\Gamma}{dy} = \frac{d\Gamma}{d\theta}\frac{d\theta}{dy} = 2bV_\infty \sum_1^N n A_n \cos n\theta \frac{d\theta}{dy}$$

$$\alpha(y_0) = \frac{\Gamma(y_0)}{\pi V_\infty c(y_0)} + \alpha_{L=0}(y_0) + \frac{1}{4\pi V_\infty}\int_{-b/2}^{b/2} \frac{(d\Gamma/dy)\,dy}{y_0 - y}$$

$$\alpha(\theta_0) = \frac{2b}{\pi c(\theta_0)} \sum_1^N A_n \sin n\theta_0 + \alpha_{L=0}(\theta_0) + \frac{1}{\pi}\int_0^\pi \frac{\sum_1^N n A_n \cos n\theta}{\cos\theta - \cos\theta_0} d\theta$$

Let us choose N different spanwise stations, and let us evaluate Equation at each of these N stations. We then obtain a system of *N* independent algebraic equations with *N* unknowns, namely, *A1*, *A2*,... , A_N.

GENERAL WINGS

$$L = \int_{-b/2}^{b/2} \rho V_\infty \Gamma(y)\, dy$$

$$y = \frac{b}{2}\cos\theta$$

$$dy = -\frac{b}{2}\sin\theta\, d\theta$$

$$\Rightarrow \quad L = \rho V_\infty \left[2bV_\infty \sum_{n=1}^{N} A_n \frac{b}{2} \int_0^\pi \sin n\theta \, \sin\theta \, d\theta \right]$$

The orthogonality property of the sine functions:

$$\int_0^\pi \sin n\theta \, \sin m\theta \, d\theta = \begin{cases} \pi/2 & (\text{if } n = m) \\ 0 & (\text{if } n \neq m) \end{cases}$$

$$L = \frac{\pi}{2} \rho V_\infty^2 b^2 A_1 \quad \Rightarrow \quad C_L = \frac{L}{\frac{1}{2}\rho V_\infty^2 S} = \pi A_1 \frac{b^2}{S} = A_1 \pi AR$$

GENERAL WINGS

$$\alpha_i = \frac{1}{4\pi V_\infty}\int_{-b/2}^{b/2}\frac{d\Gamma}{dy}\frac{dy}{y_o - y} = \frac{1}{\pi}\sum_{n=1}^{N} nA_n \int_0^{\pi}\frac{\cos n\theta}{\cos\theta - \cos\theta_o}\,d\theta$$

$$\alpha_i(\theta_o) = \sum_{n=1}^{N} nA_n \frac{\sin n\theta_o}{\sin\theta_o}$$

The leading n = 1 term is the same as the elliptic loading case, with the expected uniform induced angle.

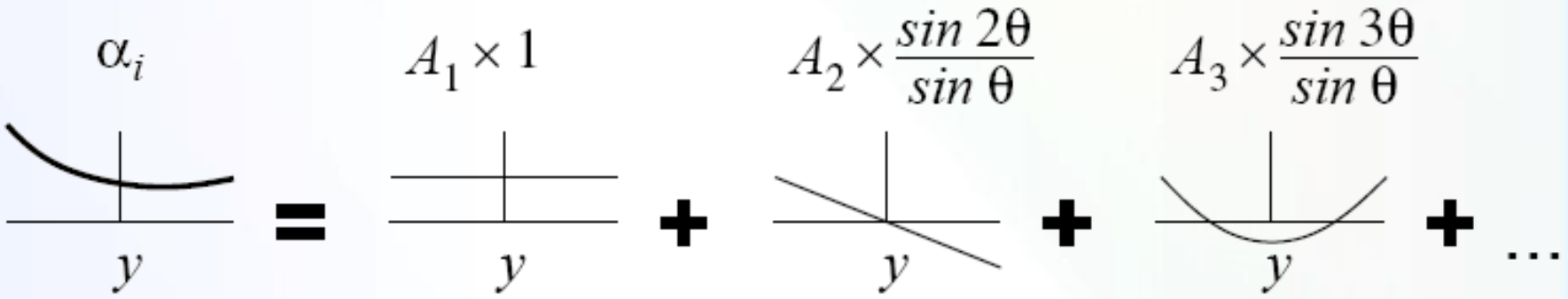

GENERAL WINGS
INDUCED DRAG

$$D_i' = L_i' \alpha_i \qquad D_i = \int_{-b/2}^{b/2} L'(y)\alpha_i(y)\,dy$$

$$D_i = \rho_\infty V_\infty \int_{-b/2}^{b/2} \Gamma(y)\alpha_i(y)\,dy$$

$$C_{D,i} = \frac{2b^2}{S} \int_0^\pi \left(\sum_1^N A_n \sin n\theta \right) \left(\sum_1^N n A_n \sin n\theta \right) d\theta$$

$$\int_0^\pi \sin m\theta \sin k\theta = \begin{cases} 0 & \text{for } m \neq k \\ \pi/2 & \text{for } m = k \end{cases}$$

$$C_{D,i} = \frac{2b^2}{S} \left(\sum_1^N n A_n^2 \right) \frac{\pi}{2} = \pi \mathrm{AR} \sum_1^N n A_n^2$$

GENERAL WINGS
INDUCED DRAG

$$C_{D,i} = \frac{2b^2}{S}\left(\sum_1^N nA_n^2\right)\frac{\pi}{2} = \pi \mathrm{AR}\sum_1^N nA_n^2$$

$$= \pi \mathrm{AR}\left(A_1^2 + \sum_2^N nA_n^2\right)$$

$$= \pi \mathrm{AR}\, A_1^2\left[1 + \sum_2^N n\left(\frac{A_n}{A_1}\right)^2\right]$$

$\delta = \sum_2^N n(A_n/A_1)^2$

$$C_{D,i} = \frac{C_L^2}{\pi \mathrm{AR}}(1+\delta)$$

$$e \equiv \frac{1}{1+\delta}$$

$$C_{D,i} = \frac{C_L^2}{\pi e \mathrm{AR}}$$

span efficiency

$$e \leq 1$$

The minimum drag corresponding to elliptic loading, for which e = 1.

THE SUPERMARINE SPITFIRE

LOAD DISTRIBUTIONS ON TYPICAL PLANFORMS

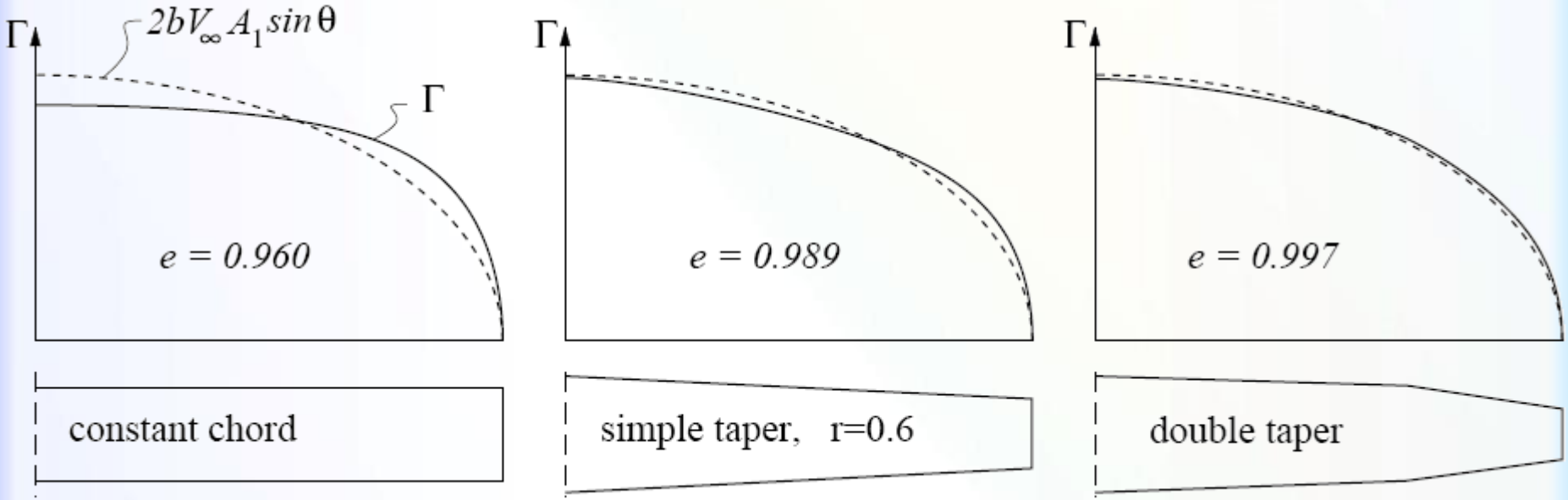

WING COMPONENTS

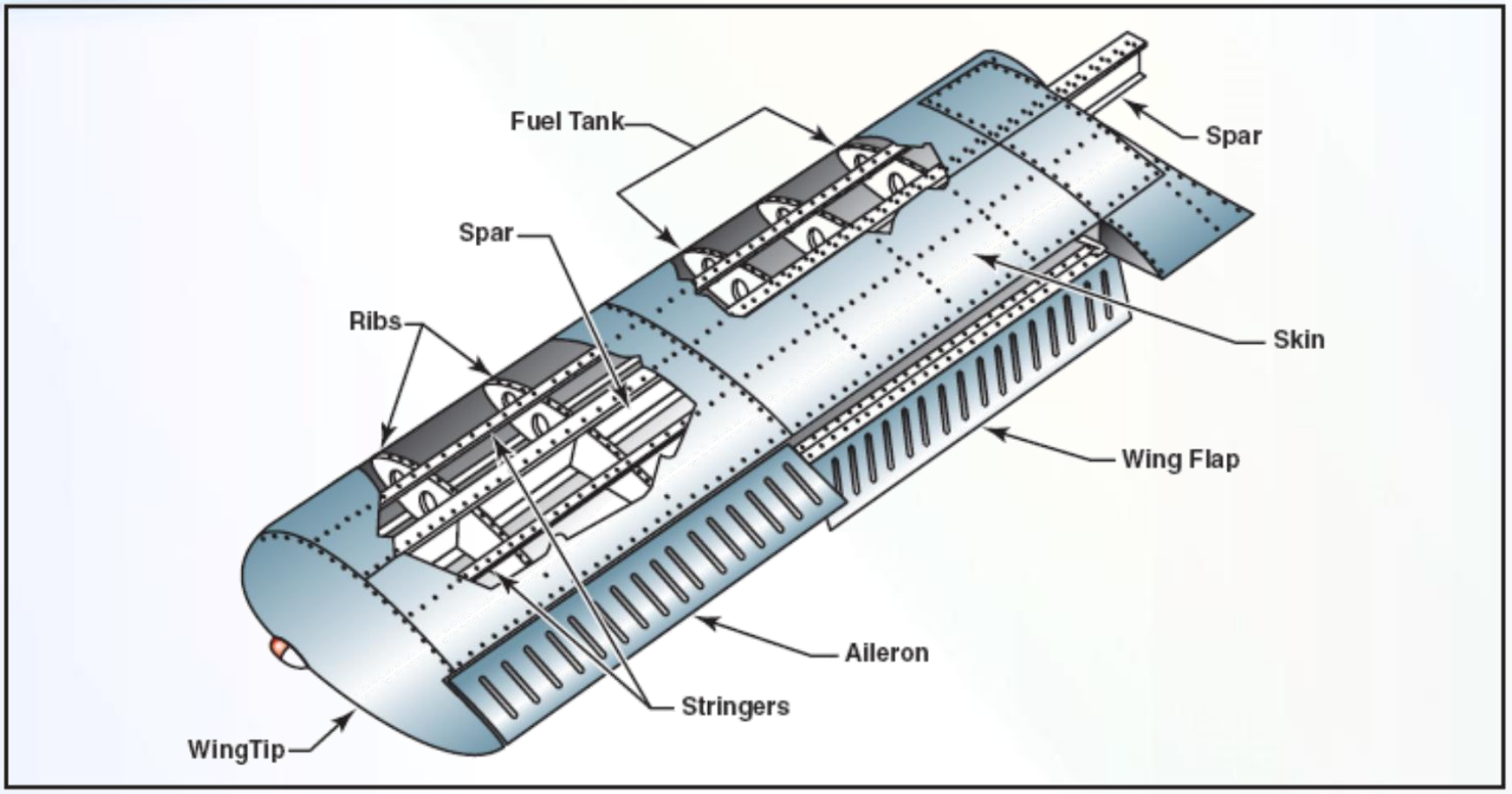

EFFECTS OF TRAILING EDGE FLAPS

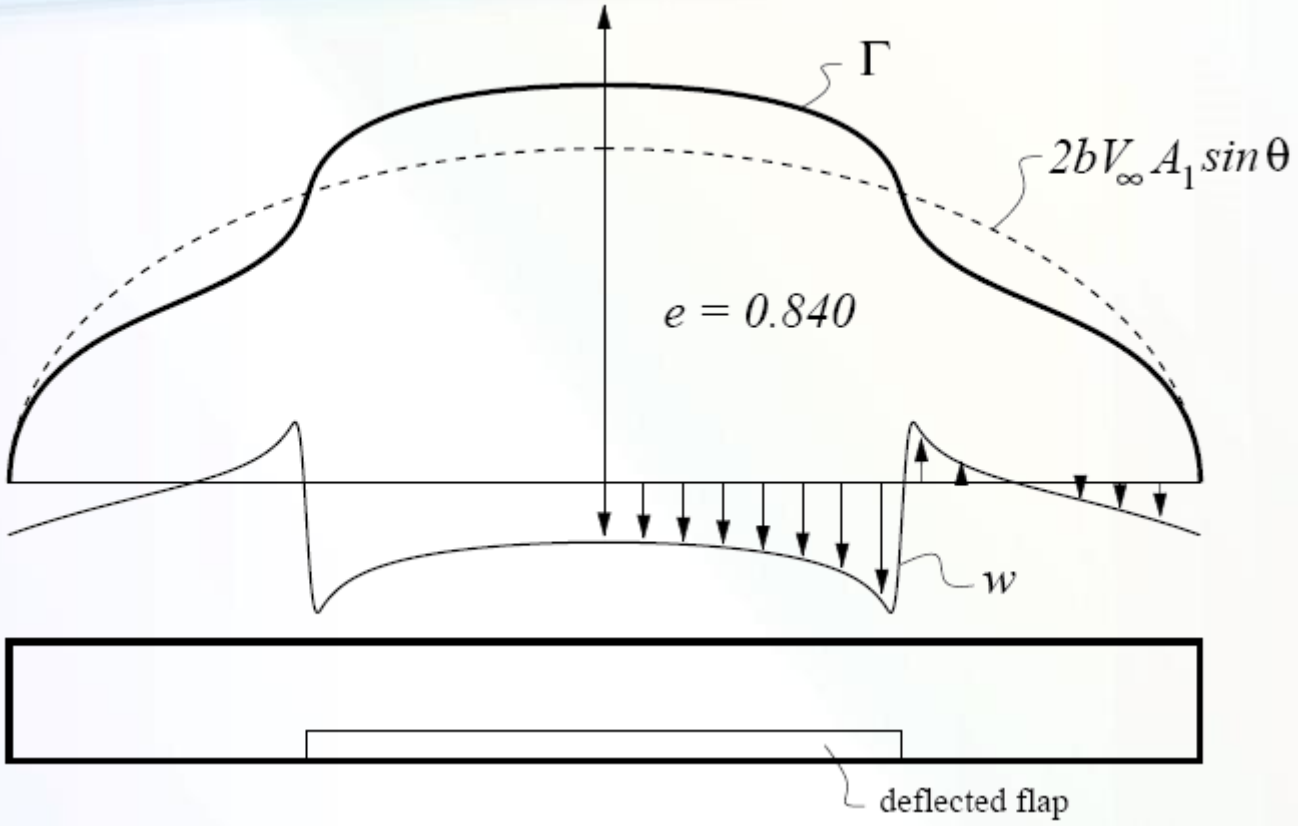

Note also the strongly non-uniform downwash distribution resulting from this distorted loading.

EFFECT OF ASPECT RATIO

Induced drag factor δ as a function of taper ratio.

$$e \equiv \frac{1}{1+\delta}$$

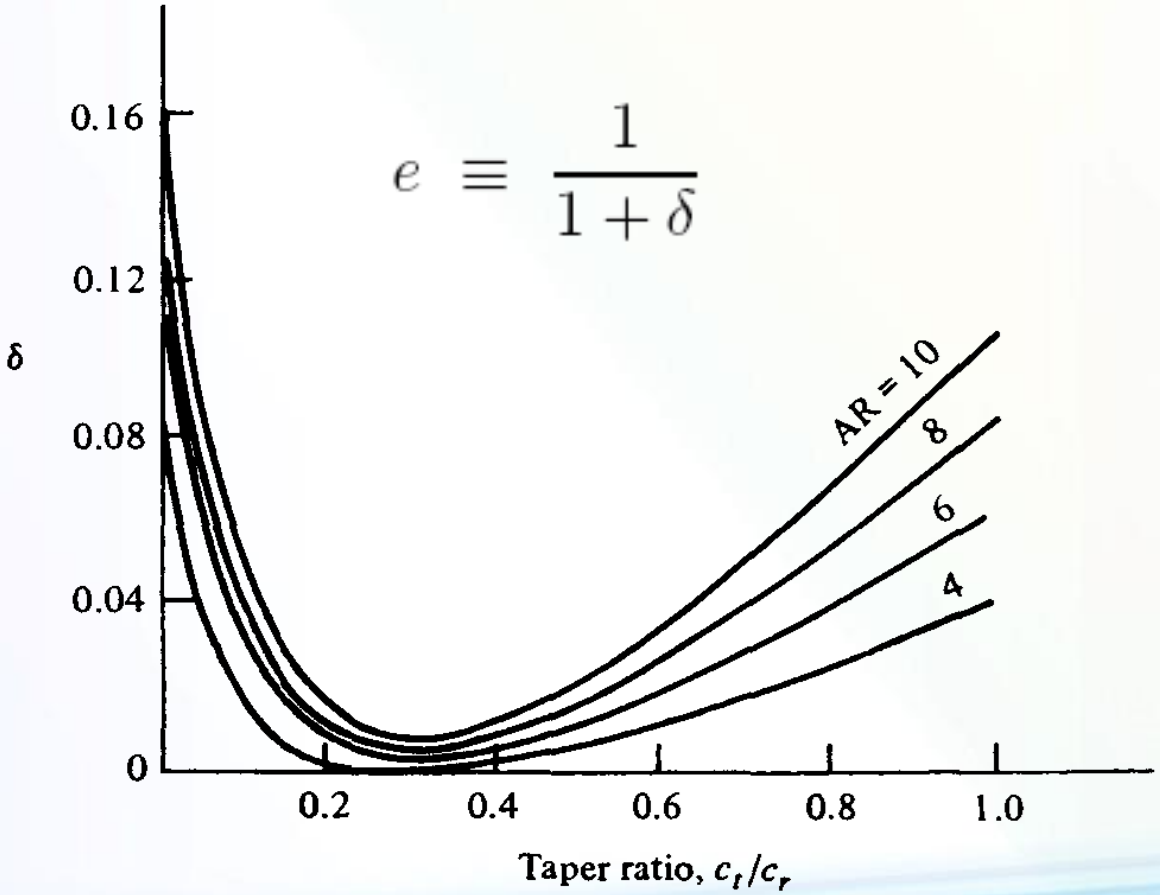

EFFECT OF ASPECT RATIO

$$C_D = c_d + \frac{C_L^2}{\pi e \mathrm{AR}}$$

If we consider two wings with different aspect ratios AR_1 and AR_2

$$C_{D,1} = c_d + \frac{C_L^2}{\pi e \mathrm{AR}_1}$$

$$C_{D,2} = c_d + \frac{C_L^2}{\pi e \mathrm{AR}_2}$$

Assume that the wings are at the same C_L

$$C_{D,1} = C_{D,2} + \frac{C_L^2}{\pi e}\left(\frac{1}{\mathrm{AR}_1} - \frac{1}{\mathrm{AR}_2}\right)$$

EFFECT OF ASPECT RATIO

For historical interest, we reproduce here Prandtl's actual graphs.
Note that, in his nomenclature,
C_a = lift coefficient and
C_w =drag coefficient

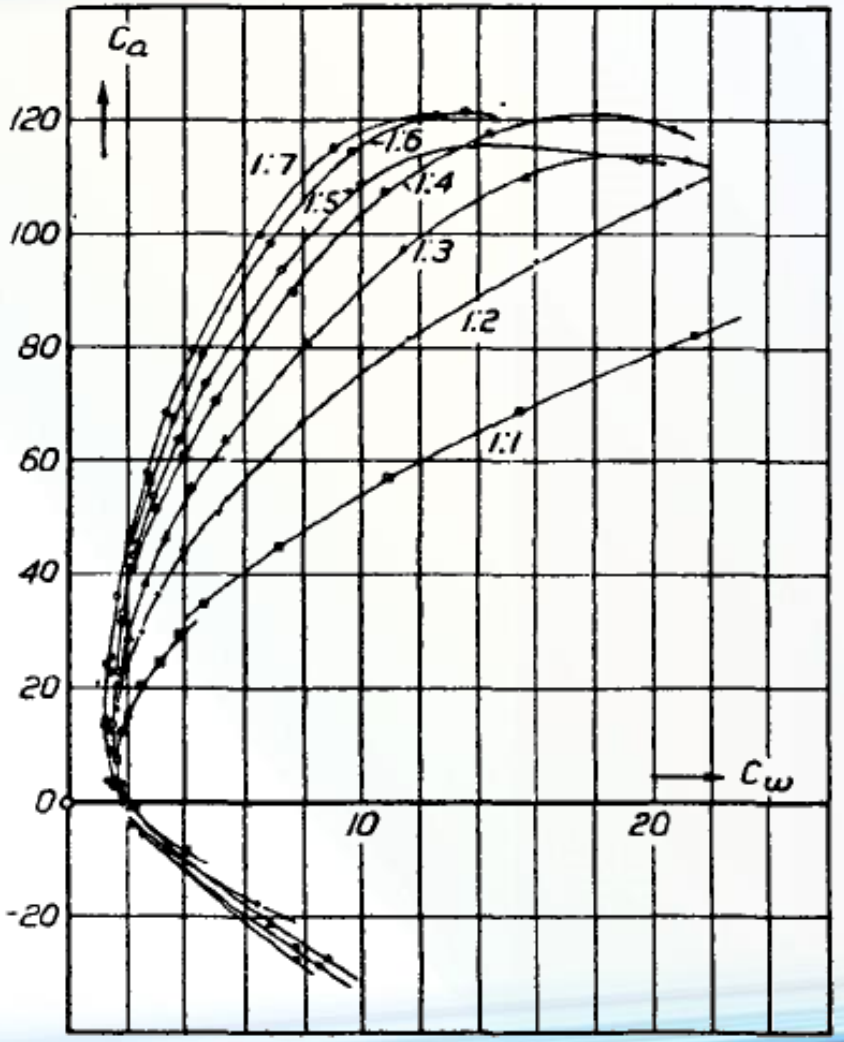

EFFECT OF ASPECT RATIO

$$C_{D,1} = C_{D,2} + \frac{C_L^2}{\pi e}\left(\frac{1}{5} - \frac{1}{\mathrm{AR}_2}\right)$$

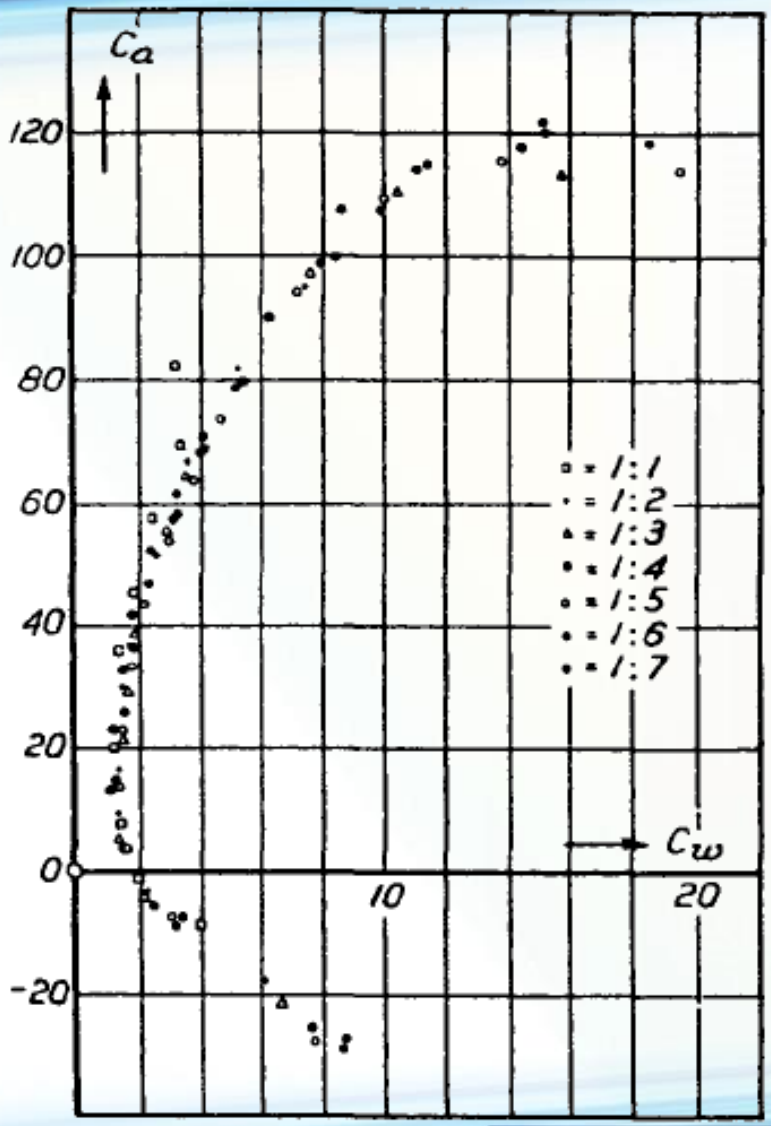

LIFT SLOPE REDUCTION

The downwash behind any finite wing modifies the wing's lift slope

Consider the c_ℓ-angle relation at a typical spanwise location

$$\frac{dC_L}{d(\alpha - \alpha_i)} = a_0 \qquad C_L = a_0(\alpha - \alpha_i) + \text{const}$$

$$C_L = a_0\left(\alpha - \frac{C_L}{\pi \text{AR}}\right) + \text{const} \qquad \frac{dC_L}{d\alpha} = a = \frac{a_0}{1 + a_0/\pi \text{AR}}$$

For a nearly-elliptic loading, we have $c_\ell \simeq C_L$

For a finite wing of general planform, the equation is slightly modified, as given below:

$$a = \frac{a_0}{1 + (a_0/\pi \text{AR})(1 + \tau)}$$

τ is a function of the Fourier coefficients A_n. Values of τ typically range between 0.05 and 0.25.

LIFT SLOPE REDUCTION

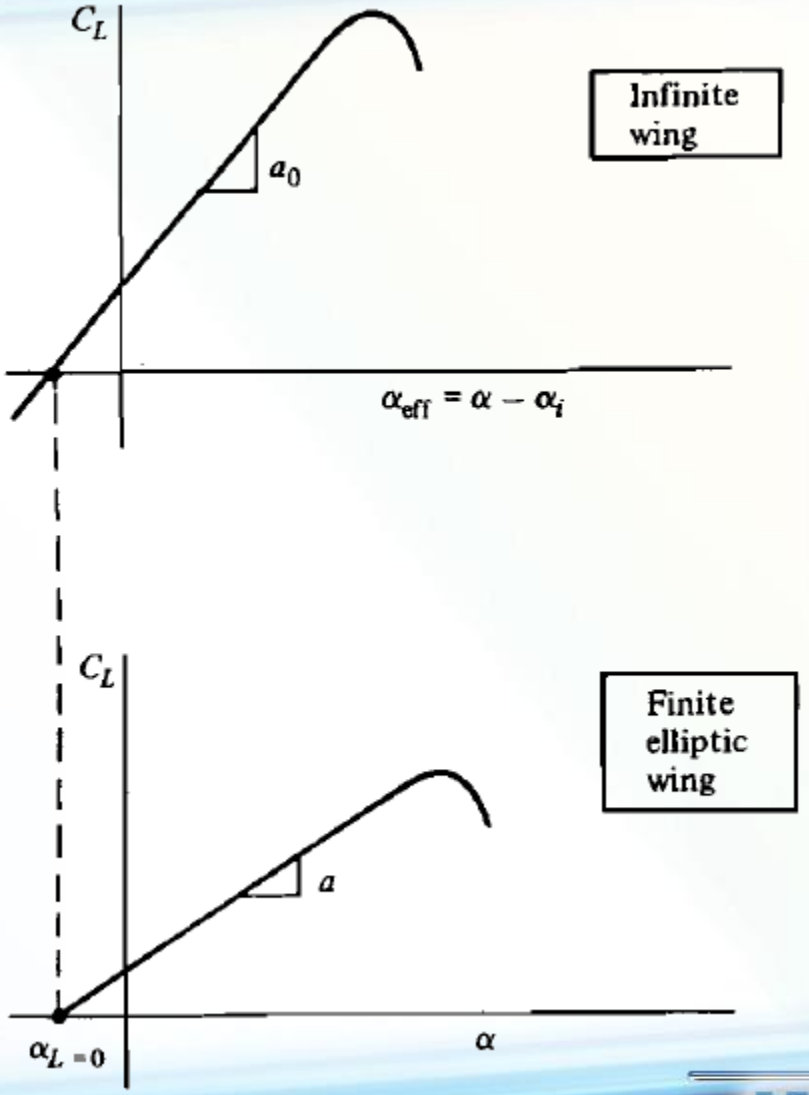

EFFECT OF ASPECT RATIO ON LIFT SLOPE

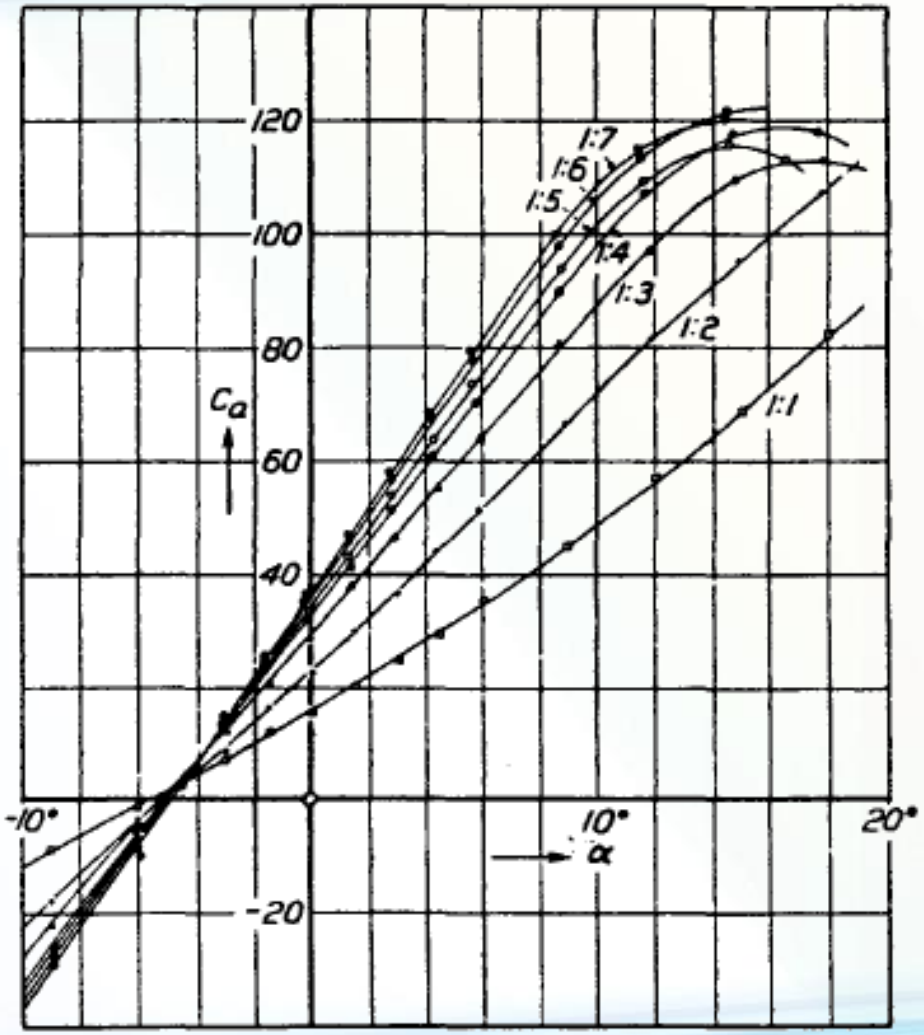

EXAMPLE 1

Consider a finite wing with an aspect ratio of 8 and a taper ratio of 0.8. The airfoil section is thin and symmetric. Calculate the lift and induced drag coefficients for the wing when it is at an angle of attack of 5°. Assume that $\delta = \tau$.

, assuming $a_0 = 2\pi$

$$a = \frac{a_0}{1 + a_0/\pi \text{AR}(1+\tau)} = \frac{2\pi}{1 + 2\pi(1.055)/8\pi} = 4.97 \text{ rad}^{-1}$$

$$= 0.0867 \text{ degree}^{-1}$$

Since the airfoil is symmetric, $\alpha_{L=0} = 0°$. Thus,

$$C_L = a\alpha = (0.0867 \text{ degree}^{-1}(5°) = \boxed{0.4335}$$

$$C_{D,i} = \frac{C_L^2}{\pi \text{AR}}(1+\delta) = \frac{(0.4335)^2(1+0.055)}{8\pi} = \boxed{0.00789}$$

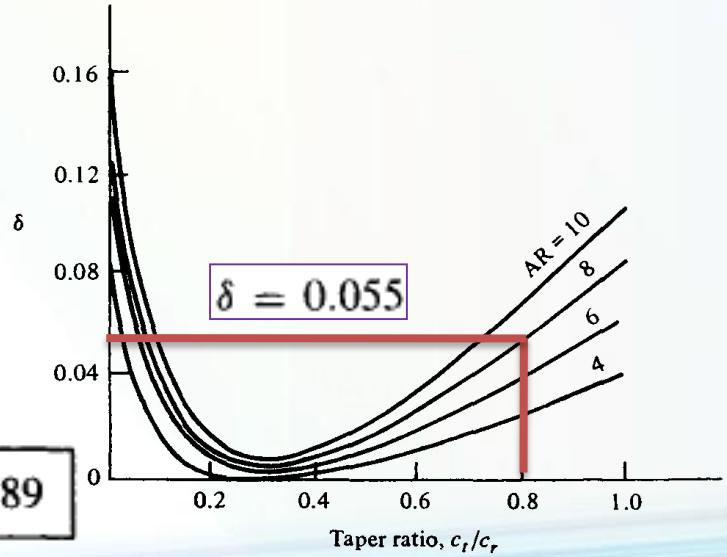

EXAMPLE 2

Consider a rectangular wing with an aspect ratio of 6, an induced drag factor $\delta = 0.055$, and a zero-lift angle of attack of $-2°$. At an angle of attack of $3.4°$, the induced drag coefficient for this wing is 0.01. Calculate the induced drag coefficient for a similar wing (a rectangular wing with the same airfoil section) at the same angle of attack, but with an aspect ratio of 10. Assume that the induced factors for drag and the lift slope, δ and τ, respectively, are equal to each other (i.e., $\delta = \tau$). Also, for AR = 10, $\delta = 0.105$.

First, let us calculate C_L for the wing with aspect ratio 6

$$C_L^2 = \frac{\pi \text{AR} C_{D,i}}{1+\delta} = \frac{\pi(6)(0.01)}{1+0.055} = 0.1787$$

$$\Rightarrow \quad C_L = 0.423$$

The lift slope of this wing is therefore

$$\frac{dC_L}{d\alpha} = \frac{0.423}{3.4° - (-2°)} = 0.078/\text{degree} = 4.485/\text{rad}$$

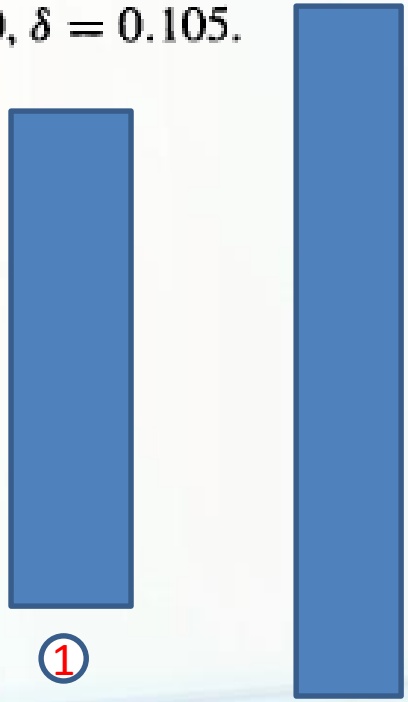

EXAMPLE 2 (CONT.)

The lift slope for the airfoil (the infinite wing) can be obtained

$$\frac{dC_L}{d\alpha} = a = \frac{a_0}{1 + (a_0/\pi \mathrm{AR})(1 + \tau)}$$

$$4.485 = \frac{a_0}{1 + [(1.055)a_0/\pi(6)]} = \frac{a_0}{1 + 0.056a_0}$$

Solving for a_0 → $a_0 = 5.989/\mathrm{rad}.$

Since the second wing (with AR = 10) has the same airfoil section, then:

$$a = \frac{a_0}{1 + (a_0/\pi \mathrm{AR})(1 + \tau)} = \frac{5.989}{1 + [(5.989)(1.105)/\pi(10)]} = 4.95/\mathrm{rad}$$

$$= 0.086/\mathrm{degree}$$

EXAMPLE 2 (CONT.)

The lift coefficient for the second wing is therefore

$$C_L = a(\alpha - \alpha_{L=0}) = 0.086[3.4^\circ - (-2^\circ)] = 0.464$$

The induced drag coefficient is

$$C_{D,i} = \frac{C_L^2}{\pi \mathrm{AR}}(1+\delta) = \frac{(0.464)^2(1.105)}{\pi(10)} = \boxed{0.0076}$$

EXAMPLE 3

Consider an airplane that with $\alpha_{L=0}$=-2°, the lift slope of the airfoil section is 0.1 per degree, the lift efficiency factor τ = 0.04, and the wing aspect ratio is 7.96. At the cruising condition, the lift coefficient equal to 0.21. Calculate the angle of attack of the airplane.

The lift slope of the airfoil section in radians is:

$$a_0 = 0.1 \text{ per degree} = 0.1(57.3) = 5.73 \text{ rad}$$

$$a = \frac{a_0}{1 + (a_0/\pi \text{AR})(1 + \tau)}$$

$$a = \frac{5.73}{1 + \left(\frac{5.73}{7.96\pi}\right)(1 + 0.04)} = 4.627 \text{ per rad}$$

$$a = \frac{4.627}{57.3} = 0.0808 \text{ per degree}$$

$$C_L = a(\alpha - \alpha_{L=0})$$

we have

$$\alpha = \frac{C_L}{a} + \alpha_{L=0} = \frac{0.21}{0.0808} + (-2) = \boxed{0.6^\circ}$$

EXAMPLE 4

We considered the Beechcraft Baron 58 flying such that the wing is at a 4-degree angle of attack. The wing of this airplane has an NACA 23015 airfoil at the root, tapering to a 23010 airfoil at the tip. The data for the NACA 23015 airfoil is available. The airfoil lift and drag coefficients at $\alpha = 4°$, namely, $c_l = 0.54$ and $c_d = 0.0068$, Consider the wing of the airplane at a 4-degree angle of attack. The wing has an aspect ratio of 7.61 and a taper ratio of 0.45. Calculate C_L *and* C_D *for the wing.*

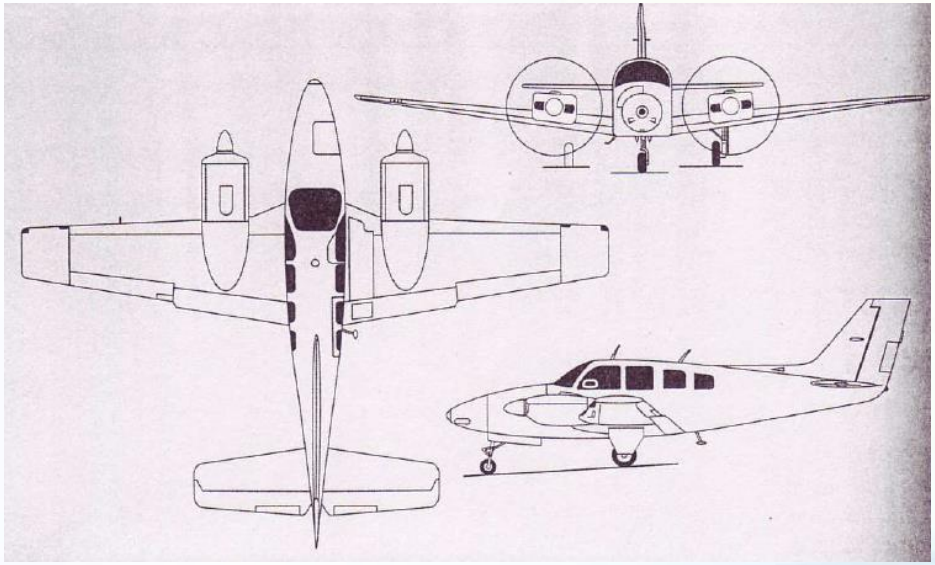

EXAMPLE 4 (CONT.)

$$a_0 = 0.113(57.3) = 6.47 \text{ per rad}$$

$$\delta = 0.01$$

$$e = \frac{1}{1+\delta} = \frac{1}{1+0.01} = 0.99$$

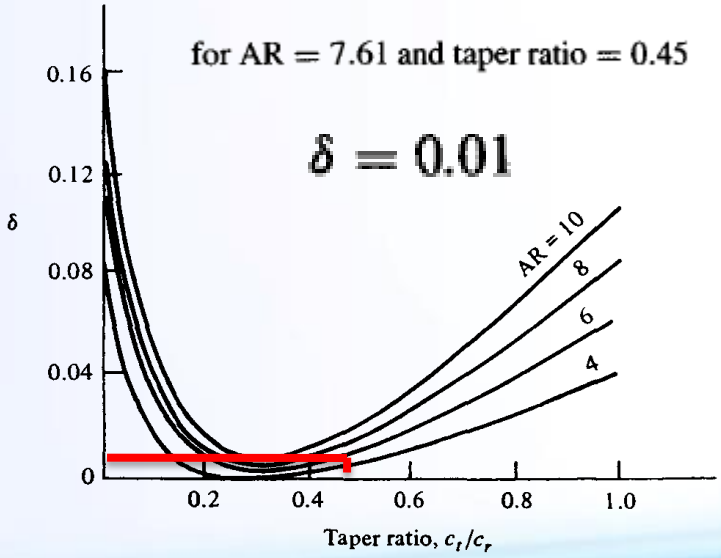

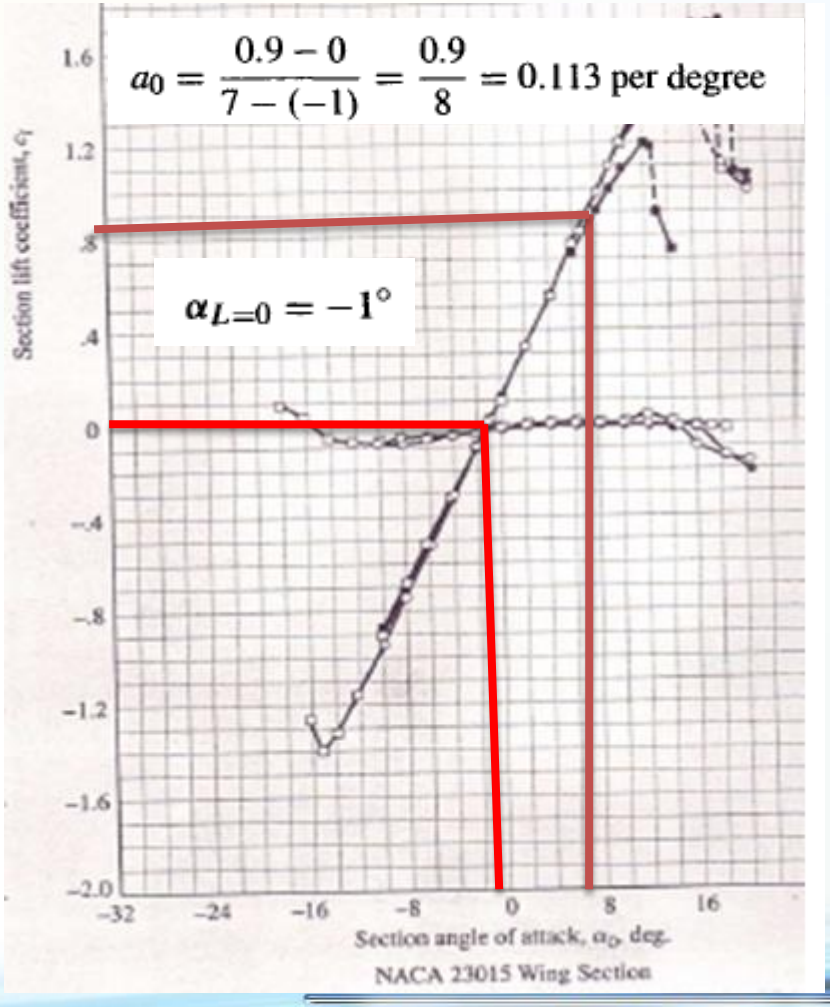

EXAMPLE 4 (CONT.)

assuming $\tau = \delta$,

$$a = \frac{a_0}{1 + \left(\frac{a_0}{\pi \mathrm{AR}}\right)(1 + \tau)}$$

$$\frac{a_0}{\pi \mathrm{AR}} = \frac{6.47}{\pi(7.61)} = 0.271$$

$$(1 + \tau) = 1 + 0.01 = 1.01$$

$$a = \frac{6.47}{1 + (0.271)(1.01)} = 5.08 \text{ per rad}$$

$$a = \frac{5.08}{57.3} = 0.0887 \text{ per degree}$$

$$C_L = a(\alpha - \alpha_{L=0})$$

For $\alpha = 4°$, we have

$$C_L = 0.0887[4 - (-1)] = 0.0887(5)$$

$$C_L = \boxed{0.443}$$

$$C_D = c_d + \frac{C_L^2}{\pi e \mathrm{AR}}$$

EXAMPLE 4 (CONT.)

Here, c_d is the section drag coefficient given in data. Note that in data, c_d is plotted versus the section lift coefficient c_l. To accurately read c_d from data, we need to know the value of c_l actually sensed by the airfoil section on the finite wing, that is, the value of the airfoil c_l for the airfoil at its effective angle of attack, α_{eff}. To estimate α_{eff} we will assume an elliptical lift distribution over the wing. We know this is not quite correct, but with a value of $\delta = 0.01$, it is not very far off. for an elliptical lift distribution, the induced angle of attack is:

$$\alpha_i = \frac{C_L}{\pi \, \mathrm{AR}} = \frac{(0.443)}{\pi(7.61)} = 0.0185 \text{ rad}$$

$$\alpha_i = (0.0185)(57.3) = 1.06^\circ \Rightarrow \alpha_{\text{eff}} = \alpha - \alpha_i = 4^\circ - 1.06^\circ = 2.94^\circ \approx 3^\circ$$

$$c_l = a_0(\alpha_{\text{eff}} - \alpha_{L=0})$$

$$= 0.113[3 - (-1)] = 0.113(4) = 0.452$$

EXAMPLE 4 (CONT.)

$$c_l = 0.452,$$

taking the data at the highest Reynolds number shown:

$$c_d = 0.0065$$

$$C_D = c_d + \frac{C_L^2}{\pi e \mathrm{AR}}$$

$$= 0.0065 + \frac{(0.443)^2}{\pi(0.99)(7.61)}$$

$$= 0.0065 + 0.0083 = \boxed{0.0148}$$

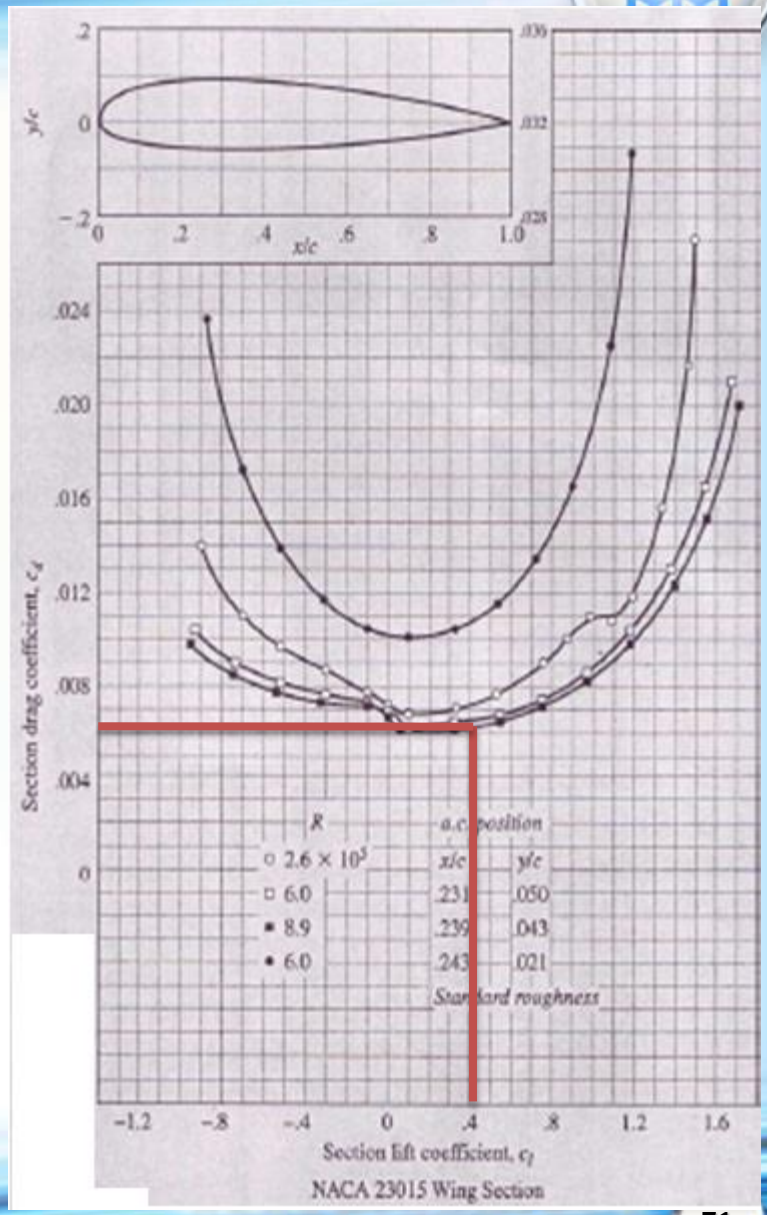

A NUMERICAL NONLINEAR LIFTING-LINE METHOD

Consider the most general case of a finite wing of given planform and geometric twist, with different airfoil sections at different spanwise stations. Assume that we have experimental data for the lift curves of the airfoil sections, including the nonlinear regime (i.e., assume we have the conditions of the following Figure for all the given airfoil sections). A numerical iterative solution for the finite-wing properties can be obtained as follows:

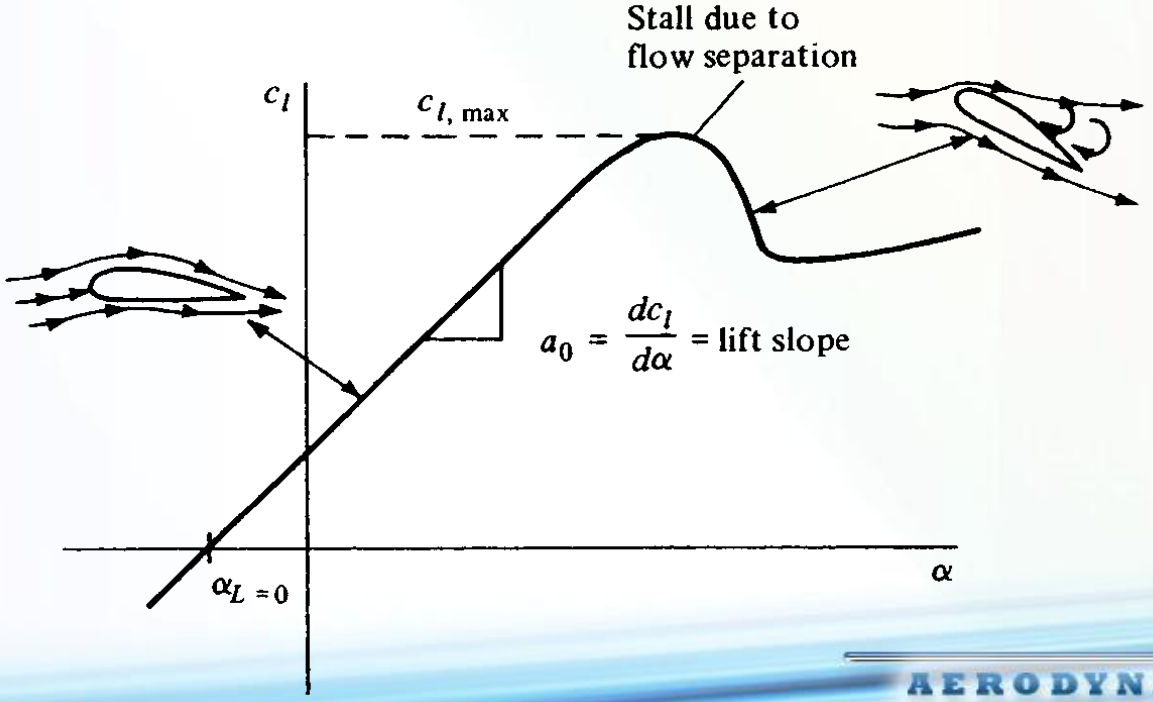

A NUMERICAL NONLINEAR LIFTING-LINE METHOD

1. Divide the wing into a number of spanwise stations, as shown in The following Figure. Here $k + 1$ stations are shown, with n designating any specific station.

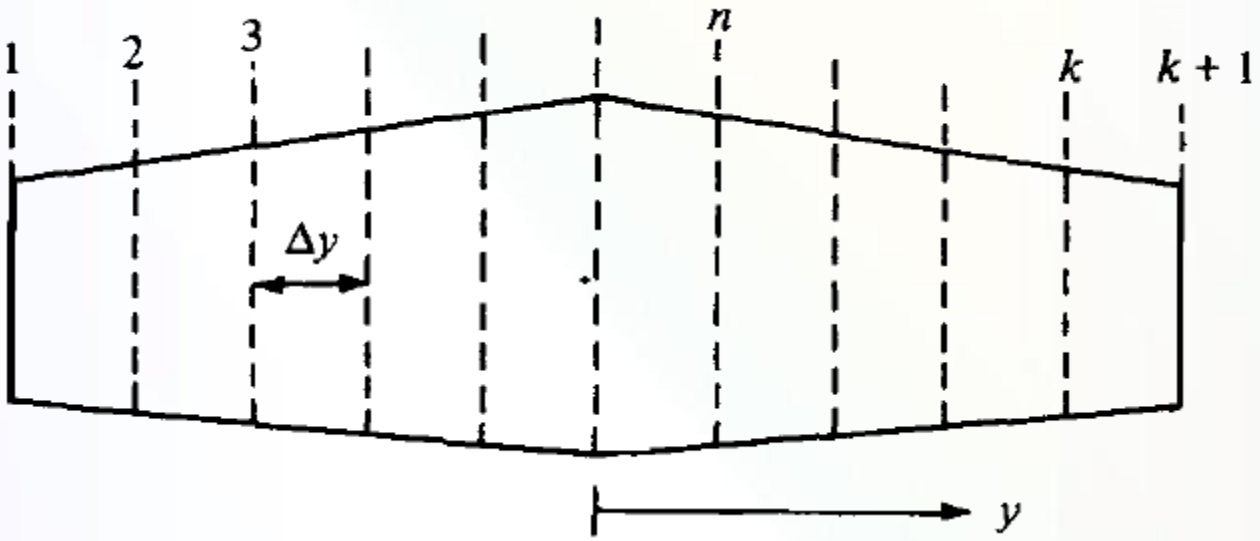

2. For the given wing at a given a, assume the lift distribution along the span; that is, assume values for Γ at all the stations $\Gamma_1, \Gamma_2, \ldots, \Gamma_n, \ldots, \Gamma_{k+1}$. An elliptical lift distribution is satisfactory for such an assumed distribution.

A NUMERICAL NONLINEAR LIFTING-LINE METHOD

3. With this assumed variation of Γ, calculate the induced angle of attack α_i at each of the stations:

$$\alpha_i(y_n) = \frac{1}{4\pi V_\infty} \int_{-b/2}^{b/2} \frac{(d\Gamma/dy)\, dy}{y_n - y}$$

The integral is evaluated numerically. If Simpson's rule is used

$$\alpha_i(y_n) = \frac{1}{4\pi V_\infty} \frac{\Delta y}{3} \sum_{j=2,4,6}^{k} \frac{(d\Gamma/dy)_{j-1}}{(y_n - y_{j-1})} + 4\frac{(d\Gamma/dy)_j}{y_n - y_j} + \frac{(d\Gamma/dy)_{j+1}}{y_n - y_{j+1}}$$

where Δy is the distance between stations.
when $y_n = y_{j-1}$, y_j, or y_{j+1}, a singularity occurs (a denominator goes to zero). When this singularity occurs, it can be avoided by replacing the given term by its average value based on the two adjacent sections.

A NUMERICAL NONLINEAR LIFTING-LINE METHOD

4. Using α_i from step 3, obtain the effective angle of attack α_{eff} at each station from

$$\alpha_{\text{eff}}(y_n) = \alpha - \alpha_i(y_n)$$

5. With the distribution of α_{eff} calculated from step 4, obtain the section lift coefficient $(c_l)_n$ at each station. These values are read from the known lift curve for the airfoil.

6. From $(c_l)_n$ obtained in step 5, a *new* circulation distribution is calculated from the Kutta-Joukowski theorem and the definition of lift coefficient:

$$L'(y_n) = \rho_\infty V_\infty \Gamma(y_n) = \tfrac{1}{2}\rho_\infty V_\infty^2 c_n (c_l)_n$$

Hence,

$$\Gamma(y_n) = \tfrac{1}{2} V_\infty c_n (c_l)_n$$

where c_n is the local section chord. Keep in mind that in all the above steps, n ranges from 1 to $k + 1$.

A NUMERICAL NONLINEAR LIFTING-LINE METHOD

7. The new distribution of Γ obtained in step 6 is compared with the values that were initially fed into step 3. If the results from step 6 do not agree with the input to step 3, then a new input is generated. If the previous input to step 3 is designated as Γ_{old} and the result of step 6 is designated as Γ_{new},

then the new input to step 3 is determined from

$$\Gamma_{input} = \Gamma_{old} + D(\Gamma_{new} - \Gamma_{old})$$

where D is a damping factor for the iterations. Experience has found that the iterative procedure requires heavy damping, with typical values of D on the order of 0.05.

8. Steps 3 to 7 are repeated a sufficient number of cycles until Γ_{new} and Γ_{old} agree at each spanwise station to within acceptable accuracy. If this accuracy is stipulated to be within 0.01 percent for a stretch of five previous iterations, then a minimum of 50 and sometimes as many as 150 iterations may be required for convergence.

A NUMERICAL NONLINEAR LIFTING-LINE METHOD

9. From the converged $\Gamma(y)$, the lift and induced drag coefficients are obtained

$$C_L = \frac{L}{q_\infty S} = \frac{2}{V_\infty S} \int_{-b/2}^{b/2} \Gamma(y)\, dy \qquad C_{D,i} = \frac{D_i}{q_\infty S} = \frac{2}{V_\infty S} \int_{-b/2}^{b/2} \Gamma(y) \alpha_i(y)\, dy$$

The integrations in these equations can again be carried out by Simpson's rule.

A NUMERICAL NONLINEAR LIFTING-LINE METHOD

Typical results

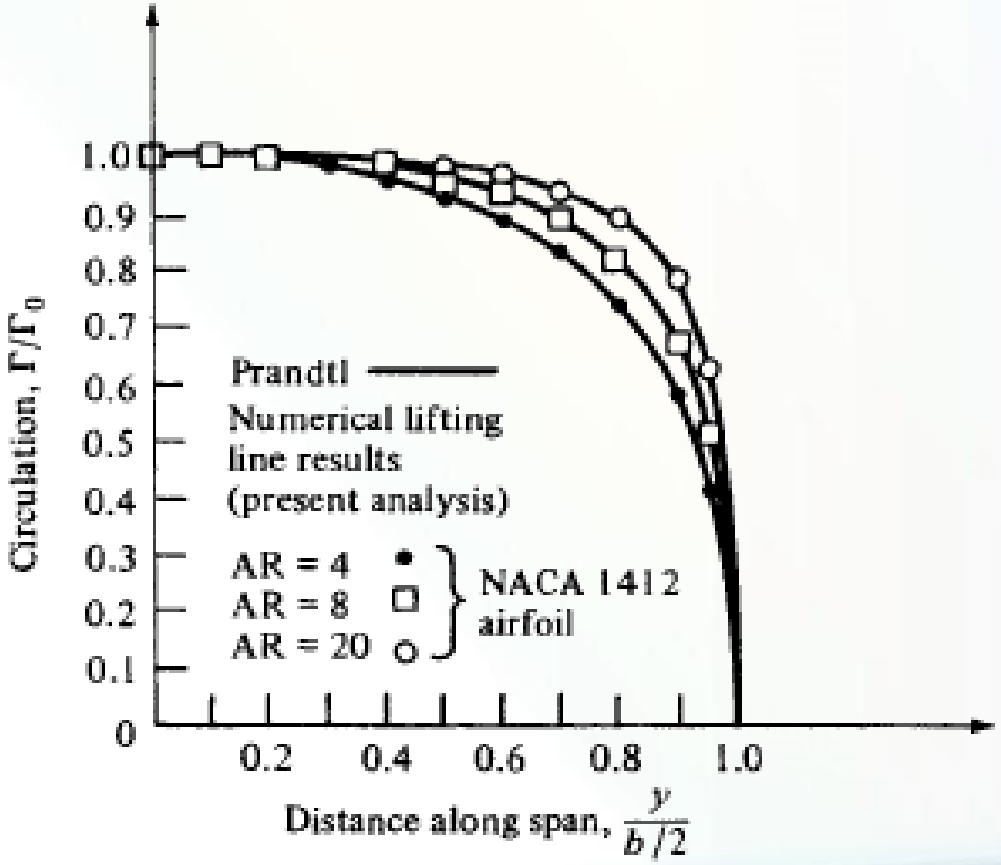

A NUMERICAL NONLINEAR LIFTING-LINE METHOD

An example of the use of the numerical method for the nonlinear regime is shown in this figure:

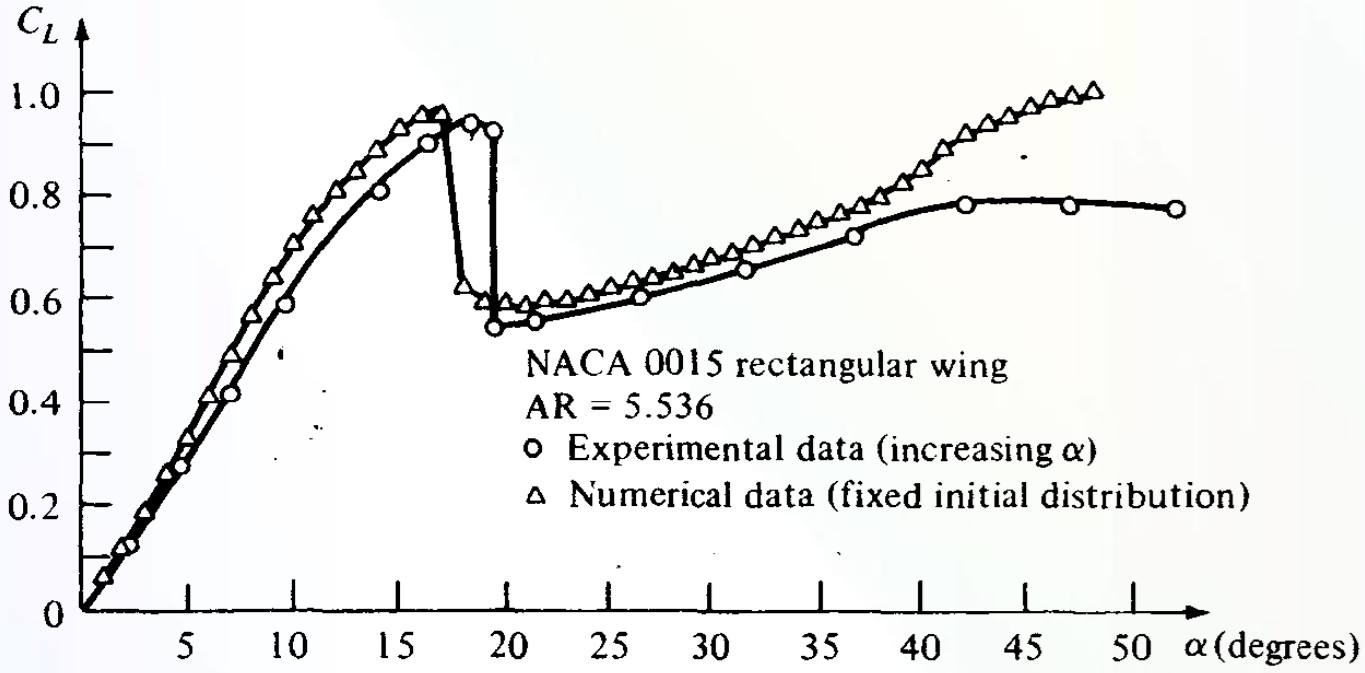

The numerical lifting-line solution at high angle of attack agrees with the experiment to within 20 percent, and much closer for many cases.

Reduction of Induced Drag

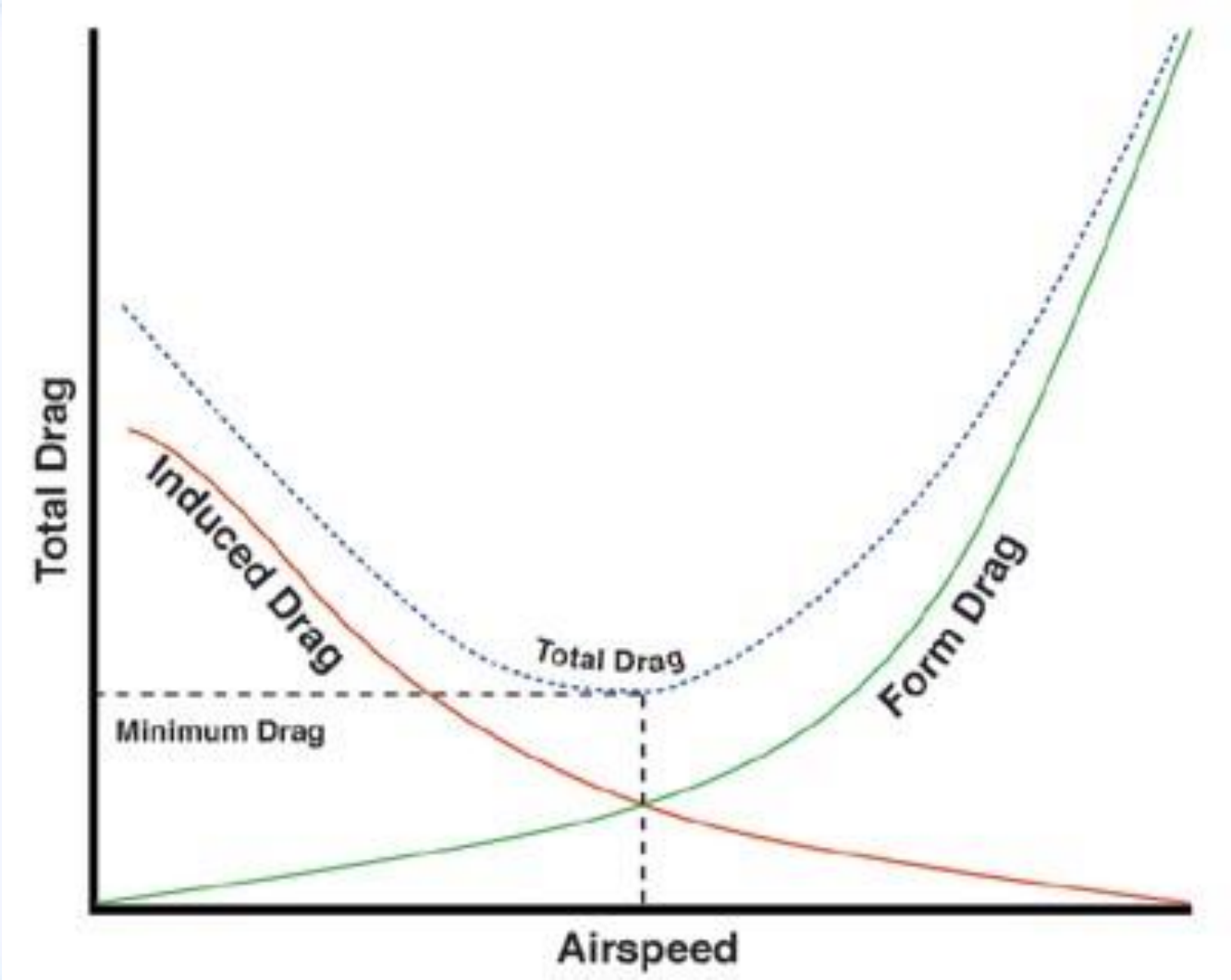

Reduction of Induced Drag

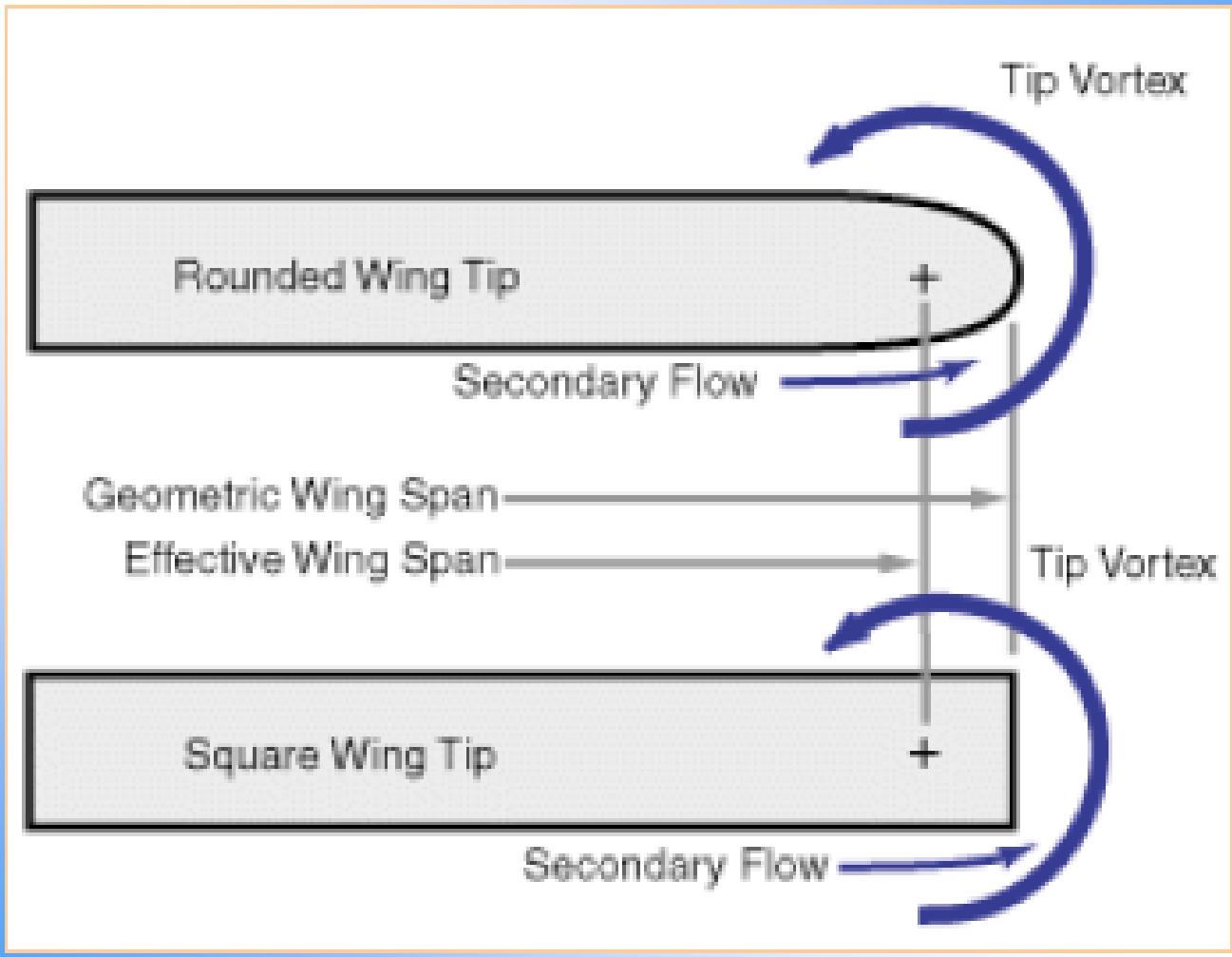

Reduction of Induced Drag

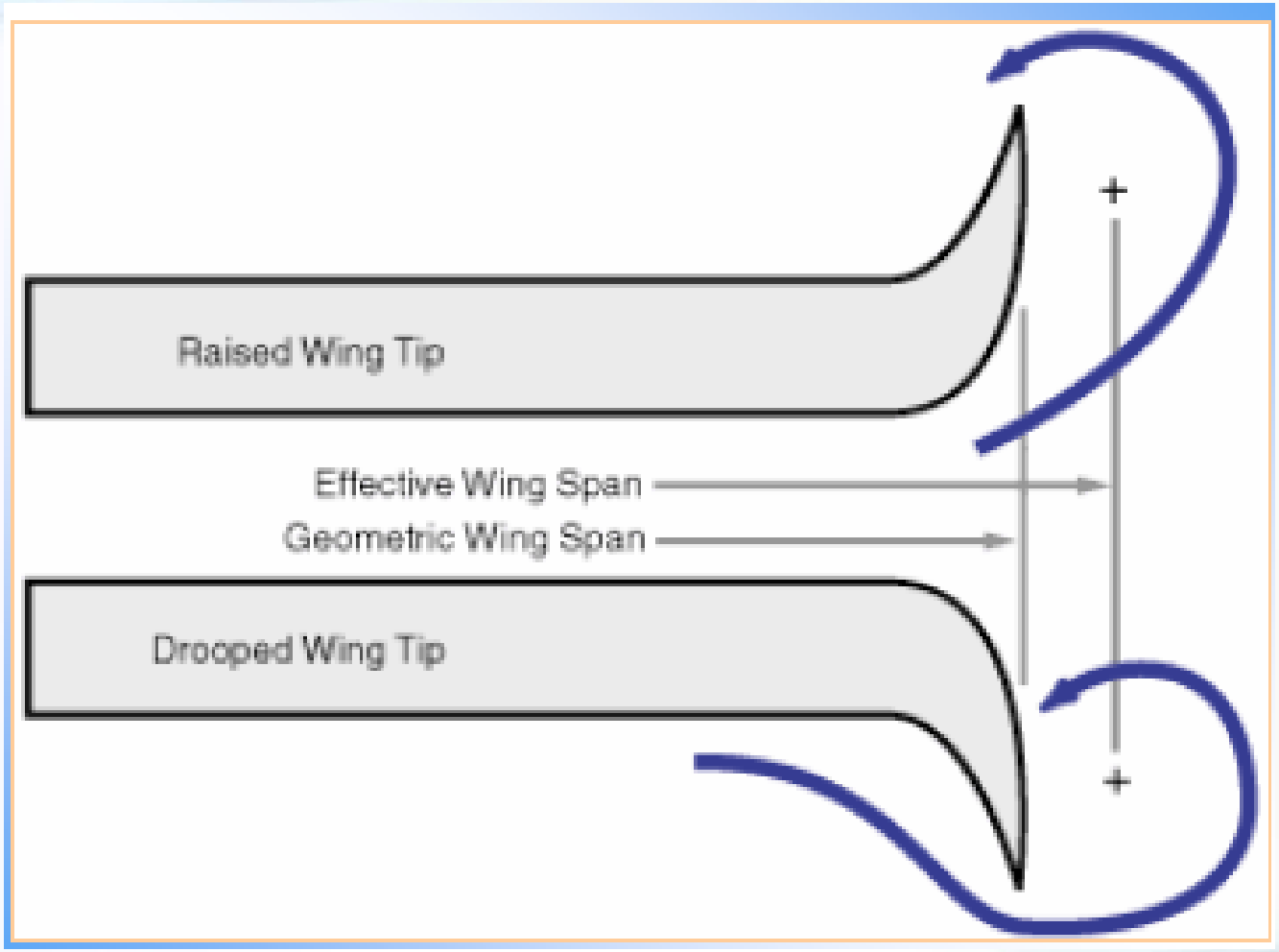

Reduction of Induced Drag

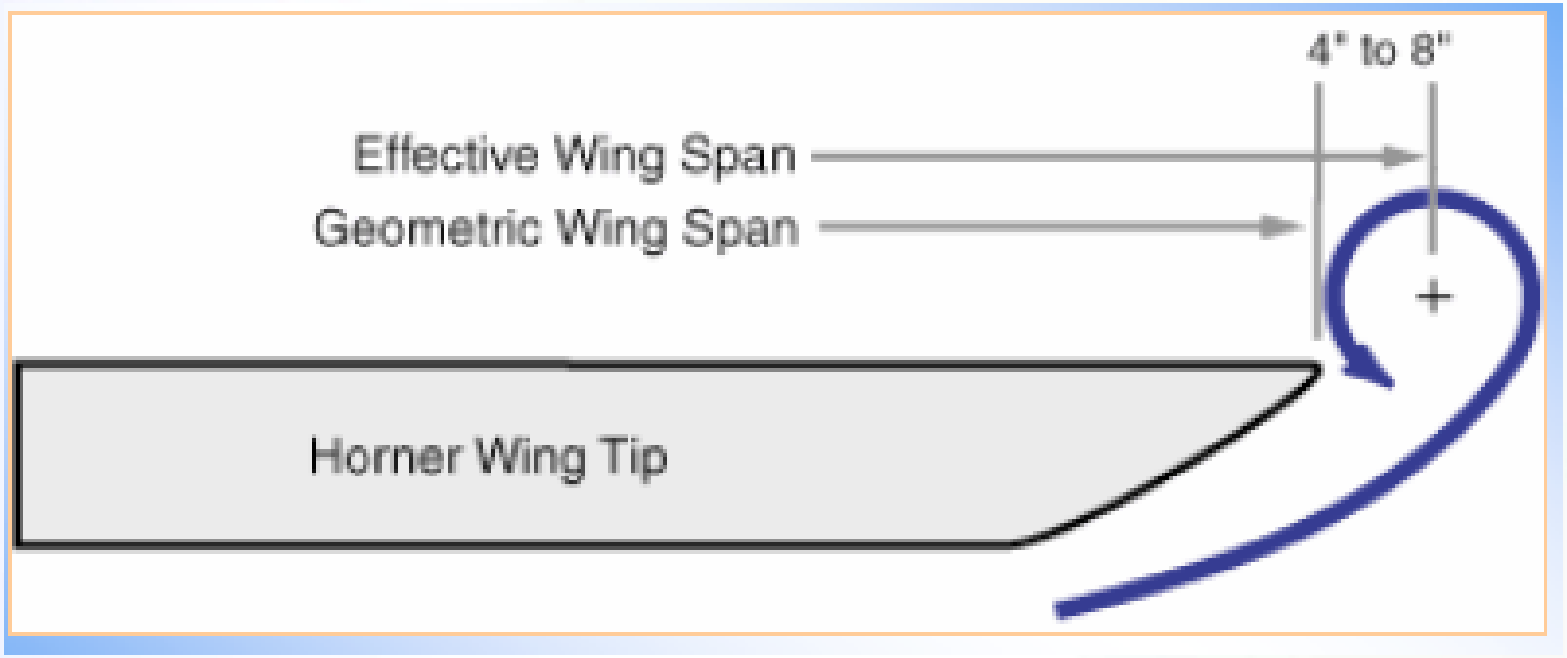

Reduction of Induced Drag

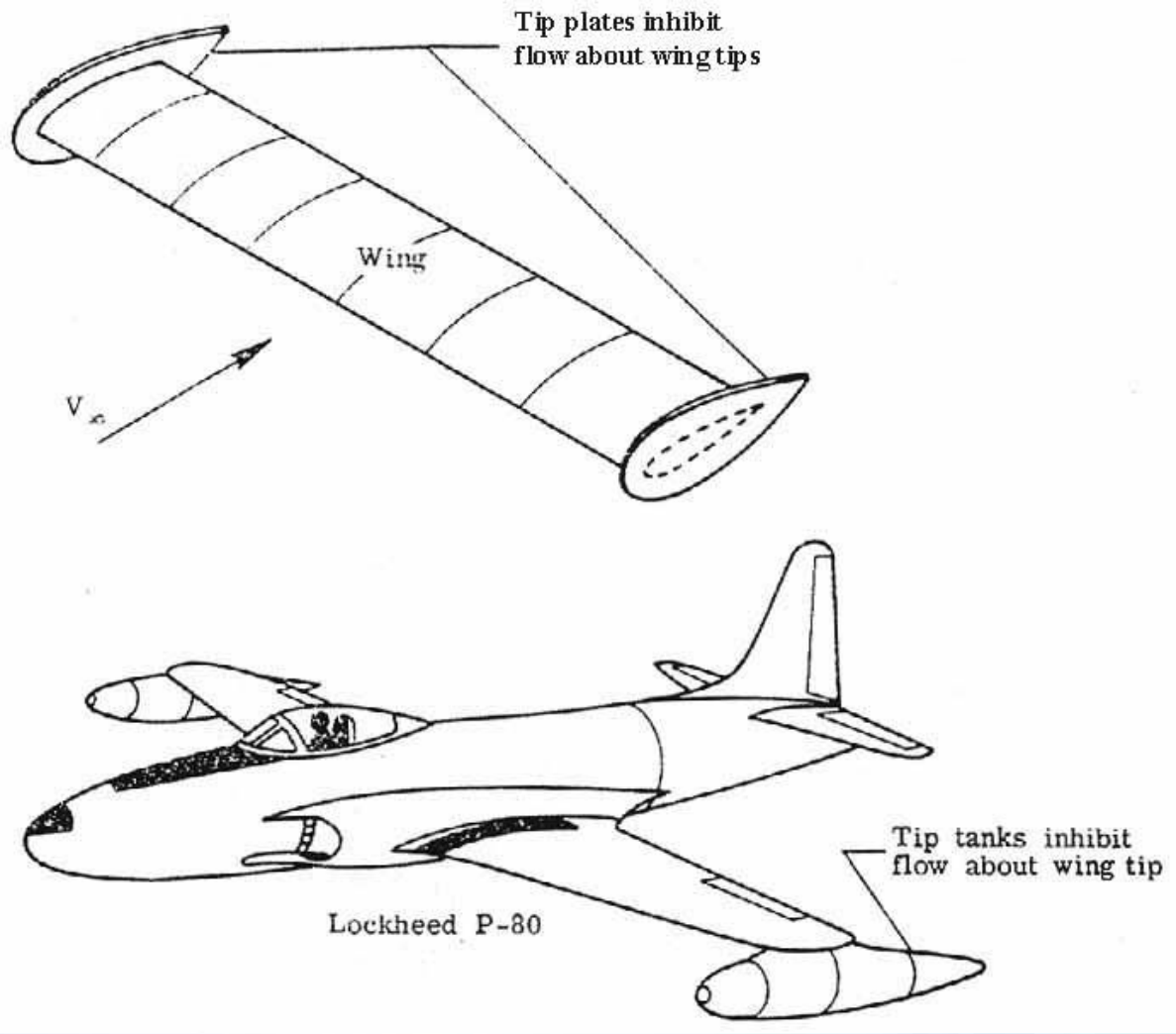

Reduction of Induced Drag

Reduction of Induced Drag

THE LIFTING-SURFACE THEORY AND THE VORTEX LATTICE NUMERICAL METHOD

Prandtl's classical lifting-line theory gives reasonable results for *straight wings at moderate to high aspect ratio*.

For low-aspect-ratio straight wings, swept wings, and delta wings, classical lifting-line theory is inappropriate.

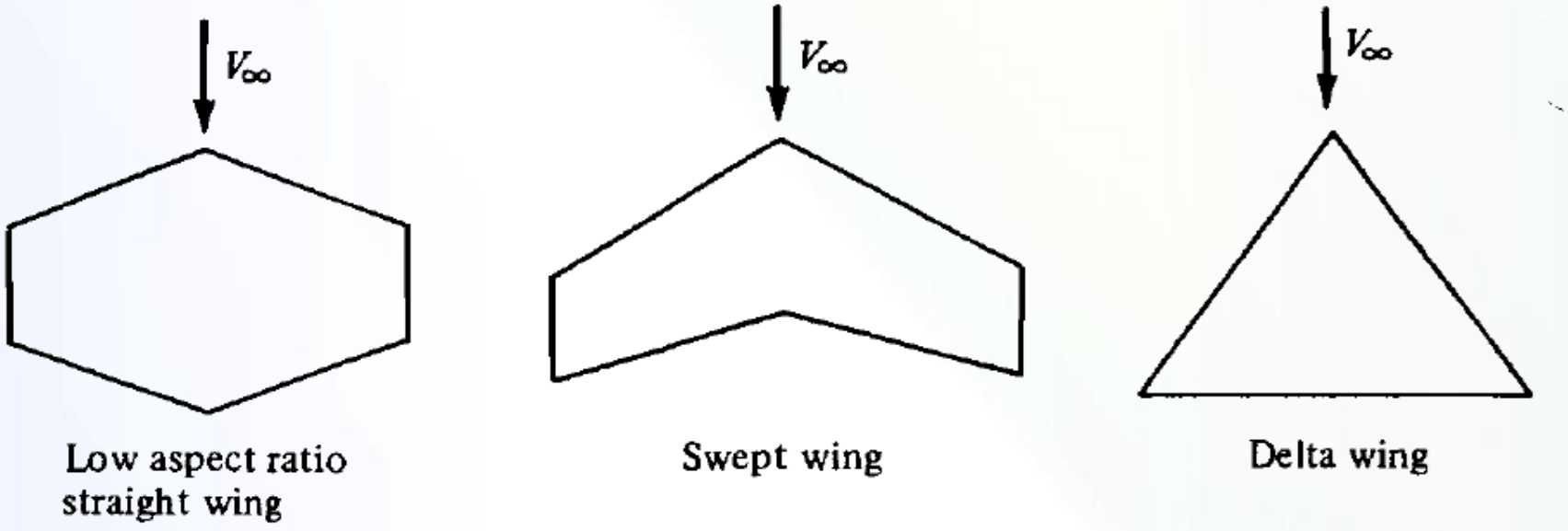

For such planforms, a more sophisticated model must be used.

VORTEX LATTICE METHOD (VLM)

- The VLM represents the wing as a planar surface on which a grid of horseshoe vortices is superimposed.

- The velocities induced by each horseshoe vortex at a specified control point are calculated using the law of Biot-Savart.

- A summation is performed for all control points on the wing to produce a set of linear algebraic equations for the horseshoe vortex strengths that satisfy the boundary condition of no flow through the wing.

- The vortex strengths are related to the wing circulation and the pressure differential between the upper and lower wing surfaces.

VORTEX LATTICE METHOD (VLM)

1. The wing surface is divided into several trapezoidal sub regions (*finite elements* or *lattices*)

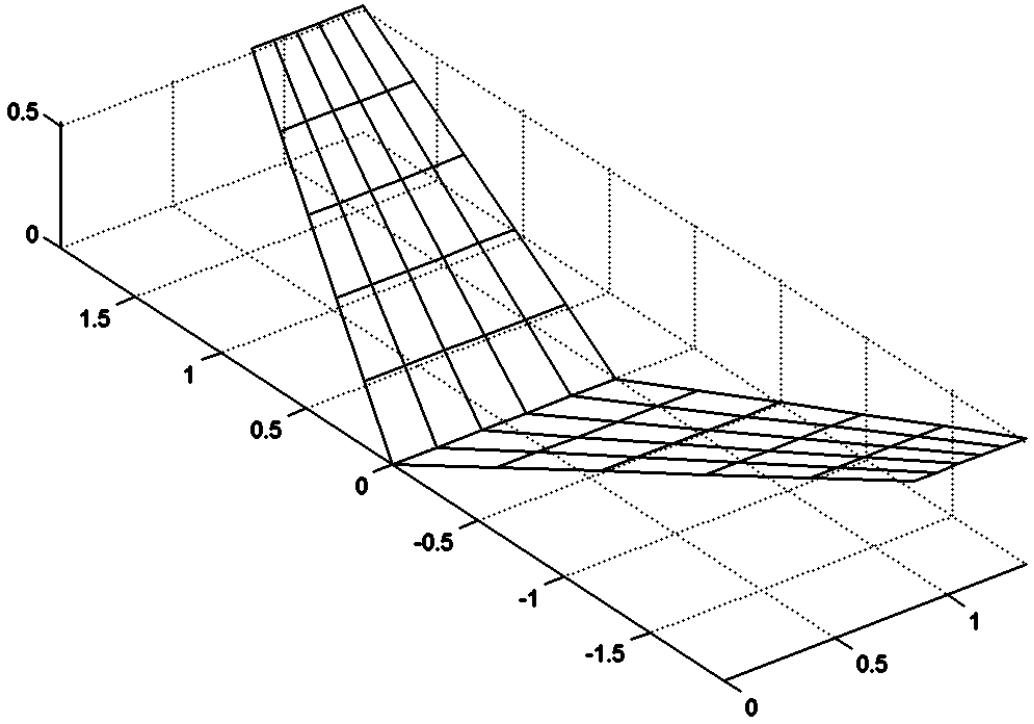

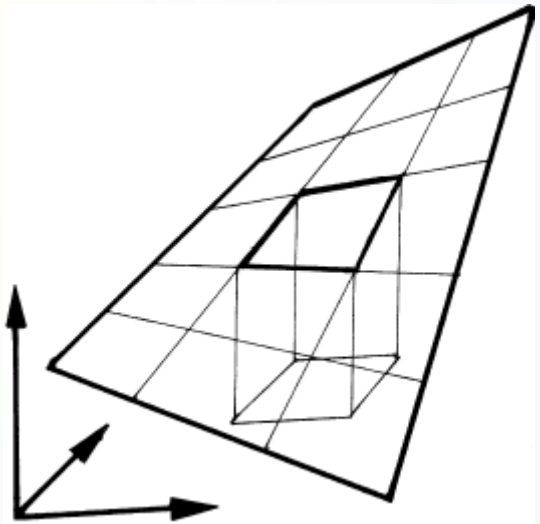

2. A horseshoe vortex is placed on each lattice.

- Place the bound vortex of the horseshoe vortex on the 1/4 chord element line of each panel.
- Place the control point on the 3/4 chord point of each panel at the midpoint in the spanwise direction.

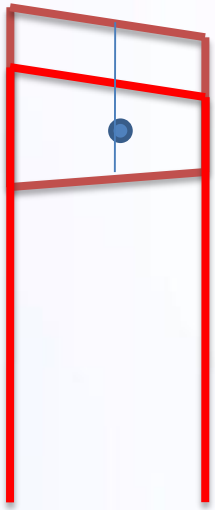

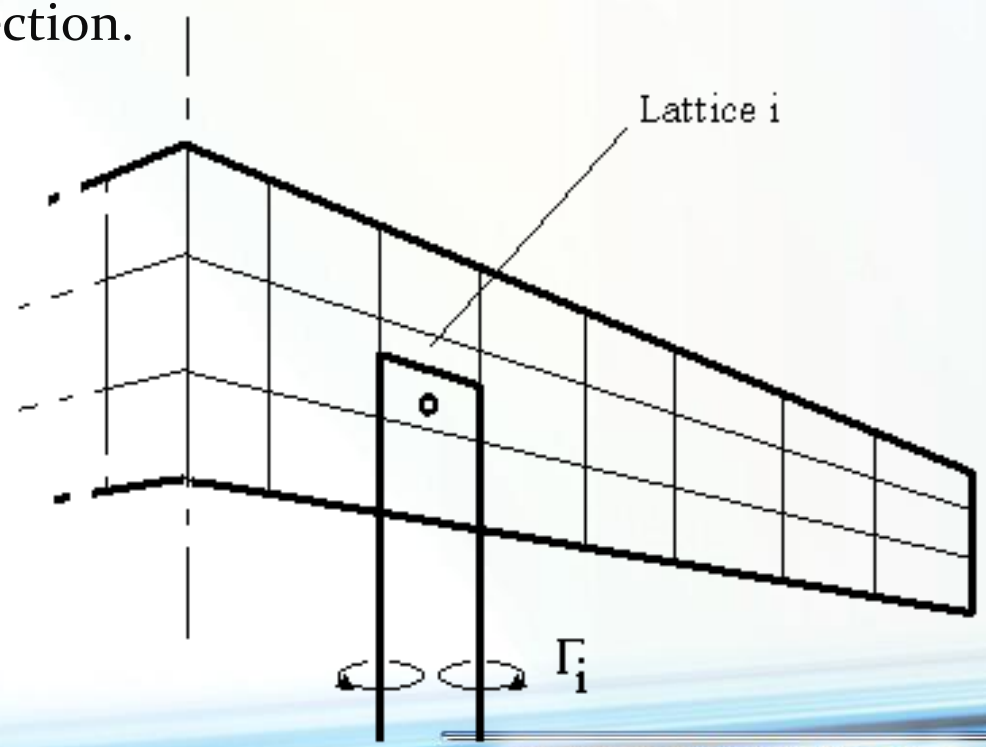

VORTEX LATTICE METHOD (VLM)

- **Comments**
  - This is known as the “1/4 - 3/4 rule.”
  - It’s not a theoretical law, simply a placement that works well and has become a rule of thumb.
  - The 1/4 - 3/4 rule is widely used, and has proven to be sufficiently accurate in practice.

VORTEX LATTICE METHOD (VLM)

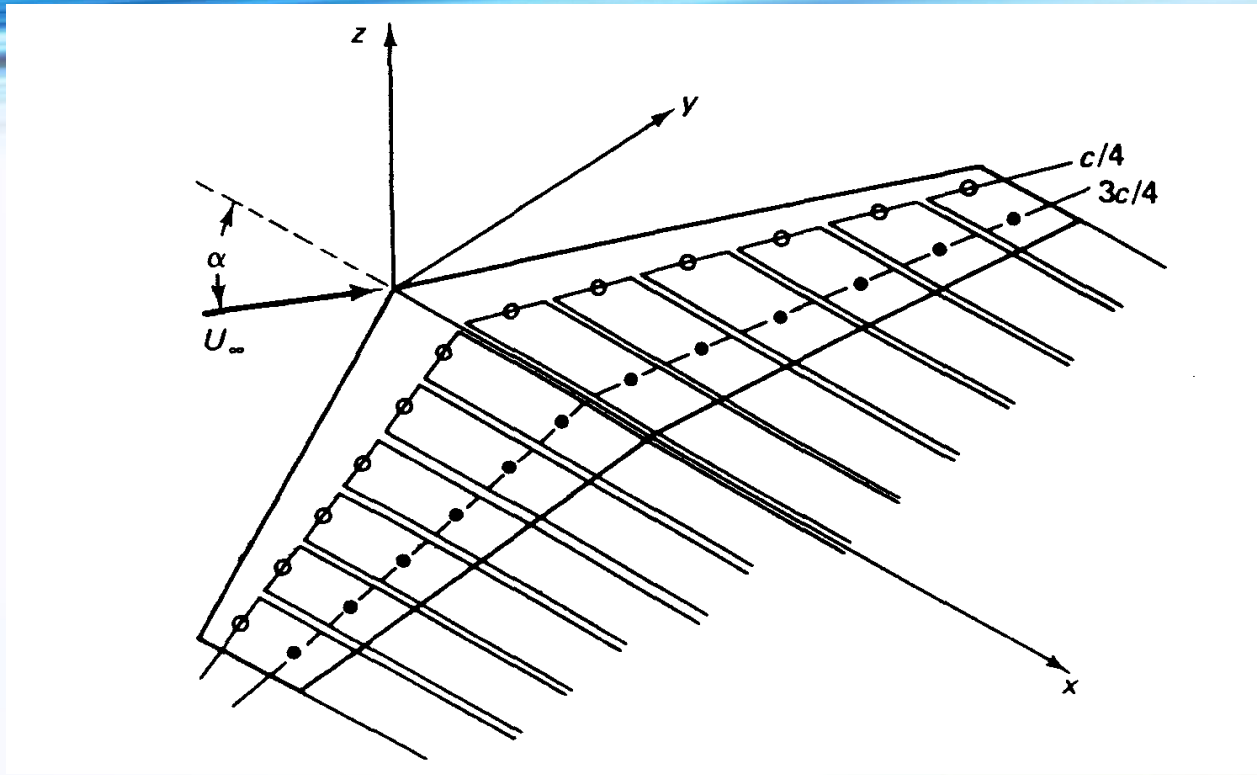

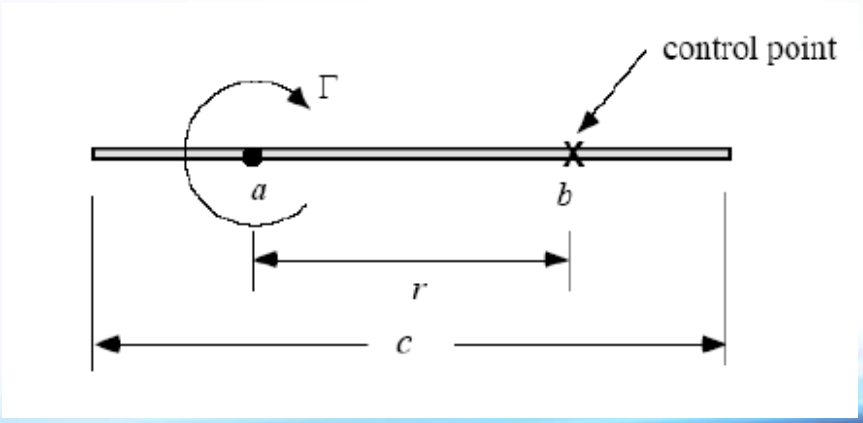

VORTEX LATTICE METHOD (VLM)

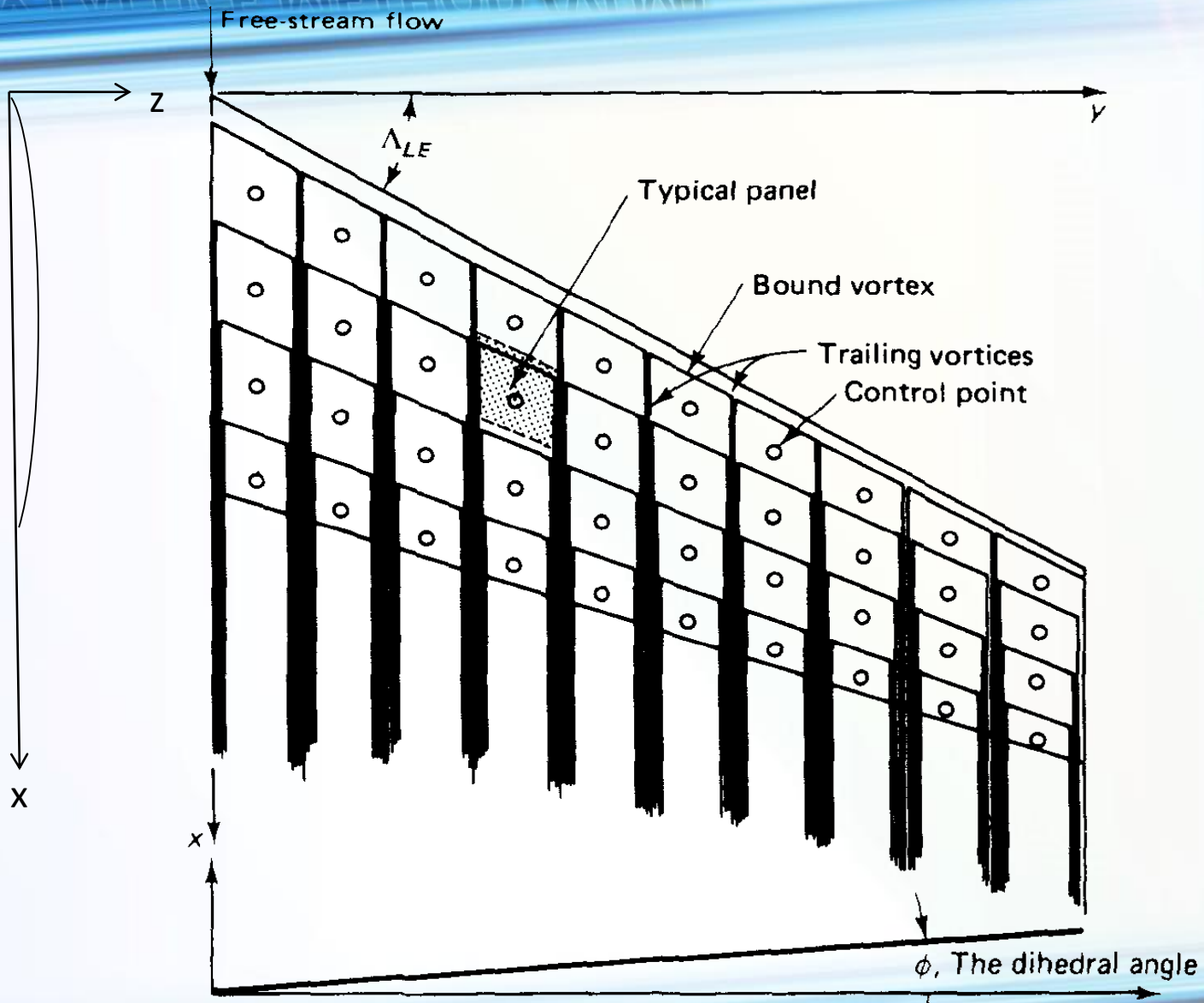

THE HORSESHOE VORTEX INDUCED VELOCITY

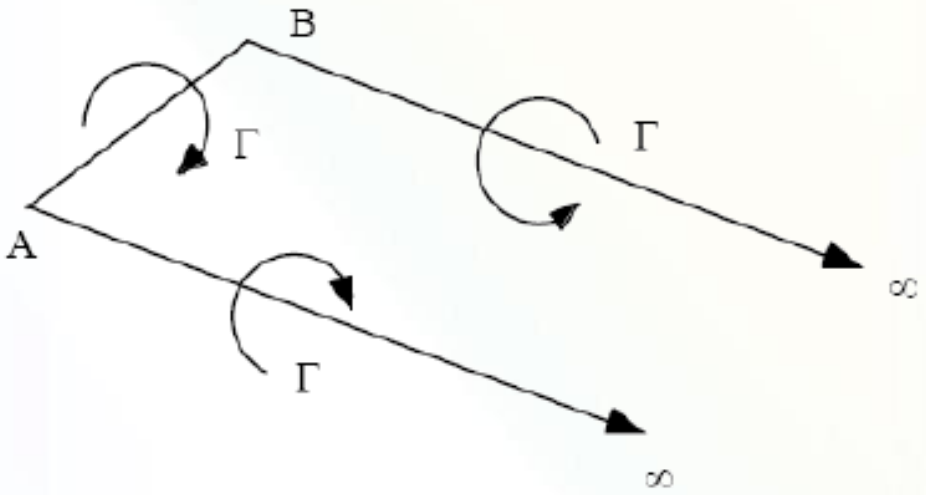

$$\mathbf{V} = \mathbf{V}_{AB} + \mathbf{V}_{A\infty} + \mathbf{V}_{B\infty}$$

THE HORSESHOE VORTEX INDUCED VELOCITY

- The velocity induced by a vortex filament of strength Γ and a length of *dl* is given by the *law of Biot and Savart*.

$$\vec{V}_p = \frac{\Gamma}{4\pi}\int \frac{d\vec{l}\times\vec{r}_{pq}}{\left|\vec{r}_{pq}\right|^3}$$

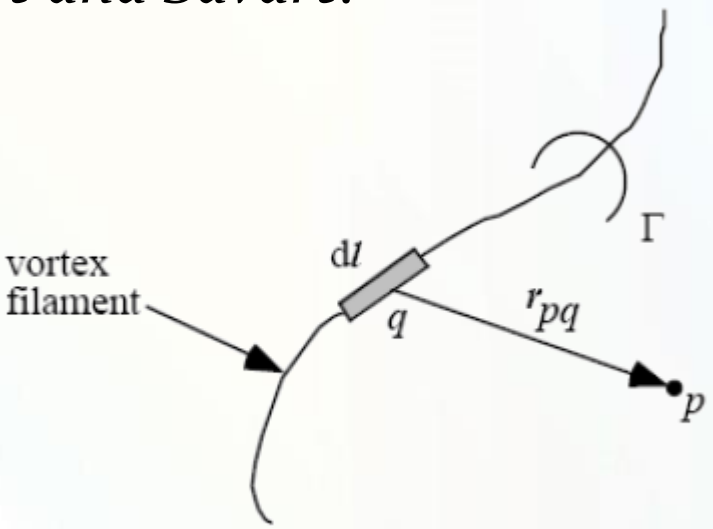

- Since we are interested in the flow field induced by a horseshoe vortex which consists of three straight segments, let us use this equation to calculate the effect of each segment separately.

THE HORSESHOE VORTEX INDUCED VELOCITY

- Let AB be such a segment, with the vorticity vector directed from A to B. Let C be a point in space whose normal distance from the line AB is r_p.

$$r = \frac{r_p}{\sin\theta}$$

$$dl = r_p(\csc^2\theta)\, d\theta$$

- We can integrate between A and B to find the magnitude of the induced velocity:

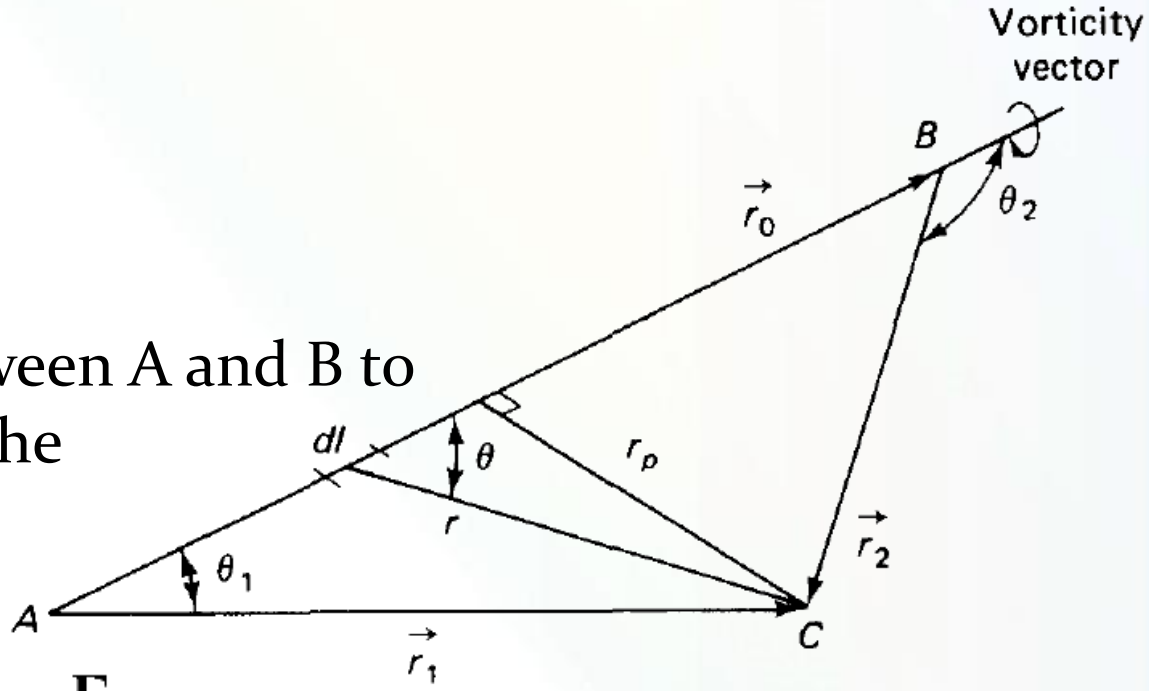

$$V = \frac{\Gamma_n}{4\pi r_p}\int_{\theta_1}^{\theta_2} \sin\theta\, d\theta = \frac{\Gamma_n}{4\pi r_p}(\cos\theta_1 - \cos\theta_2)$$

THE HORSESHOE VORTEX INDUCED VELOCITY

The semi-infinite vortex

$$V_p = \frac{\Gamma}{4\pi h}(1 + \cos\theta_0)$$

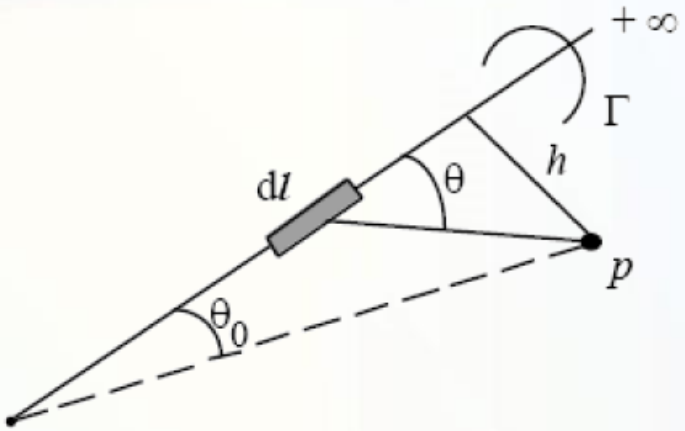

The finite vortex

$$V_p = \frac{\Gamma}{4\pi h}(\cos\theta_1 - \cos\theta_2)$$

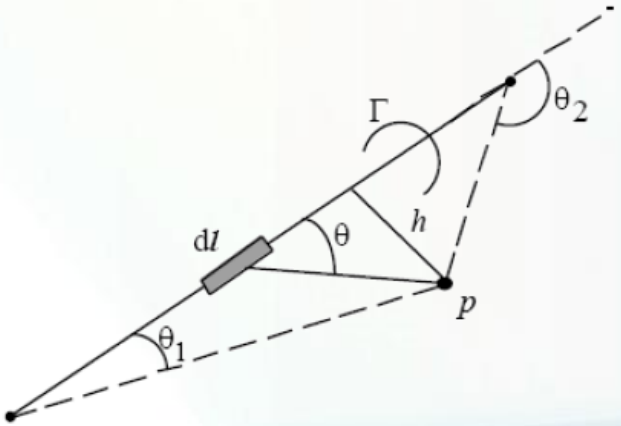

THE HORSESHOE VORTEX INDUCED VELOCITY

$$V_p = \frac{\Gamma}{4\pi r_p}(\cos\theta_1 - \cos\theta_2)$$

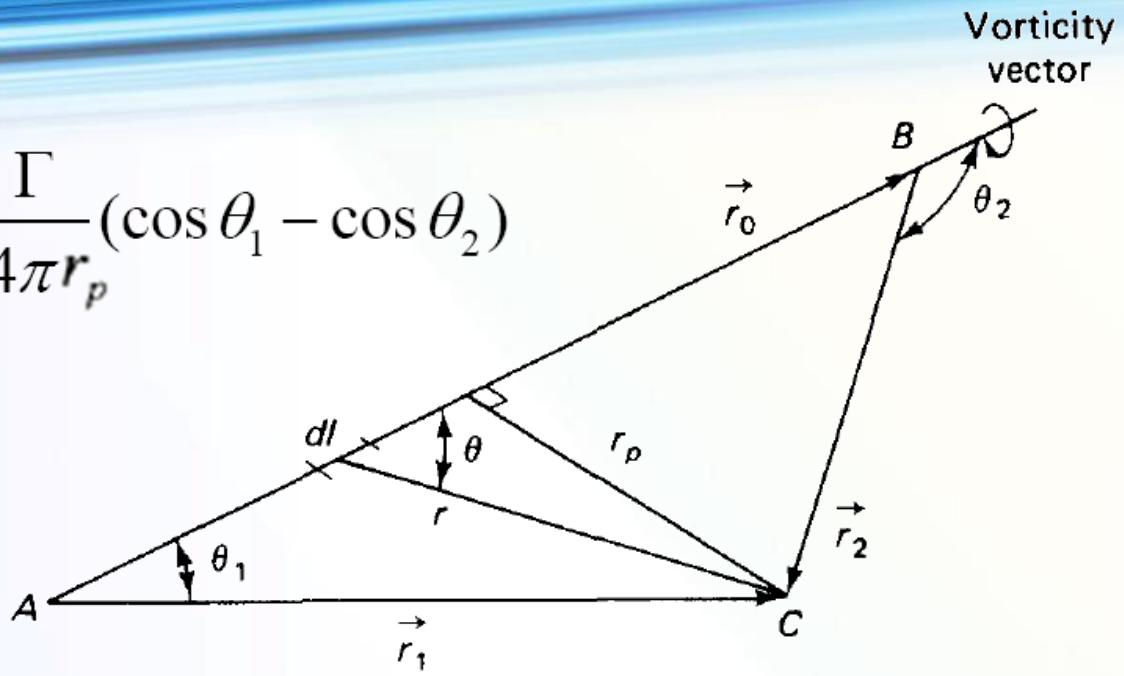

$$r_p = \frac{|\vec{r}_1 \times \vec{r}_2|}{r_0}$$

$$\cos\theta_1 = \frac{\vec{r}_0 \cdot \vec{r}_1}{r_0 r_1}$$

$$\cos\theta_2 = \frac{\vec{r}_0 \cdot \vec{r}_2}{r_0 r_2}$$

The direction of the induced velocity is given by the unit vector:

$$\frac{\vec{r}_1 \times \vec{r}_2}{|\vec{r}_1 \times \vec{r}_2|}$$

$$\vec{V} = \frac{\Gamma_n}{4\pi} \frac{\vec{r}_1 \times \vec{r}_2}{|\vec{r}_1 \times \vec{r}_2|^2} \left[\vec{r}_0 \cdot \left(\frac{\vec{r}_1}{r_1} - \frac{\vec{r}_2}{r_2} \right) \right]$$

THE HORSESHOE VORTEX INDUCED VELOCITY

$$\vec{V} = \frac{\Gamma_n}{4\pi} \frac{\vec{r}_1 \times \vec{r}_2}{|\vec{r}_1 \times \vec{r}_2|^2} \left[\vec{r}_0 \cdot \left(\frac{\vec{r}_1}{r_1} - \frac{\vec{r}_2}{r_2} \right) \right]$$

- This is the basic expression for the calculation of the induced velocity by the horseshoe vortices in the VLM. It can be used regardless of the assumed orientation of the vortices.

- We shall now use this equation to calculate the velocity that is induced at a general point in space (x, y, z) by the horseshoe vortex. This horseshoe vortex may be assumed to represent that for a typical wing panel.

THE HORSESHOE VORTEX INDUCED VELOCITY

For the bound vortex, segment *AB*:

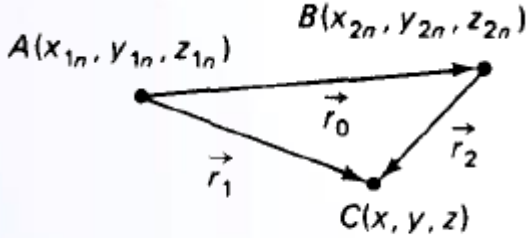

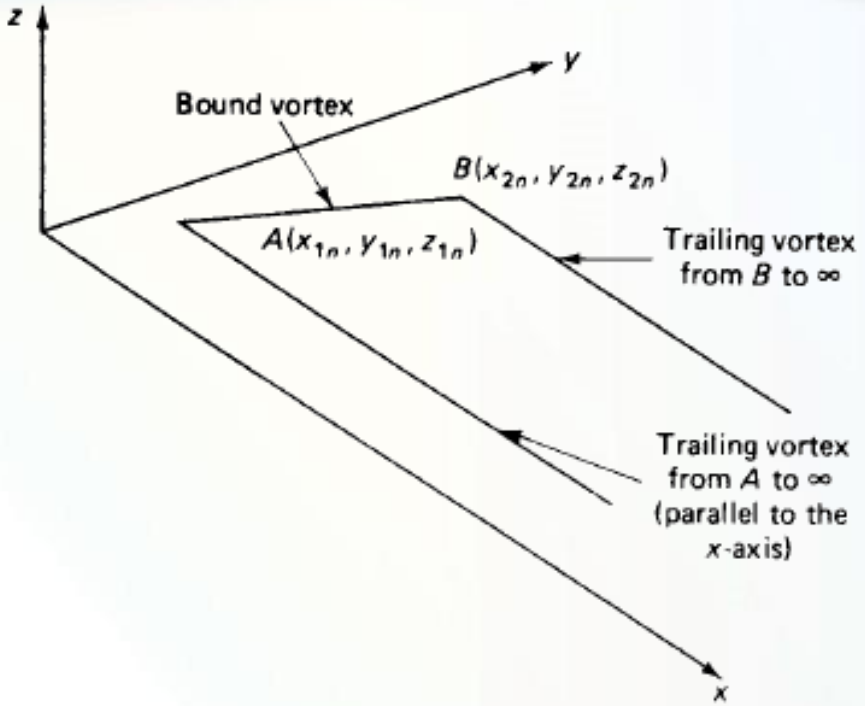

$$\vec{r}_0 = \overrightarrow{AB} = (x_{2n} - x_{1n})\hat{i} + (y_{2n} - y_{1n})\hat{j} + (z_{2n} - z_{1n})\hat{k}$$

$$\vec{r}_1 = (x - x_{1n})\hat{i} + (y - y_{1n})\hat{j} + (z - z_{1n})\hat{k}$$

$$\vec{r}_2 = (x - x_{2n})\hat{i} + (y - y_{2n})\hat{j} + (z - z_{2n})\hat{k}$$

THE HORSESHOE VORTEX INDUCED VELOCITY

$$\vec{V} = \frac{\Gamma_n}{4\pi} \frac{\vec{r}_1 \times \vec{r}_2}{|\vec{r}_1 \times \vec{r}_2|^2} \left[\vec{r}_0 \cdot \left(\frac{\vec{r}_1}{r_1} - \frac{\vec{r}_2}{r_2} \right) \right]$$

$$\vec{V}_{AB} = \frac{\Gamma_n}{4\pi} \{\mathrm{Fac1}_{AB}\}\{\mathrm{Fac2}_{AB}\}$$

$$\{\mathrm{Fac1}_{AB}\} = \frac{\vec{r}_1 \times \vec{r}_2}{|\vec{r}_1 \times \vec{r}_2|^2}$$

$$\begin{aligned}
&= \{[(y - y_{1n})(z - z_{2n}) - (y - y_{2n})(z - z_{1n})]\hat{i} \\
&\quad - [(x - x_{1n})(z - z_{2n}) - (x - x_{2n})(z - z_{1n})]\hat{j} \\
&\quad + [(x - x_{1n})(y - y_{2n}) - (x - x_{2n})(y - y_{1n})]\hat{k}\}/ \\
&\quad \{[(y - y_{1n})(z - z_{2n}) - (y - y_{2n})(z - z_{1n})]^2 \\
&\quad + [(x - x_{1n})(z - z_{2n}) - (x - x_{2n})(z - z_{1n})]^2 \\
&\quad + [(x - x_{1n})(y - y_{2n}) - (x - x_{2n})(y - y_{1n})]^2\}
\end{aligned}$$

THE HORSESHOE VORTEX INDUCED VELOCITY

$$\vec{V} = \frac{\Gamma_n}{4\pi} \frac{\vec{r}_1 \times \vec{r}_2}{|\vec{r}_1 \times \vec{r}_2|^2} \left[\vec{r}_0 \cdot \left(\frac{\vec{r}_1}{r_1} - \frac{\vec{r}_2}{r_2} \right) \right]$$

$$\vec{V}_{AB} = \frac{\Gamma_n}{4\pi} \{\text{Fac1}_{AB}\}\{\text{Fac2}_{AB}\}$$

$$\{\text{Fac2}_{AB}\} = \left(\vec{r}_0 \cdot \frac{\vec{r}_1}{r^1} - \vec{r}_0 \cdot \frac{\vec{r}_2}{r^2} \right)$$

$$= \{[(x_{2n} - x_{1n})(x - x_{1n}) + (y_{2n} - y_{1n})(y - y_{1n}) + (z_{2n} - z_{1n})(z - z_{1n})]/$$

$$\sqrt{(x - x_{1n})^2 + (y - y_{1n})^2 + (z - z_{1n})^2}$$

$$- [(x_{2n} - x_{1n})(x - x_{2n}) + (y_{2n} - y_{1n})(y - y_{2n}) + (z_{2n} - z_{1n})(z - z_{2n})]/$$

$$\sqrt{(x - x_{2n})^2 + (y - y_{2n})^2 + (z - z_{2n})^2}\}$$

THE HORSESHOE VORTEX INDUCED VELOCITY

To calculate the velocity induced by the filament that extends from *A to* ∞*:*

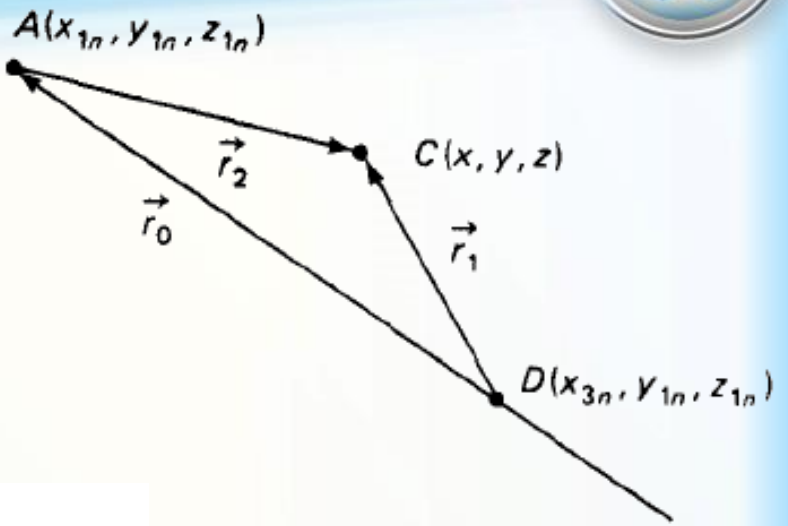

$$\vec{r}_0 = \overrightarrow{DA} = (x_{1n} - x_{3n})\hat{i}$$

$$\vec{r}_1 = (x - x_{3n})\hat{i} + (y - y_{1n})\hat{j} + (z - z_{1n})\hat{k}$$

$$\vec{r}_2 = (x - x_{1n})\hat{i} + (y - y_{1n})\hat{j} + (z - z_{1n})\hat{k}$$

$$\overrightarrow{V_{AD}} = \frac{\Gamma_n}{4\pi}\{\text{Fac1}_{AD}\}\{\text{Fac2}_{AD}\}$$

$$\{\text{Fac1}_{AD}\} = \frac{(z - z_{1n})\hat{j} + (y_{1n} - y)\hat{k}}{[(z - z_{1n})^2 + (y_{1n} - y)^2](x_{3n} - x_{1n})}$$

$$\{\text{Fac2}_{AD}\} = (x_{3n} - x_{1n})\left\{\frac{x_{3n} - x}{\sqrt{(x - x_{3n})^2 + (y - y_{1n})^2 + (z - z_{1n})^2}}\right.$$

$$\left. + \frac{x - x_{1n}}{\sqrt{(x - x_{1n})^2 + (y - y_{1n})^2 + (z - z_{1n})^2}}\right\}$$

Letting x_3 go to ∞, the first term of $\{\text{Fac2}_{AD}\}$ goes to 1.0.

THE HORSESHOE VORTEX INDUCED VELOCITY

$$\overrightarrow{V_{A\infty}} = \frac{\Gamma_n}{4\pi}\left\{\frac{(z - z_{1n})\hat{j} + (y_{1n} - y)\hat{k}}{[(z - z_{1n})^2 + (y_{1n} - y)^2]}\right\}\left[1.0 + \frac{x - x_{1n}}{\sqrt{(x - x_{1n})^2 + (y - y_{1n})^2 + (z - z_{1n})^2}}\right]$$

Similarly, the velocity induced by the vortex filament that extends from B to ∞

$$\overrightarrow{V_{B\infty}} = -\frac{\Gamma_n}{4\pi}\left\{\frac{(z - z_{2n})\hat{j} + (y_{2n} - y)\hat{k}}{[(z - z_{2n})^2 + (y_{2n} - y)^2]}\right\}\left[1.0 + \frac{x - x_{2n}}{\sqrt{(x - x_{2n})^2 + (y - y_{2n})^2 + (z - z_{2n})^2}}\right]$$

THE HORSESHOE VORTEX INDUCED VELOCITY

The velocity induced at the *m*th control point by the vortex representing the *n*th panel will be designated as $\vec{V}_{m,n}$

$$\vec{V}_{m,n} = \vec{C}_{m,n}\Gamma_n \quad \Rightarrow \quad \vec{V}_m = \sum_{n=1}^{2N} \vec{C}_{m,n}\Gamma_n$$

We have $2N$ of these equations, one for each of the control points

The strengths of the horseshoe vortices are not known

APPLICATION OF THE BOUNDARY CONDITIONS

The resultant flow is tangent to the wing at each and every control point (which is located at the midspan of the three-quarter-chord line of each elemental panel). If the flow is tangent to the wing, the component of the induced velocity normal to the wing at the control point balances the normal component of the free-stream velocity.

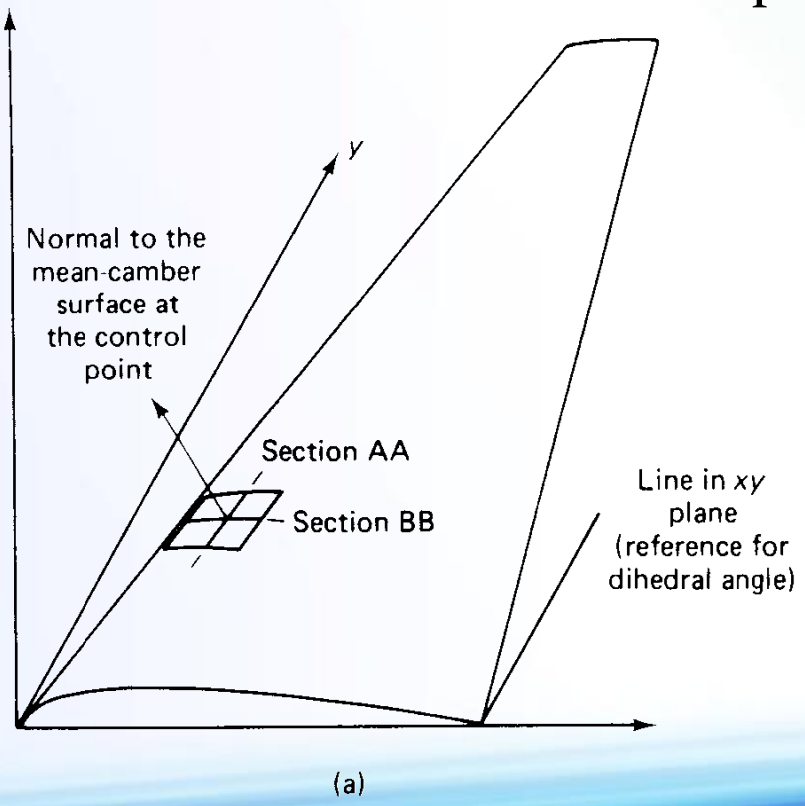

(a)

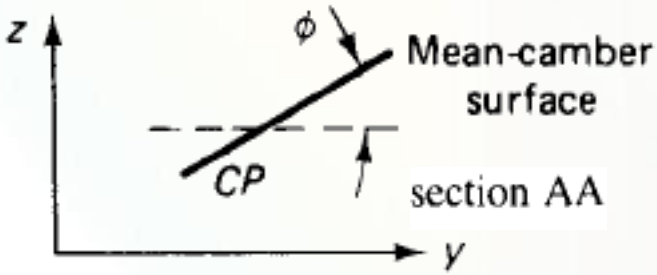

(b)

ϕ is the dihedral angle

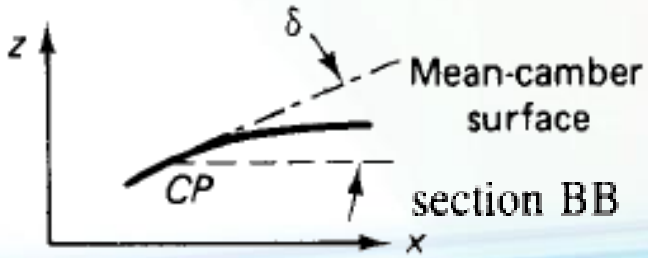

(c)

$$\delta = \tan^{-1}\left(\frac{dz}{dx}\right)_m$$

δ is the slope of the mean camber line

APPLICATION OF THE BOUNDARY CONDITIONS

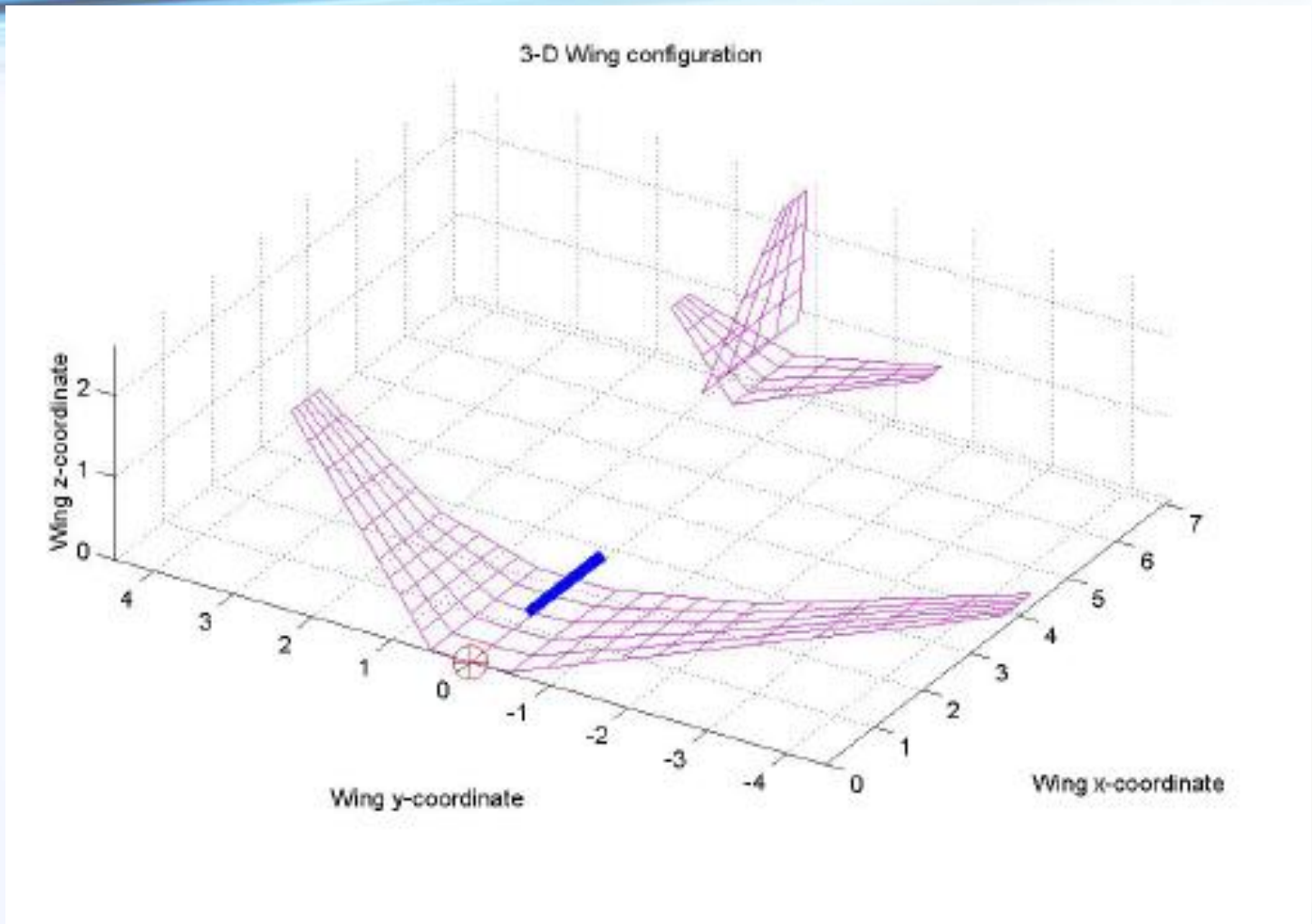

APPLICATION OF THE BOUNDARY CONDITIONS

The tangency requirement yields the relation

$$-u_m \sin\delta\cos\phi - v_m \cos\delta \sin\phi + w_m \cos\phi\cos\delta + U_\infty \sin(\alpha - \delta)\cos\phi = 0$$

For wings where the slope of the mean camber line is small and are at small angles of attack, this equation can be replaced by the approximation:

$$w_m - v_m \tan\phi + U_\infty\left[\alpha - \left(\frac{dz}{dx}\right)_m\right] = 0$$

RELATIONS FOR A PLANAR WING

Let us apply these equations to a relatively simple geometry. A planar wing (i.e., one that lies in the *xy plane),*

For a planar wing, $z_{1n} = z_{2n} = 0$ for all the bound vortices. Furthermore, $z_m = 0$ for all the control points

$$\vec{V}_{AB} = \frac{\Gamma_n}{4\pi} \frac{\hat{k}}{(x_m - x_{1n})(y_m - y_{2n}) - (x_m - x_{2n})(y_m - y_{1n})} \left[\frac{(x_{2n} - x_{1n})(x_m - x_{1n}) + (y_{2n} - y_{1n})(y_m - y_{1n})}{\sqrt{(x_m - x_{1n})^2 + (y_m - y_{1n})^2}} - \frac{(x_{2n} - x_{1n})(x_m - x_{2n}) + (y_{2n} - y_{1n})(y_m - y_{2n})}{\sqrt{(x_m - x_{2n})^2 + (y_m - y_{2n})^2}} \right]$$

RELATIONS FOR A PLANAR WING

Let us apply these equations to a relatively simple geometry. A planar wing (i.e., one that lies in the *xy plane),*

For a planar wing, $z_{1n} = z_{2n} = 0$ for all the bound vortices. Furthermore, $z_m = 0$ for all the control points

$$\overrightarrow{V_{A\infty}} = \frac{\Gamma_n}{4\pi} \frac{\hat{k}}{y_{1n} - y_m} \left[1.0 + \frac{x_m - x_{1n}}{\sqrt{(x_m - x_{1n})^2 + (y_m - y_{1n})^2}} \right]$$

$$\overrightarrow{V_{B\infty}} = -\frac{\Gamma_n}{4\pi} \frac{\hat{k}}{y_{2n} - y_m} \left[1.0 + \frac{x_m - x_{2n}}{\sqrt{(x_m - x_{2n})^2 + (y_m - y_{2n})^2}} \right]$$

RELATIONS FOR A PLANAR WING

Note that, for the planar wing, all three components of the vortex representing the *n*th panel induce a velocity at the control point of the *m*th panel which is in the *z* direction (i.e., a downwash). Therefore, we can simplify equations by combining the components into one expression:

$$w_{m,n} = \frac{\Gamma_n}{4\pi}\left\{\frac{1}{(x_m - x_{1n})(y_m - y_{2n}) - (x_m - x_{2n})(y_m - y_{1n})}\right.$$
$$\left[\frac{(x_{2n} - x_{1n})(x_m - x_{1n}) + (y_{2n} - y_{1n})(y_m - y_{1n})}{\sqrt{(x_m - x_{1n})^2 + (y_m - y_{1n})^2}}\right.$$
$$\left. - \frac{(x_{2n} - x_{1n})(x_m - x_{2n}) + (y_{2n} - y_{1n})(y_m - y_{2n})}{\sqrt{(x_m - x_{2n})^2 + (y_m - y_{2n})^2}}\right]$$
$$+ \frac{1.0}{y_{1n} - y_m}\left[1.0 + \frac{x_m - x_{1n}}{\sqrt{(x_m - x_{1n})^2 + (y_m - y_{1n})^2}}\right]$$
$$\left. - \frac{1.0}{y_{2n} - y_m}\left[1.0 + \frac{x_m - x_{2n}}{\sqrt{(x_m - x_{2n})^2 + (y_m - y_{2n})^2}}\right]\right\}$$

Summing the contributions of all the vortices to the downwash at the control point of the *m*th panel:

$$w_m = \sum_{n=1}^{2N} w_{m,n}$$

RELATIONS FOR A PLANAR WING

Since we are considering a planar wing:

$$(dz/dx)_m = 0 \qquad \phi = 0$$

The component of the free-stream velocity perpendicular to the wing is $U_\infty \sin \alpha$ at any point on the wing. The resultant flow will be tangent to the wing if the total vortex-induced downwash at the control point of the *m*th panel, balances the normal component of the free-stream velocity:

$$w_m + U_\infty \sin \alpha = 0$$

For small angles of attack,

$$w_m = -U_\infty \alpha$$

EXAMPLE

Let us use the relations developed in this section to calculate the lift coefficient for a swept wing. So that the calculation procedures can be easily followed, let us consider a wing with a relatively simple geometry. Plot C_L-α of the wing.

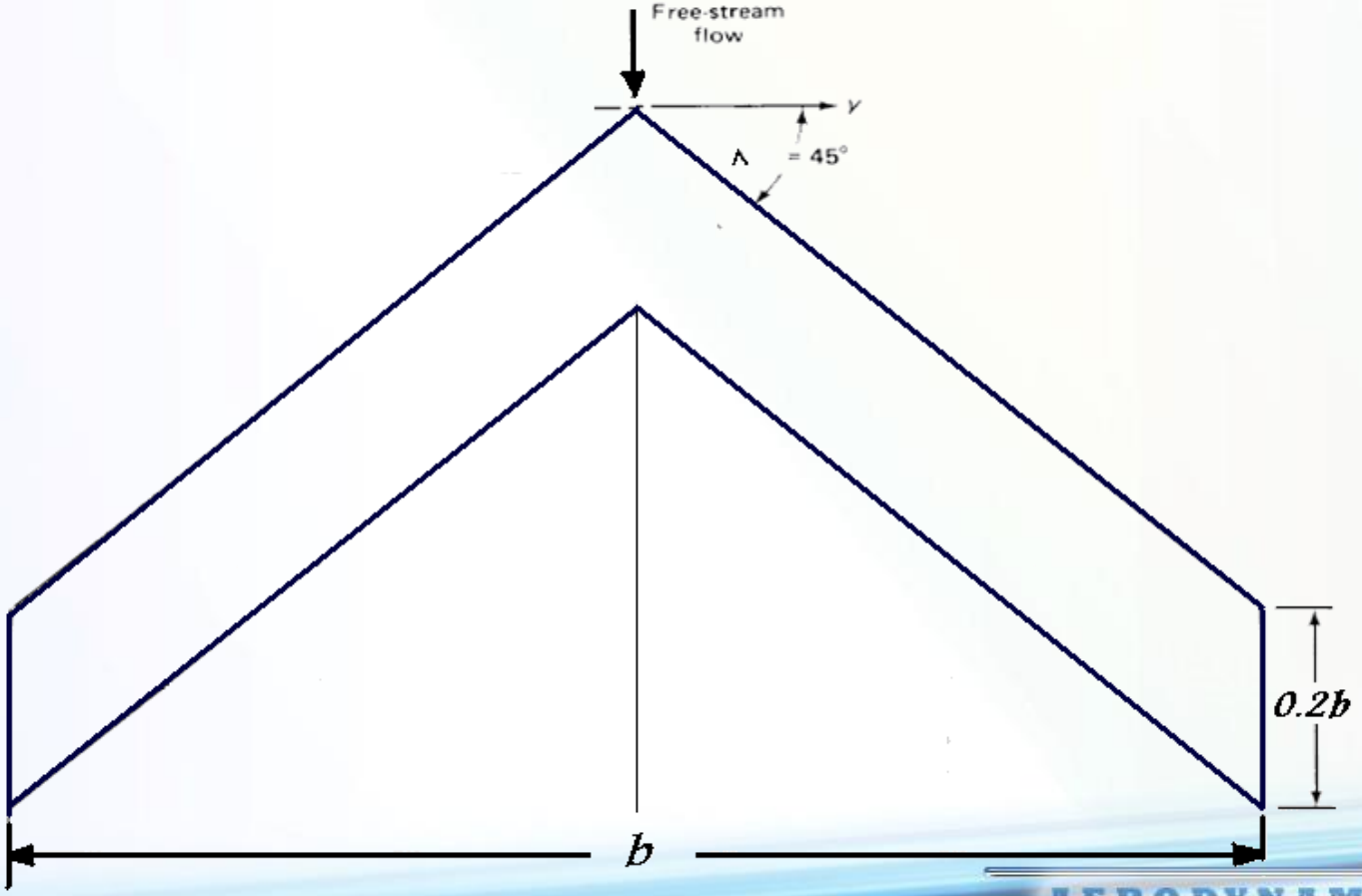

EXAMPLE (CONT.)

The wing has an aspect ratio of 5, a taper ratio of unity (i.e., $c_t = c_r$). and an uncambered section (i.e., it is a flat plate). Since the taper ratio is unity, the leading edge, the quarter-chord line, the three-quarter-chord line, and the trailing edge all have the same sweep, 45 deg.

$$\mathrm{AR} = 5 = \frac{b^2}{S}$$

For a swept, untapered wing

$$S = bc$$

It is clear that $b = 5c$. Using this relation, it is possible to calculate all of the necessary coordinates in terms of the parameter b. Therefore, the solution does not require that we know the physical dimensions of the configuration.

EXAMPLE (CONT.)

The flow field under consideration is symmetric with respect to the y=o plane (*xz* plane); that is, there is no yaw. Thus, the lift force acting at a point on the starboard wing (+y) is equal to that at the corresponding point on the port wing (-y).

Because of symmetry, we need only to solve for the strengths of the vortices of the starboard wing.

We must remember to include the contributions of the horseshoe vortices of the port wing to the velocities induced at these control points (of the starboard wing).

Tangency condition:

$$w_m = \sum_{n=1}^{N} w_{m,ns} + \sum_{n=1}^{N} w_{m,np}$$

the symbols *s* and *p* represent the starboard and port wings, respectively

EXAMPLE (CONT.)

The planform of the starboard wing is divided into four panels, each panel extending from the leading edge to the trailing edge. By limiting ourselves to only four spanwise panels.

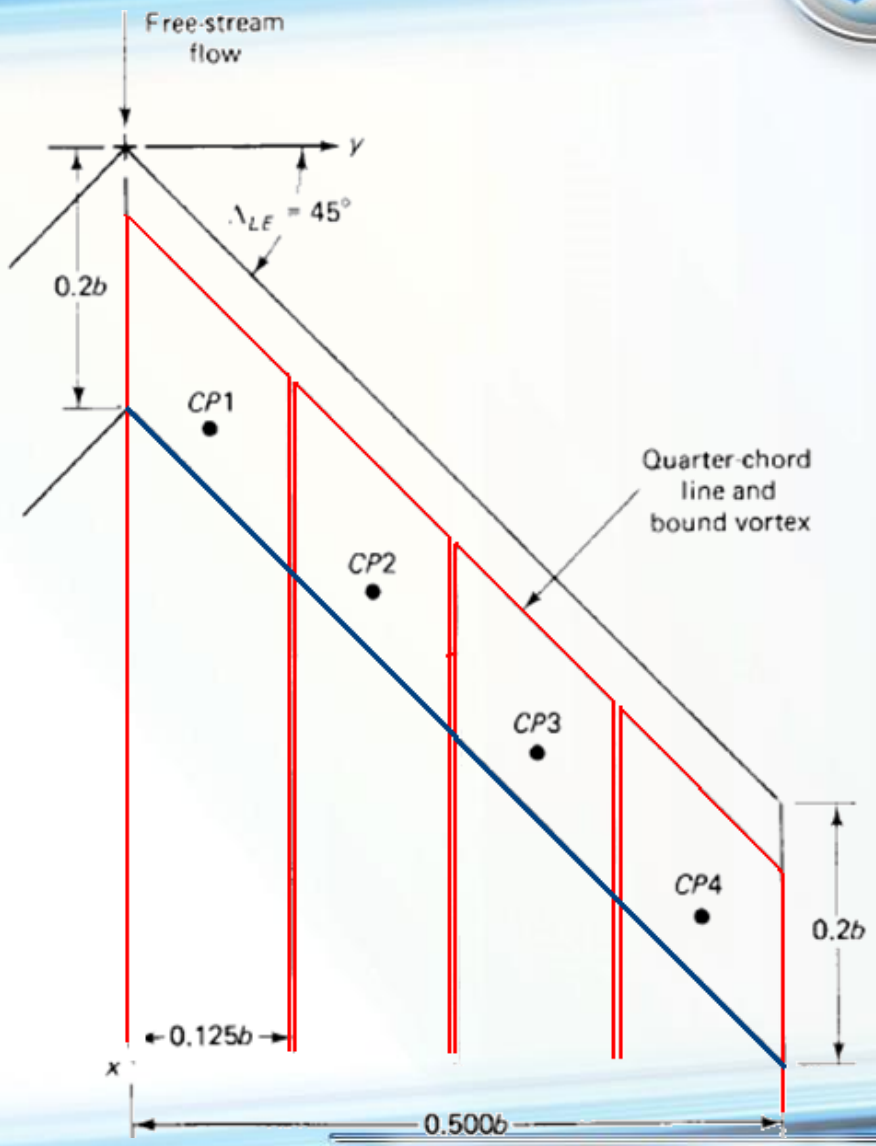

EXAMPLE (CONT.)

The planform of the starboard wing is divided into four panels, each panel extending from the leading edge to the trailing edge. By limiting ourselves to only four spanwise panels.

coordinates of the bound vortices and of the control points of the starboard wing

Panel	x_m	y_m	x_{1n}	y_{1n}	x_{2n}	y_{2n}
1	0.2125b	0.0625b	0.0500b	0.0000b	0.1750b	0.1250b
2	0.3375b	0.1875b	0.1750b	0.1250b	0.3000b	0.2500b
3	0.4625b	0.3125b	0.3000b	0.2500b	0.4250b	0.3750b
4	0.5875b	0.4375b	0.4250b	0.3750b	0.5500b	0.5000b

EXAMPLE (CONT.)

The downwash velocity at the CP of panel 1 induced by the horseshoe vortex of panel 1 of the starboard wing:

$$w_{1,1s} = \frac{\Gamma_1}{4\pi}\left\{\frac{1.0}{(0.1625b)(-0.0625b) - (0.0375b)(0.0625b)}\right.$$

$$\left[\frac{(0.1250b)(0.1625b) + (0.1250b)(0.0625b)}{\sqrt{(0.1625b)^2 + (0.0625b)^2}}\right.$$

$$- \frac{(0.1250b)(0.0375b) + (0.1250b)(-0.0625b)}{\sqrt{(0.0375b)^2 + (-0.0625b)^2}}$$

$$+ \frac{1.0}{-0.0625b}\left[1.0 + \frac{0.1625b}{\sqrt{(0.1625b)^2 + (0.0625b)^2}}\right]$$

$$\left.\left. - \frac{1.0}{0.0625b}\left[1.0 + \frac{0.0375b}{\sqrt{(0.0375b)^2 + (0.0625b)^2}}\right]\right\}\right.$$

$$= \frac{\Gamma_1}{4\pi b}(-16.3533 - 30.9335 - 24.2319)$$

$$w_{1,1s} = \frac{\Gamma_1}{4\pi b}(-71.5187)$$

EXAMPLE (CONT.)

The downwash velocity at the CP of panel 1 (of the starboard wing) induced by I the horseshoe vortex of panel 1 of the port wing:

$$w_{1,1p} = \frac{\Gamma_1}{4\pi}\left\{\frac{1.0}{(0.0375b)(0.0625b) - (0.1625b)(0.1875b)}\right.$$
$$\left[\frac{(-0.1250b)(0.0375b) + (0.1250b)(0.1875b)}{\sqrt{(0.0375b)^2 + (0.1875b)^2}}\right.$$
$$- \frac{(-0.1250b)(0.1625b) + (0.1250b)(0.0625b)}{\sqrt{(0.1625b)^2 + (0.0625b)^2}}$$
$$+ \frac{1.0}{-0.1875b}\left[1.0 + \frac{0.0375b}{\sqrt{(0.0375b)^2 + (0.1875b)^2}}\right]$$
$$\left.\left. - \frac{1.0}{-0.0625b}\left[1.0 + \frac{0.1625b}{\sqrt{(0.1625b)^2 + (0.0625b)^2}}\right]\right\}\right.$$
$$= \frac{\Gamma_4}{4\pi b}(18.5150)$$

EXAMPLE (CONT.)

Similarly, the downwash velocity at the CP of panel 2 induced by the horseshoe vortex of panel 4 of the starboard wing:

$$w_{2,4s} = \frac{\Gamma_4}{4\pi b}\left\{\frac{1.0}{(-0.0875b)(-0.3125b) - (-0.2125b)(-0.1875b)}\right.$$
$$\left[\frac{(0.1250b)(-0.0875b) + (0.1250b)(-0.1875b)}{\sqrt{(-0.0875b)^2 + (-0.1875b)^2}}\right.$$
$$\left.\left. - \frac{(0.1250b)(-0.2125b) + (0.1250b)(-0.3125b)}{\sqrt{(-0.2125b)^2 + (-0.3125b)^2}}\right]\right.$$
$$+ \frac{1.0}{0.1875b}\left[1.0 + \frac{-0.0875b}{\sqrt{(-0.0875b)^2 + (-0.1875b)^2}}\right]$$
$$\left. - \frac{1.0}{0.3125b}\left[1.0 + \frac{-0.2125b}{\sqrt{(-0.2125b)^2 + (-0.3125b)^2}}\right]\right\}$$

$$= \frac{\Gamma_4}{4\pi b}(-0.60167 + 3.07795 - 1.40061)$$

$$= \frac{\Gamma_4}{4\pi b}(1.0757)$$

EXAMPLE (CONT.)

Evaluating all of the various components (or influence coefficients), we find that at control point 1:

$$w_1 = \frac{1}{4\pi b}[(-71.5187\Gamma_1 + 11.2933\Gamma_2 + 1.0757\Gamma_3 + 0.3775\Gamma_4)_s + (+18.5150\Gamma_1 + 2.0504\Gamma_2 + 0.5887\Gamma_3 + 0.2659\Gamma_4)_p$$

At CP 2:

$$w_2 = \frac{1}{4\pi b}[(+20.2174\Gamma_1 - 71.5187\Gamma_2 + 11.2933\Gamma_3 + 1.0757\Gamma_4)_s + (+3.6144\Gamma_1 + 1.1742\Gamma_2 + 0.4903\Gamma_3 + 0.2503\Gamma_4)_p$$

At CP 3:

$$w_3 = \frac{1}{4\pi b}[(+3.8792\Gamma_1 + 20.2174\Gamma_2 - 71.5187\Gamma_3 + 11.2933\Gamma_4)_s + (+1.5480\Gamma_1 + 0.7227\Gamma_2 + 0.3776\Gamma_3 + 0.2179\Gamma_4)_p]$$

At CP 4:

$$w_4 = \frac{1}{4\pi b}[(+1.6334\Gamma_1 + 3.8792\Gamma_2 + 20.2174\Gamma_3 - 71.5187\Gamma_4)_s + (+0.8609\Gamma_1 + 0.4834\Gamma_2 + 0.2895\Gamma_3 + 0.1836\Gamma_4)_p]$$

EXAMPLE (CONT.)

Since it is a planar wing with no dihedral, the no-flow condition of equation requires that

$$w_1 = w_2 = w_3 = w_4 = -U_\infty \alpha$$

$$\begin{aligned}
-53.0037\Gamma_1 + 13.3437\Gamma_2 + 1.6644\Gamma_3 + 0.6434\Gamma_4 &= -4\pi b U_\infty \alpha \\
+23.8318\Gamma_1 - 70.3445\Gamma_2 + 11.7836\Gamma_3 + 1.3260\Gamma_4 &= -4\pi b U_\infty \alpha \\
+5.4272\Gamma_1 + 20.9401\Gamma_2 - 71.1411\Gamma_3 + 11.5112\Gamma_4 &= -4\pi b U_\infty \alpha \\
+2.4943\Gamma_1 + 4.3626\Gamma_2 + 20.5069\Gamma_3 - 71.3351\Gamma_4 &= -4\pi b U_\infty \alpha
\end{aligned}$$

EXAMPLE (CONT.)

Solving for Γ_1, Γ_2, Γ_3 and Γ_4, we find that

$$\Gamma_1 = +0.02728(4\pi b U_\infty \alpha)$$

$$\Gamma_2 = +0.02869(4\pi b U_\infty \alpha)$$

$$\Gamma_3 = +0.02841(4\pi b U_\infty \alpha)$$

$$\Gamma_4 = +0.02490(4\pi b U_\infty \alpha)$$

the lift acting on the *n*th panel is $\Delta l_n = l = \rho_\infty U_\infty \Gamma_n$

Since the flow is symmetric, the total lift for the wing is

$$L = 2\int_0^{0.5b} \rho_\infty U_\infty \Gamma(y)\, dy$$

EXAMPLE (CONT.)

$$L = 2\rho_\infty U_\infty \sum_{n=1}^{4} \Gamma_n \Delta y_n$$

Since $\Delta y_n = 0.1250b$ for each panel,

$$L = 2\rho_\infty U_\infty 4\pi b U_\infty \alpha(0.02728 + 0.02869 + 0.02841 + 0.02490)0.1250b$$
$$= \rho_\infty U_\infty^2 b^2 \pi\alpha(0.10928)$$

To calculate the lift coefficient, recall that S = bc and b = 5c for this wing. Therefore,

$$C_L = \frac{L}{q_\infty S} = 1.0928\pi\alpha$$

$$C_{L_\alpha} = \frac{dC_L}{d\alpha} = 3.43314 \text{ per radian} = 0.05992 \text{ per degree}$$

EXAMPLE (CONT.)

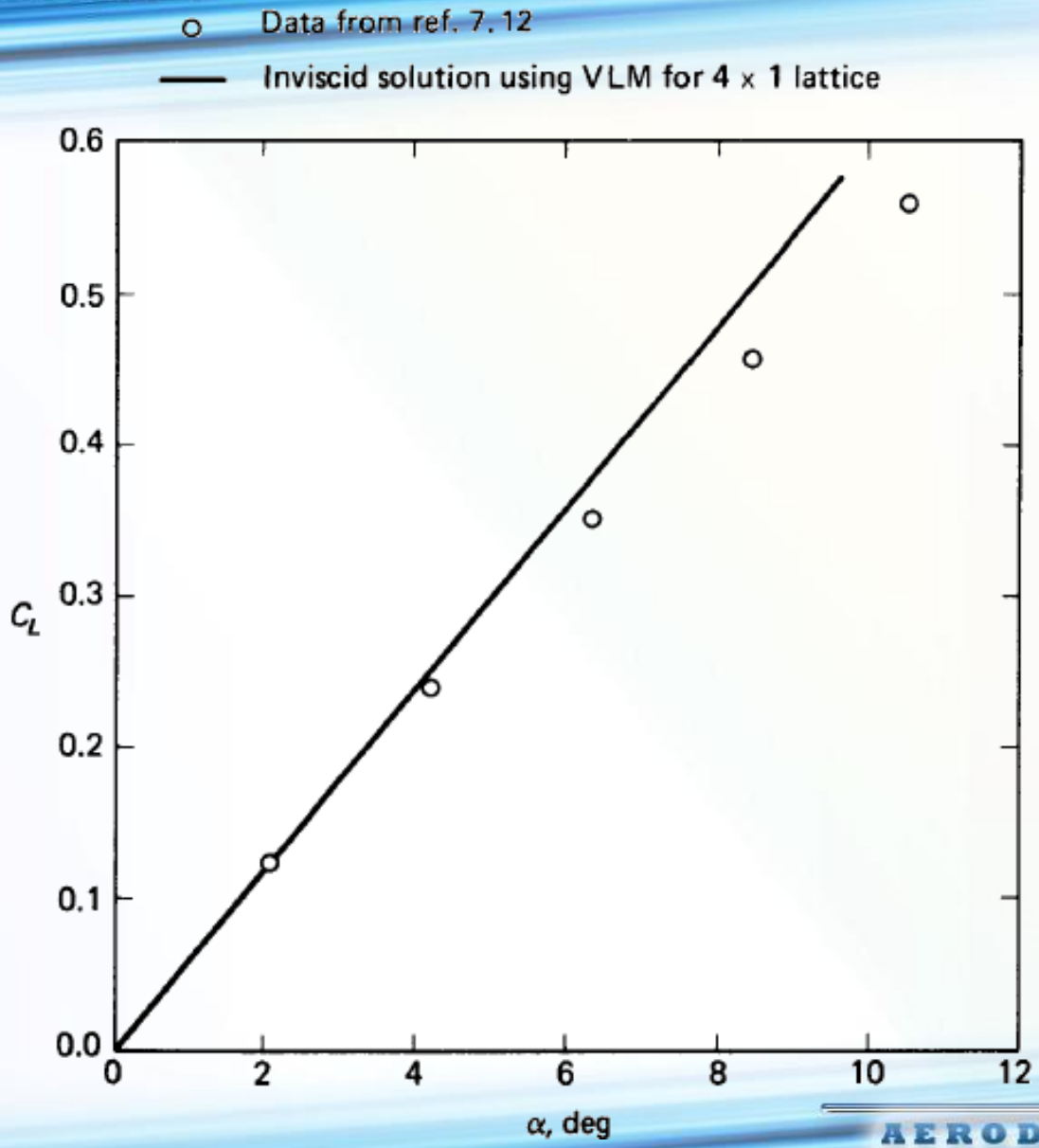

EXAMPLE (CONT.)

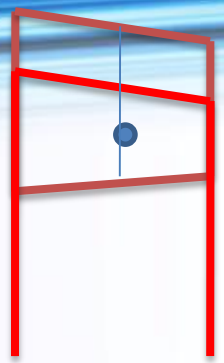

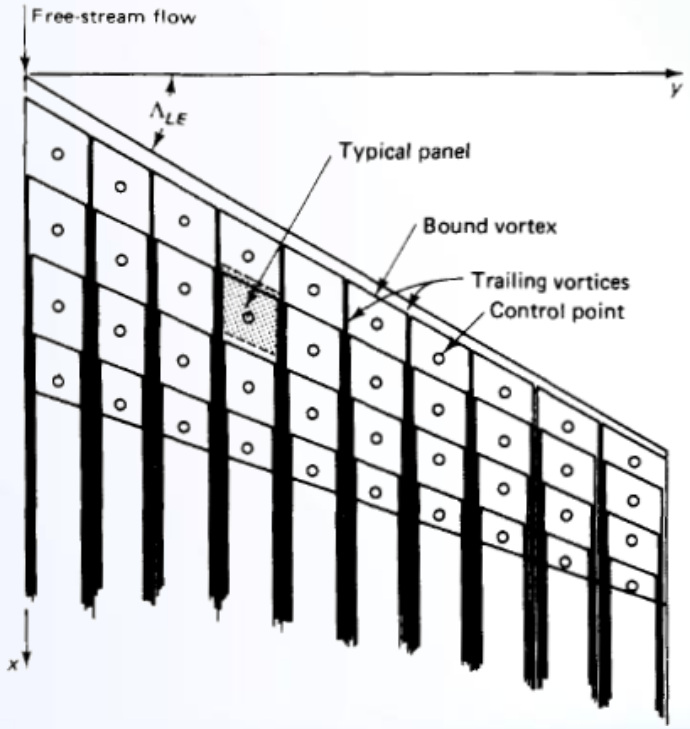

$$C_l = \frac{l}{\frac{1}{2}\rho_\infty U_\infty^2 c_{av}} = \frac{2\Gamma}{U_\infty c_{av}}$$

$$\frac{C_l c}{c_{av}} = \sum_{j=1}^{J_{max}} \left(\frac{l}{q_\infty c_{av}} \right)_j$$

where c_{av} is the average chord (and is equal to S/b), c is the local chord, and j is the index for an elemental panel in the chordwise row.

$$C_L = \int_0^1 \frac{C_l c}{c_{av}} d\left(\frac{2y}{b}\right)$$

EXAMPLE (CONT.)

The theoretical distribution is compared with the experimentally determined spanwise load distribution for an angle of attack of 4.2 deg. The increased loading of the outer wing sections promotes premature boundary-layer separation there. This unfavorable behavior is amplified by the fact that the spanwise velocity component causes the already decelerated fluid particles in the boundary layer to move toward the wing tips. This transverse flow results in a large increase in the boundary-layer thickness near the wing tips. Thus, at large angles of attack, premature separation may occur on the suction side of the wing near the tip. If significant tip stall occurs on the swept wing, there is a loss of the effectiveness of the control surfaces and a forward shift in the wing center of pressure that creates an unstable, nose-up increase in the pitching moment.

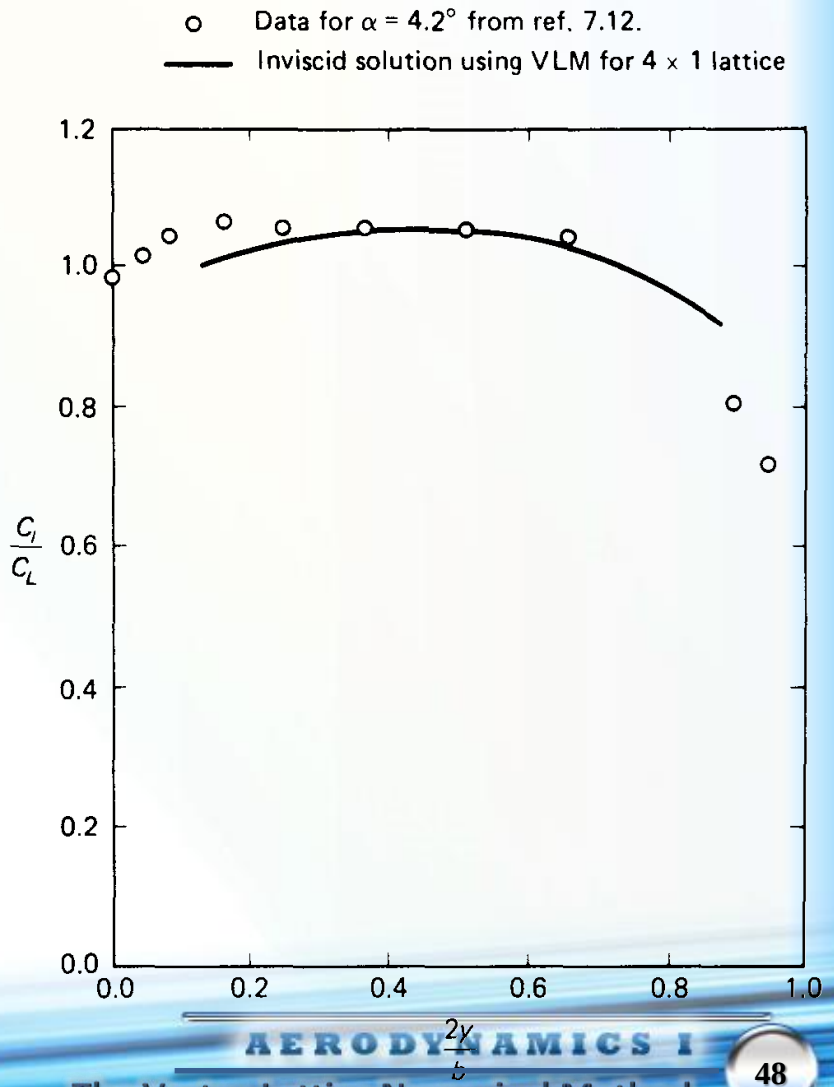

BOUNDARY-LAYER FENCE

Boundary-layer fences are often used to break up the spanwise flow on swept wings.

The essential effect of the boundary-layer fence does not so much consist in the prevention of the transverse flow but, much more important, in that the fence divides each wing into an inner and an outer portion.

Both transverse flow and boundary-layer separation may be present, but to a reduced extent.

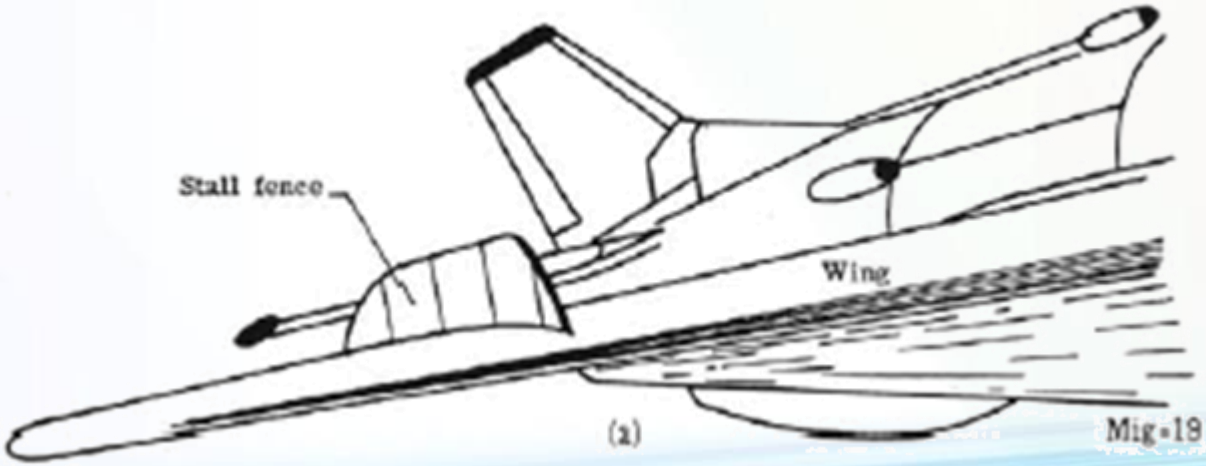

BOUNDARY-LAYER FENCE

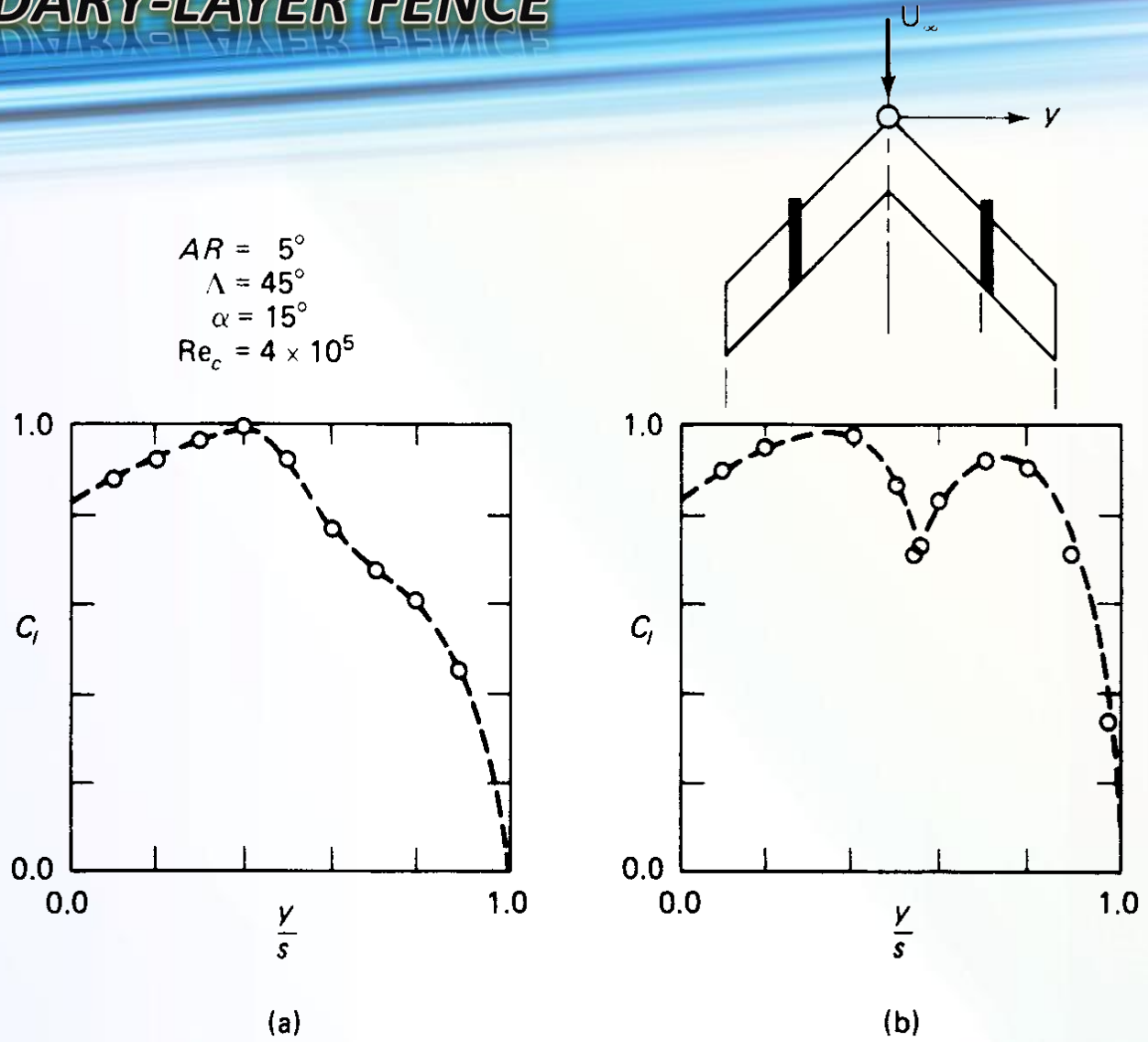

Effect of a boundary-layer fence on the spanwise distribution of the local lift coefficient: (a) without fence; (b) with fence.

EXAMPLE (CONT.)

The induced drag coefficient may be calculated using the relation given

$$C_{D_i} = \frac{1}{S}\int_{-0.5b}^{+0.5b} C_l c\alpha_i \, dy$$

where α_i which is the induced incidence, given by

$$\alpha_i = -\frac{1}{8\pi}\int_{-0.5b}^{+0.5b} \frac{C_l c}{(y-\eta)^2}\, d\eta$$

For a symmetrical loading

$$\alpha_i = -\frac{1}{8\pi}\int_{0}^{0.5b} \left[\frac{C_l c}{(y-\eta)^2} + \frac{C_l c}{(y+\eta)^2}\right] d\eta$$

Tornado© VLM code for MATLAB

Winglet Geometry

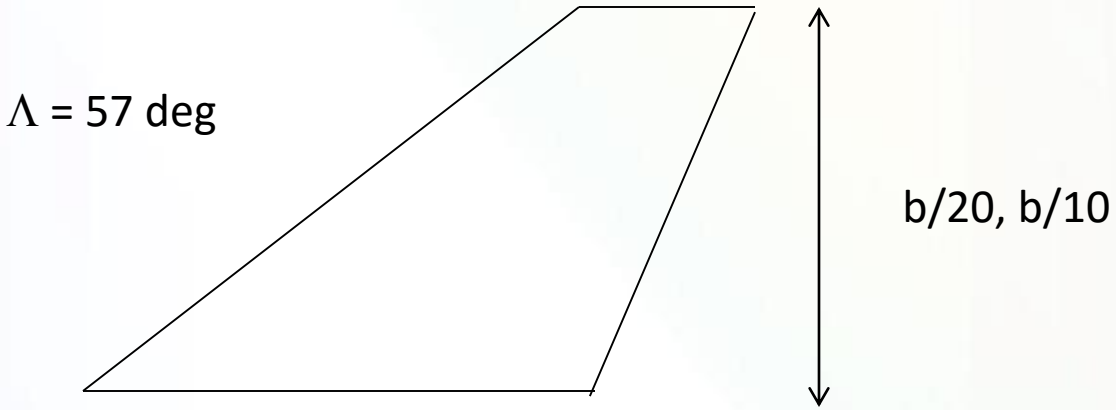

Taper => $\lambda = 0.3$

Aircraft Configuration

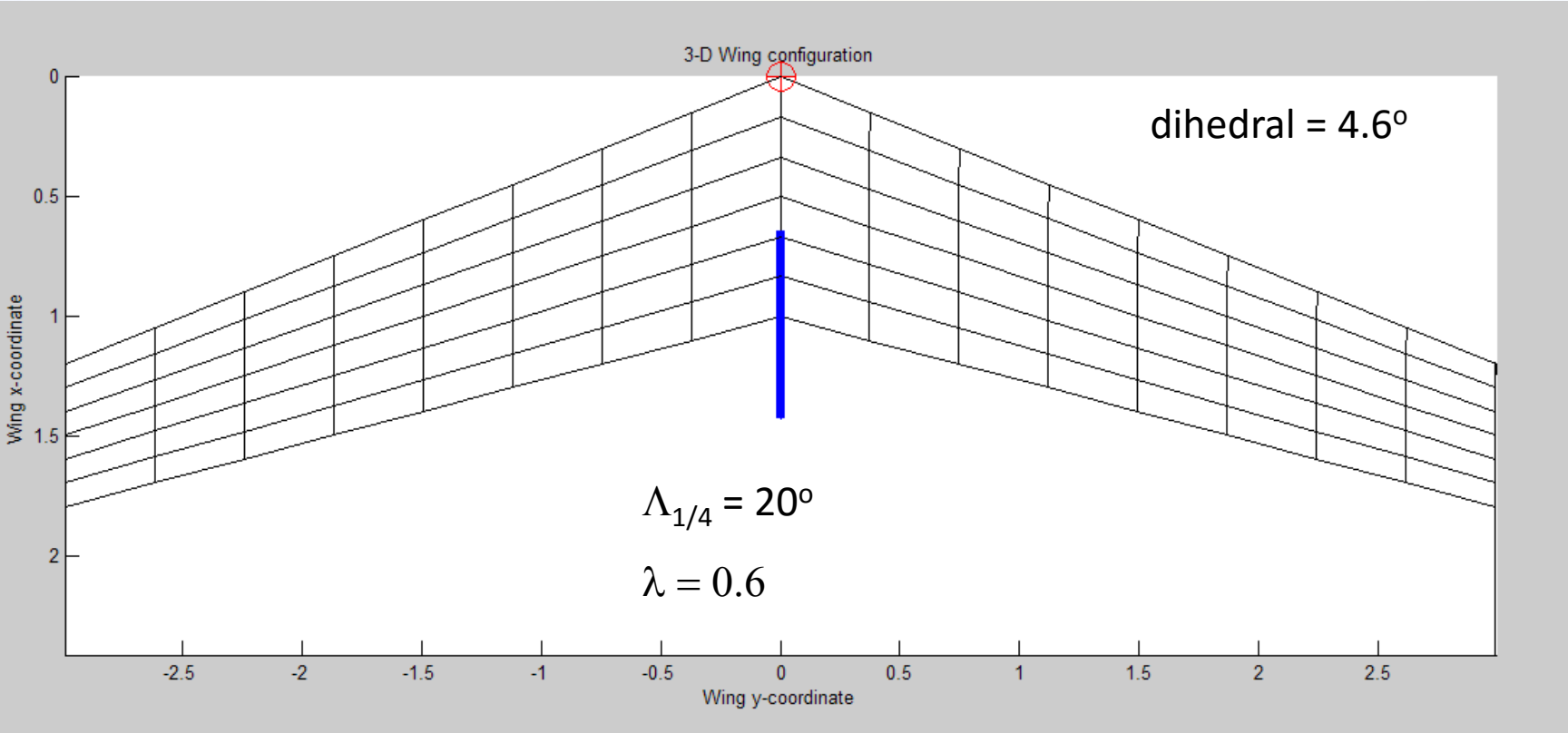

Winglet Modeling (Cont.)

Original Configuration

$\alpha = 8^o$

L/D = 51

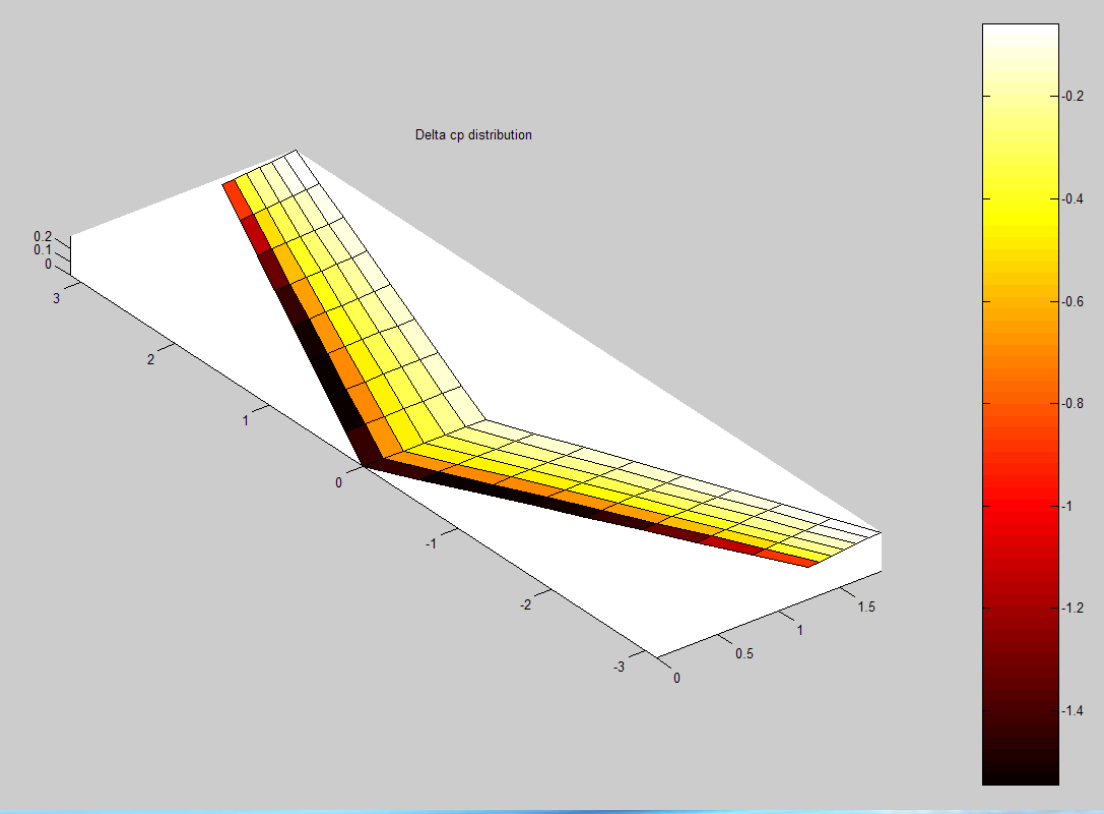

Winglet Modeling (Cont.)

Small Version

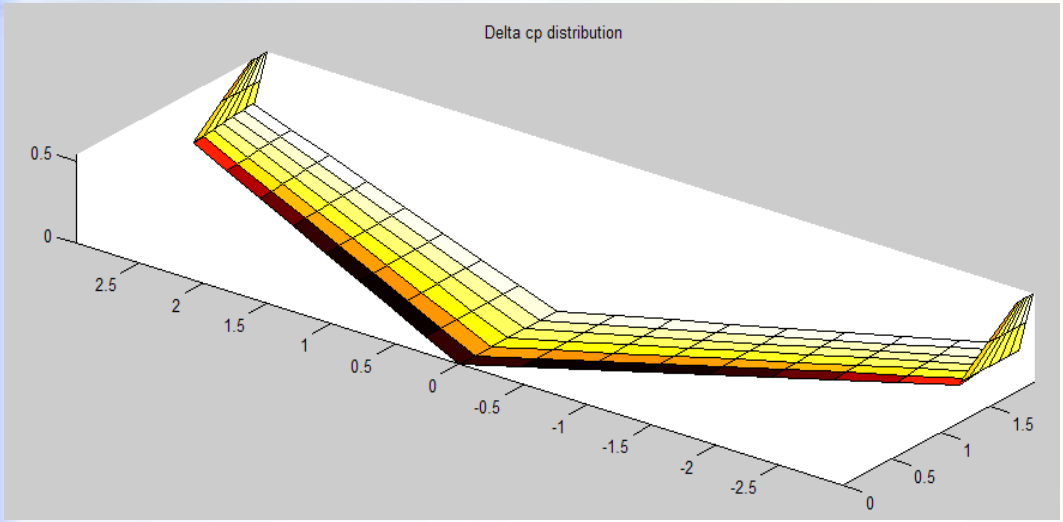

11% drag reduction

(7% when compared to an extended wing)

8% drag reduction

(4% when compared to an extended wing)

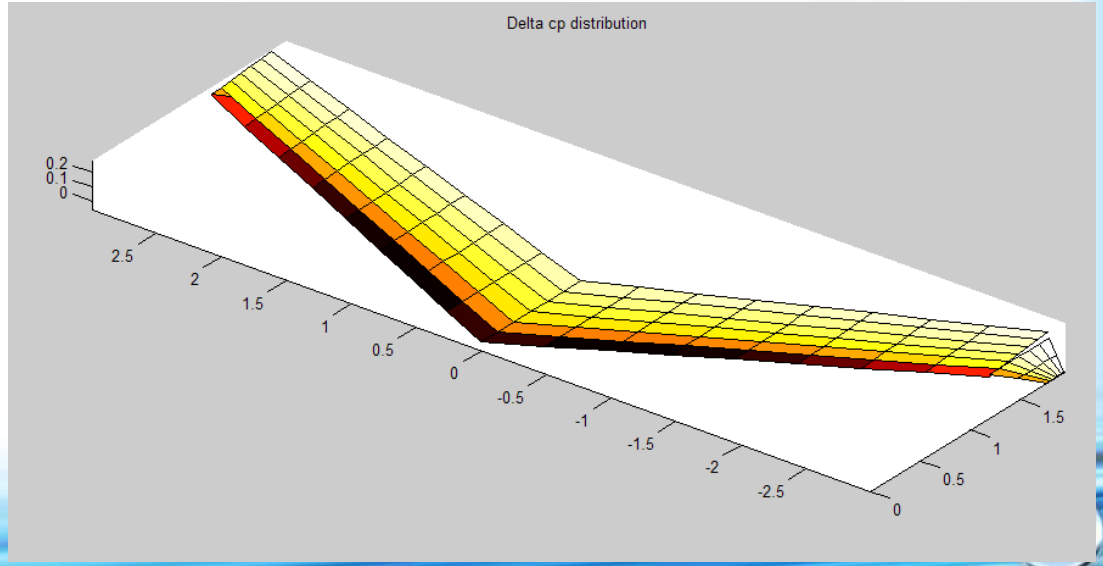

Winglet Modeling (Cont.)

Large Version

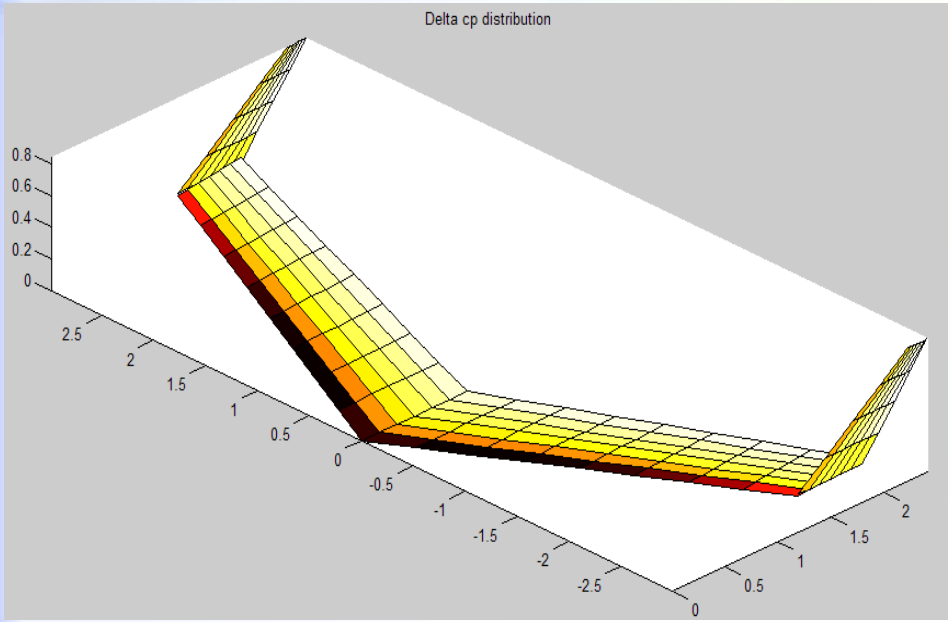

22% drag reduction

(14% when compared to an extended wing)

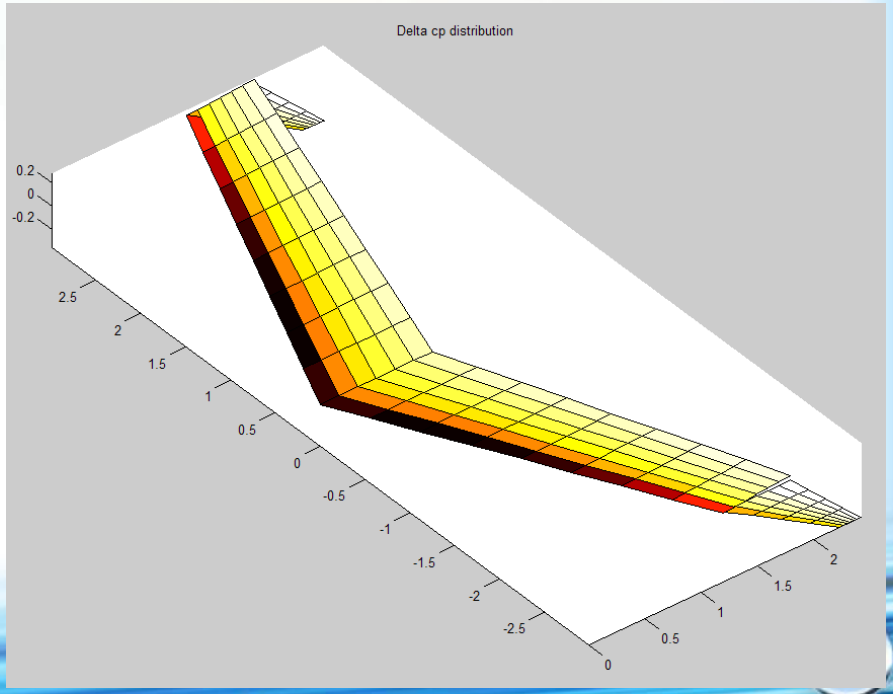

12% drag reduction

(4% when compared to an extended wing)

Winglet Modeling (Cont.)

Side View

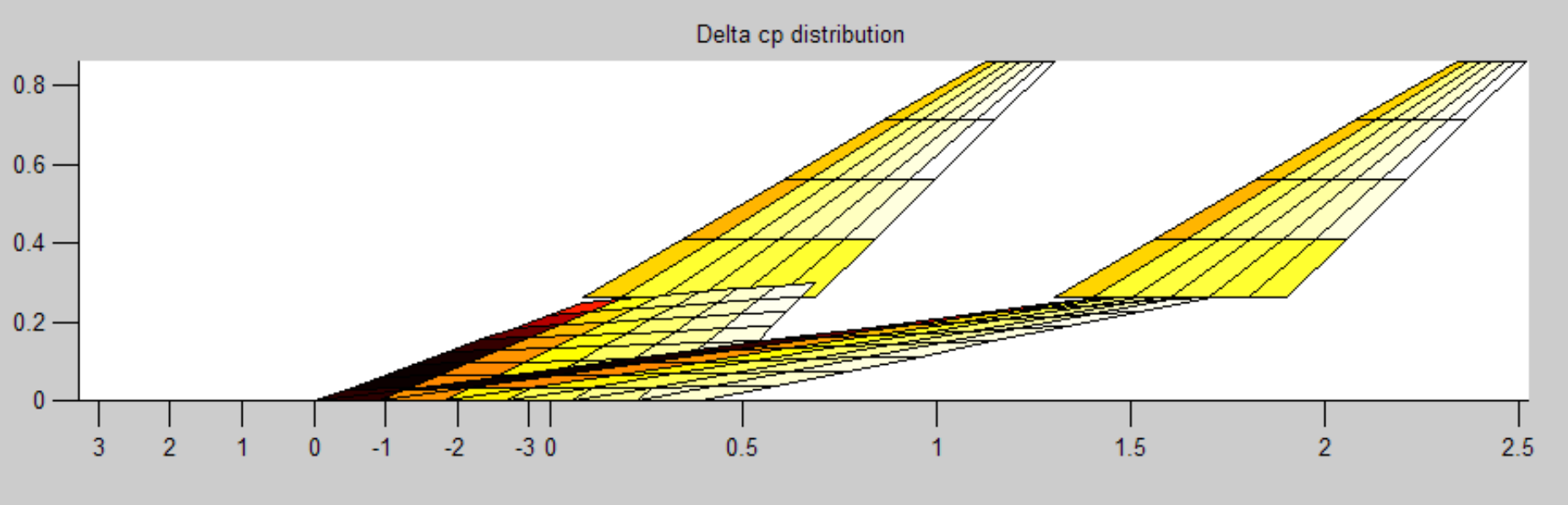

INTRODUCTION TO THREE-DIMENSIONAL INCOMPRESSIBLE FLOWS

- To this point in our aerodynamic discussions, we have been working mainly in a two-dimensional world; the flows over the bodies treated so far, involved only two dimensions in a single plane *(planar flows)*.

- The relative simplicity of dealing with two dimensions is self-evident and is the reason why a large bulk of aerodynamic theory deals with two-dimensional flows.

- The two-dimensional analyses go a long way toward understanding many practical flows, but they also have distinct limitations.

INTRODUCTION TO THREE-DIMENSIONAL INCOMPRESSIBLE FLOWS

- The real world of aerodynamic applications is three-dimensional. However, because of the addition of one more independent variable, the analyses generally become more complex.

- Our purpose is to introduce some very basic considerations of three-dimensional incompressible flow.

INTRODUCTION TO THREE-DIMENSIONAL INCOMPRESSIBLE FLOWS

- For an irrotational flow, there exists a scalar function ϕ such that

$$\mathbf{V} = \nabla\phi$$

- If the flow is also incompressible, the velocity potential is given by Laplace's equation

$$\nabla^2\phi = 0$$

- Solutions of this equation for flow over a body must satisfy the flow-tangency boundary condition on the body

$$\mathbf{V} \cdot \mathbf{n} = 0$$

where *n* is a unit vector normal to the body surface.

INTRODUCTION TO THREE-DIMENSIONAL INCOMPRESSIBLE FLOWS

- ϕ is, in general, a function of three-dimensional space.

- **Cartesian coordinates** $\phi = \phi(x, y, z)$

$$\nabla^2\phi = \frac{\partial^2\phi}{\partial x^2} + \frac{\partial^2\phi}{\partial y^2} + \frac{\partial^2\phi}{\partial z^2} = 0$$

- **Cylindrical coordinates** $\phi = \phi(r, \theta, z)$

$$\nabla^2\phi = \frac{1}{r}\frac{\partial}{\partial r}\left(r\frac{\partial\phi}{\partial r}\right) + \frac{1}{r^2}\frac{\partial^2\phi}{\partial\theta^2} + \frac{\partial^2\phi}{\partial z^2} = 0$$

- **Spherical coordinates** $\phi = \phi(r, \theta, \Phi)$

$$\nabla^2\phi = \frac{1}{r^2\sin\theta}\left[\frac{\partial}{\partial r}\left(r^2\sin\theta\frac{\partial\phi}{\partial r}\right) + \frac{\partial}{\partial\theta}\left(\sin\theta\frac{\partial\phi}{\partial\theta.}\right) + \frac{\partial}{\partial\Phi}\left(\frac{1}{\sin\theta}\frac{\partial\phi}{\partial\Phi}\right)\right] = 0$$

THREE-DIMENSIONAL SOURCE

Return to Laplace's equation written in spherical coordinates,

$$\nabla^2 \phi = \phi_{rr} + \frac{2}{r}\phi_r + \frac{1}{r^2}\left(\phi_{\theta\theta} + \cot\theta\,\phi_\theta + \csc^2\theta\,\phi_{\Phi\Phi}\right)$$

Consider the velocity potential given by

$$\phi = -\frac{C}{r}$$

where C is a constant and r is the radial coordinate from the origin.

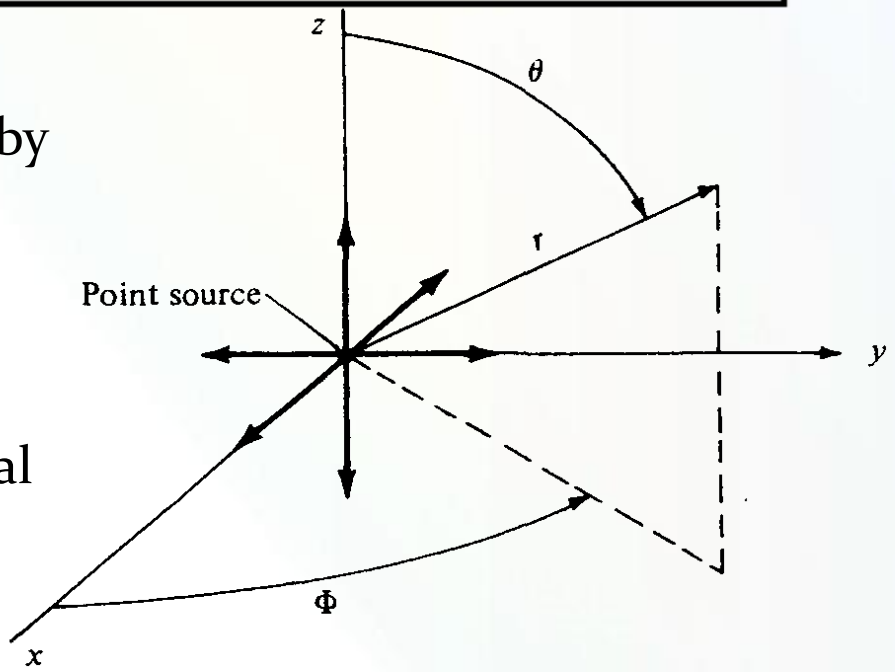

THREE-DIMENSIONAL SOURCE VELOCITY COMPONENTS

$$\mathbf{V} = \nabla\phi$$

$$\nabla\phi = \frac{\partial\phi}{\partial r}\mathbf{e_r} + \frac{1}{r}\frac{\partial\phi}{\partial\theta}\mathbf{e}_\theta + \frac{1}{r\sin\theta}\frac{\partial\phi}{\partial\Phi}\mathbf{e}_\Phi$$

$$\mathbf{V} = \nabla\phi = \frac{C}{r^2}\mathbf{e}_r$$

$$V_r = \frac{C}{r^2}$$
$$V_\theta = 0$$
$$V_\Phi = 0$$

THREE-DIMENSIONAL SOURCE

To evaluate the constant C, consider a sphere of radius r and surface S centered at the origin

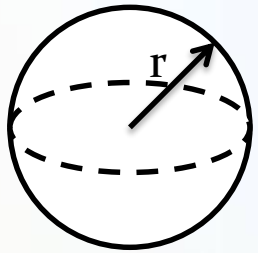

$$\text{Mass flow} = \oiint_S \rho \mathbf{V} \cdot \mathbf{dS}$$

The volume flow:

$$\lambda = \oiint_S \mathbf{V} \cdot \mathbf{dS}$$

$$V_r = C/r^2$$

$$\lambda = \frac{C}{r^2} 4\pi r^2 = 4\pi C \quad \Rightarrow \quad C = \frac{\lambda}{4\pi}$$

$$V_r = \frac{\lambda}{4\pi r^2}$$

λ is defined as the strength of the source.

THREE-DIMENSIONAL DOUBLET

Consider a sink and source of equal but opposite strength located at points *O* and A

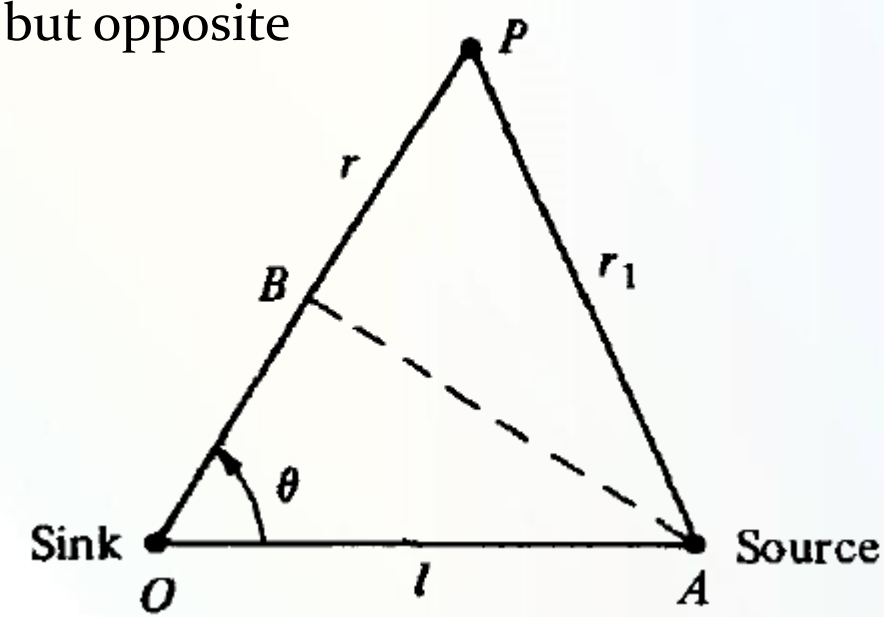

The velocity potential at *P is:*

$$\phi = -\frac{\lambda}{4\pi}\left(\frac{1}{r_1} - \frac{1}{r}\right)$$

$$\phi = -\frac{\lambda}{4\pi}\frac{r - r_1}{r r_1}$$

THREE-DIMENSIONAL DOUBLET

Let the source approach the sink as their strengths become infinite; that is, let $l \to 0$ as $\lambda \to \infty$

In the limit, as $l \to 0$, $r - r_1 \to OB = l\cos\theta$, and $rr_1 \to r^2$.

$$\phi = -\lim_{\substack{l\to 0\\ \lambda\to\infty}} \frac{\lambda}{4\pi}\frac{r-r_1}{rr_1} = -\frac{\lambda}{4\pi}\frac{l\cos\theta}{r^2}$$

$$\mu = \lambda l. \quad \Rightarrow \quad \boxed{\phi = -\frac{\mu}{4\pi}\frac{\cos\theta}{r^2}}$$

$$\mathbf{V} = \nabla\phi = \frac{\mu}{2\pi}\frac{\cos\theta}{r^3}\mathbf{e}_r + \frac{\mu}{4\pi}\frac{\sin\theta}{r^3}\mathbf{e}_\theta + 0\mathbf{e}_\Phi$$

THREE-DIMENSIONAL DOUBLET

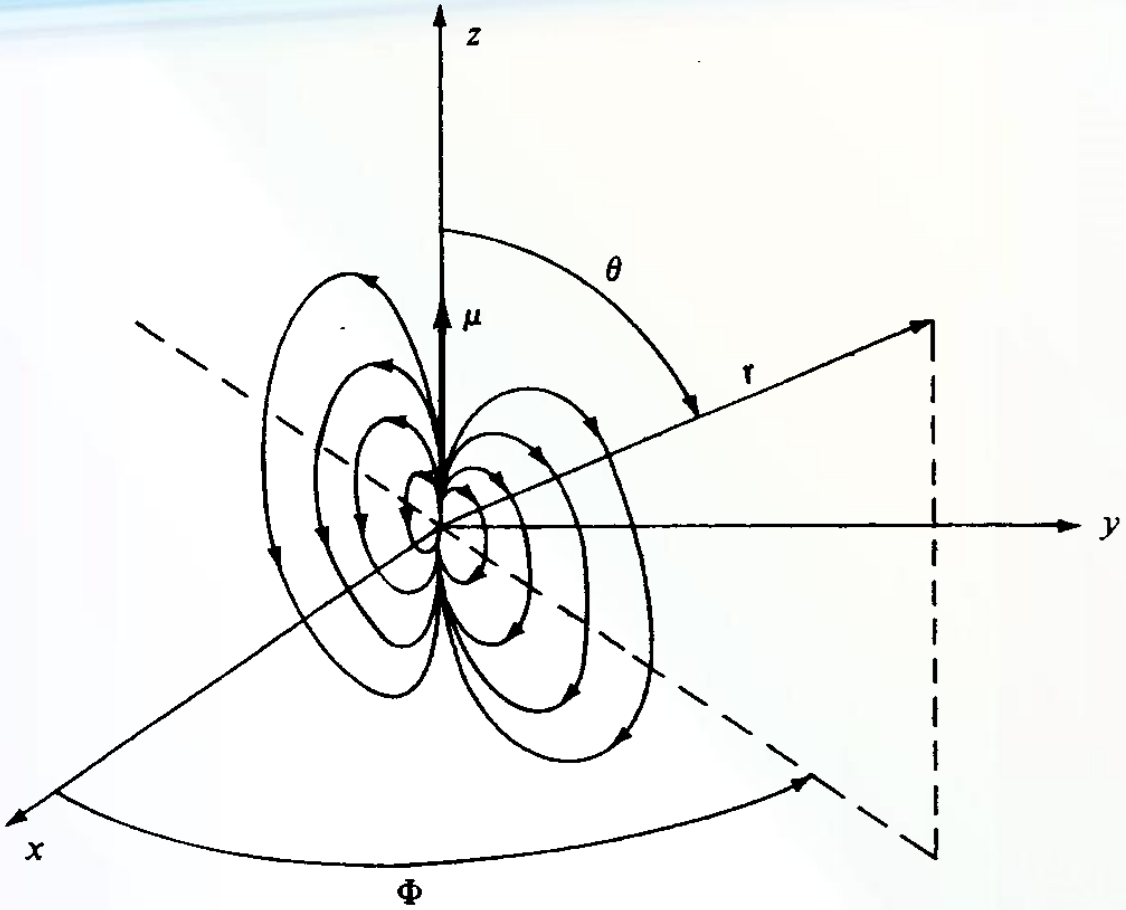

The velocity field depends only on *r and* θ. Such a flow is defined as *axisymmetric* flow.

FLOW OVER A SPHERE

Consider the flow induced by the three-dimensional doublet.

Superimpose on this flow a uniform velocity field of magnitude V_∞ in the negative z direction

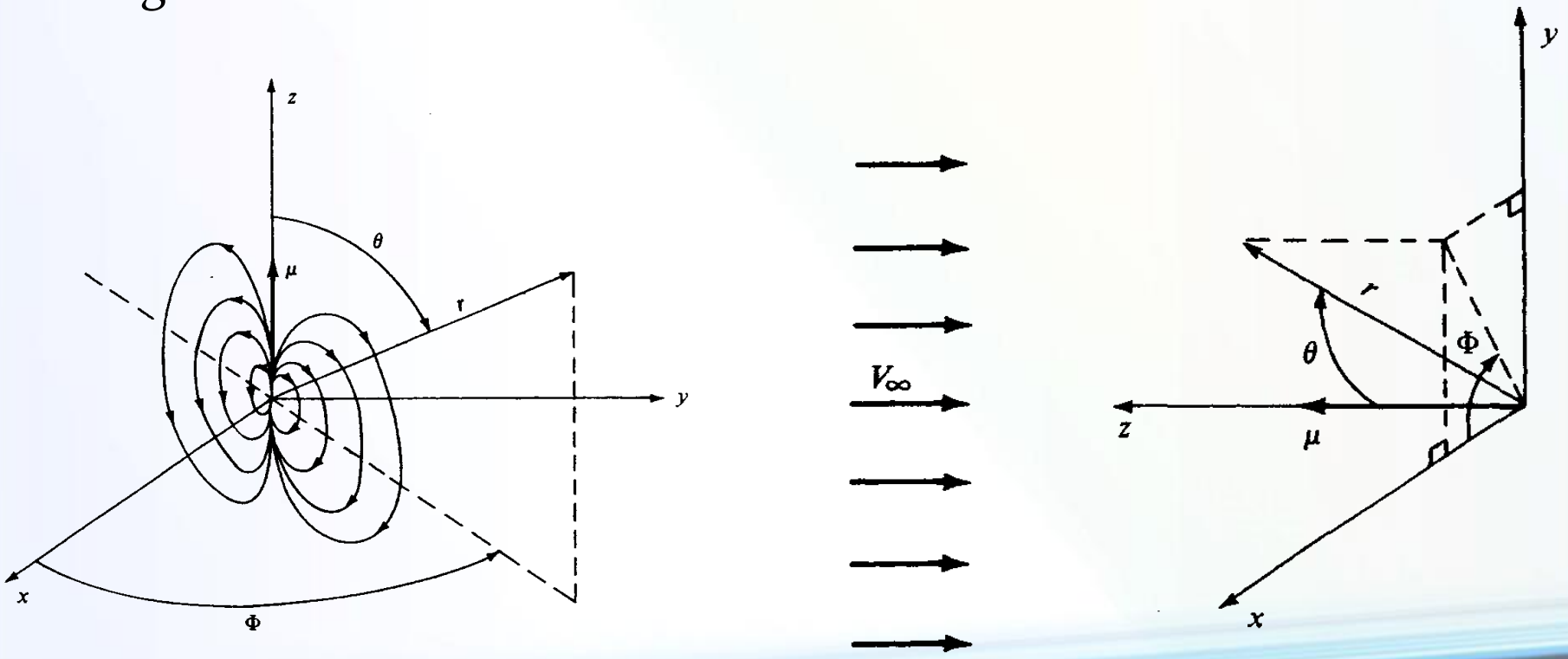

The spherical coordinates of the freestream are:

$$V_r = -V_\infty \cos\theta$$

$$V_\theta = V_\infty \sin\theta$$

$$V_\Phi = 0$$

Combined flow:

$$V_r = -V_\infty \cos\theta + \frac{\mu}{2\pi}\frac{\cos\theta}{r^3} = -\left(V_\infty - \frac{\mu}{2\pi r^3}\right)\cos\theta$$

$$V_\theta = V_\infty \sin\theta + \frac{\mu}{4\pi}\frac{\sin\theta}{r^3} = \left(V_\infty + \frac{\mu}{4\pi r^3}\right)\sin\theta$$

$$V_\Phi = 0$$

FLOW OVER A SPHERE (STAGNATION POINTS)

To find the stagnation points in the flow

$$V_r = V_\theta = 0$$

$$\text{with } V_r = 0 \quad \Rightarrow \quad V_\infty - \frac{\mu}{2\pi R^3} = 0 \quad \Rightarrow \quad R = \left(\frac{\mu}{2\pi V_\infty}\right)^{1/3}$$

$$V_\theta = 0 \text{ gives } \sin\theta = 0 \quad \Rightarrow \quad \theta = 0 \text{ and } \pi$$

Hence, there are two stagnation points, both on the *z axis*,

$$\left[\left(\frac{\mu}{2\pi V_\infty}\right)^{1/3}, 0\right] \quad \text{and} \quad \left[\left(\frac{\mu}{2\pi V_\infty}\right)^{1/3}, \pi\right]$$

FLOW OVER A SPHERE (TANGENTIAL VELOCITY)

The incompressible flow over a sphere of radius R is **qualitatively similar** to the flow over the cylinder, but **quantitatively different**.

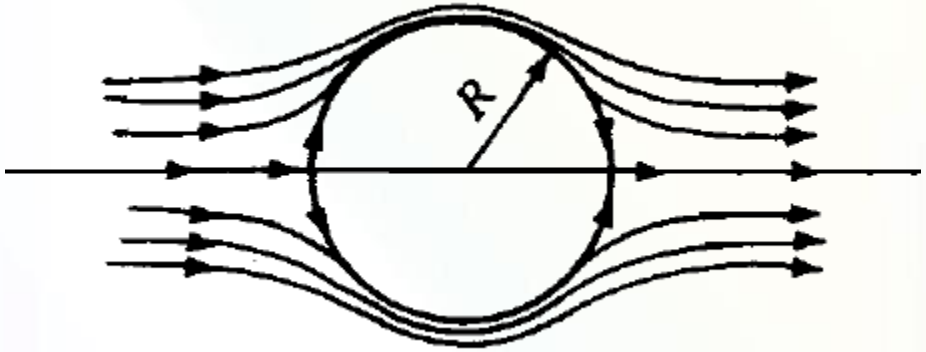

On the surface of the sphere, where $r = R$, the tangential velocity is

$$V_\theta = \tfrac{3}{2} V_\infty \sin\theta$$

The pressure distribution on the surface of the sphere is

$$C_p = 1 - \tfrac{9}{4} \sin^2\theta$$

THREE-DIMENSIONAL RELIEVING EFFECT

	Cylinder	Sphere
Location of maximum velocity	$\theta = \frac{\pi}{2}$	$\theta = \frac{\pi}{2}$
Maximum velocity	$2V_\infty$	$1.5V_\infty$
Maximum pressure coefficient	1	1
Minimum pressure coefficient	-3	-5/4

The flow over a sphere is somewhat *relieved* in comparison with the flow over a cylinder. The flow over a sphere has an extra dimension in which to move out of the way of the solid body; the flow can move sideways as well as up and down. In contrast, the flow over a cylinder is more constrained; it can only move up and down.

THE FLOW OVER A SPHERE
THE REAL CASE

The qualitative features of the real flow over a sphere are similar to those discussed for a cylinder (*the phenomenon of flow separation, the variation of drag coefficient with a Reynolds number, the precipitous drop in drag coefficient when the flow transits from laminar to turbulent ahead of the separation point at the critical Reynolds number, and the general structure of the wake*).

These items are similar for both cases. However, because of the three-dimensional relieving effect, the flow over a sphere is quantitatively different from that for a cylinder.

THE FLOW OVER A SPHERE
THE REAL CASE

The flow over sphere – **Re=17.9**

THE FLOW OVER A SPHERE
THE REAL CASE

The flow over sphere – **Re=25.5**

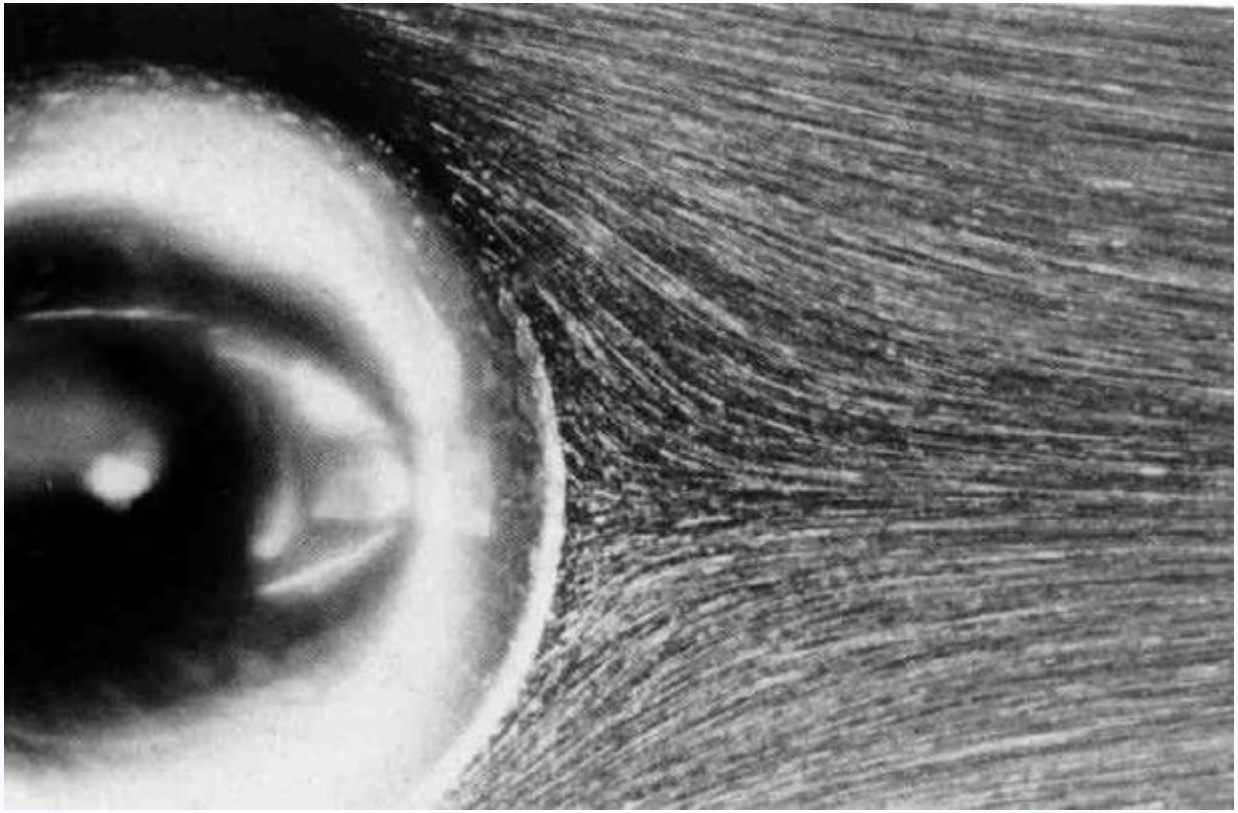

Although it is not obvious, the flow is just to have separated at the rear at this Reynolds number.

THE FLOW OVER A SPHERE
THE REAL CASE

The flow over sphere – **Re=26.8**

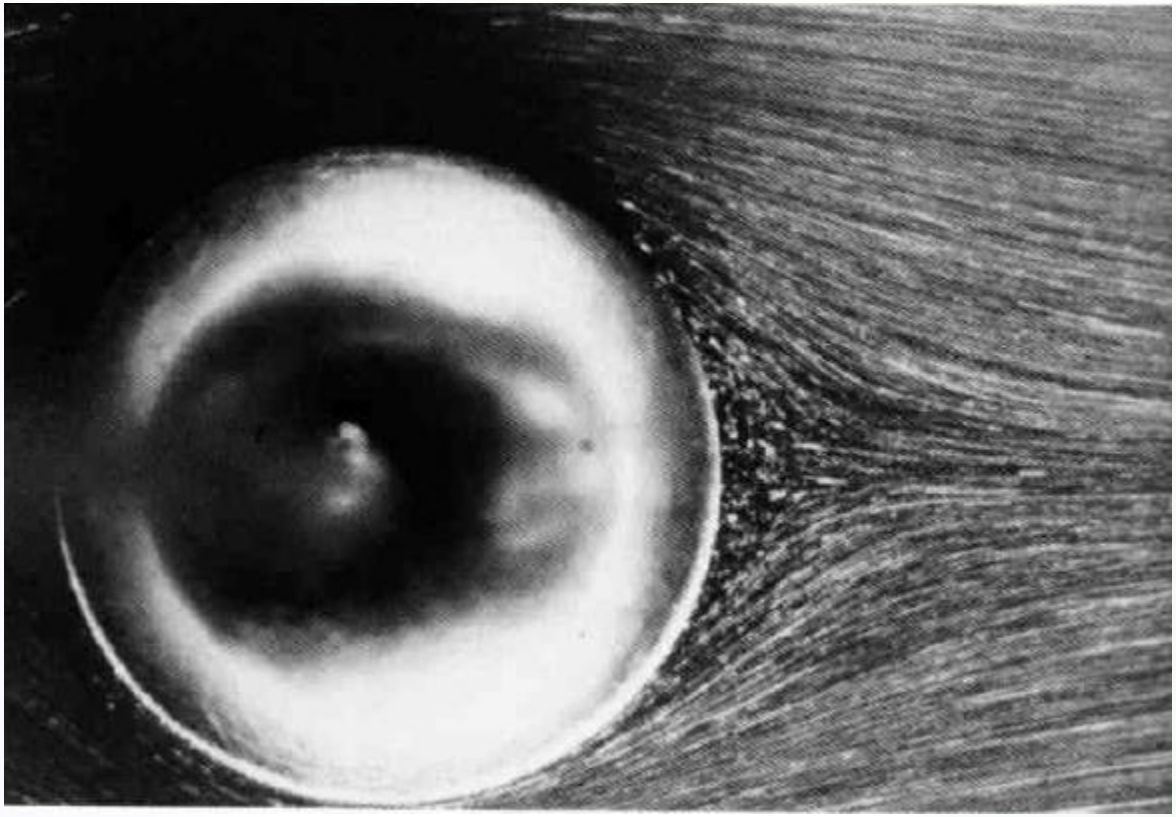

The flow is clearly separated over the rear of the sphere..

THE FLOW OVER A SPHERE
THE REAL CASE

The flow over sphere – **Re=56.5**

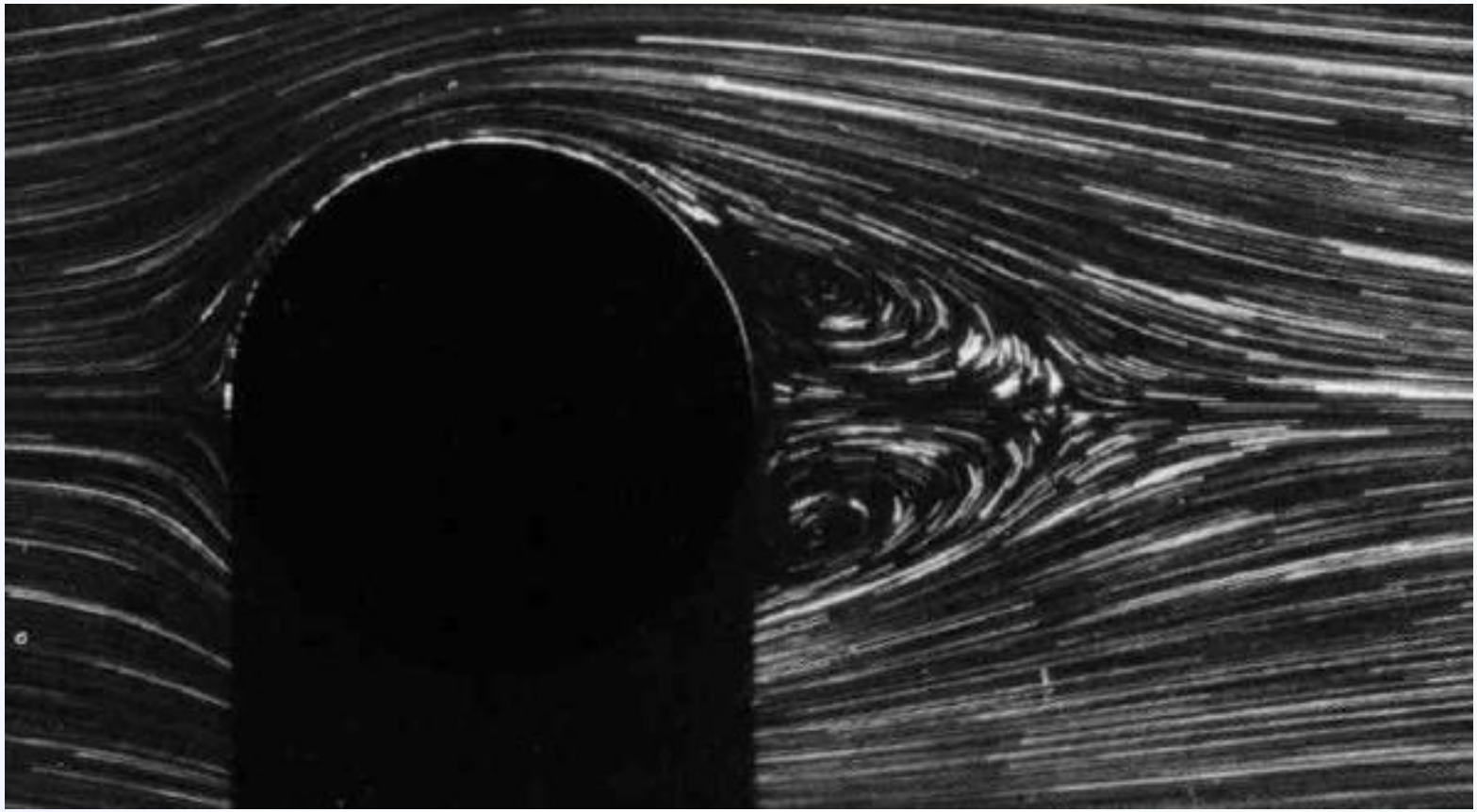

THE FLOW OVER A SPHERE
THE REAL CASE

The flow over sphere – **Re=104**

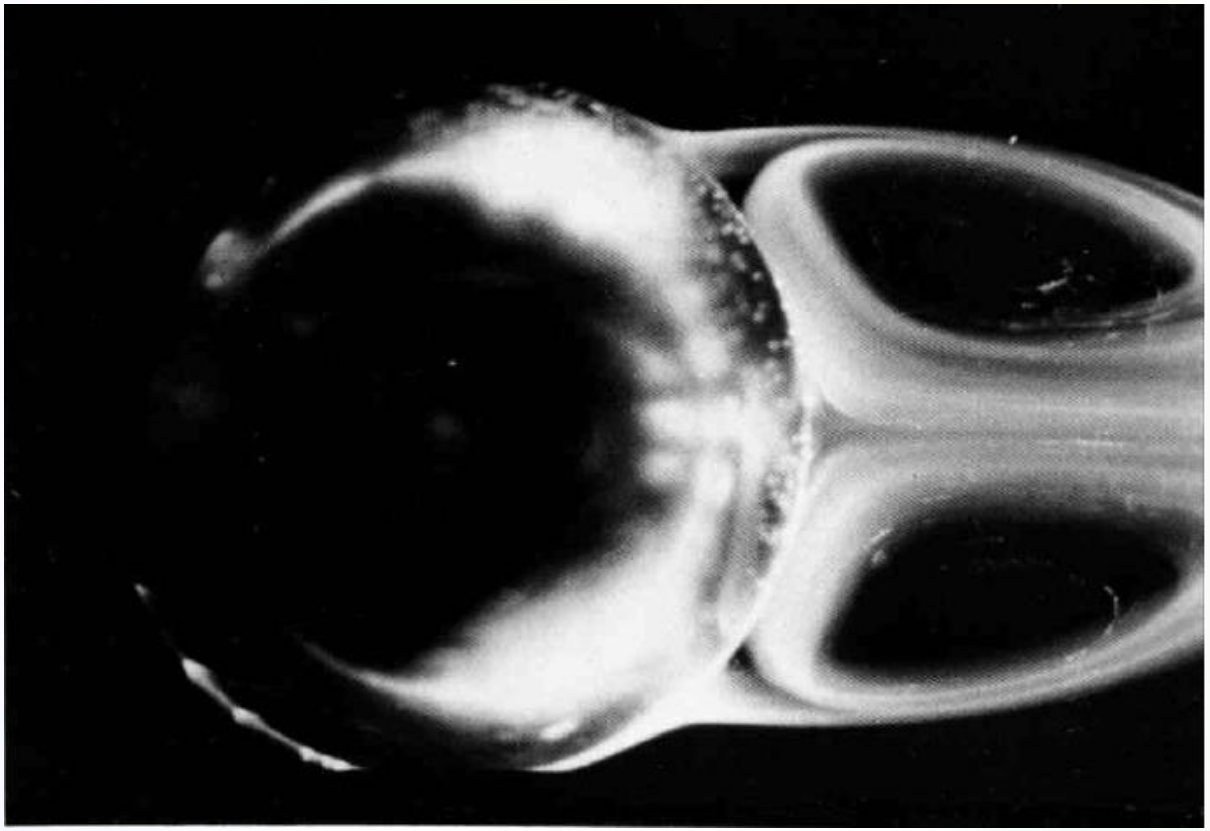

THE FLOW OVER A SPHERE
THE REAL CASE

The flow over sphere – **Re=118**

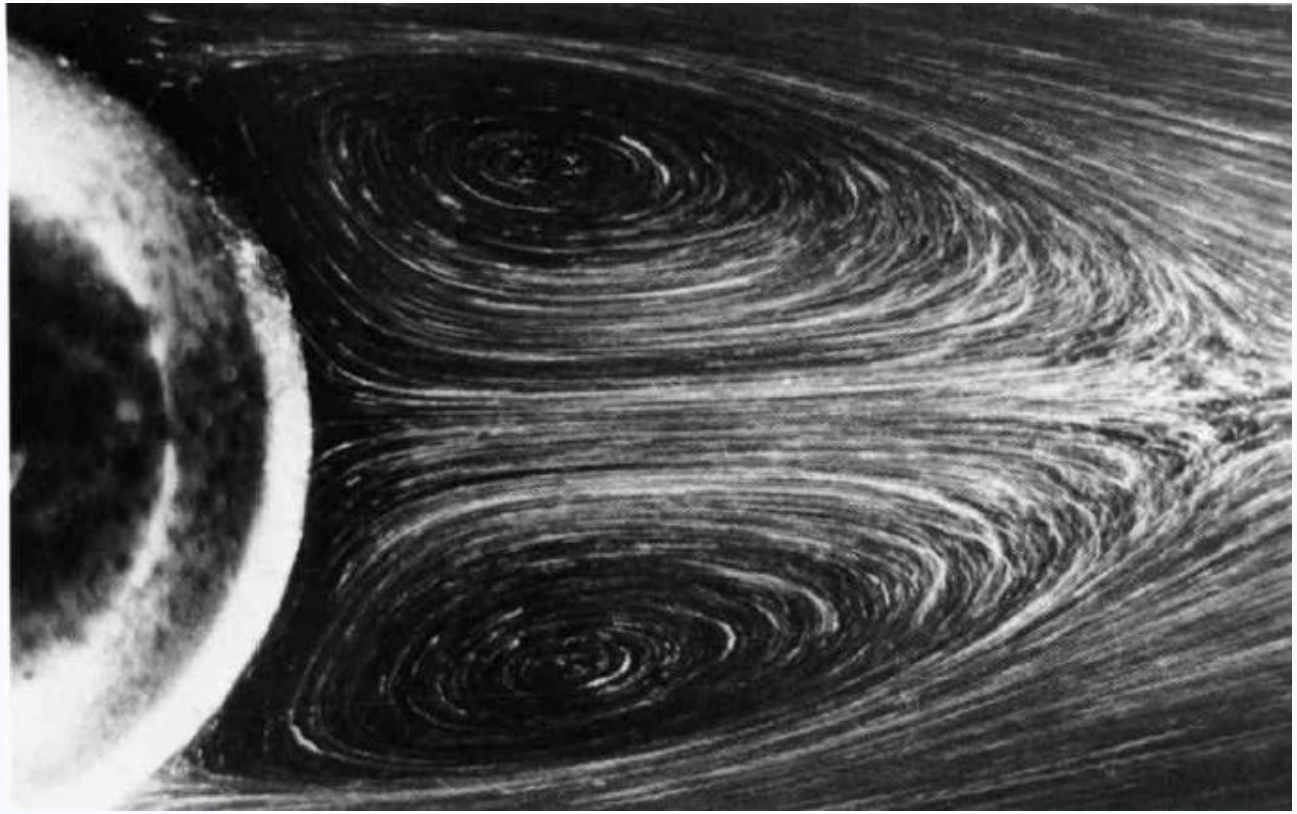

The flow is clearly separated over the rear of the sphere.

THE FLOW OVER A SPHERE
THE REAL CASE

The flow over sphere – **Re=202**

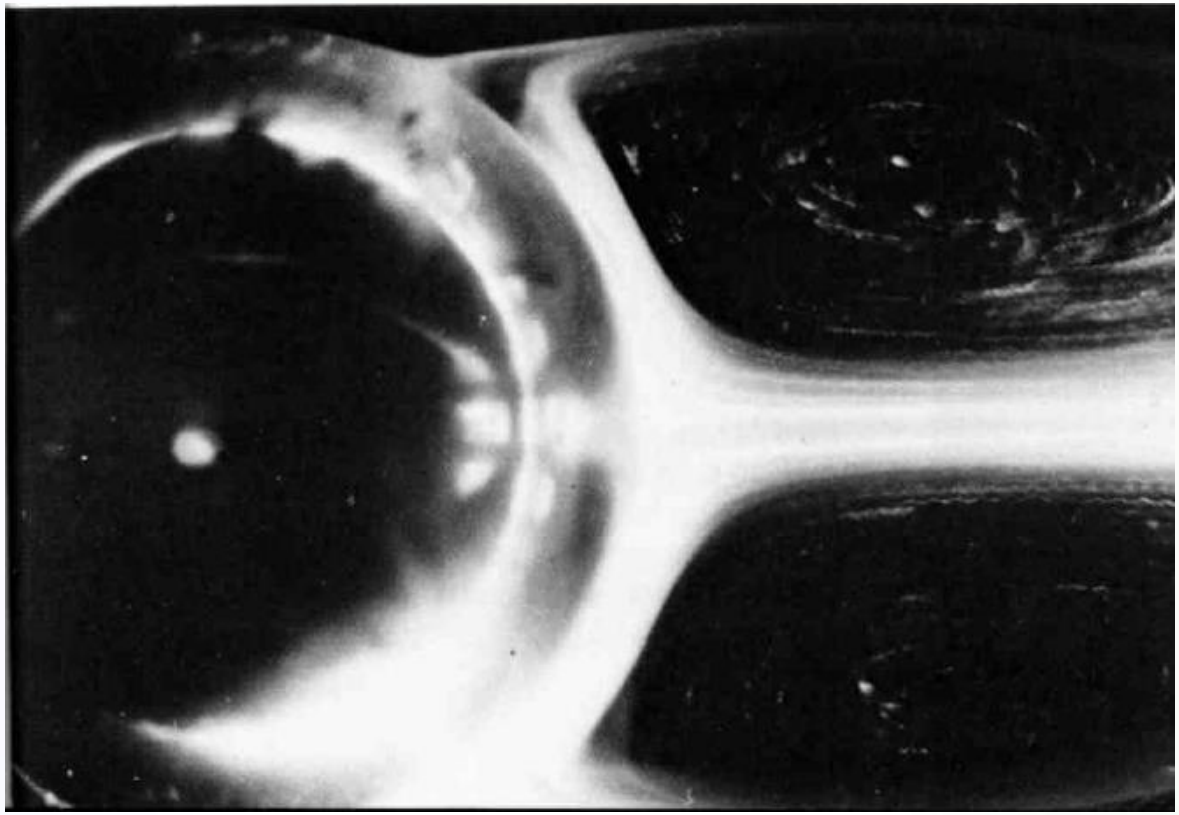

THE FLOW OVER A SPHERE
THE REAL CASE

The flow over sphere – **Re=15000**

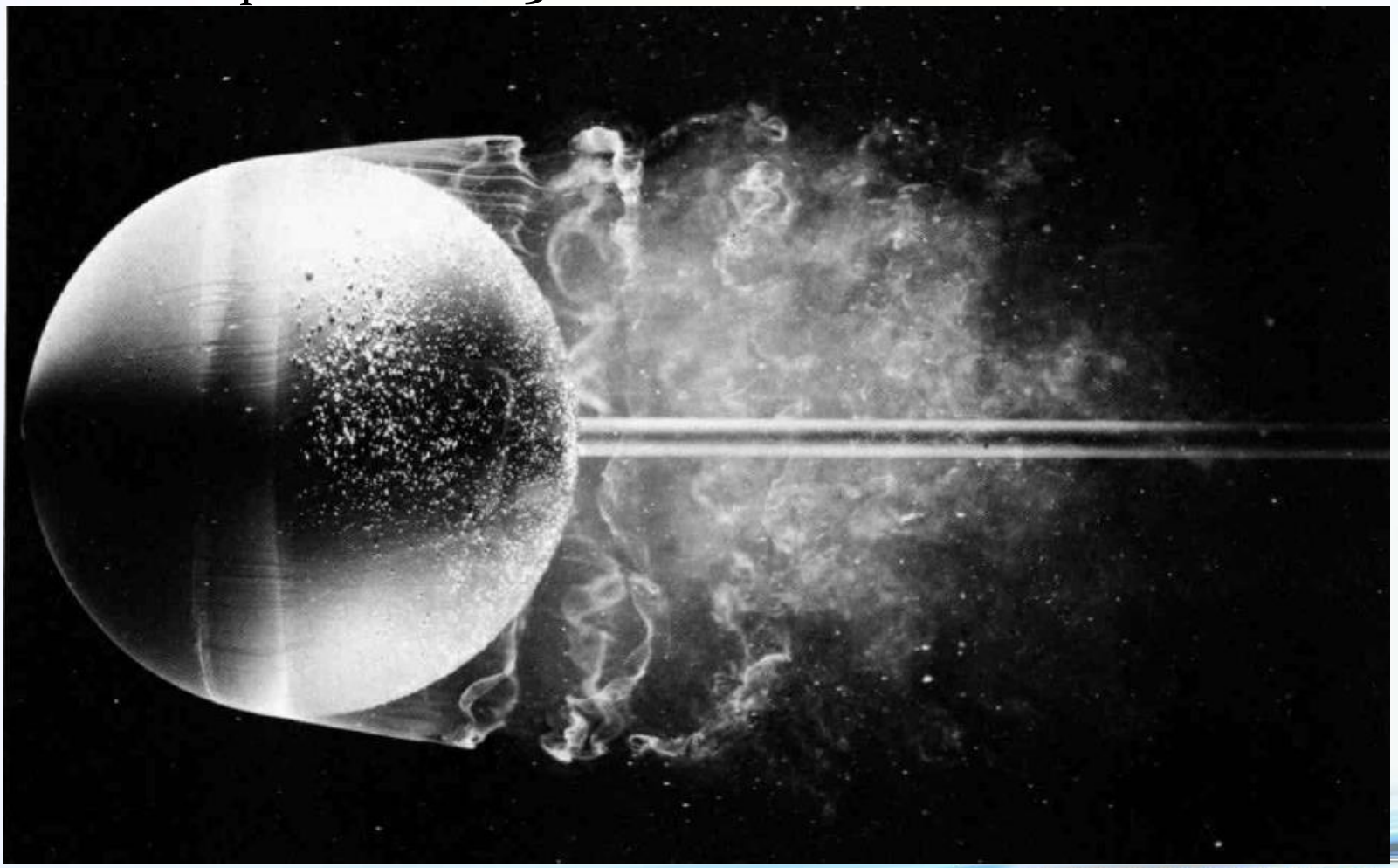

THE FLOW OVER A SPHERE
THE REAL CASE

The flow over sphere – **Re=30000** *(Turbulent flow. Forced by a trip wire hoop ahead of the equator, causing the laminar flow to become turbulent suddenly)*

Because the flow is turbulent, separation takes place much farther over the back surface of sphere.

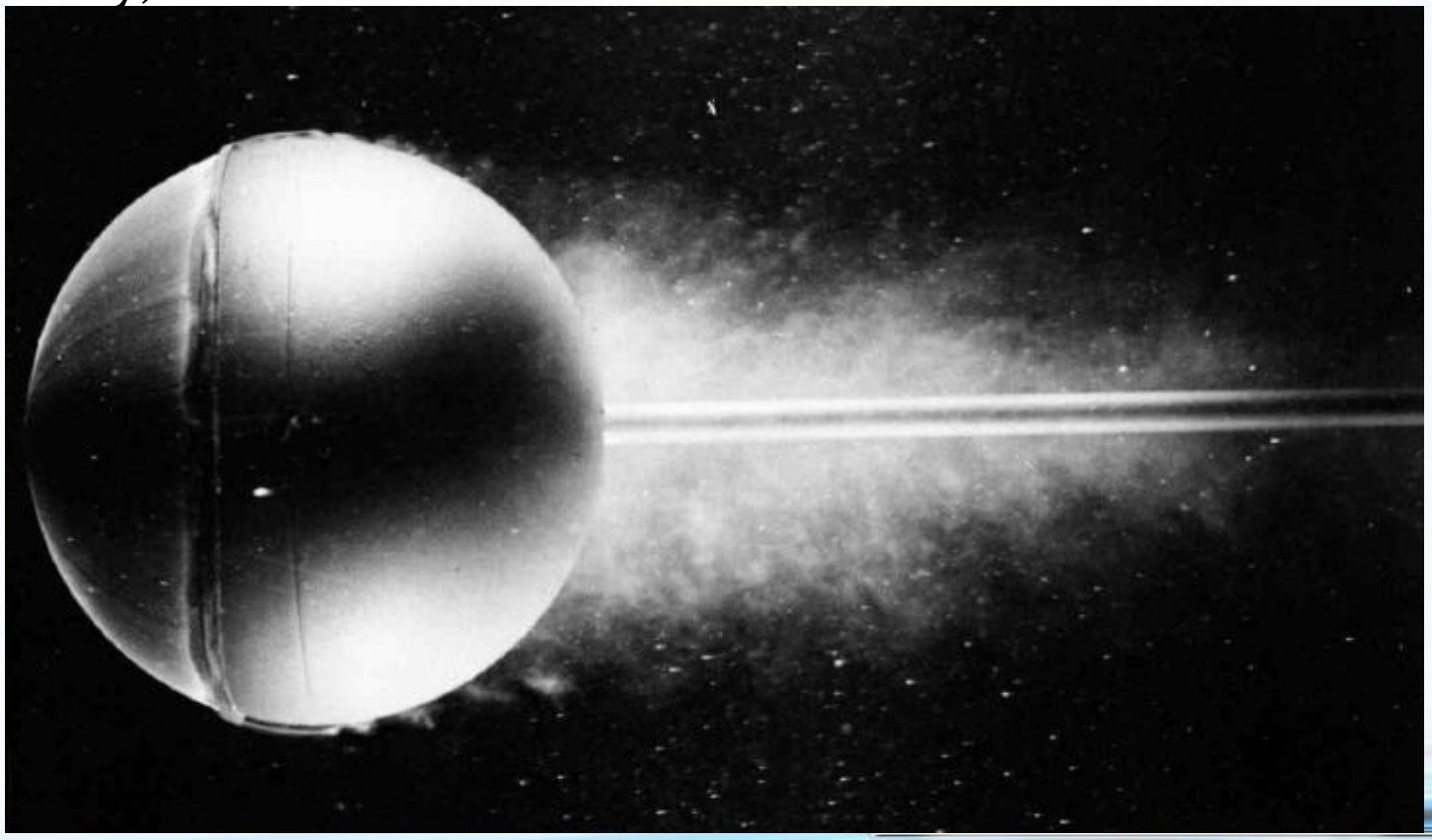

THE FLOW OVER A SPHERE
THE REAL CASE

Variation of drag coefficient C_D with the Reynolds number

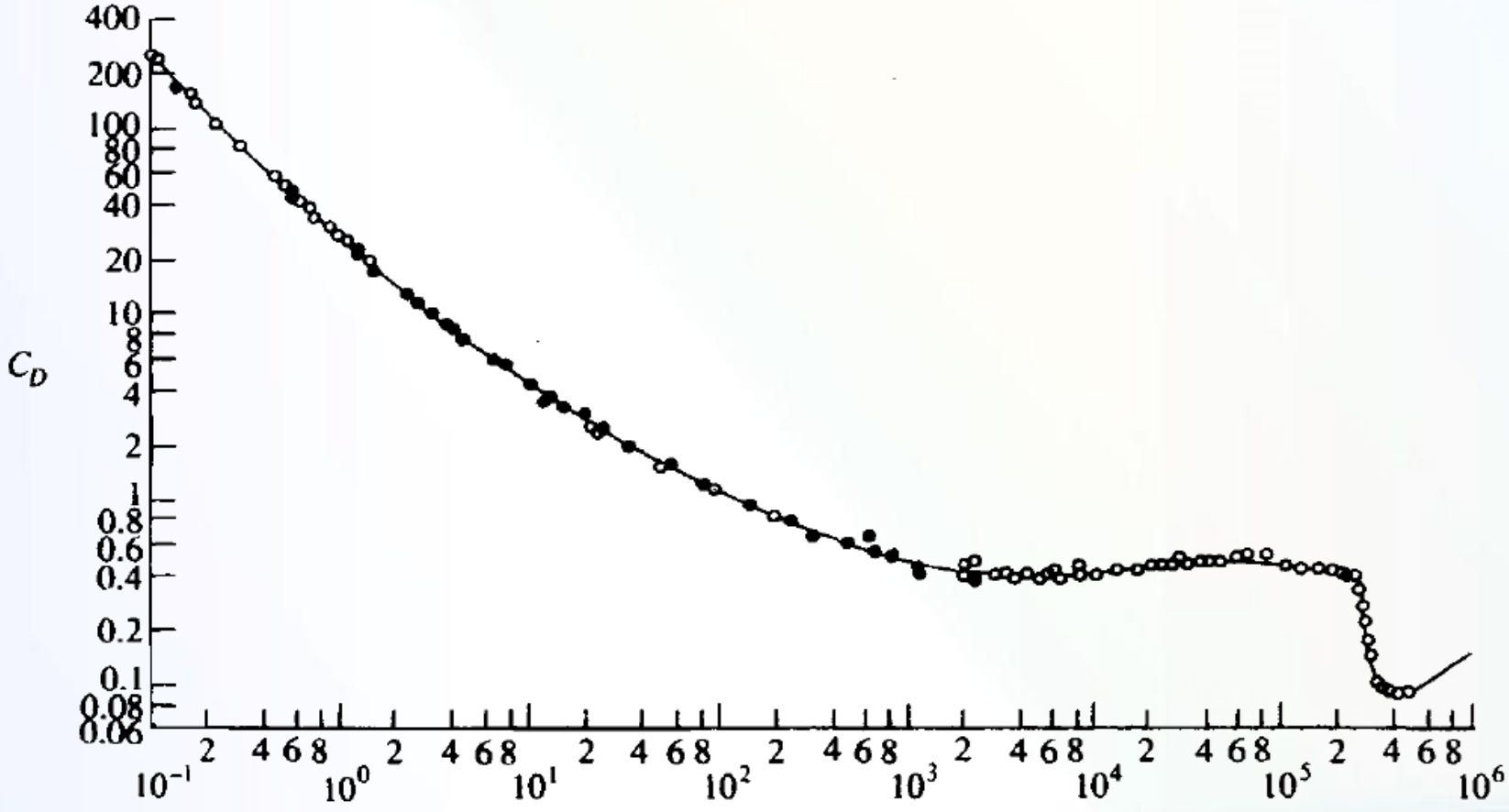

THE FLOW OVER A SPHERE AND CIRCULAR CYLINDER

the C_D variations are qualitatively similar, both with a precipitous decrease in C_D near a critical Reynolds number of 300,000, coinciding with natural transition from laminar to turbulent flow.

However, quantitatively the two curves are quite different. In the Reynolds number range most appropriate to practical problems, that is, for Re>1000, the values of C_D for the sphere are considerably smaller than those for a cylinder-a classic example of the three-dimensional relieving effect.

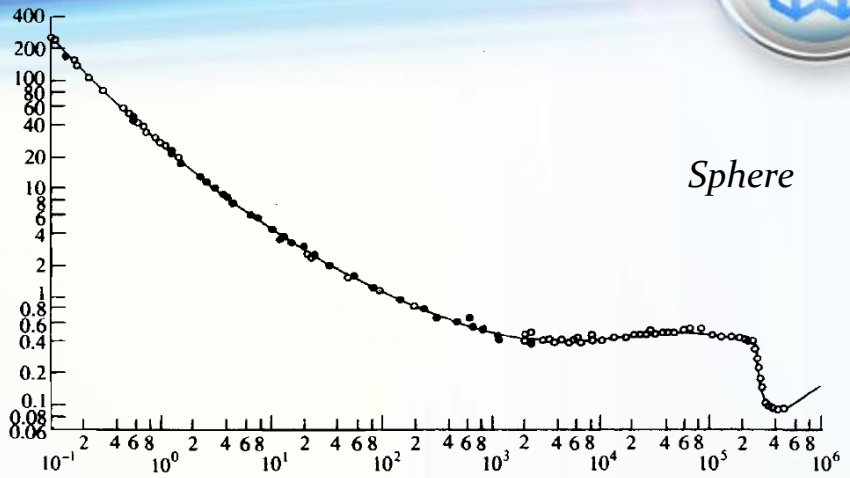

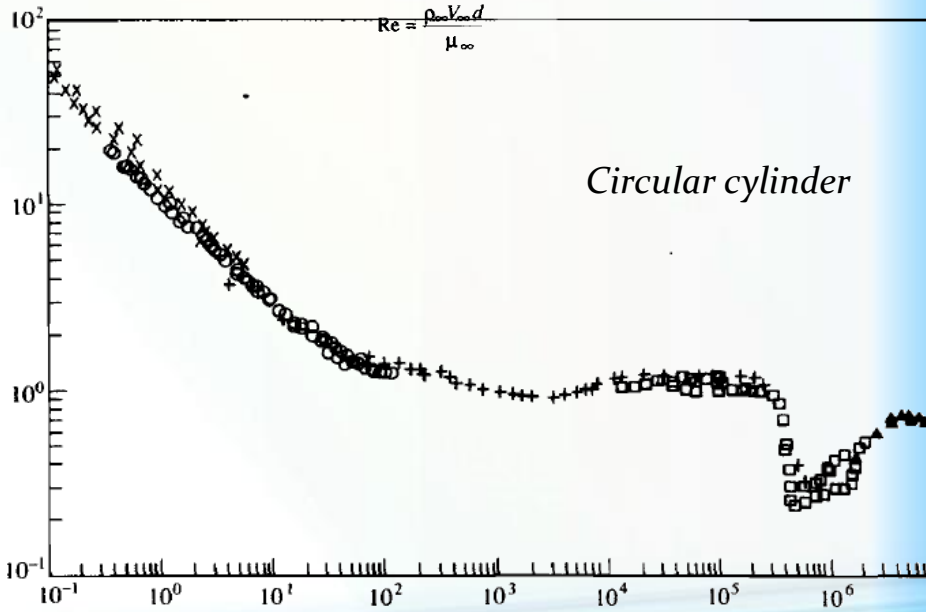

THE FLOW OVER A SPHERE AND CIRCULAR CYLINDER

The value of C_D for *Re* slightly less than the critical value is about 1 and drops to 0.3 for *Re* slightly above the critical value. In contrast, for the sphere, C_D is about 0.4 in the Reynolds number range below the critical value and drops to about 0.1 for Reynolds numbers above the critical value.

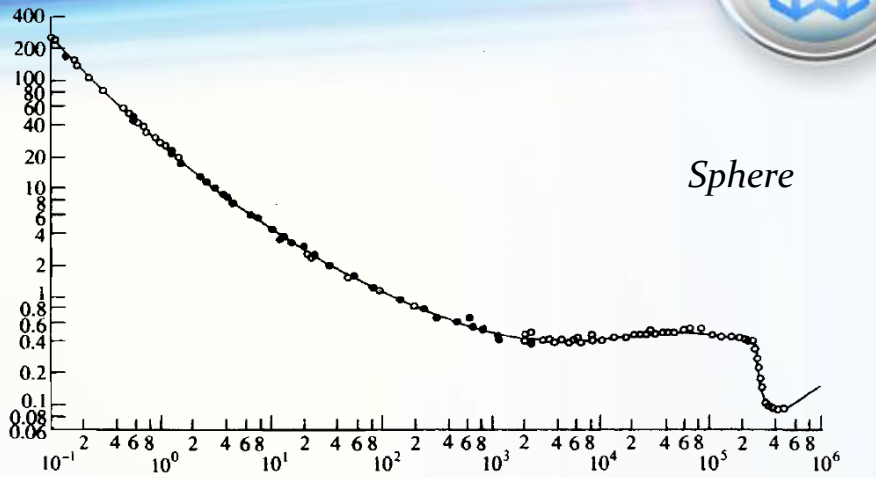

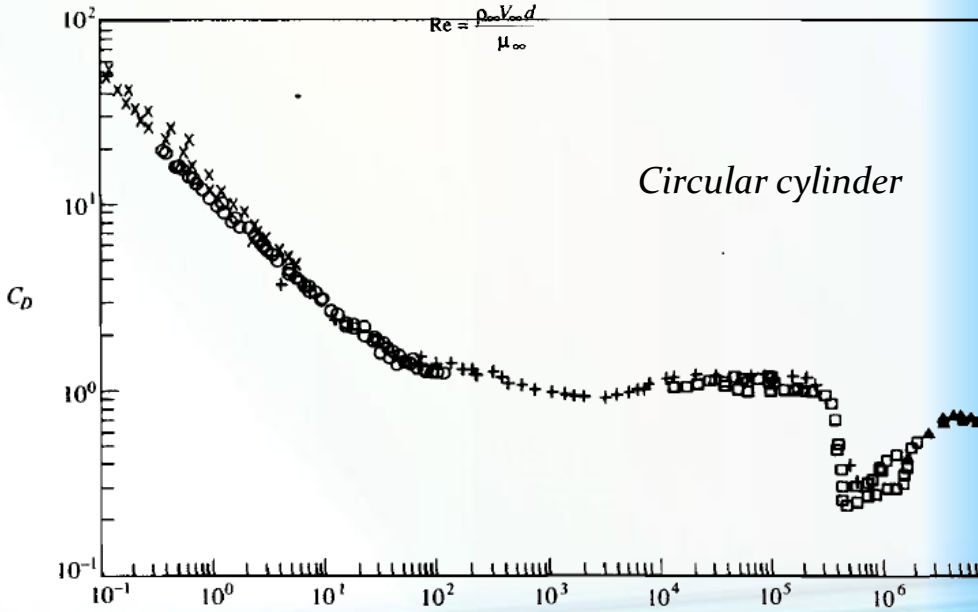

Introduction to Three-Dimensional Incompressible Flows

KN Toosi University of Technology
Aerospace engineering Faculty

To this point in our aerodynamic discussions, we have been working mainly in a two-dimensional world;

Fortunately, the two-dimensional analyses go a long way toward understanding many practical flows, but they also have distinct limitations.

The real world of aerodynamic applications is three- dimensional. However, because of the addition of one more independent variable, the analyses generally become more complex.

The real world of aerodynamic applications is three-dimensional. However, because of the addition of one more independent variable, the analyses generally become more complex.

Governing Equation

$$\nabla^2 \phi = 0$$

For flow over a body must satisfy the flow-tangency boundary condition on the body, that is:

$$\mathbf{V} \cdot \mathbf{n} = 0$$

φ is, in general, a function of three-dimensional space

Some elementary three-dimensional incompressible flows

THREE-DIMENSIONAL SOURCE

Return to Laplace's equation written in spherical coordinates,

$$\nabla^2 \phi = \phi_{rr} + \frac{2}{r}\phi_r + \frac{1}{r^2}\left(\phi_{\theta\theta} + \cot\theta\,\phi_\theta + \csc^2\theta\,\phi_{\Phi\Phi}\right)$$

Consider the velocity potential given by

$$\phi = -\frac{C}{r}$$

where *C is a constant and r is the radial coordinate from the origin.*

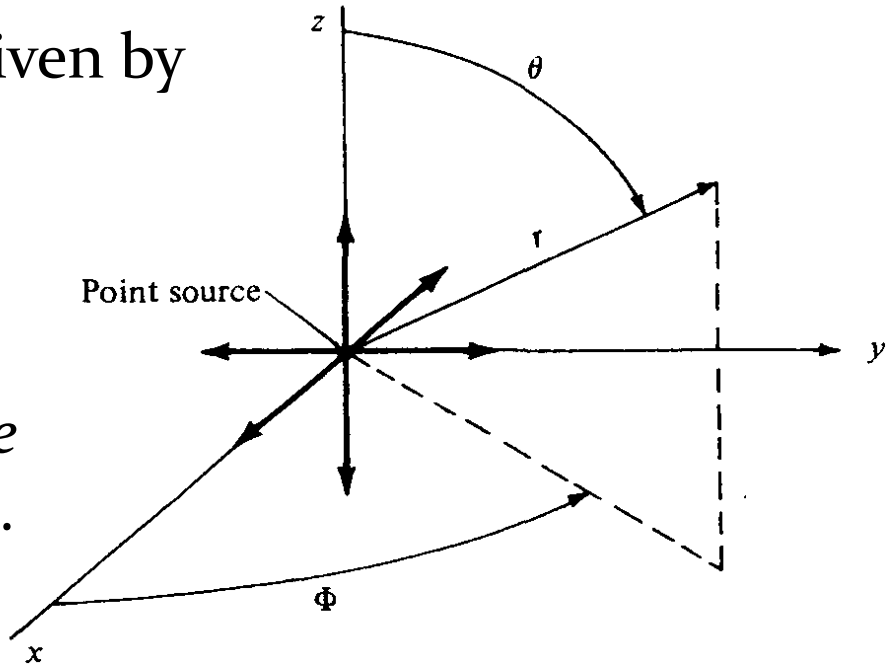

$$\nabla p = \frac{\partial p}{\partial r}\mathbf{e}_r + \frac{1}{r}\frac{\partial p}{\partial \theta}\mathbf{e}_\theta + \frac{1}{r\sin\theta}\frac{\partial p}{\partial \Phi}\mathbf{e}_\Phi$$

$$\mathbf{V} = \nabla\phi = \frac{C}{r^2}\mathbf{e}_r$$

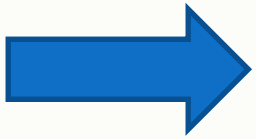

$$V_r = \frac{C}{r^2}$$
$$V_\theta = 0$$
$$V_\Phi = 0$$

To evaluate the constant C

$$\text{Mass flow} = \oiint_S \rho \mathbf{V} \cdot \mathbf{dS}$$

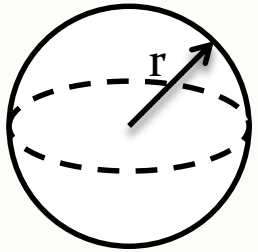

The volume flow:

$$\lambda = \oiint_S \mathbf{V} \cdot \mathbf{dS}$$

$$V_r = C/r^2$$

$$\lambda = \frac{C}{r^2} 4\pi r^2 = 4\pi C \quad \Rightarrow \quad C = \frac{\lambda}{4\pi}$$

$$V_r = \frac{\lambda}{4\pi r^2}$$

λ is defined as the strength of the source.

THREE-DIMENSIONAL DOUBLET

KN Toosi University of Technology
Aerospace engineering Faculty

Consider a sink and source of equal but opposite strength located at points *O* and A

The velocity potential at *P is:*

$$\phi = -\frac{\lambda}{4\pi}\left(\frac{1}{r_1} - \frac{1}{r}\right)$$

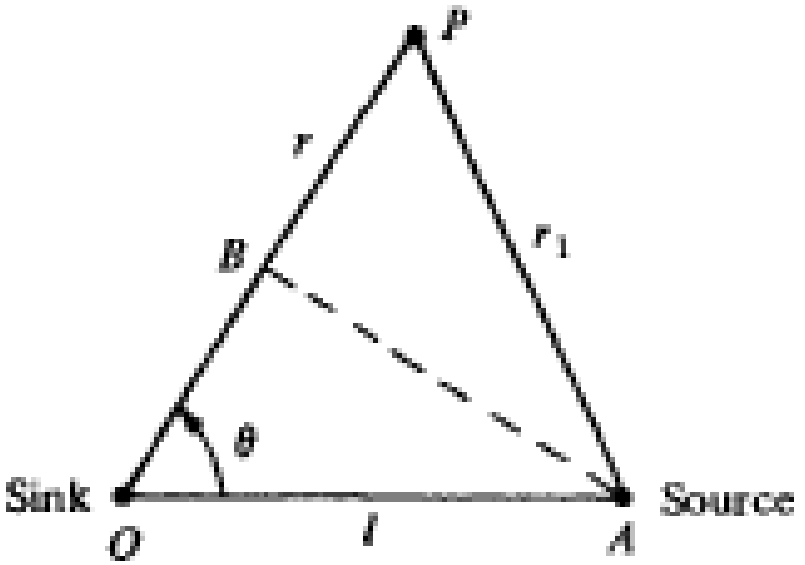

$$\phi = -\frac{\lambda}{4\pi}\frac{r - r_1}{r r_1}$$

$$l \to 0 \qquad \text{as} \qquad \lambda \to \infty$$

In the limit, as $l \to 0$, $r - r_1 \to OB = l\cos\theta$, and $rr_1 \to r^2$.

$$\phi = -\lim_{\substack{l\to 0 \\ \lambda\to\infty}} \frac{\lambda}{4\pi}\frac{r - r_1}{rr_1} = -\frac{\lambda}{4\pi}\frac{l\cos\theta}{r^2}$$

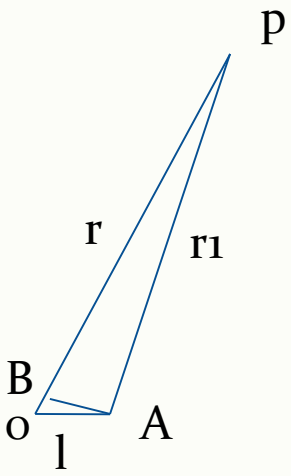

$$\mu = \lambda l.$$

$$\boxed{\phi = -\frac{\mu}{4\pi}\frac{\cos\theta}{r^2}}$$

$$\mathbf{V} = \nabla\phi = \frac{\mu}{2\pi}\frac{\cos\theta}{r^3}\mathbf{e}_r + \frac{\mu}{4\pi}\frac{\sin\theta}{r^3}\mathbf{e}_\theta + 0\mathbf{e}_\Phi$$

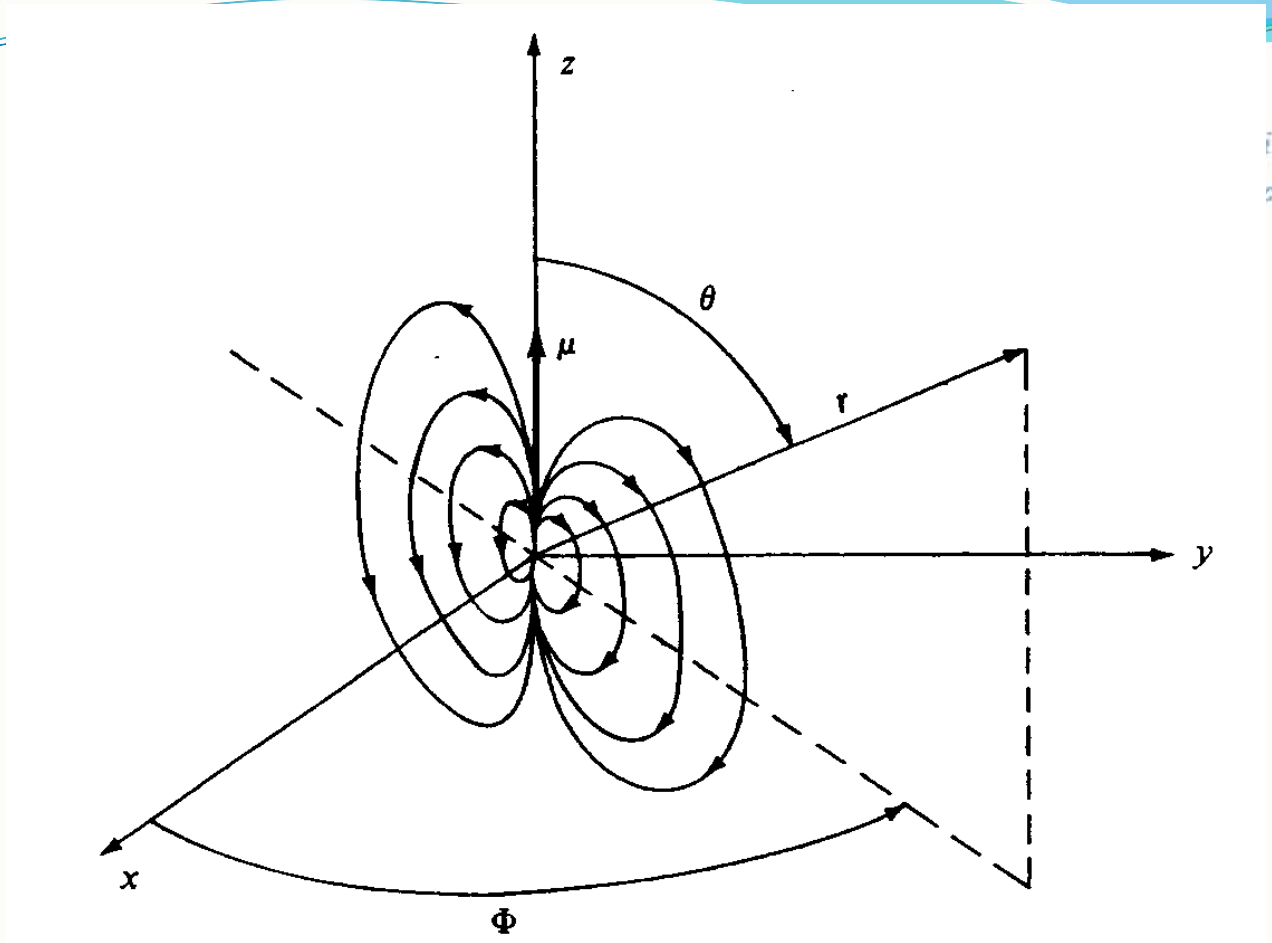

The velocity field depends only on *r and θ*. *Such a flow is defined* as *axisymmetric flow.*

FLOW OVER A SPHERE

The superposition of a uniform flow and a three-dimensional doublet.

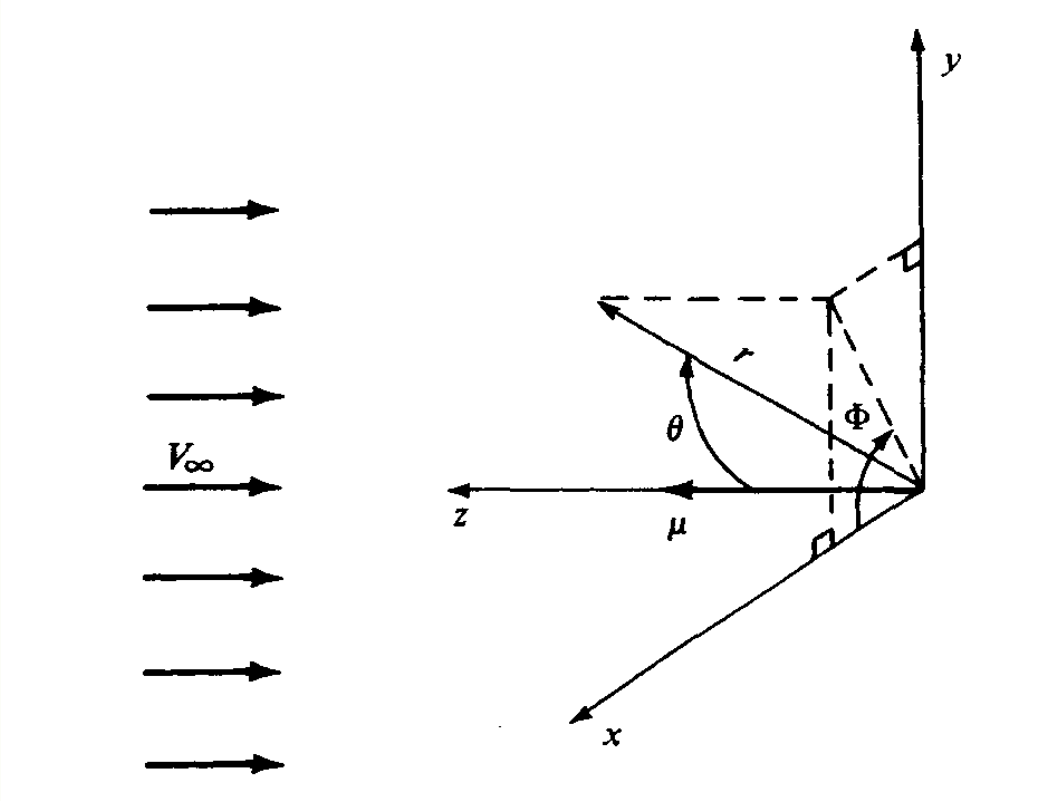

The spherical coordinates of the freestream are:

$$V_r = -V_\infty \cos\theta$$
$$V_\theta = V_\infty \sin\theta$$
$$V_\Phi = 0$$

combined flow:

$$V_r = -V_\infty \cos\theta + \frac{\mu}{2\pi}\frac{\cos\theta}{r^3} = -\left(V_\infty - \frac{\mu}{2\pi r^3}\right)\cos\theta$$
$$V_\theta = V_\infty \sin\theta + \frac{\mu}{4\pi}\frac{\sin\theta}{r^3} = \left(V_\infty + \frac{\mu}{4\pi r^3}\right)\sin\theta$$
$$V_\Phi = 0$$

To find the stagnation points in the flow

$$V_r = V_\theta = 0$$

with $V_r = 0$ $\Rightarrow$ $V_\infty - \dfrac{\mu}{2\pi R^3} = 0$ $\Rightarrow$ $R = \left(\dfrac{\mu}{2\pi V_\infty}\right)^{1/3}$

$V_\theta = 0$ gives $\sin\theta = 0$ $\Rightarrow$ $\theta = 0$ and π

Hence, there are two stagnation points, both on the *z axis*,

$$\left[\left(\frac{\mu}{2\pi V_\infty}\right)^{1/3}, 0\right] \quad \text{and} \quad \left[\left(\frac{\mu}{2\pi V_\infty}\right)^{1/3}, \pi\right]$$

$$R = \left(\frac{\mu}{2\pi V_\infty}\right)^{1/3}$$

$$V_r = -\left(V_\infty - \frac{\mu}{2\pi r^3}\right)\cos\theta$$

$$V_r = -\left(V_\infty - \frac{\mu}{2\pi R^3}\right)\cos\theta = -\left[V_\infty - \frac{\mu}{2\pi}\left(\frac{2\pi V_\infty}{\mu}\right)\right]\cos\theta$$

$$= -(V_\infty - V_\infty)\cos\theta = 0$$

Thus, $V_r = 0$ when $r = R$ for *all values* of θ and Φ.

This is precisely the flow-tangency condition for flow over a sphere of radius ***R***.

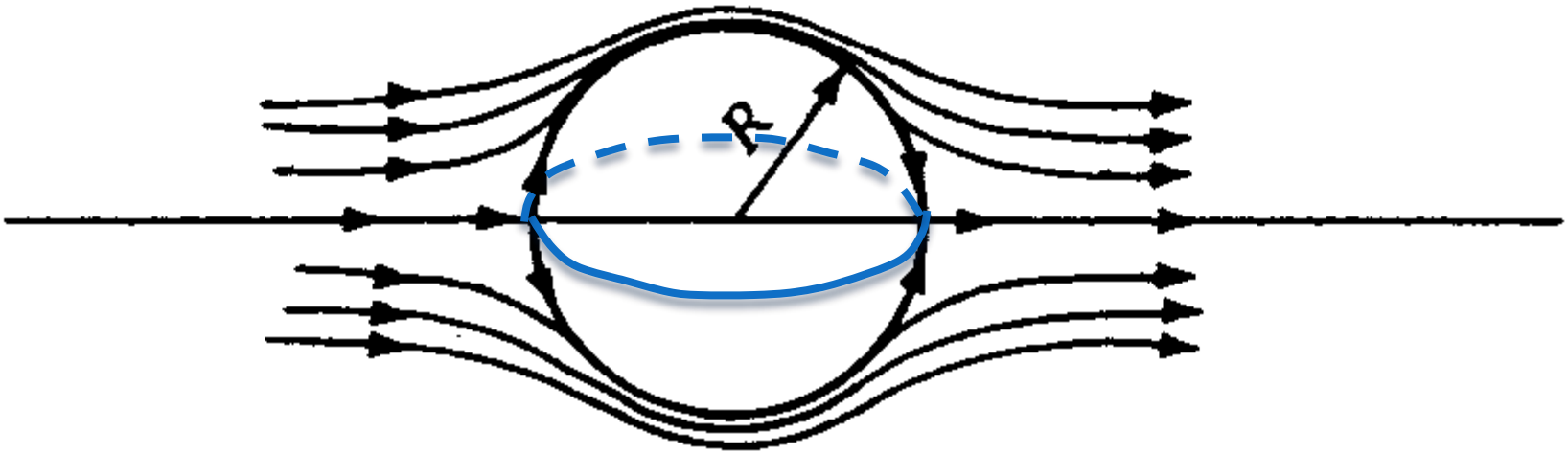
R

$r = R$

$$V_\theta = \left(V_\infty + \frac{\mu}{4\pi R^3} \right) \sin\theta$$

$$R = \left(\frac{\mu}{2\pi V_\infty} \right)^{1/3}$$

$$\mu = 2\pi R^3 V_\infty$$

$$V_\theta = \left(V_\infty + \frac{1}{4\pi} \frac{2\pi R^3 V_\infty}{R^3} \right) \sin\theta$$

$$\boxed{V_\theta = \tfrac{3}{2} V_\infty \sin\theta}$$

The maximum velocity occurs at the top and bottom points of the sphere, and its magnitude is **(3/2)V_∞.**

For the two-dimensional flow, the maximum velocity is **2V_∞**.

Three-dimensional relieving effect

The pressure distribution on the surface of the sphere:

$$C_p = 1 - \left(\frac{V}{V_\infty}\right)^2 = 1 - \left(\frac{3}{2}\sin\theta\right)^2 \Rightarrow \boxed{C_p = 1 - \frac{9}{4}\sin^2\theta}$$

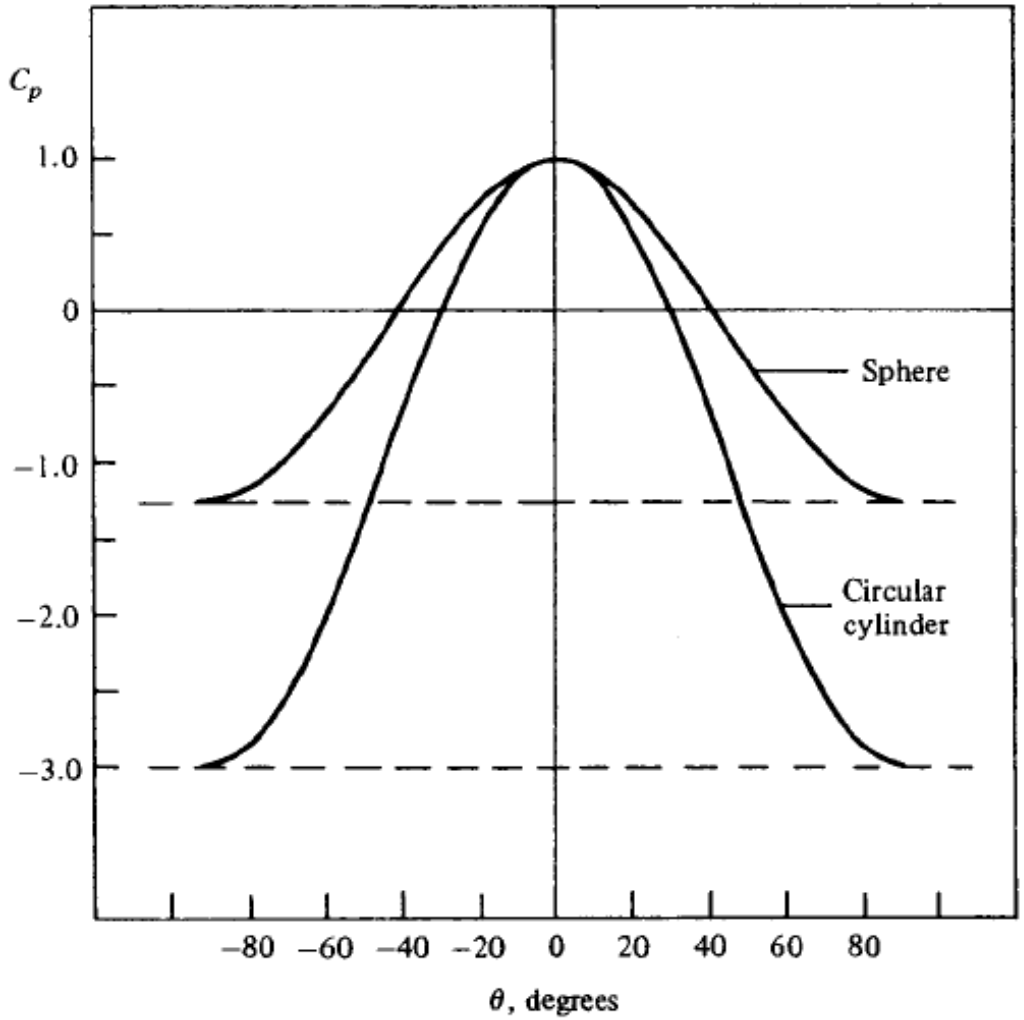

GENERAL THREE-DIMENSIONAL FLOWS: PANEL TECHNIQUES

KN Toosi University of Technology
Aerospace engineering Faculty

Three-dimensional, inviscid, incompressible flows are almost always calculated by means of numerical panel techniques.

The general idea behind all 3 D panel methods is to cover the three-dimensional body with panels over which there is an unknown distribution of singularities (such as point sources, doublets, or vortices).

For a nonlifting body such as illustrated in the following figure, a distribution of source panels is sufficient. However, for a lifting body, both source and vortex panels (or their equivalent) are necessary.

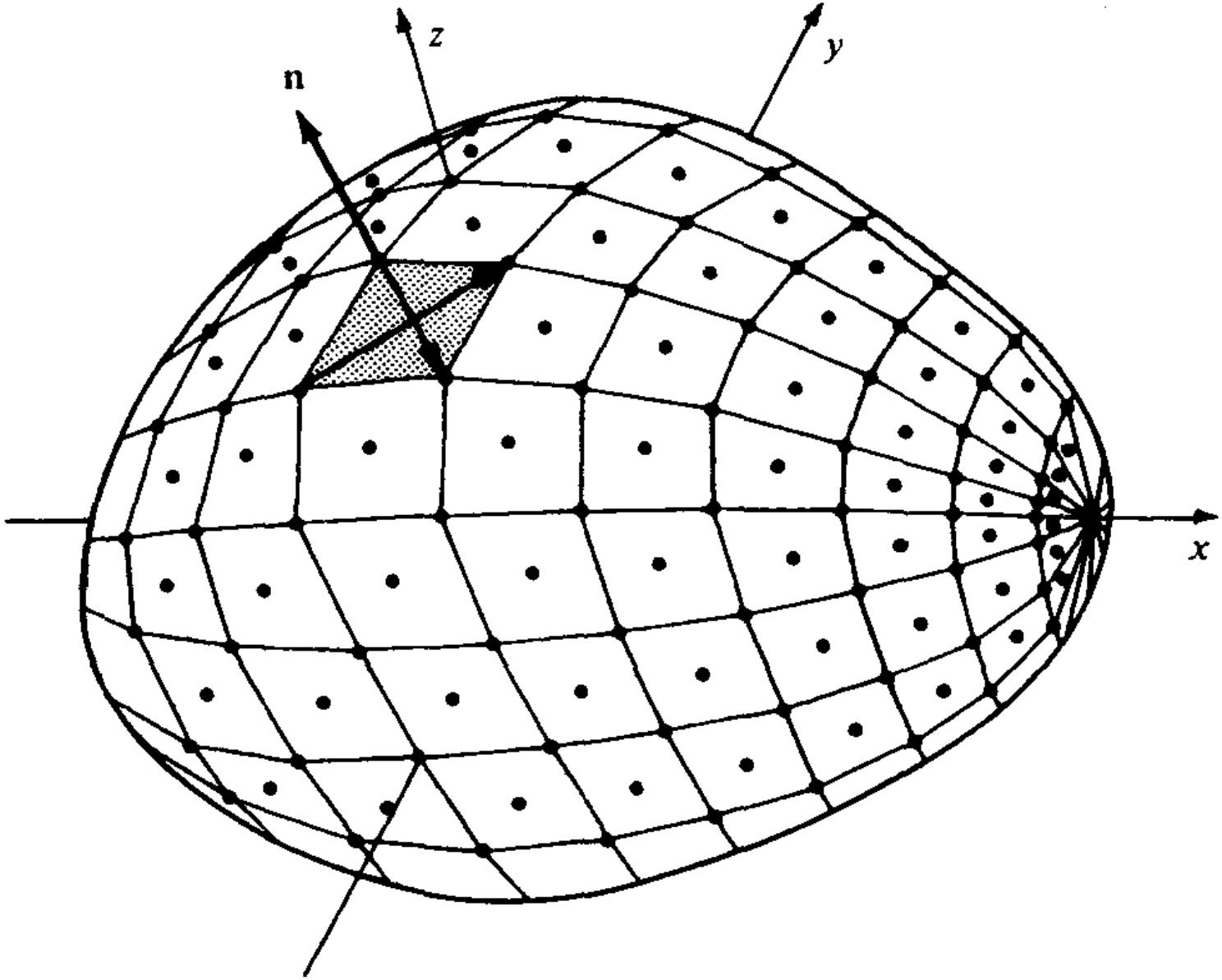
n
z
y
x

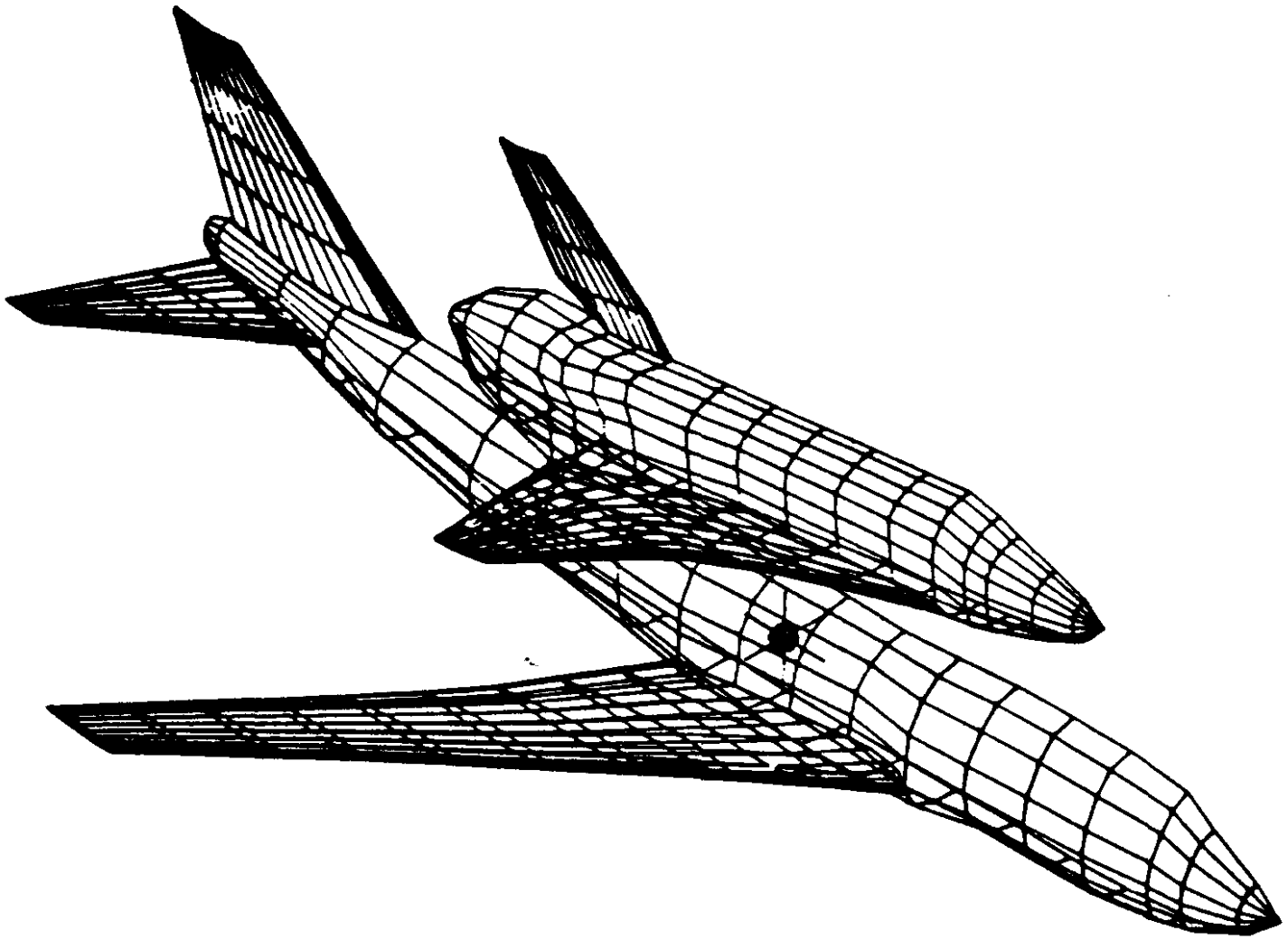

Panel distribution for the analysis of the Boeing 747 carrying the space shuttle orbiter.

APPLIED AERODYNAMICS: THE FLOW OVER A SPHERE—THE REAL CASE

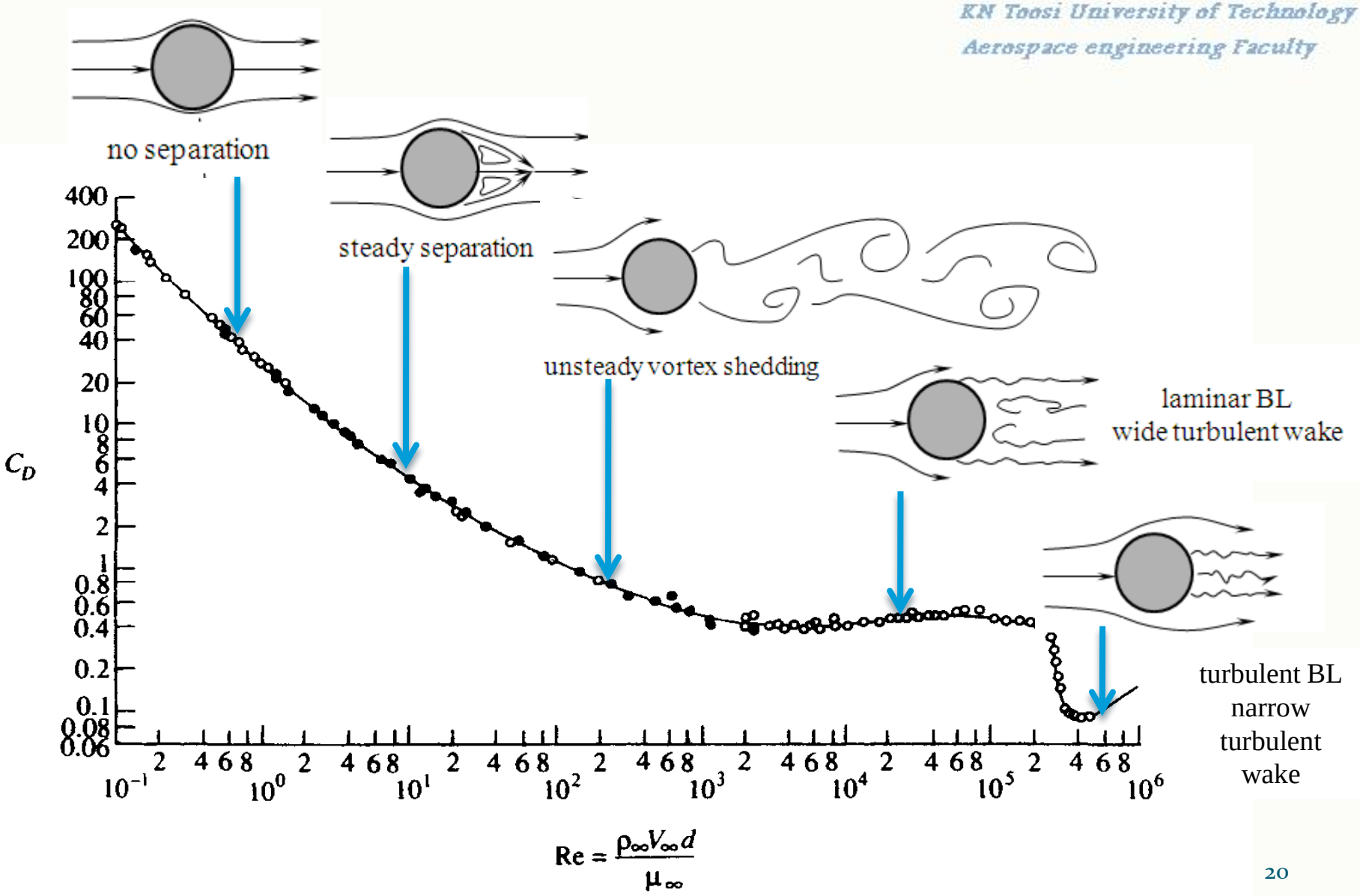

Tripping the boundary layer

- Here we see how the addition of a trip wire to induce transition to turbulence changes the separation line further to the rear of the sphere, reducing the size of the wake and thus drastically diminishing overall drag.
- This well-known fact can be taken advantage of in a number of applications, such as dimples in golf balls and turbulence generation devices on airfoils.

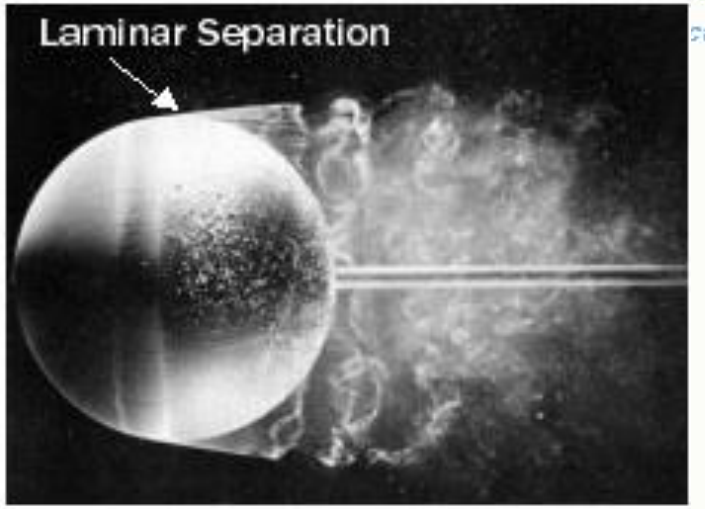

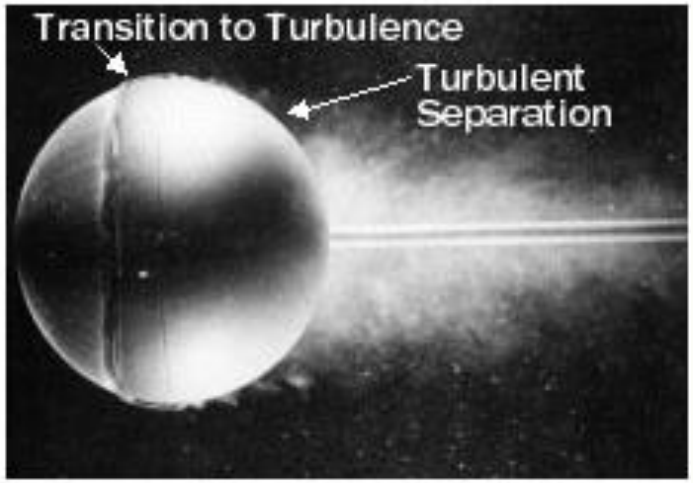

Sports balls

- Many games involve balls designed to use drag reduction brought about by surface roughness.
- Many sports balls have some type of surface roughness, such as the seams on baseballs or cricket balls and the fuzz on tennis balls.
- It is the Reynolds number (not the speed, per se) that determines whether the boundary layer is laminar or turbulent. Thus, the larger the ball, the lower the speed at which a rough surface can be of help in reducing the drag.

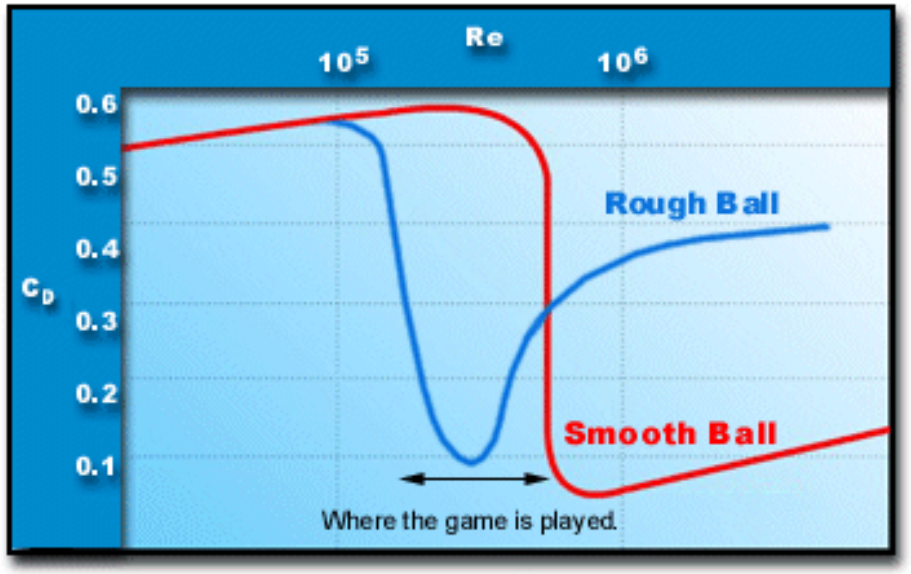

- Typically sports ball games that use surface roughness to promote an early transition of the boundary layer from a laminar to a turbulent flow are played over a Reynolds number range that is near the "trough" of the Cd versus Re curve, where drag is lowest.